

CR 114442

AVAILABLE TO THE PUBLIC

V/STOL TILT-ROTOR STUDY TASK II

RESEARCH AIRCRAFT DESIGN (NASA CONTRACT NAS2-6599)

VOLUME II REPORT 300-099-006

(NASA-CR-114442) V/STOL TILT-ROTOR STUDY,
TASK 2. VOLUME 2: RESEARCH AIRCRAFT
DESIGN (Bell Helicopter Co.) 254 p HC
\$14.75

CSCD 01C

N73-21927

63/02
69387
Unclass



BELL
HELICOPTER COMPANY

POST OFFICE BOX 482 • FORT WORTH TEXAS 76101 A  COMPANY

CR 114442

AVAILABLE TO THE PUBLIC

V/STOL TILT-ROTOR STUDY TASK II

RESEARCH AIRCRAFT DESIGN (NASA CONTRACT NAS2-6599)

VOLUME II REPORT 300-099-006



**BELL
HELICOPTER COMPANY**

POST OFFICE BOX 482 • FORT WORTH, TEXAS 76101 A **Textron** COMPANY

TABLE OF CONTENTS

	<u>Page</u>
I. SUMMARY	I-1
II. RESEARCH FLIGHT INVESTIGATIONS	II-1
A. IDENTIFICATION OF NEEDED FLIGHT INVESTIGATIONS	II-1
1. Objective	II-1
2. Flight Investigations	II-3
B. CAPABILITY OF RESEARCH AIRCRAFT	II-9
1. Performance Capability	II-9
2. Range of Parameter Variation	II-10
3. Ability to Test Other Proprotor Configurations	II-12
4. Applicability of Results	II-13
C. LIMITATION OF RESEARCH AIRCRAFT	II-14
1. Technical Characteristics	II-14
2. Operational Characteristics	II-14
III. DESIGN DESCRIPTION	III-1
A. GENERAL	III-1
B. DESIGN CRITERIA	III-10
C. PROPROTOR	III-11
1. Blades	III-11
2. Hub (300-010-100)	III-12
D. DRIVE SYSTEM (300-960-004)	III-12
E. POWERPLANT	III-14
1. Engine	III-14
2. Induction System (300-960-003)	III-14
3. Oil System	III-14
4. Fuel System	III-15
F. AIRFRAME	III-15
1. Wing (300-960-007)	III-15
2. Fuselage (300-960-008)	III-16
3. Empennage	III-17
4. Landing Gear	III-17

TABLE OF CONTENTS - Continued

	<u>Page</u>
G. AIRCRAFT SYSTEMS	III-17
1. Conversion System	III-17
2. Hydraulic System	III-18
3. Electrical System	III-19
H. AIRCRAFT CONTROLS	III-20
1. Proprotor Controls (300-960-002)	III-20
2. Flight Control	III-21
3. Stability and Control Augmentation System	III-21
4. Proprotor Governor System	III-22
5. Power Management	III-22
IV. WEIGHT ANALYSIS	IV-1
A. ROTOR GROUP	IV-2
B. WING GROUP	IV-2
C. TAIL GROUP	IV-3
D. BODY GROUP	IV-4
E. ALIGHTING GEAR GROUP	IV-5
F. CONTROLS GROUP	IV-7
G. ENGINE SECTION AND NACELLE GROUP	IV-7
H. PROPULSION GROUP	IV-7
1. Engine Installation	IV-7
2. Conversion System	IV-8
3. Air Induction System	IV-8
4. Exhaust System	IV-8
5. Lubrication System, Engine	IV-8
6. Fuel System	IV-8
7. Engine Controls	IV-8
8. Starting System	IV-8
9. Proprotor Pitch-Governor Control	IV-8
10. Drive System	IV-9
I. INSTRUMENT GROUP	IV-9
J. HYDRAULICS GROUP	IV-11
K. ELECTRICAL GROUP	IV-11

TABLE OF CONTENTS - Continued

	<u>Page</u>
L. ELECTRONIC GROUP	IV-12
M. FURNISHINGS AND EQUIPMENT GROUP	IV-12
N. AIR-CONDITIONING EQUIPMENT GROUP	IV-12
V. PERFORMANCE	V-1
A. SUMMARY	V-1
B. AIRFRAME AERODYNAMICS	V-1
1. Lift Analysis	V-1
2. Drag Analysis	V-3
3. Proprotor Power Required	V-3
4. Powerplant Performance	V-4
5. Hover Ceilings	V-5
6. Rate of Climb	V-5
7. Flight Envelope and Maximum Speeds	V-5
8. Specific Range	V-5
9. Payload Range and Endurance	V-5
10. STOL Performance	V-5
VI. DYNAMICS	VI-1
A. COUPLED NATURAL FREQUENCIES	VI-1
1. Proprotor Natural Frequencies	VI-1
2. Wing-Pylon-Fuselage Natural Frequencies	VI-1
3. Drive System Natural Frequencies	VI-3
B. BLADE FLAPPING ENVELOPE IN AIRPLANE MODE	VI-3
C. PROPROTOR STABILITY	VI-4
1. Analytical Method	VI-4
2. Stability Characteristics of the Coupled Modes	VI-7
3. Model 300 Stability Boundaries	VI-7
4. Sensitivity to Loss of Stiffness	VI-8
D. RIDE COMFORT	VI-9
1. Rotor Harmonic Induced Vibration	VI-8
2. Response to Atmospheric Turbulence in Airplane Mode	VI-9

TABLE OF CONTENTS - Concluded

	<u>Page</u>
VII. STABILITY AND CONTROL	VII-1
A. HOVER AND LOW-SPEED FLIGHT	VII-2
1. Stick-Fixed Static Stability	VII-2
2. Control Power and Damping	VII-2
B. CONVERSION FLIGHT	VII-3
1. Stick-Fixed Static Stability	VII-3
2. Control Phasing and Control Power	VII-4
C. AIRPLANE FLIGHT	VII-4
1. Stick-Fixed Static Stability	VII-4
2. Control Power	VII-4
3. Dynamic Stability	VII-4
VIII. NOISE	VIII-1
A. WIND-TUNNEL EXPERIMENTAL DATA	VIII-1
B. COMPARISON BETWEEN THEORY AND EXPERIMENTAL DATA	VIII-1
C. PREDICTED NOISE CHARACTERISTICS	VIII-2
D. GROUND NOISE EXPOSURE	VIII-2
E. COMPARISON WITH OTHER MODES OF TRANSPORTATION	VIII-3
IX. REFERENCES	IX-1

LIST OF TABLES

<u>Table</u>		<u>Page</u>
III-I	Basic Data	III-2
III-II	Dimensional Data	III-3
III-III	Control Travels	III-7
III-IV	Inertia	III-9
III-V	Basic Design Criteria	III-10
IV-I	Model 300 Group Weight Statement	IV-1
IV-II	Mission Gross Weights	IV-3
IV-III	Tail Surface Unit Weights	IV-3
IV-IV	Fuselage Weight Penalties	IV-4
IV-V	Fuselage Parameters and Symbols	IV-6
IV-VI	Rolling Gear Component Data	IV-6
IV-VII	Alighting Gear Group Weight Comparison	IV-7
IV-VIII	Drive System Component Weights	IV-9
IV-IX	Instrument Group Weights	IV-10
IV-X	Electrical Group Weights	IV-11
IV-XI	Furnishings and Equipment Group Weights	IV-12
V-I	Performance Summary	V-2
V-II	Engine Installation Losses	V-5

ILLUSTRATIONS

<u>Figure</u>		<u>Page</u>
I-1	Model 300 Research Aircraft	I-2
II-1	Model 300 Payload Capacity for Test Equipment and/or Mission Simulation Versus Takeoff Altitude	II-16
II-2	Model 300 Flight-Test Endurance	II-17
II-3	Model 300 Flight-Test Envelope and Dive Profile	II-18
II-4	Model 300 Test Range of Disc Loading and Wing Loading	II-19
II-5	Model 300 Test Tip Speed and Gross Weight Range for Hover	II-20
II-6	Model 300 Test Tip Speed Range for Airplane Cruise	II-21
II-7	Comparison of Model 300 Proprotor Inflow and Mach Test Range with D302 Conceptual Aircraft	II-22
II-8	Model 300 with Soft Inplane Proprotor, Symmetric Modes	II-23
II-9	Model 300 with Soft Inplane Proprotor, Stability Margin of Symmetric Modes Versus RPM	II-24
II-10	Comparison of Model 300 Proprotor Blade Collective Modes with D302 Conceptual Aircraft	II-25
II-11	Comparison of Model 300 Symmetric Modes with D302 Conceptual Aircraft	II-26
III-1	Twenty-Five-Foot Proprotor Parameters	III-24
III-2	Proprotor Stiffness and Mass Distriburions	III-25
III-3	Wing Stiffness and Panel Point Weight	III-26
III-4	Fuselage Stiffness and Panel Point Weight	III-27
III-5	Vertical Tail Stiffness	III-28

ILLUSTRATIONS - Continued

<u>Figure</u>		<u>Page</u>
III-6	Horizontal Tail Stiffness	III-29
III-7	Collective Pitch Versus Conversion Angle	III-30
III-8	Differential Collective Pitch Versus Conversion Angle	III-31
III-9	Fore and Aft Cyclic Pitch Versus Conversion Angle	III-32
III-10	Differential Cyclic Pitch Versus Conversion Angle	III-33
III-11	Differential Cyclic Pitch Versus Airspeed	III-34
III-12	Flaperon Deflection Versus Flap Position	III-35
III-13	Typical Hydraulic Boost Cylinder	III-36
III-14	Schematic of Proprotor Control Geometry	III-37
III-15	Model 300 Design Airspeed Versus Altitude	III-38
IV-1	Fuselage Weight Estimation Parameters	IV-13
V-1	Airframe Lift Coefficient Versus Fuselage Angle of Attack	V-7
V-2	Airframe Drag Coefficient Versus Fuselage Angle of Attack	V-8
V-3	Airframe Drag Coefficient Versus Lift Coefficient	V-9
V-4	Drag Coefficient Versus Mach Number	V-10
V-5	Proprotor Hovering Power Required Versus Thrust	V-11
V-6	Hovering Figure of Merit	V-12
V-7	Proprotor Shaft Horsepower Required Versus True Airspeed, Helicopter Mode	V-13
V-8	Lift Distribution Between Proprotor and Airframe in Helicopter Level Flight	V-14

ILLUSTRATIONS - Continued

<u>Figure</u>		<u>Page</u>
V-9	Proprotor Shaft Horsepower Required Versus True Airspeed, Conversion Mode	V-15
V-10	Proprotor Efficiency Versus Shaft Horsepower, Sea Level	V-16
V-11	Proprotor Efficiency Versus Shaft Horsepower, 10,000 Feet	V-17
V-12	Proprotor Efficiency Versus Shaft Horsepower, 20,000 Feet	V-18
V-13	Proprotor Shaft Horsepower Required Versus True Airspeed, Airplane Mode, Sea Level	V-19
V-14	Proprotor Shaft Horsepower Required Versus True Airspeed, Airplane Mode, 10,000 Feet	V-20
V-15	Proprotor Shaft Horsepower Required Versus True Airspeed, Airplane Mode, 20,000 Feet	V-21
V-16	Twin-Engine Proprotor, Shaft Horsepower Available, Helicopter Mode	V-22
V-17	Fuel Flow, Helicopter Mode	V-23
V-18	Proprotor Shaft Horsepower Available, 30-Minute Power	V-24
V-19	Proprotor Shaft Horsepower Available, Maximum Continuous Power	V-25
V-20	Fuel Flow, Airplane Mode	V-26
V-21	Hover Ceilings	V-27
V-22	Rate of Climb Versus True Airspeed, Conversion Mode	V-28
V-23	Maximum Rate of Climb, Airplane Mode	V-29
V-24	Flight Envelope and Maximum Speed, Airplane Mode	V-30
V-25	Nautical Miles Per Pound of Fuel Versus True Airspeed, Airplane Mode, Sea Level	V-31

ILLUSTRATIONS - Continued

<u>Figure</u>		<u>Page</u>
V-26	Nautical Miles Per Pound of Fuel Versus True Airspeed, Airplane Mode, 10,000 Feet	V-32
V-27	Nautical Miles Per Pound of Fuel Versus True Airspeed, Airplane Mode, 20,000 Feet	V-33
V-28	Payload Range	V-34
V-29	Model 300 Endurance	V-35
V-30	Model 300 STOL Takeoff Distance	V-36
VI-1	Model 300 Proprotor Collective Mode Natural Frequencies	VI-12
VI-2	Model 300 Proprotor Cyclic Mode Natural Frequencies	VI-13
VI-3	Structural Model of Wing-Pylon System	VI-14
VI-4	Structural Models of Wing-Pylon-Fuselage System	VI-15
VI-5	Model 300 Airframe Natural Frequencies, Symmetric	VI-16
VI-6	Model 300 Airframe Natural Frequencies, Asymmetric	VI-16
VI-7	Analytical Model of Model 300 Drive System	VI-17
VI-8	Model 300 Drive System Natural Frequencies and Modes	VI-18
VI-9	Airplane Mode Flapping Envelope, Sea Level	VI-19
VI-10	Airplane Mode Flapping Envelope, 20,000 Feet	VI-20
VI-11	Model 300 Blade Flapping Modes, Root Variation with Airspeed	VI-21
VI-12	Model 300 Proprotor Coupled Flapping and Inplane Bending Modes, Root Variation with Airspeed	VI-22

ILLUSTRATIONS - Continued

<u>Figure</u>		<u>Page</u>
VI-13	Model 300 Cantilevered Wing, Root Variation with Airspeed	VI-23
VI-14	Model 300 Symmetric Modes, Root Variation with Airspeed	VI-24
VI-15	Model 300 Asymmetric Modes, Root Variation with Airspeed	VI-25
VI-16	Model 300 Airplane Mode Stability Boundary Versus Proprotor RPM, Symmetric Modes	VI-26
VI-17	Model 300 Airplane Mode Stability Boundary Versus RPM, Asymmetric Free-Free Modes	VI-27
VI-18	Model 300 Airplane Mode Stability Boundary Versus Altitude, Symmetric Modes	VI-28
VI-19	Model 300 Airplane Mode Stability Boundary Versus Altitude, Asymmetric Modes	VI-29
VI-20	Model 300 Conversion Mode Stability Boundary Versus Altitude, Symmetric Modes	VI-30
VI-21	Model 300 Conversion Mode Stability Boundary Versus Altitude, Asymmetric Modes	VI-
VI-22	Model 300 Dynamic Stability Margin in Airplane Mode	VI-32
VI-23	Effect of Loss of Wing Torsional Stiffness on Stability Boundary	VI-33
VI-24	Cabin Vibration Level Versus Conversion Angle and Airspeed	VI-34
VI-25	Crew Station Vibration Level Versus Conversion Angle and Airspeed	VI-35
VI-26	Pylon Vibration Level Versus Conversion Angle and Airspeed	VI-36
VI-27	Procedure for Calculating Response to Atmospheric Turbulence	VI-37
VI-28	Model 300 Frequency Response to Unit Sinusoidal Gust Field	VI-38

ILLUSTRATIONS - Continued

<u>Figure</u>		<u>Page</u>
VI-29	Turbulence Field Power Spectral Density (Von Karman Type)	VI-39
VI-30	Model 300 Center of Gravity Acceleration Response Spectral Density	VI-40
VI-31	Model 300 Crew Station RMS Acceleration Response to One Foot Per Second RMS Turbulence	VI-41
VI-32	Model 300 Center of Gravity RMS Acceleration Response to One Foot Per Second RMS Turbulence	VI-42
VI-33	Model 300 RMS Lateral Acceleration Response to One Foot Per Second RMS Lateral Turbulence	VI-43
VI-34	Model 300 Proprotor Contribution to Acceleration Response to Turbulence, Crew Station RMS	VI-44
VI-35	Wing Elasticity Contribution to Model 300 Acceleration Response to Turbulence	VI-45
VI-36	Comparison of Acceleration Response of Model 300 and a CTOL Airplane (Beech 99) to Turbulence	VI-46
VII-1	Model 300 Conversion Angle and Stick Position Versus Airspeed, Aft Center of Gravity	VII-6
VII-2	Model 300 Conversion Angle and Stick Position Versus Airspeed, Forward Center of Gravity	VII-7
VII-3	Model 300 Hover Control Power and Damping, SCAS-Off	VII-8
VII-4	Model 300 Damping Comparison with Other Aircraft and MIL-H-8501A, VHF Requirements	VII-9
VII-5	Model 300 Control Power Versus Airspeed	VII-10
VII-6	Model 300 Roll Performance Versus Airspeed, SCAS Off	VII-11

ILLUSTRATIONS - Concluded

<u>Figure</u>		<u>Page</u>
VII-7	Model 300 Conversion Corridor	VII-12
VII-8	Model 300 Short Period Characteristics - Airplane Mode	VII-13
VII-9	Model 300 Longitudinal Short Period Frequency Characteristics, Airplane Mode	VII-14
VII-10	Model 300 Dutch Roll Characteristics - Airplane Mode	VII-15
VIII-1	Comparison of Model 300 Proprotor and Conventional Rotor Noise Levels Measured in Ames 40- by 80-Foot Wind Tunnel	VIII-4
VIII-2	Comparison of Calculated and Measured Proprotor Noise-Hover	VIII-5
VIII-3	Comparison of Calculated and Measured Proprotor Noise-80 Knots	VIII-6
VIII-4	Model 300 External Noise as a Function of Mode of Operation	VIII-7
VIII-5	Take Off and Approach Profiles	VIII-8
VIII-6	Model 300 Noise Exposure Footprints	VIII-9
VIII-7	Model 300 Noise-Time Histories for Various Modes of Operation	VIII-10
VIII-8	Comparison of Noise of Model 300 and Other Modes of Transportation	VIII-11

I. SUMMARY

A tilt-proprotor research aircraft design study has been performed under Task II of the NASA V/STOL Tilt-Rotor Aircraft Study, Contract NAS2-6599. The research aircraft, the Bell Model 300, is well suited for NASA proof-of-concept flight research investigations to establish the technology base needed for the confident design of operational aircraft.

The Model 300 (Figure I-1) is a twin-engine, high-wing aircraft with 25-foot three-bladed proprotors mounted on pylons at the wing tips. Each pylon houses a Pratt and Whitney PT6C-40(VX) engine with a 30-minute rating of 1150 horsepower. Empty weight is 7390 pounds. The normal gross weight for VTOL is 12,400 pounds and the STOL gross weight is 15,000 pounds.

The maximum level flight speed of the Model 300 is 312 knots. The aircraft can hover out of ground effect at 4600 feet on a standard day at normal gross weight. At a typical flight test weight of 10,700 pounds, it can hover at 4000 feet on a 95°F day.

Technology development, component detail design, and development of dynamic components for the Model 300 research aircraft have been underway since 1968 as part of Bell Helicopter Company's Independent Research and Development Program and by means of Government-sponsored model and full-scale wind-tunnel test programs.

The approach to the design study consisted of updating and extending the design study of a tilt-proprotor proof-of-concept aircraft performed for NASA in 1969, Reference 1. Bases for updating the original design study include information resulting from: (1) having completed one-half of the aircraft detail design, (2) fabrication of the dynamic components which account for approximately one-third of the aircraft empty weight, (3) two full-scale wind-tunnel tests of the 25-foot proprotor completed in 1970 in the NASA-Ames large-scale tunnel (an Army/NASA program, Reference 2), and (4) one-fifth scale aeroelastic tests in 1970 and one-fifth scale aerodynamic tests of the complete aircraft in 1971 conducted in the NASA-Langley Transonic-Dynamics Tunnel in joint NASA/Bell programs.

Section II presents the aircraft's capability to perform the needed flight research investigations. Subsequent sections describe the aircraft and present the results of weight, performance, dynamics, stability and control, and noise analyses.

The Model 300 can perform the needed flight research investigation which will enable the aeronautical community to proceed with confidence on the design and development of useful tilt-rotor aircraft.

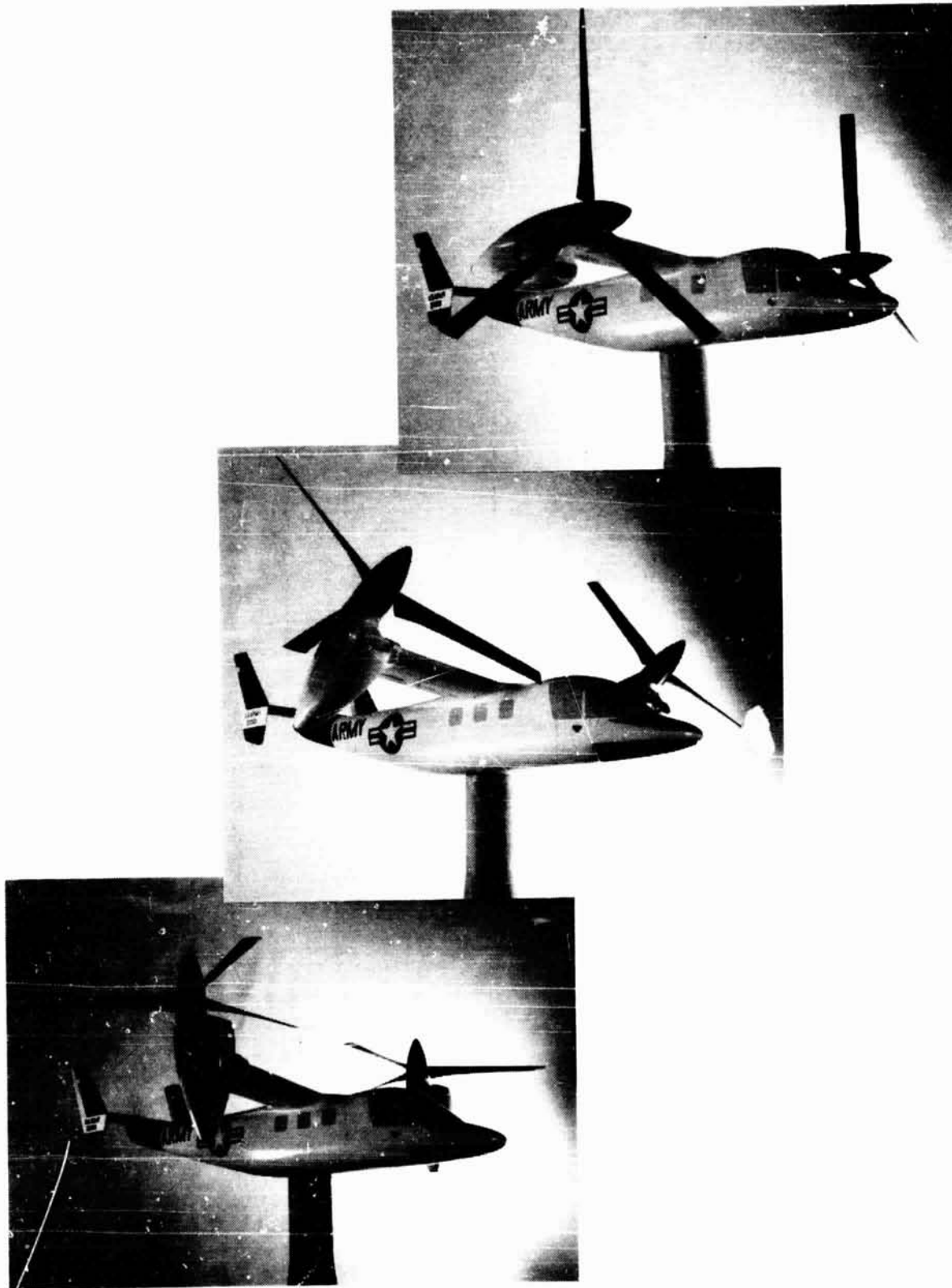


Figure I-1. Model 300 Research Aircraft.

II. RESEARCH FLIGHT INVESTIGATIONS

A. IDENTIFICATION OF NEEDED FLIGHT INVESTIGATIONS

1. Objective

Flight investigations with a tilt-proprotor aircraft are needed to (1) establish the viability of the concept to perform military and commercial missions, (2) establish a technology base for the confident design of such aircraft, and (3) provide the potential user, regulating agency, and the community and military planner with the factual information required for the introduction of such aircraft into transportation systems.

NASA can accomplish these objectives in a research aircraft program. Flight research would evaluate proprotor/pylon dynamic stability, short-period aircraft stability, low-speed handling characteristics in and out of ground effect, proprotor propulsive efficiency, proprotor flapping in gusts and maneuvers, steep descent and approach capability, gust sensitivity and riding qualities, downwash and ingestion, noise, and pollution.

a. Proof of Concept

The foremost need for a research aircraft flight investigation is to verify that the tilt-proprotor aircraft has the characteristics to make it suitable to fill the role of a productive civil and/or military VTOL aircraft. The range of speed, size, and hovering characteristics, wherein the tilt-proprotor offers advantages over other concepts for V/STOL, is lacking. Actual flight research is needed on an aircraft operating in the speed ranges projected, and the gathering of comparable flight data on handling qualities, maneuverability, aerodynamic efficiency, noise, and ride quality. Furthermore, analysis based on flight experience is needed to show the degree to which cost factors such as mechanical complexity and structural and aerodynamic refinement might be increased in raising these qualities to various levels. Then cost effectiveness studies and operations analysis can show meaningful results for use by civil and military program planners. Only when a confirmed potential advantage is thus found will there be incentive to use this concept.

b. Technology Base

Flight research is needed to establish a technology base which will enable the aeronautical community to proceed with confidence on the design of useful tilt-proprotor aircraft. Specific areas of needed research for the confident design of the conceptual aircraft were assessed in Task I of this study, Volume I. The conceptual design aircraft is typical of a first-generation tilt-proprotor aircraft which could be operational in the 1980-85 time frame. Its design and development will require that technology

be available in 1975. Flight research is needed to provide a sound basis for this technology.

Thus far, the tilt-proprotor concept has had flight experience only at low speeds (up to 160 knots) with piston engine power. Tunnel testing of scale models has revealed problems and produced various solutions. Realistically, we might expect that operation at higher speeds, greater (turbine) power, and with various structural and aerodynamic arrangements may reveal new problems, or at least added constraints, in the application of design techniques developed thus far for the type.

The NASA-Ames full-scale 25-foot proprotor tests, Reference 2, have shown that technology is adequate for the design of such an aircraft, but actual flight-test verification is needed. In particular, the total aircraft design solution used for the Bell D302 conceptual aircraft and the Bell Model 300 research aircraft designs needs flight verification. Thorough flight-test documentation is needed in all of the technical disciplines: aerodynamics, structures, dynamics, aeroelasticity, and stability and control.

Known problem areas such as coupled proprotor/pylon/wing dynamic stability, short-period aircraft stability, proprotor propulsive efficiency, proprotor flapping in gusts and maneuvers, and oscillatory loads and vibration should receive special attention. However, even more important than these is the need to define any unknown problems and the technology required for their solution.

c. Operation and Regulation Certification Criteria

Agencies which will be planning transportation systems and certifying and regulating the aircraft, potential operators, and communities that must accept and accommodate the new VTOL aircraft will all need factual information on its specific flight and environmental characteristics, and its impact on ecology. Examples of the information they will need are:

Handling characteristics during hover in and out of ground effect, conversion, and cruise

- Steep descent and approach characteristics
- Emergency procedures (autorotation, etc.)
- Real estate required for V/STOL ports
- Maneuver capability
- Design load factors
- Riding qualities (gust sensitivity)

- Vibration levels
- Steady and oscillatory proprotor loads
- Noise
- Pollution
- Downwash and ingestion
- Single engine and STOL capability
- Mission suitability and performance
- Flight limitations
- Operating flexibility and flight procedures

2. Flight Investigations

NASA flight research investigations needed to meet the above objectives for proof of concept, establishment of a technology base, and for operation regulation and certification criteria are outlined below. This outline and discussion lumps the tests for each of the objectives together as if it were all to be done in one big program. However, the research flight tests would probably be conducted as several separate programs spanning over several years. The first program might be a coarse coverage of most of the areas of interest with subsequent test programs directed at detailed quantitative results in specific areas.

For convenience of presentation, the needed flight investigations are discussed in groupings relating to aircraft configuration and speed.

The Model 300 research aircraft has the capability for performing flight research in all of the areas of investigation. Its capabilities and limitations to perform these investigations are discussed later in following subsections.

a. Helicopter Low-Speed Flight (0-40 Knots)

(1) Performance

Measure hover power required as a function of height above the ground and gross weight to air density ratio and determine the flap setting to minimize wing down load.

(2) Handling Qualities

Evaluate rotor/wing/ground interference effects on roll stability at various heights in and out of ground effect with different flap settings and with SCAS (stability and control augmentation system) on and off.

Perform precision hover and other tasks in calm and gusty air to determine control power and damping requirements in pitch, roll, and yaw.

Investigate trim and transient characteristics in forward, side-ward, and rearward flight for speeds up to 40 knots and determine the effects of conversion angle (from 75 to 95 degrees), center of gravity, and flap settings.

(3) Environmental Effects

Measure vibration and internal and sideline noise in hover as a function of aircraft heading, disc loadings ranging from 9 to 15 pounds per square foot, and tip speeds varying from 600 to 800 feet per second.

Evaluate downwash effects at various hover heights on dust and spray recirculation and crew visibility, and measure flow profiles around the aircraft to define the environment for ground personnel as a function of disc loading.

Measure inlet temperature rise to determine heat ingestion as a function of height and aircraft heading to wind.

(4) Operational Characteristics

Explore different pilot techniques for slowing down, flaring, and landing, and determine pilot work load for steady flight when operating on the back side of the power curve, in and out of ground effect.

Conduct simulations of picking up a rescuee with a hoist over land and over water. Determine approach profile to minimize dust or spray for such operations.

Determine transient and steady-state maneuver requirements (g capability) in hover and slow-speed maneuvers. Simulate operation at these minimum levels by operating in these maneuvers with rotor speed reduced to limit maximum thrust available.

b. Helicopter Forward Flight (40-100 Knots)

(1) Performance

Measure power required versus airspeed as a function of gross weight to air-density ratio, conversion angle, and flap setting. Determine rate of climb and service ceiling as a function of air-speed and conversion angle.

(2) Flight Handling Qualities

Determine the longitudinal control effects due to the rotor's downwash on the horizontal tail. Measure fore and aft stick position versus yaw angle at several airspeeds.

Measure stick position stability and stick-fixed and free dynamic stability as a function of airspeed, conversion angle, and aircraft center of gravity.

Evaluate yaw control required for coordinated maneuvers as a function of airspeed.

Evaluate control characteristics SCAS on and off and establish control power and damping requirements in pitch, roll, and yaw.

(3) Environmental Effects

Measure flyover and sideline noise for a range of disc loadings from 9 to 15 pounds per square foot and tip speeds from 600 to 800 feet per second.

Measure internal noise and vibration for all flight conditions.

(4) Operational Characteristics

Define boundaries for maximum climb and partial power and autorotative descent angles as limited by buffeting from positive and/or negative wing stall, uncomfortable attitude, visibility, etc.

Simulate IFR work tasks and approach conditions to determine usable ranges of glide slope, speed, and conversion angle for commercial operations.

Evaluate maneuverability as a function of airspeed and conversion angle, and establish steady-state and transient maneuver requirements (g capability).

Evaluate different departure and approach operating techniques and profiles to minimize flyover and sideline noise levels.

c. Helicopter High-Speed Flight (100-140 Knots)

(1) Performance

Determine maximum level flight speed versus conversion angle and flap setting as limited by power available.

(2) Controllability

Determine maximum flight speed versus conversion angle, flap setting, and power as limited by longitudinal control.

(3) Dynamic Loads

Determine maximum flight speed versus conversion angle, flap setting, and power as limited by oscillatory loads on proprotor and pylon and/or vibration level in the cockpit.

(4) Maneuverability

Evaluate retreating blade stall in maneuvers at maximum speed as limited by controllability, oscillatory loads, and vibration.

d. Conversion Flight (80-170 Knots)

(1) Performance

Determine conversion envelope as a function of altitude, temperature, and gross weight to air-density ratio as limited by power available.

(2) Flight Handling Qualities

Determine conversion envelope as limited by wing stall and/or controllability.

Evaluate roll control power as a function of conversion angle and airspeed and proximity to stall.

Conduct maneuvers at various conversion angles and establish the desired level of control power and damping for pitch, roll, and yaw.

(3) Dynamic Loads

Determine conversion corridor as limited by stall buffet, rotor induced vibration, and/or oscillatory rotor loads.

(4) Maneuverability

Evaluate maneuverability as a function of airspeed and conversion angle, and establish steady state and transient maneuver requirements (g capability).

(5) Environmental Effects

Measure vibration, internal noise, and flyover noise as a function of conversion angle and airspeed in level flight, climb, and approaches.

(6) Operational Characteristics

Determine the most practical data presentation (such as aircraft angle of attack) for the boundaries of the conversion envelope to enable a pilot to stay within the conversion corridor without the need for monitoring airspeed, power, altitude, and gross weight during conversion.

Evaluate the ability to convert and reconvert while accelerating or decelerating, climbing, turning, or letting down.

Conduct simulated IFR flight to determine work load during conversion while enroute, on approach, etc.

e. Airplane Flight (140-300 Knots)

(1) Performance

Determine rate of climb, service ceiling, specific range, and maximum power limit speed as a function of gross weight at the normal cruise tip speed.

Measure power required to obtain a qualitative indication of propulsive efficiency as a function of tip speed from 400 to 700 feet per second throughout the airspeed range.

(2) Flight Handling Qualities

Measure roll control performance at low airspeed, flaps up and down, and establish roll control power requirements.

Measure control stick and pedal force characteristics in trim flight and in maneuvering flight.

Evaluate the effect of altitude and airspeed on short-period longitudinal stability and Dutch roll stability.

Determine, if any, the effect of having a highly damped spiral mode.

(3) Aeroelastic Stability

By the use of inflight shakers, measure the frequency and damping of major prop rotor, airframe, and empennage modes as a function of airspeed and altitude.

(4) Rotor Behavior

Measure flapping amplitude and oscillatory blade loading in cruise and maneuvers.

(5) Riding Qualities

Evaluate vertical, lateral, and fore and aft response characteristics in turbulence and determine what level of alleviation, if any, should be required for this type of aircraft.

(6) Environmental Effects

Measure vibration and flyover and internal noise levels as a function of power and airspeed.

f. Dive Flight (300 to 360 Knots)

Evaluate the effects of compressibility on propulsive efficiency, rotor behavior, and aeroelastic stability by progressively increasing dive speed until some limit is reached for tip speeds ranging from 500 to 700 feet per second.

g. STOL Takeoff

(1) Takeoff Distance

Measure takeoff distance as a function of conversion angle (from 70 to 90 degrees, flap setting, gross weight, and altitude.

(2) Maneuver Capability

Evaluate maneuver capability and flight-handling qualities to establish criteria for levels of g capability and control power for STOL operation.

(3) Environmental Effects

Measure sideline noise exposure as a function of gross weight.

(4) Operating Characteristics

Determine combination of conversion angle, lift-off speed, and flap setting which will provide adequate safety and maneuverability for the full STOL gross weight and altitude capability of the aircraft.

h. Emergency Conditions

(1) Performance

Determine single-engine rate of climb, service ceiling, and minimum speeds for helicopter, conversion, and airplane flight. Measure power off rate of sink versus airspeed, conversion angle, flap setting, and rpm as a function of gross weight and altitude.

(2) Operational Procedures

Define takeoff profiles and operating gross weight/altitude envelopes that will permit safe return to the takeoff point and/or proceeding to the cruise mode in the event of a single engine failure. Develop landing techniques for zero-speed touchdown on a single engine. Establish flight techniques and define gross weight, altitude, and airspeed operating profiles that will permit safe entry from airplane windmilling flight into helicopter autorotational flight. Evaluate flare and touchdown techniques to determine the minimum safe touchdown speed as a function of altitude and propotor disc loading.

i. Mission Simulation

A demonstrated capability for tilt-propotor aircraft to perform useful missions is required for successful "proof-of-concept." This can be accomplished as part of NASA flight investigation with the research aircraft.

Demonstrate the level of ability of the aircraft to perform a variety of possible civil and military missions. Measure payload/lift capability, range, endurance, and fuel consumption. Fly specified flight profiles with simulated mission payloads. Conduct takeoff and landings from various terrain under a variety of atmospheric conditions. Evaluate approach and landing procedures and profiles to establish criteria and provide data for flight regulations and the design of terminal area navigation and traffic control systems, and layout of V/STOL ports.

B. CAPABILITY OF RESEARCH AIRCRAFT

The Model 300 tilt-propotor aircraft is suitable for performing the NASA research flight tests in all of the areas of flight investigation outlined previously. Specific capability for performing research flight tests is discussed in this section. Areas of needed investigation where the Model 300 has only limited capabilities are discussed in subsection C below.

1. Performance Capability

General performance of the aircraft is described in Section V of this report. In this section, performance capability of the aircraft is discussed and presented in a form which may be more useful to the flight research investigator.

a. Payload

Nearly all of the VTOL concepts researched to date with test aircraft have failed to demonstrate that they are viable solutions for potential VTOL missions. This result has been due primarily to the lack of a demonstratable vertical-lift payload capability. If positive conclusions are to be drawn from the program, it is essential that the tilt-propotor research aircraft successfully accomplish the role of a concept demonstrator as well as perform technology test tasks. The Model 300 research aircraft has the vertical-lift payload capability to demonstrate proof of concept. Figure II-1 shows the payload capability for simulating mission payloads and/or carrying test equipment. With a crew of two and full fuel on board, as much as 4500 pounds of payload can be lifted on an out-of-ground-effect hovering takeoff. With reduced fuel load, the aircraft can hover above 16,000 feet. At the STOL gross weight of 15,000 pounds, payloads up to 5500 pounds can be lifted with a running takeoff at elevations over 7000 feet. Figure II-1 also shows that even on hot days (95°F) there is substantial payload capability in the hover and STOL takeoff modes.

b. Endurance

Endurance of the aircraft with normal fuel load of 1600 pounds is more than adequate to gather considerable data on each test

flight. Figure II-2 shows the time available at a test point as a function of test airspeed, altitude, and aircraft mode. For instance, the Model 300 can hover for 1.6 hours, or cruise at 260 knots at 20,000 feet for 2.0 hours.

c. Test Envelope

The Model 300 has a large airspeed-altitude flight envelope available for flight research as shown in Figure II-3. The aircraft is designed for a cruise airspeed of 260 knots KEAS and a cruise Mach number of 0.50. Maximum level flight speed is 311 knots at 6000 feet.

d. Dive Profile

To explore characteristics which would limit the maximum airspeed of the concept, the aircraft can dive to investigate speeds beyond its level flight capability. The design dive speed is an equivalent airspeed of 300 knots up to a Mach number of 0.575. A dive profile is shown on Figure II-3 which would permit the Model 300 to operate with its proprotor deep into compressibility (where the total rotor torque available would be required to overcome profile power with little or no thrust). A stable test condition could be established for 20 seconds at a flight Mach number of 0.57 while passing through 14,000 to 12,000 feet altitude. A maximum true airspeed of 360 knots could be reached, recovery would be made above 10,000 feet, and the dive would be entered at approximately 18,000 feet with a dive angle of approximately 9 degrees. Conducting these dives while maintaining different tip speeds would permit evaluation of compressibility effects on the proprotor. This is discussed in more detail below.

2. Range of Parameter Variation

It is desirable to be able to evaluate aircraft characteristics as they are affected by some of the major design variables. Capability of the Model 300 to evaluate the effects of disc loading, wing loading, tip speed, proprotor inflow ratio, and proprotor Mach number is described below.

a. Disc Loading and Wing Loading

It is desirable to be able to evaluate the environmental effects of the proprotor hovering over various types of terrain and in a variety of simulated operational conditions. Since it is known that downwash effects and noise are related to disc loading, the research aircraft should be capable of evaluating the sensitivity of these effects to changes in design disc loading. Figure II-4 shows that by varying gross weight, disc loading of the Model 300 may be varied from 8.1 to 14.3 pounds per square foot for out-of-ground-effect hovering takeoff, or for a STOL takeoff, disc loading as high as 15.3 pounds can be flown with the Model 300.

Figure II-4 shows that wing loading may be varied from 44 to 83 pounds per square foot to evaluate its effects on STOL takeoff and landing performance, riding qualities in turbulence in the airplane mode, and handling qualities and performance in conversion and airplane modes of flight.

b. Tip Speed

Proprotor tip speed is an important operating and design parameter in the helicopter as well as the airplane modes of flight. In particular, noise generated in hover and the propulsive efficiency in cruise are closely related to tip speed. The test tip speed range available for hover is shown in Figure II-5. At the normal gross weight of 12,400 pounds, tip speed may be varied from 650 feet per second to 814 feet per second while maintaining an out-of-ground-effect hover at sea level on a standard day. By reducing gross weight, tip speeds as low as 525 feet per second may be tested in hover. This wide range of tip speeds is made available by overspeeding the proprotor up to its design overspeed limit, and by underspeeding the rotor and reducing gross weight as required to maintain a small thrust margin for maneuvering. While testing in the underspeed range, it may be necessary to avoid one-per-rev resonant conditions if the proprotors are not in good track and balance. The modes which could be excited by one per rev and three per rev are indicated in Figure II-5. In hover there should be little three-per-rev excitation and, with good track and balance, operation even in the shaded areas may be possible.

The tip speed range available for test in the airplane cruise mode of flight is shown in Figure II-6. A range from 400 to 700 feet per second is available by overspeeding and underspeeding the rotor. The upper limit of 700 feet per second is the maximum tip speed which can be governed by the proprotor governor. The design cruise tip-speed range of the Model 300 is from 540 to 660 feet per second. Within this tip speed range there is the first asymmetric wing beam and wing chord modes which could be excited by one per rev out-of-balance and out-of-track. However, experience with the 25-foot proprotor in the NASA-Ames tunnel and with the one-fifth-scale aeroelastic model indicates that vibration from these modes is insignificant and should not cause a test limitation for the aircraft. Outside of the design overspeed-underspeed range but within the 400 to 700 feet-per-second range, there are several modes which can be excited strongly and must be avoided. These are indicated by the shaded areas on Figure II-6. It should be practical to test in the range from 400 to 475 feet per second and from 675 to 700 feet per second in addition to the range from 540 to 660 feet per second.

c. Proprotor Cruise Aerodynamic Conditions

Testing over a range of tip speeds in cruise, as described above, is needed for a complete evaluation of blade flapping behavior.

and dynamic stability, as well as cruise propulsive efficiency. Propulsive efficiency is basic to a broad evaluation of the concept as it relates to the economics of how the aircraft can perform a mission in comparison to other aircraft or vehicles. Proprotor blade compressibility effects are detrimental to high propulsive efficiency. The usable flight speed range of the proprotor concept is therefore limited at the upper end by flight Mach number. Figure II-7 shows the proprotor inflow and blade Mach number range for several test conditions of the Model 300 aircraft and compares these with the D302 conceptual aircraft defined in Task I of this study, Volume I. Mach number along the span of the proprotor blade varies from the flight Mach number, M_0 , at the centerline to the Mach number at the tip of the blade, M_{tip} , Mac helical.

The highest cruise tip Mach number and inflow ratio of the Model D302 aircraft occur at its maximum cruise speed of 354 knots at 23,000 feet. Tip Mach number is 0.77 and inflow ratio is 1.15. At this altitude and at normal gross weight, the Model 300 can test at speeds up to 280 knots in level flight. With the normal cruise tip speed of 600 feet per second, tip Mach number is 0.75, and λ equals 0.79. Inflow ratio can be increased to λ equal to 1.265 by operating the Model 300 proprotors at a tip speed of 400 feet per second and tip Mach number to 0.82 by operating at 700 feet per second.

Higher tip Mach numbers and inflow ratios can be reached by diving the Model 300. Tip Mach number is 0.79 at 360 knots and 12,000 feet with a tip speed of 600 feet per second. By overspeeding to a tip speed of 700 feet per second, tip Mach number is increased to 0.87.

3. Ability to Test Other Proprotor Configurations

The semi-rigid gimbal-mounted proprotor is basic to the total design solution of the Model 300 aircraft. However, this does not necessarily mean that other proprotor configurations could not be tested on the Model 300 aircraft. This possibility was examined very briefly for the soft-inplane proprotor.

The inplane stiffness of the Model 300 proprotor was decreased to 0.65 per rev and the flapping natural frequency tuned to 1.2 per rev. The stability of the symmetric free-free modes was calculated for airplane flight. Figure II-8 is a root locus of this configuration at 458 rpm. Figure II-9 shows the stability boundary as a function of rpm. Above 410 rpm, the short-period flight mode is the first mode to become unstable; below 410 rpm, a coupled flapping--inplane bending mode becomes unstable. A small region of air resonance (mechanical instability) is predicted at low airspeeds. The high speed boundary is satisfactory and the low-speed air resonance is well below the minimum flying speed in airplane mode.

These results are encouraging, but from such an over-simplification of the problem, no firm conclusion can be reached. An exact representation of blade inertia and stiffness, in particular blade torsional characteristics which are typical of soft-inplane rotor configurations, must be included in the analysis. Also, the characteristics of the automatic proprotor control system, which may be essential to minimize blade loads of a soft inplane rotor during flight in turbulence and maneuvers, must also be included in the evaluation. A careful evaluation of the air/ground resonance in helicopter and conversion mode would of course have to be made.

The ability to test other proprotor configurations can only be determined after thorough analysis of each configuration in all flight modes. This is beyond the scope of the present study.

4. Applicability of Results

The NASA research flight investigations will produce technology that is applicable to the largest tilt-proprotor aircraft envisioned at this time. In many areas of investigation, the test data itself will be scaleable to larger sizes. However, the important thing is not that the test data be directly applicable, but that the NASA research will provide the know-how (technology) for the confident development of useful operational aircraft.

Technology and data obtained with the Model 300 research aircraft is, however, directly scaleable to the design of the military and/or commercial tilt-rotor V/STOL aircraft defined in Task I of this study, Volume I, because the technical approach to the total aircraft design solution for the Model 300 research aircraft is identical with the design solution for the Bell D302 conceptual aircraft. This design solution is also applicable to other aircraft designed to be operational in the 1980-1985 time frame.

Comparison of several of the technical design aspects of the Model 300 and the D302 are made in Figures II-10 and II-11 to illustrate that data and technology from the research flight investigations will be applicable to the design of operational aircraft.

Figure II-10 compares the relative location of the blade natural frequencies to the exciting frequencies for the proprotor of the Model 300 research aircraft and the D302 conceptual design. Figure II-11 compares the coupled proprotor/pylon/wing/flight modes of the two aircraft. It is seen that on a nondimensional basis, i.e., in terms of per rev, relative location of natural frequencies is basically the same for the two aircraft. Not only in the area of dynamics, but also in other areas, the technical design of the Model 300 is similar to the D302 and representative of tilt-proprotor aircraft that could be operational in the 1980-85 time frame.

C. LIMITATION OF RESEARCH AIRCRAFT

The Model 300 research aircraft is well suited for NASA flight investigations to accomplish the objectives of proof of concept, establish a technology base, and provide operation regulations and certification criteria. There are limits, however, to what a given aircraft can do. These limits for the research aircraft, as they relate to the objectives of the research flight investigation, are discussed below.

1. Technical Characteristics

The Model 300 can very adequately provide flight results to establish the technology base for operational aircraft. This technology will be applicable to the largest transport aircraft that are envisioned at this time. However, for missions requiring dash speeds of 400 knots or more, research emphasis should be placed on evaluating prop rotor compressibility effects. As discussed in Section II.B.2 above, some data of this type can be obtained with the Model 300. The aircraft can dive to flight Mach numbers of 0.57.

The addition of auxiliary jet engines to the aircraft would eliminate the need for diving and would make the aircraft better suited for compressibility testing. With jet engines, the Model 300 would be capable of evaluating prop rotors designed to operate at speeds of 400 knots and above.

2. Operational Characteristics

The research aircraft is limited in some areas to the extent it can explore and define the operational characteristics of the concept. This is a result of the lack of operational systems and equipment in the research aircraft and its small size. Installation of additional equipment can minimize some of these limitations. Limitations with respect to size and equipment are discussed below.

The Model 300 research aircraft has the aerodynamic capability to evaluate the STOL performance of the tilt-prop rotor concept. Except for the landing gear, the structure is adequate to meet FAA requirements up to gross weights of 15,000 pounds. The main landing gear oleo used on the Model 300 is from an executive turboprop airplane and is good for a design landing weight of 9500 pounds. The limit sink speed would be reduced to 80 percent at 15,000 pounds gross weight. Run-on landings would have to be limited to smooth runways under steady wind conditions. This limitation could be eliminated by fitting the aircraft with a new landing gear or attaching a fixed landing gear that was designed for higher gross weights and rough terrain.

The Model 300 is not equipped with a hoist which would be desirable for evaluating the rescue characteristics over water, forests,

etc. A personnel hoist could be fitted to the aircraft which would eliminate this limitation.

Use of the research aircraft to define terminal area and enroute navigation and traffic control requirements and criteria will be limited. A thorough treatment of this area of investigation requires an automatic flight control system that is tied into a variety of navigational aids with appropriate cockpit displays. The Model 300 research aircraft could carry the weight of the needed equipment, but space on the instrument panel and control consoles is limited. To determine whether or not the needed equipment and displays can be fitted into the aircraft would require selection of equipment and a detailed cockpit design layout study. This is beyond the scope of the present study.

It must be recognized that certain ground and flight operational characteristics as well as environmental effects will be affected by size of the aircraft. However, if proper scaling is used to account for size effects, operational characteristics of the research aircraft can be extrapolated to operational aircraft.

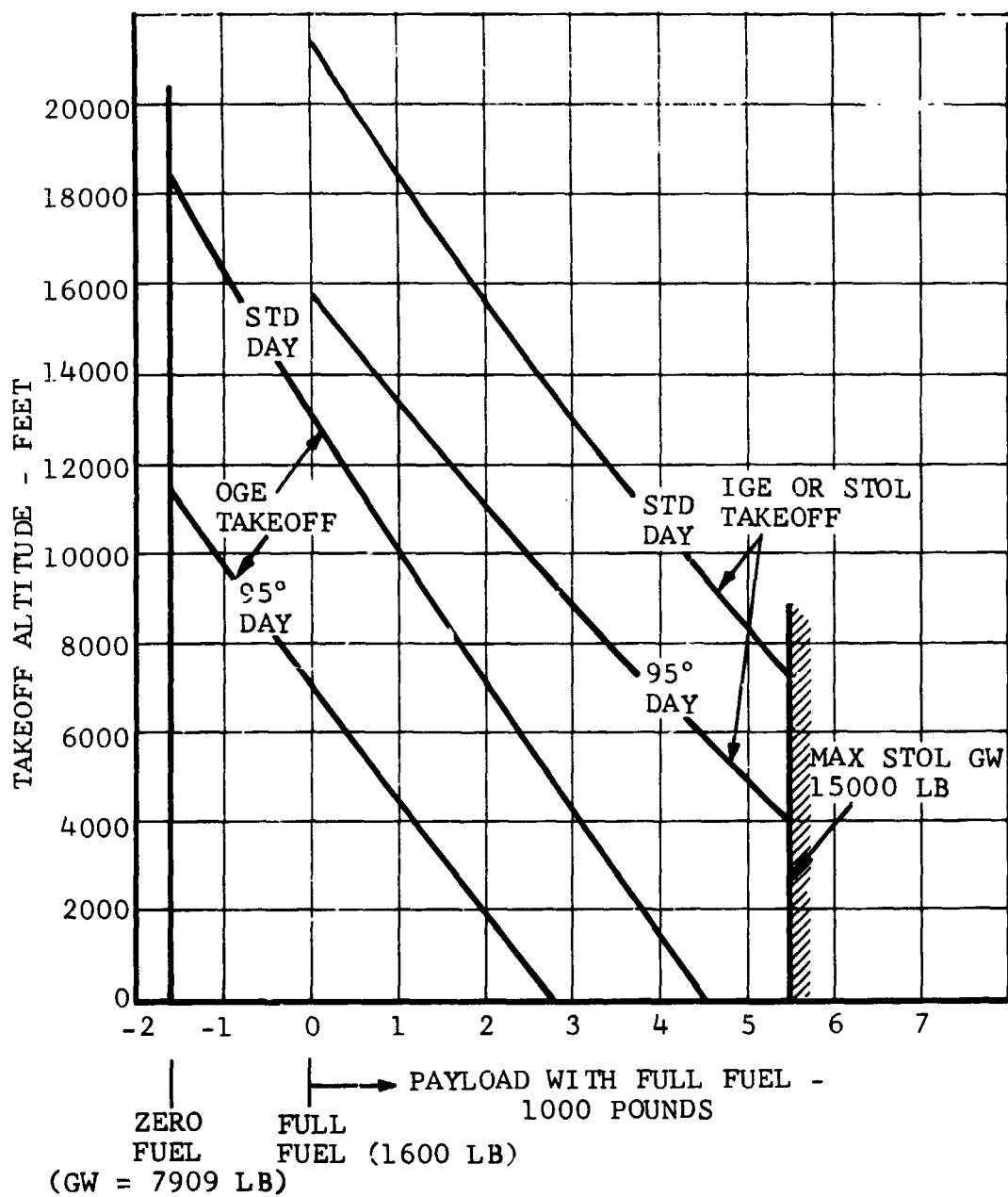


Figure II-1. Model 300 Payload Capacity for Test Equipment and/or Mission Simulation Versus Takeoff Altitude.

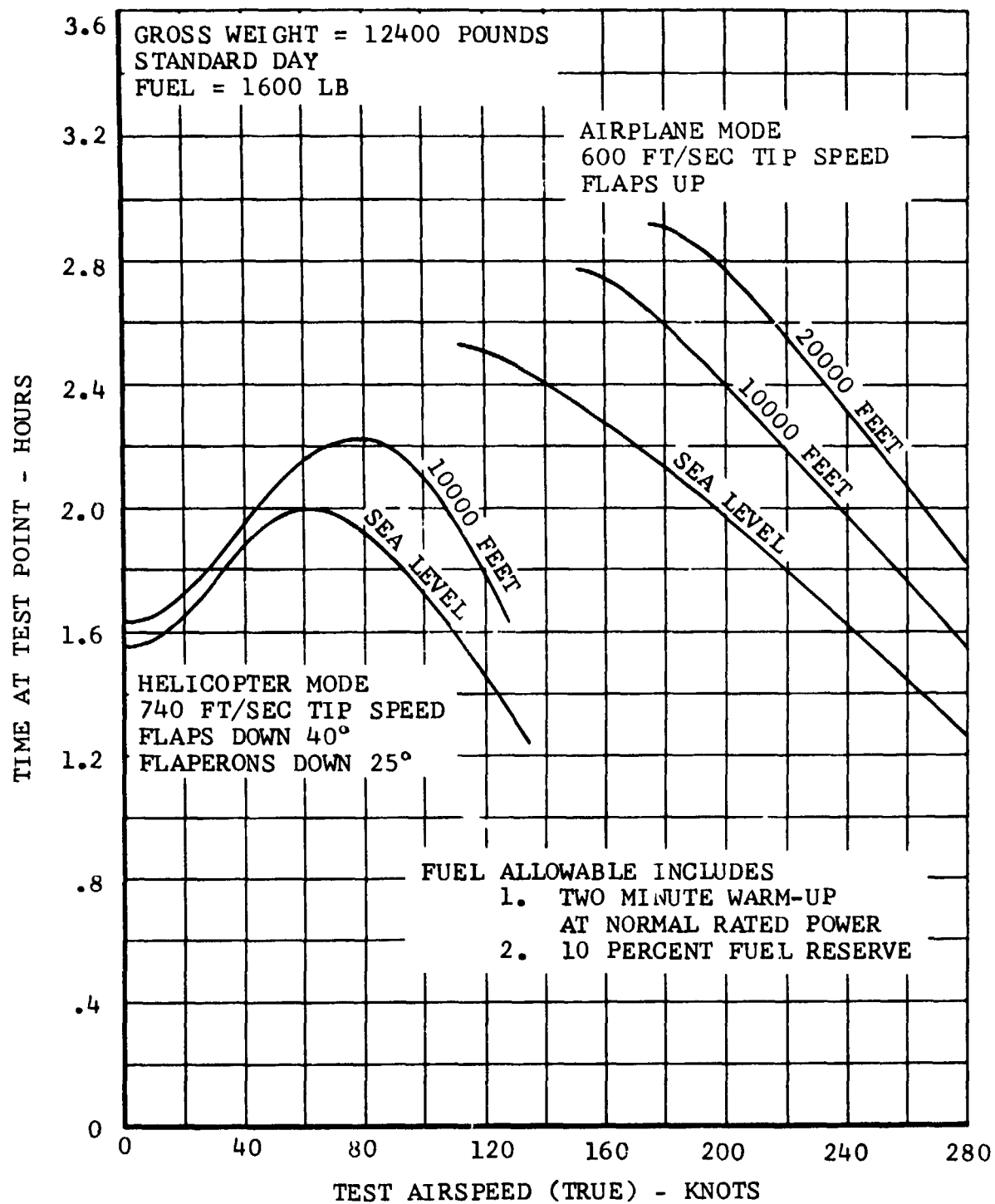


Figure II-2. Model 300 Flight Test Endurance.

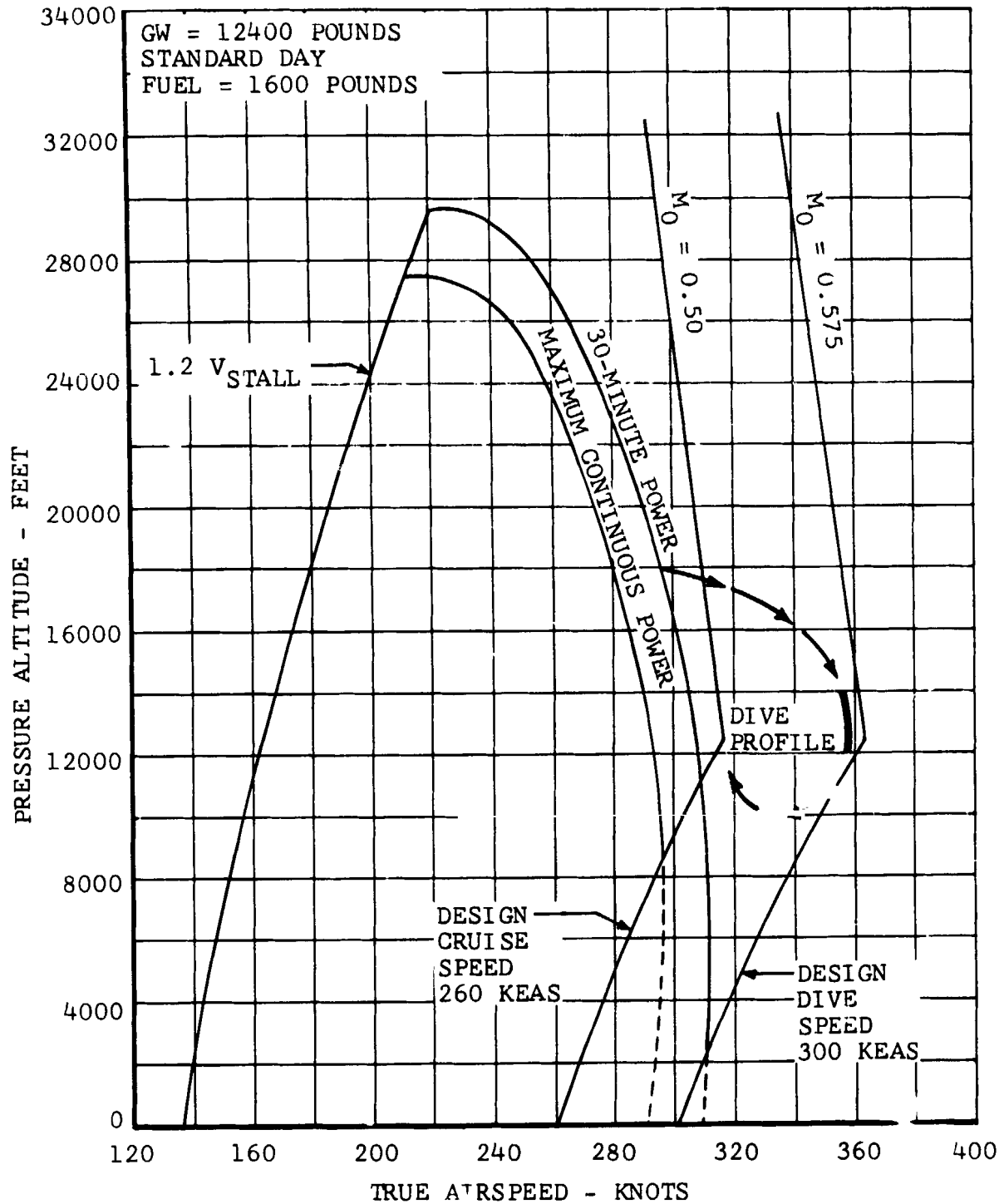


Figure II-3. Model 300 Flight-Test Envelope and Dive Profile.

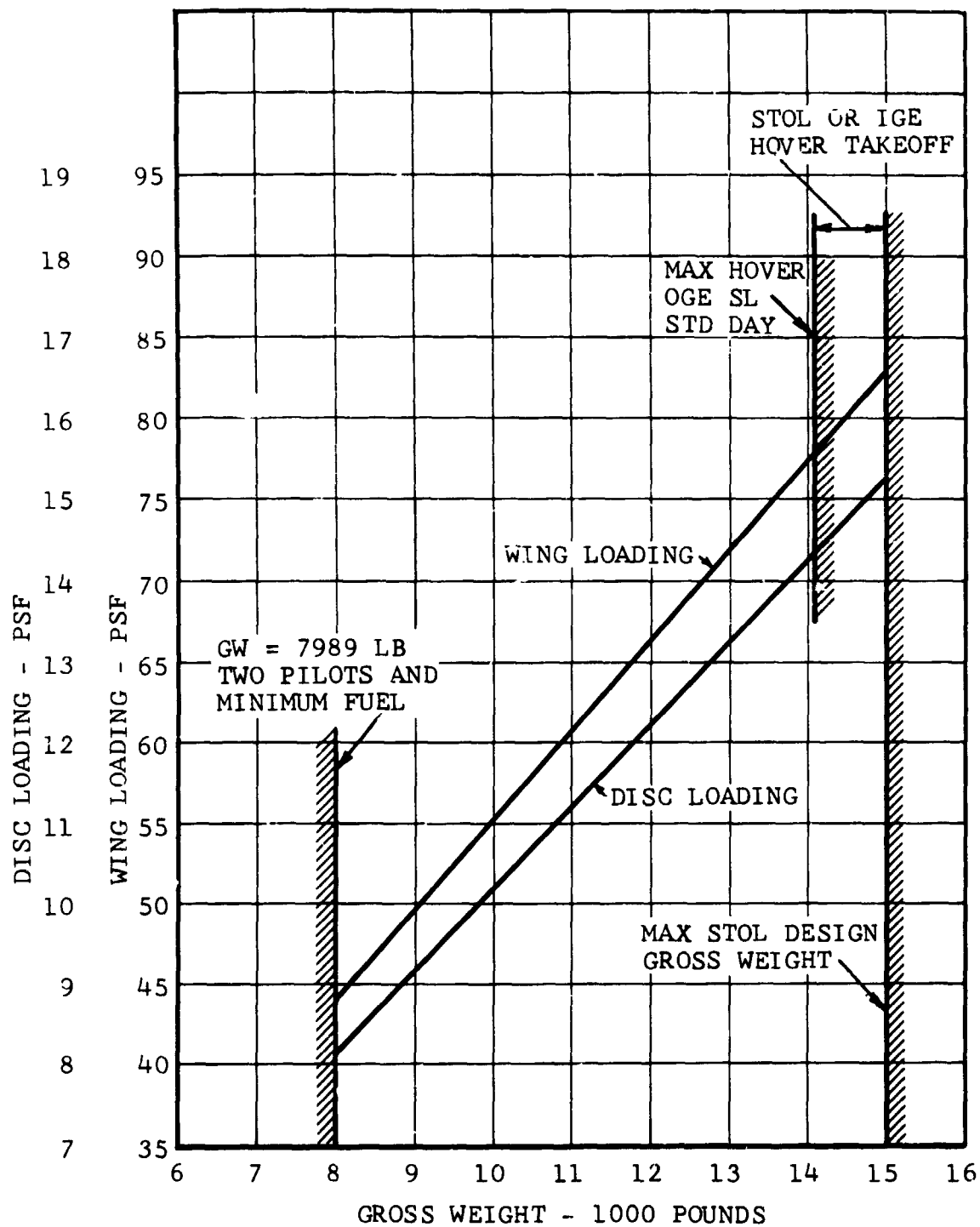


Figure II-4. Model 300 Test Range of Disc Loading and Wing Loading.

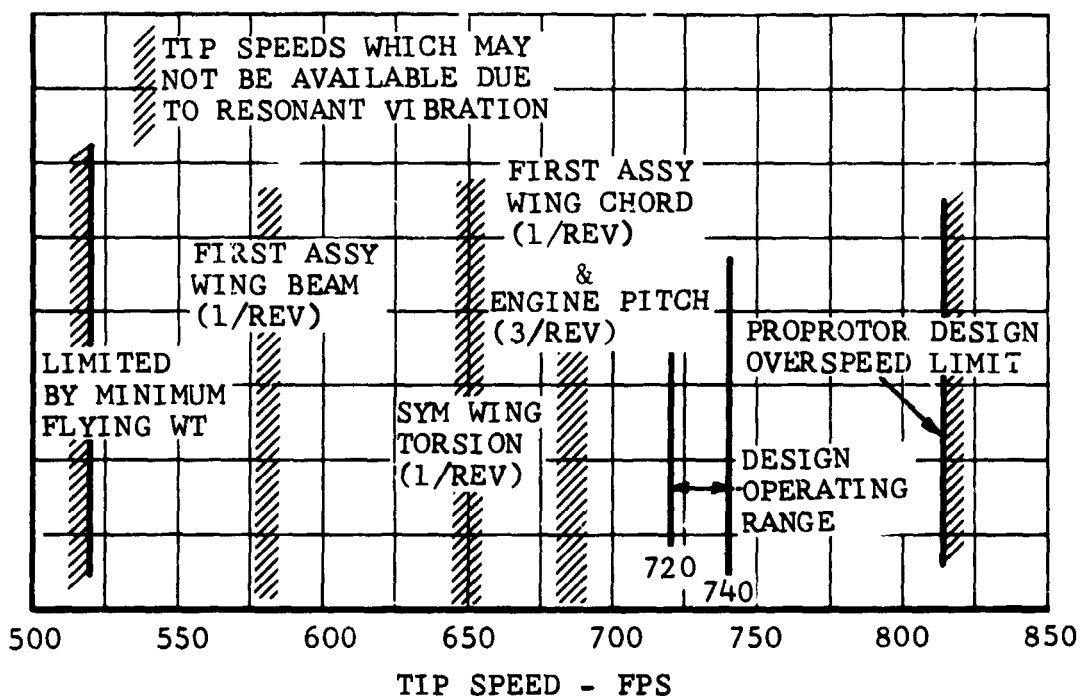
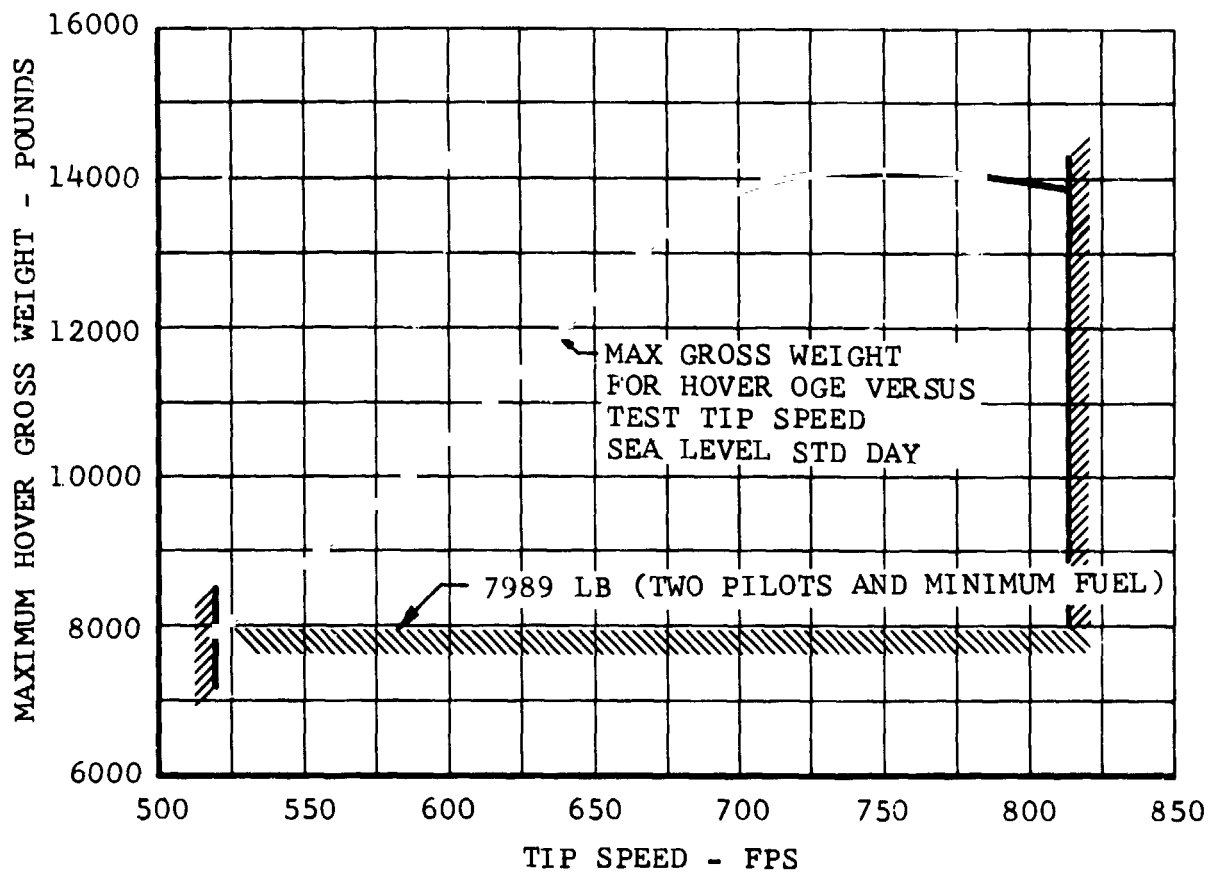


Figure II-5. Model 300 Test Tip Speed and Gross Weight Range for Hover.

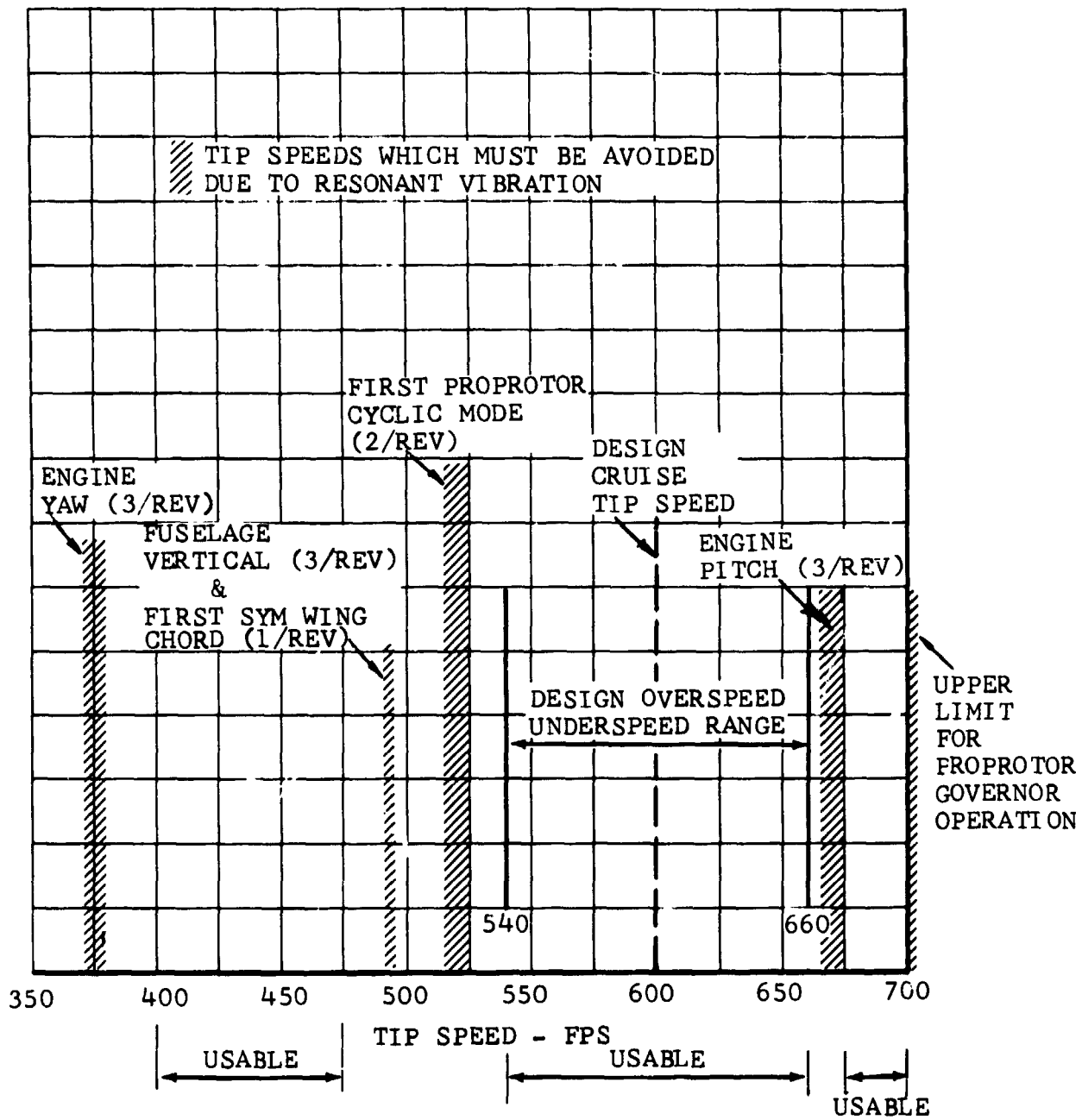


Figure II-6. Model 300 Test Tip Speed Range for Airplane Cruise.

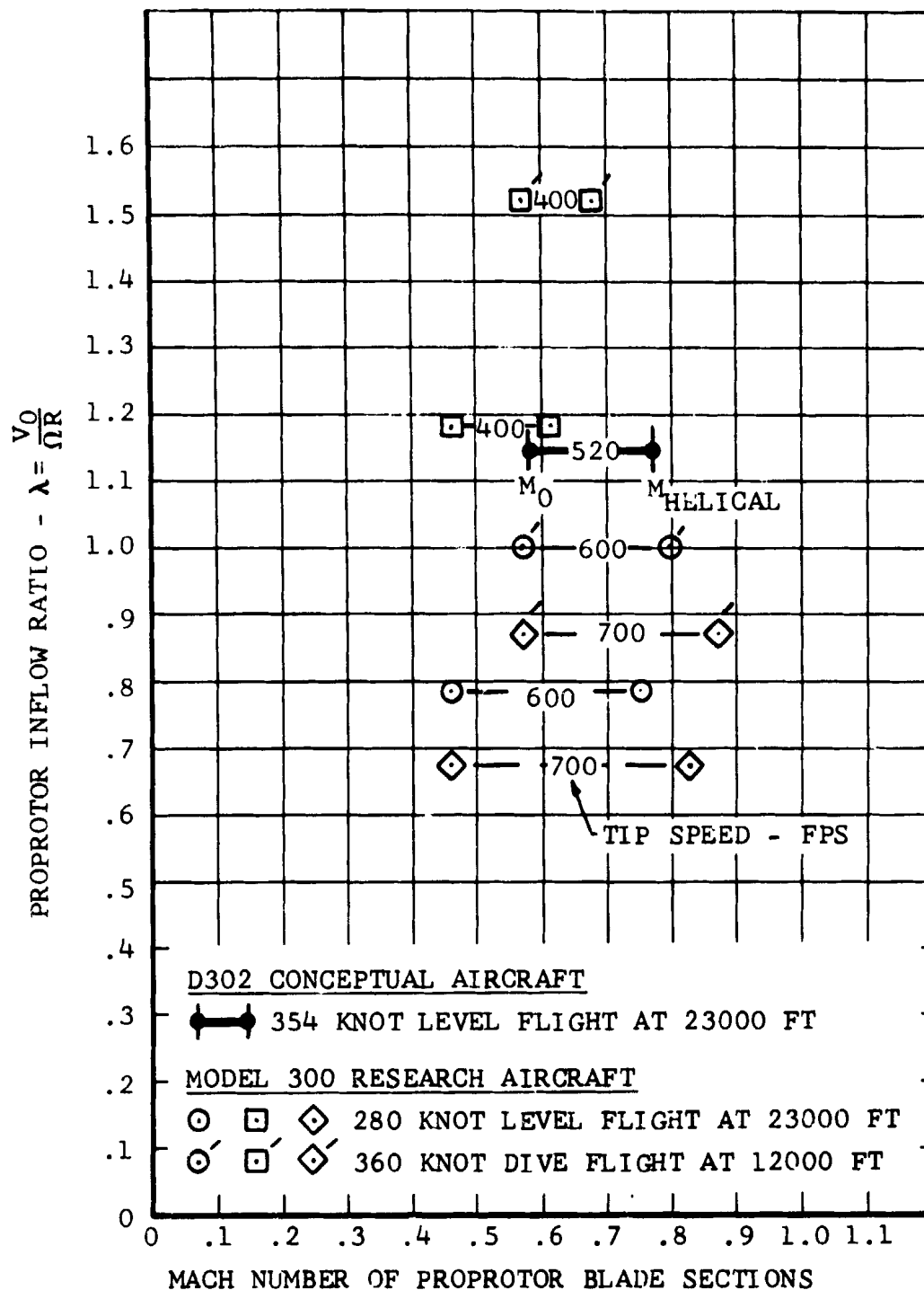


Figure II-7. Comparison of Model 300 Proprotor Inflow and Mach Test Range with D302 Conceptual Aircraft.

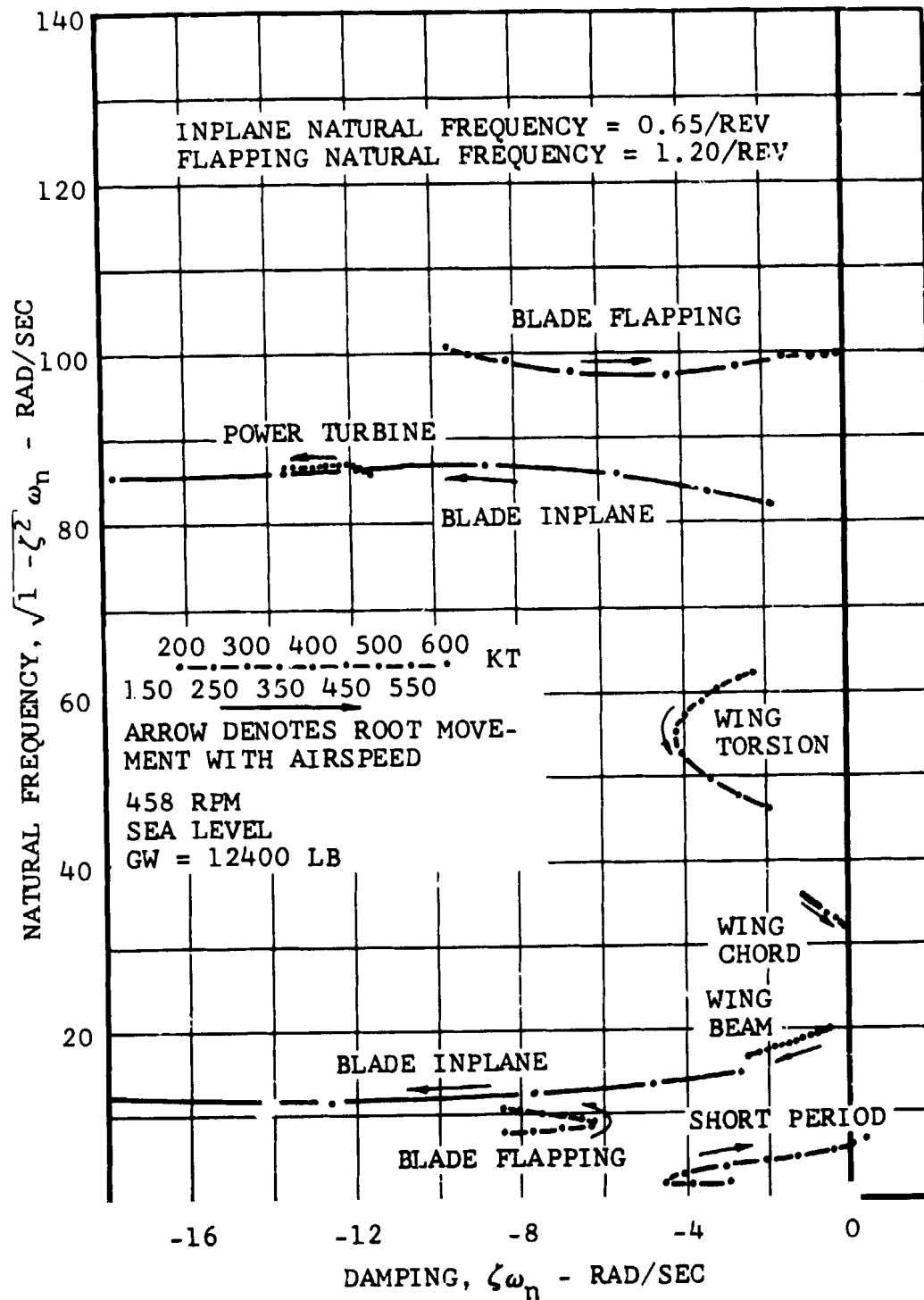


Figure II-8. Model 300 with Soft Inplane Proprotor, Symmetric Modes.

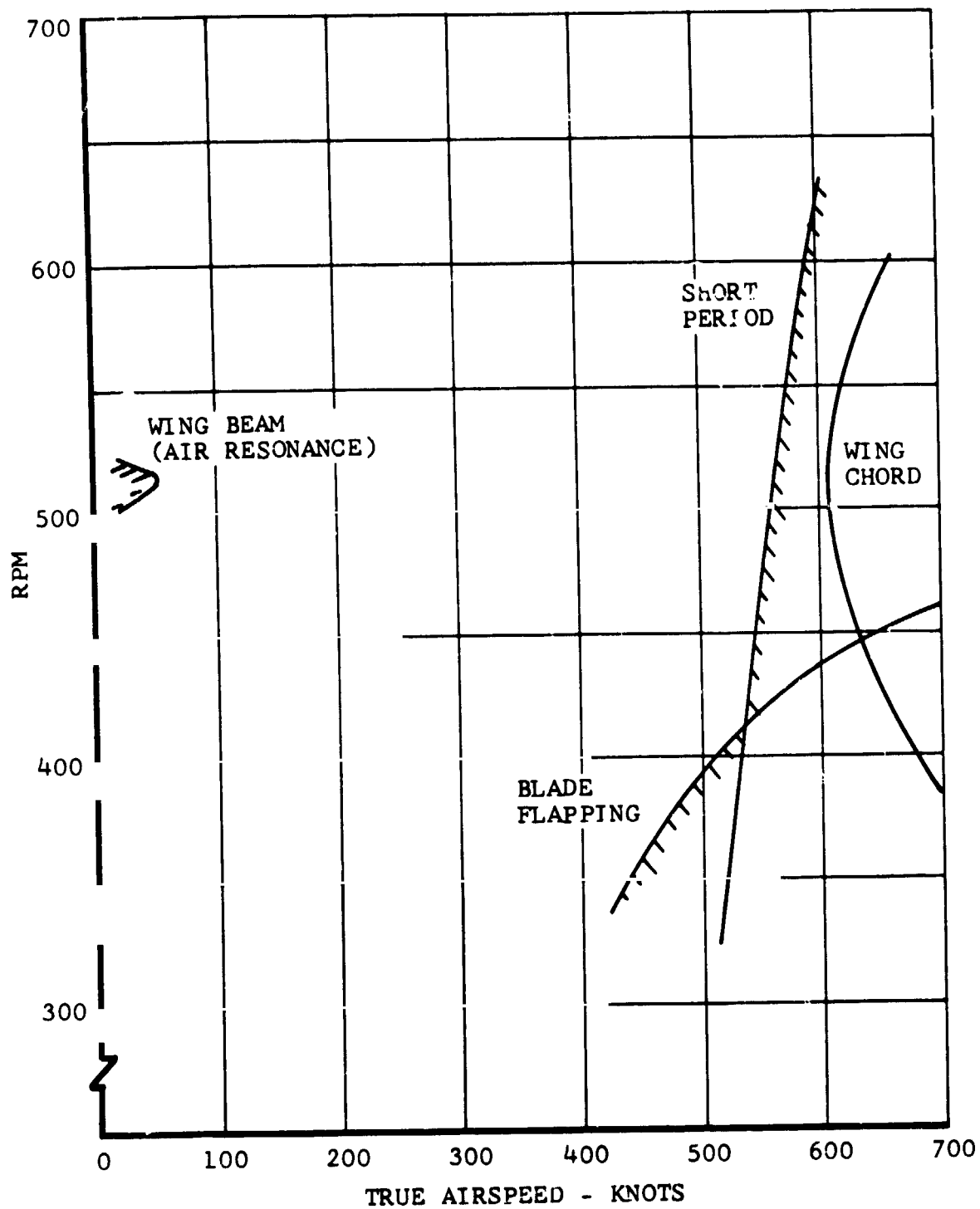


Figure II-9. Model 300 with Soft Inplane Proprotor,
Stability Margin of Symmetric Modes
Versus RPM.

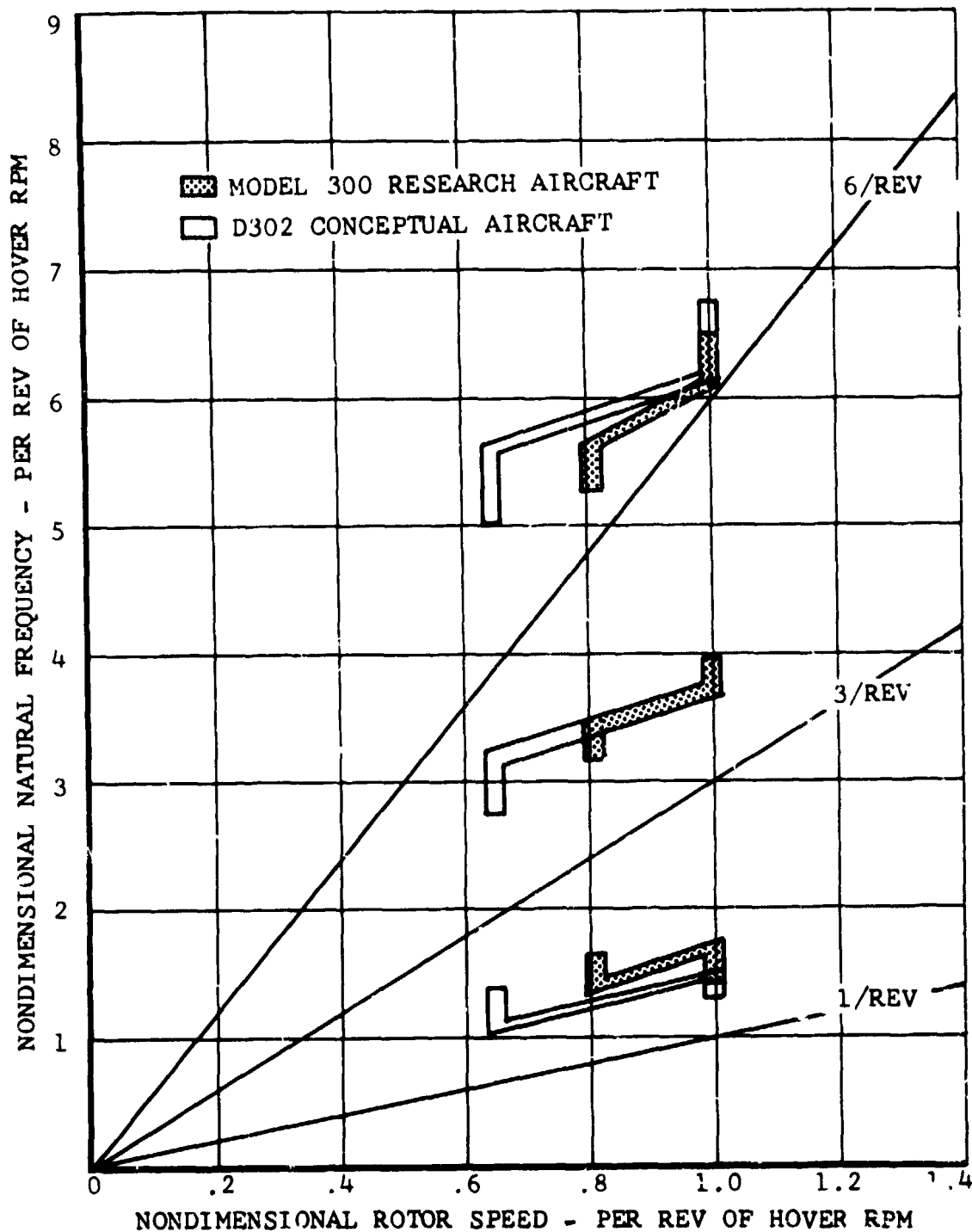


Figure II-10. Comparison of Model 300 Proprotor Blade Collective Modes with D302 Conceptual Aircraft.

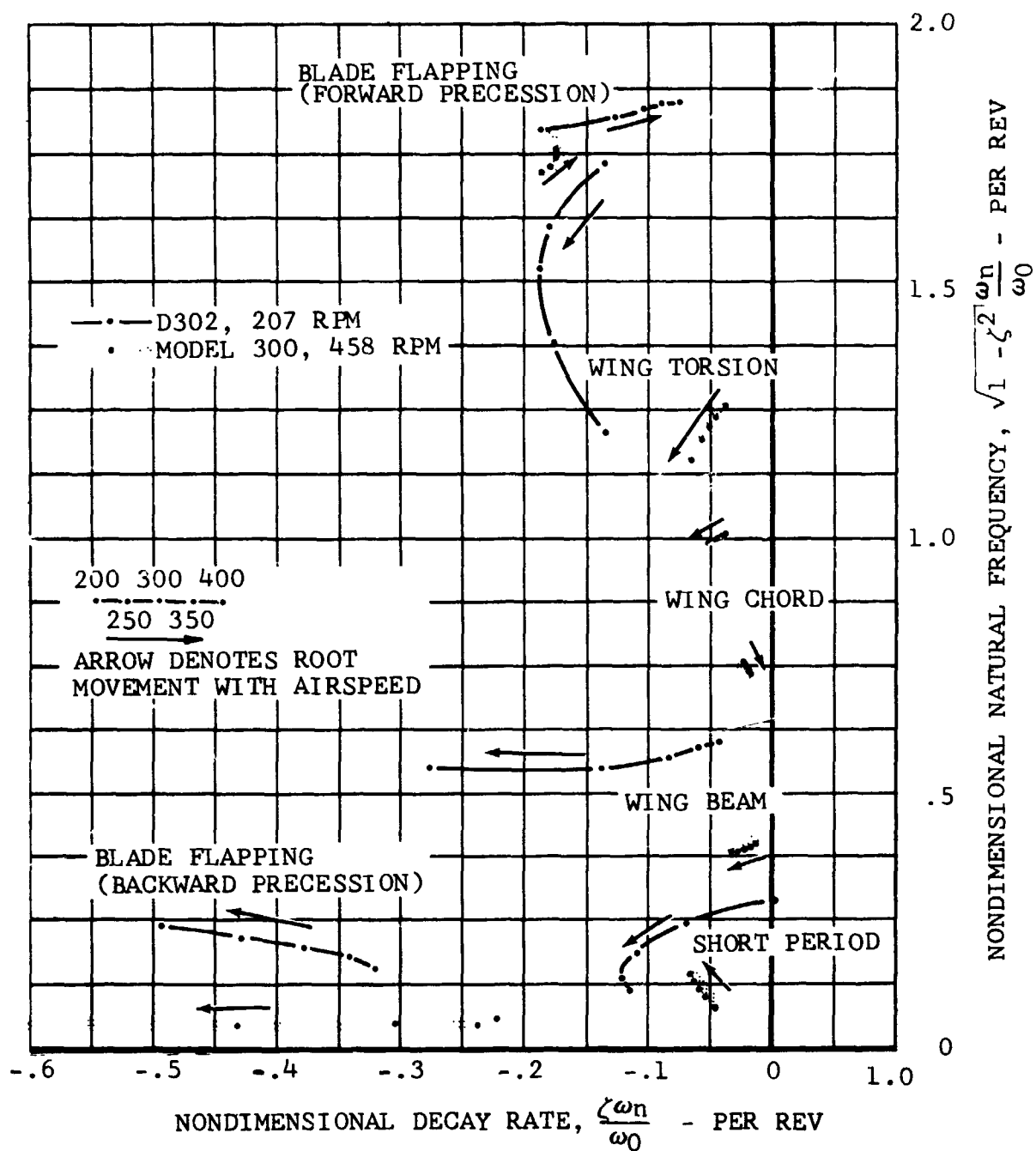


Figure II-11. Comparison of Model 300 Symmetric Modes with D302 Conceptual Aircraft.

III. DESIGN DESCRIPTION

A. GENERAL

The Model 300 tilt-prop rotor proof-of-concept aircraft has twin prop rotors at the tips of a forward-swept high wing. The prop rotors are mounted with gearboxes and turboshaft engines in self-contained propulsion system pods. The aircraft uses two 1150-horsepower Pratt and Whitney PT6C-40(VX) direct-drive engines. General arrangement of the aircraft is shown in 300-960-101 three view drawing.

The three-bladed 25-foot-diameter prop rotors are gimbal mounted with hub springs to increase longitudinal control power in helicopter mode. The prop rotors are identical in design to the prop rotor tested early in 1970 in the NASA-Ames full-scale tunnel. Disc loading is 12.6 pounds per square foot at the normal gross weight of 12,400 pounds and 15.3 pounds per square foot at the STOL gross weight of 15,000 pounds. At normal weight the wing loading is 68.5 pounds per square foot.

The cockpit is arranged for a crew of two; the aircraft can be flown from either seat. Conversion and power management procedures are simple and straightforward and permit the aircraft to be flown by a single pilot. Power is controlled in the helicopter mode by a collective stick and twist grip throttles and in airplane mode by throttle levers and a prop rotor governor. Conversion is controlled by fore and aft movement of switches on the pilot and copilot cyclic control sticks.

The canopy and forward fuselage are designed for installation of Douglas Escapac 1-E ejection seats for the research flight tests. The cabin is large enough to accommodate eight passengers in conventional seating or twelve troops in a high-density seating arrangement.

The aircraft is designed for a 2.0 g load factor in helicopter and conversion mode and +3.17 g in airplane mode. Design limit speed is 300 knots. Basic design criteria are summarized in Section B. Basic data are summarized in Table III-I, dimensional data in Table III-II, control travels in Table III-III, and aircraft inertias in Table III-IV.

The following design layouts are included in the back of this volume. Throughout the text of this section, where reference is made to these drawings, drawing number will be shown in parentheses.

300-960-101	Three View
300-960-002	Prop rotor and Controls
300-010-001	Blade Assembly
300-010-100	Prop rotor Assembly

300-960-003	Inboard Profile - Nacelle
300-960-004	Main Transmission
300-960-005	Fixed Controls - Wing
300-960-006	Fixed Controls - Fuselage
300-960-007	Wing Assembly
300-960-008	Fuselage and Empennage
300-960-009	Crew Station and General Arrangement

TABLE III-I. BASIC DATA

Aircraft Weight	
Normal Gross Weight	12400 lb
STOL Gross Weight	15000 lb
Empty Weight	7390 lb
Design Landing Weight	9500 lb
Engine (Two)	
Manufacturer	Pratt and Whitney
Model	PT6C-40(VX)
30-Minute Rating (2 x 1150)	2300 shp
Maximum Continuous Rating (2 x 995)	1990 shp
Power Loading at Normal Gross Weight	5.4 lb/hp
Power Loading at STOL Gross Weight	6.5 lb/hp
Proprotor (Two)	
Diameter	25 ft
Number of Blades Per Rotor	3
Solidity	0.089
Disc Loading at Normal Gross Weight	12.6 lb/sq ft
Disc Loading at STOL Gross Weight	15.3 lb/sq ft
Wing	
Span	34.6 ft
Area	181 sq ft
Aspect Ratio	6.6
Wing Loading at Normal Gross Weight	68.5 lb/sq ft

TABLE III-II. DIMENSIONAL DATA

Aircraft Dimensions	
Overall Length (42.1 feet)	505.0 in
Overall Width (Proprotor Turning) (57.2 feet)	686.0 in
Overall Width (Proprotors Removed) (36.4 feet)	436.0 in
Overall Height Pylons Vertical (Top of Spinner - From Static GL) at NGW (15.4 feet)	185.0 in
Overall Height (Top of Fin - From Static GL) at NGW (12.7 feet)	152.0 in
Span Between Proprotor Centerlines at Conversion Pivot Points (32.2 feet)	386.0 in
Static Ground Line Reference at WL	11.0 in
Height of Conversion Pivot Point	89.0 in
Above Static GL at NGW (7.42 feet)	39.0
Conversion Axis Location, Percent Wing MAC	39.0 in
Distance from Conversion Pivot Point	
To Horizontal Tail 1/4-Chord of MAC (21.6 feet)	260.0 in
To Vertical Tail 1/4-Chord of MAC (22.2 feet)	266.3 in
Distance from Wing 1/4-Chord of MAC	
To Conversion Axis	8.7 in
To Horizontal Tail 1/4-Chord of MAC (22.4 feet)	268.7 in
To Vertical Tail 1/4-Chord of MAC (22.9 feet)	275.0 in
Ground Clearance at NGW (GL at WL 11.0)	12.0 in
Main Gear Tread Width	110.0 in
Distance from Nose-Wheel Axle to Main-Gear Axles	214.0 in
Engine	
30-Minute Rating	
Horsepower	1550 shp
RPM (Output Shaft)	30000
Torque	2420 in-lb

TABLE III-II. Continued

Maximum Continuous Rating	
Horsepower	995 shp
RPM (Output Shaft)	30000
Torque	2090 in-lb
Dry Weight	325 lb
Drive System Gear Ratios	
Engine to Proprotor	53.1:1
Engine to Interconnect Shaft	4.69:1
Proprotor	
Number of Blades per Proprotor	3
Diameter	25.0 ft
Disc Area per Proprotor	491 sq ft
Blade Chord (See Fig. III-1)	14 in basic blade
Blade Thickness	See Figure III-1
Blade Area (3 blades)	43.75 sq ft
Solidity	0.089
Blade Airfoil Section	
Root (C_L Mast)	NACA 64-935 $a = 0.3$
Tip	NACA 64-208 $a = 0.3$
Blade Twist (See Figure III-1)	-45.0 deg
Hub Precone Angle	+1.5 deg
δ_3	-15.0 deg
Underslinging	0 deg
Mast Moment Spring (per Rotor)	2700 in-lb/deg
Flapping Design Clearance	± 12.0 deg
Blade Flapping Inertia (per Blade)	105 slug ft ²
Blade Lock Number	3.83
Direction of Rotation, Inboard	
Tip Motion, Helicopter/Airplane	Aft/Up
Pylon and Conversion Actuator	
Point of Intersection of Mast and Conversion Axis	
FS	300.0
WL	100.0
BL	193.0
Conversion Axis Wing Chord Location	39.0 percent MAC
Conversion Axis Forward Sweep	5.5 deg
Conversion Axis Dihedral (Up)	3 deg

TABLE III-II. Continued

Angle of Mast Axis to Conversion Axis	95.5 deg
Angle of Outboard Tilt of Mast Axis	
Helicopter Mode	2.5 deg
Airplane Mode	0 deg
Distance Rotor Flapping Axis to Conversion Axis	56.0 in
Conversion Range (Pylon Vertical $\theta_C = 90^\circ$)	95 to 0 deg
Actuator Length	
Extended	39.04 in
Retracted	11.0 in
Travel	28.04 in
Distance Engine C_L from Mast C_L	17.0 in
Wing	
Span (34.6 feet)	415.0 in
Span between Conversion Axis Pivot Points	386.0 in
Area (Total)	181 sq ft
Root Chord (BL 28.0)	63.06 in
Tip Chord (BL 207.5)	63.06 in
Mean Aerodynamic Chord	
Chord (BL 103.7)	63.06 in
Leading Edge at FS	275.8
1/4 Chord at FS	291.3
Airfoil Section (Constant)	NACA 64A223 Modified
Aspect Ratio	6.6
Forward Sweep	6.5 deg
Dihedral	2.0 deg
Angle of Incidence	3.0 deg
Wing Twist	0 deg
Flaperon	
Area/Side (Aft of Hinge Line)	10.1 sq ft
Span (Along Hinge Line) (7.86 feet)	94.3 in
Chord/Wing Chord	0.25
Flap	
Area/Side (Aft of Hinge Line)	5.5 sq ft
Span (Along Hinge Line) (4.25 feet)	51 in
Chord/Wing Chord	0.25
Wing Loading	
Normal Gross Weight	68.5 lb/sq ft
STOL Gross Weight	82.9 lb/sq ft

TABLE III-II. Continued

Fuselage

Length (41.0 feet)	492.0 in
Maximum Breadth	66.0 in
Maximum Depth	74 in
Cabin Length (Cockpit Plus Cargo Compartment) (15.25 feet)	183 in
Cargo Compartment Length (9.16 feet)	110 in
Cargo Compartment Width	
Maximum	60.0 in
Floor Line	48.0 in
Cargo Compartment Height	
Ahead of Wing	60.0 in
Under Wing	54.0 in
Cargo Floor Space (9.16 feet x 4 feet)	36.6 sq ft
Cargo Compartment Volume (9.16 feet x 4 feet x 4.75 feet)	174 cu ft

Vertical Tail

Span (7.68 feet)	92.2 in
Total Area	50.5 sq ft
Rudder Area (Aft of Hinge)	7.5 sq ft
Rudder Chord/Total Chord	0.15
Aspect Ratio	2.40
Sweep of 1/4 Chord (Upper)	31.6 deg
Root Chord at WL 103.0	49.04 in
Airfoil Section	NACA 0009
Tip Chord at WL 163 & 70.8	28.75 in
Airfoil Section	NACA 0009
MAC Chord (WL 115.69)	44.75 in
MAC Leading Edge at FS	555.1
MAC 1/4-Chord at FS	566.3

Horizontal Tail

Total Area	50.25 sq ft
Span (12.83 feet)	154.0 in
Aspect Ratio	3.28
Angle of Incidence	0 deg
Elevator Area (Aft of Hinge)	13.0 sq ft
Elevator Chord/Total Chord	0.30
Root Chord (BL 0)	47.0 in
Airfoil Section	NACA 64A015
Tip Chord (BL 77.0)	47.0 in
Airfoil Section	NACA 64A015
MAC Chord (BL 38.50)	47.0
MAC Leading Edge at FS	548.25
MAC 1/4-Chord at FS	560.0
Sweep of 1/4-Chordline	0 deg

TABLE III-II. Concluded

Main Gear

Number of Wheels per Side	1
Tire Size, Type and Ply Rating	8.50 x 10, Type III, 10-ply
Inflation Pressure	70 psi
Nominal Outside Diameter	25.2 in
Load Rating (Helicopter)	9200 lb
Flat-Tire Radius	7.0
Maximum Ground Speed	80 kt
Oleo Strut Stroke (Total)	10.0 in

Nose Gear

Number of Wheels	2
Wheel Spacing (Dual)	9.5 in
Tire Size, Type and Ply Rating	5.00 x 5, Type III, 6-ply
Inflation Pressure	49 psi
Nominal Outside Diameter	13.9 in
Load Rating (Helicopter)	2100 lb
Flat Tire Radius	3.8 in
Maximum Ground Speed	80 kt
Oleo Strut Stroke (Total)	9.0 in

TABLE III-III. CONTROL TRAVELS

Cockpit Controls

Cyclic Stick Fore and Aft	±6.0 in
Cyclic Stick Lateral	±6.0 in
Collective Stick	12.0 in
Rudder Pedals	±2.5 in
Pedal Adjustment	±2.0 in

Proprotor Controls

Collective Pitch at 0.75R	
Helicopter	-3, +18 deg
Conversion	See Figure III-7
Airplane	+18, +50 deg

Differential Collective Pitch
(Lateral Cyclic Stick)

Helicopter	±3.0 deg
Conversion	See Figure III-8
Airplane	±0.58 deg

TABLE III-III. Concluded

Collective Pitch Trim	
Helicopter	±0.5 deg
Conversion	±0.5 deg
Airplane	±0.5 deg
Fore and Aft Cyclic Pitch	
Helicopter	±10.0 deg
Conversion	See Figure III-9
Airplane	0
Differential Cyclic Pitch (Rudder Pedals)	
Helicopter (0-60 kt EAS)	±4.0 deg
(60-100 kt EAS)	See Figure III-11
(100 kt EAS +)	±1.0 deg
Conversion	See Figure III-10
Airplane	0 deg
Proprotor Control Geometry	See Figure III-14
Control Surfaces	
Flap and Flaperon Travels	See Figure III-12
Elevator	±20.0 deg
Elevator Trim Tab	±20.0 deg
Rudder	±20.0 deg
SCAS Authority	
Collective Pitch	±1.0 deg
Cyclic Pitch	±2.0 deg
Flaperon	±6.0 deg

TABLE III-IV. INERTIA

Aircraft Inertia in Airplane Mode	
Minimum flying weight (170 lb pilot)	7740 lb
Pitch	11660 slug ft ²
Roll	31940 slug ft ²
Yaw	42020 slug ft ²
Landing gross weight	9500 lb
Pitch	11860 slug ft ²
Roll	35030 slug ft ²
Yaw	44890 slug ft ²
Normal gross weight	12400 lb
Pitch	13030 slug ft ²
Roll	36160 slug ft ²
Yaw	45750 slug ft ²
Pylon Inertia in Airplane Mode (Includes Rotor Weight Lumped at Gimbal)	
Inertia per pylon	
Pitch, I_{yy}	322.5 slug ft ²
Roll, I_{xx}	42.4 slug ft ²
Yaw, I_{zz}	300.0 slug ft ²
Center of gravity location	
FS	277 inch
WL	94 inch
BL	194 inch
Proprotor Blade	
Flapping inertia per blade	102.7 slug ft ²
Lock Number	3.83
Feathering inertia	0.222 slug ft ²
Spanwise center of gravity	58 inch
Chordwise center of gravity from LE	4.64 inch
Chordwise center of gravity	33.1 percent chord
Spanwise center of percussion	85.5 inch
Chordwise center of percussion	3.87 inch
Chordwise center of percussion	27.6 percent chord

TABLE III-IV. Concluded

Control Surfaces About Hinge Line	
Elevator per side	0.0631 slug ft ²
Rudder per side	0.0170 slug ft ²
Flaperon per side	0.0826 slug ft ²
Flap per side	0.0442 slug ft ²

B. DESIGN CRITERIA

Criteria have been established to provide a safe and efficiently designed flight research aircraft. Basic criteria comply with the Federal Aviation Regulations. Design limits, load factors, and conditions have been established in accordance with the requirements of the FAA, "Tentative Airworthiness Standards for Verticraft/Powered Lift Transport Category Aircraft - Part XX," dated August 1970. In the areas where this document fails to provide adequate definition, the applicable requirements of the Federal Aviation Regulations for rotorcraft and airplanes were used as a guide. In the areas not covered by any of the regulations and/or where exceptions have been customarily granted, Bell design practice for helicopters has been used. The basic design criteria and design parameters for the Model 300 are given in Table III-V.

TABLE III-V. BASIC DESIGN CRITERIA

Normal Gross Weight	12400 lb
STOL Gross Weight	15000 lb
Design Landing Weight	9500 lb
Empty Weight	7390 lb
Design Operating Speed, EAS	
Helicopter	120 kt
Conversion	140-170 kt
Airplane (Speed vs Alt, Fig III-15)	260 kt
Landing Gear Down	120 kt
Flap and Flaperon	See Figure III-12
Design Limit Speed, EAS	
Helicopter	156 kt
Conversion	189 kt
Airplane (Speed vs Alt, Fig III-15)	300 kt
Landing Gear Down	133 kt
Flap and Flaperon	See Figure III-12

Table III-V. Concluded

Proprotor Maximum Operating Tip Speed and RPM		
	(fps)	(rpm)
Helicopter	740	565
Conversion	700	534
Airplane	600	458
Limit Load Factors at Gross Weight	12400 lb	15000 lb
Helicopter	2.0	
Conversion	2.0	1.65
Airplane	3.17	3.06
Transmission Design Power		
Helicopter	1060 hp	
Airplane	860 hp	
Conversion	1000 hp	
Single Engine	1150 hp	

C. PROPROTOR

The 25-foot-diameter proprotor which has been fabricated and successfully tested, is designed to flight-worthy standards and is appropriately sized for use on the Model 300 aircraft. Aerodynamic design parameters have been selected for efficient cruise in the 200- to 300-knot speed range. The same requirements for reliability, service life and maintenance as an operational helicopter were met in the detail design of this proprotor. The proprotor blades and hub are described below.

1. Blades (300-010-001)

The blades use type 17-7PH stainless steel as the basic blade material as a result of a design study in which the relative merits of aluminum, titanium and several types of stainless steel were considered. Results indicate a substantial weight savings for both steel and titanium compared with aluminum blade designs. The 17-7PH steel blade provided the desired natural frequencies and strength for minimum weight.

Thickness, taper, twist and camber distributions were selected to meet the varying structural and aerodynamic requirements for helicopter and airplane flight. NACA 64-series airfoils are used with a 64-208 at the tip and a 64-935 at the theoretical root (blade Station 0). The thick blade root section is required to provide adequate blade strength when the blade is at high pitch in airplane flight where torque and inplane-gust loading cause high bending moments about the airfoil chord line.

The basic chord of the blade is 14 inches. Chord, twist, lift coefficient and thickness distributions are shown in Figure III-1. Blade stiffness and mass distribution are shown in Figure III-2.

2. Hub (300-010-100)

The hub consists of a titanium yoke with three spindles and a universal joint assembly that is splined to the mast. A nonrotating, elastometric hub-moment spring is attached to the yoke through a bearing. The lower end of the hub-moment spring is attached to the transmission case.

The universal joint assembly consists of a steel cross with bearings mounted in aluminum pillow blocks on two opposing spindles and a steel fork with bearings on the other two spindles. These four roller bearings are not provided with inner races, but roll on the case-hardened journals of the steel cross member. A common oil reservoir is created by oil passages drilled within the cross member. Oil-level sight gages are installed on the pillow block housings. The bearing housings contain thrust bearings to carry the prop rotor H-forces, and seals to retain the oil.

The inboard and outboard pitch-change roller bearings assemble in the blade's integral root fitting. The inner race of these bearings assemble on the spindles of the yoke. A stainless steel liner is bonded to the spindle to prevent fretting between the inner race and the titanium spindle. The pitch-change bearings are oil lubricated from a reservoir located in the pitch horn.

The three wire-wound blade-retention straps have an integral steel fitting which seats at the inboard end of each spindle of the yoke. The outboard fitting, of the retention strap, is attached to the blade by a steel bolt through the blade root fitting, spar and doublers.

D. DRIVE SYSTEM (300-960-004)

The drive system consists of a main transmission assembly at each wingtip, a system of drive shafting through the wings connecting the two main transmissions, and a center gearbox mounted inside the fuselage. The PT6C-40(VX) engine attaches directly to the transmission pylon case. Each transmission is attached to a steel spindle which is supported by the two outboard wing ribs. Hydraulically-powered and mechanically-interconnected ball screw actuators support, power, and control the conversion of the pylon assembly about the transmission-spindle axis. In the airplane mode, the actuators drive the pylon into a down stop supported by the tip rib and front spar.

In normal operation, each transmission delivers power to its propotor from its own engine. The interconnecting shafts in the wings operate unloaded, except during maneuvers, single-engine operation, or asymmetrical loading conditions, where the interconnect drive shaft distributes power as required.

Design power for the transmission is shown in Table III-V and is based on the same design torque for each mode of flight with both engines operating. To permit the use of maximum power from the remaining engine in the event of an engine failure, the engine output shafting and herringbone gear stage are designed for the maximum engine output power of 1150 horsepower. The design power and torque are multiplied by several factors to arrive at limit and ultimate torques for the various stages. A distribution factor of 1.10 is applied to obtain the maximum steady power to allow for an uneven distribution of power between the propotors. A limit torque factor of 1.67 is used for those drive train components that could be subjected to loads caused by asymmetrical gust, otherwise a limit torque factor of 1.25 is used. Ultimate torque is 1.5 times limit torque.

The main transmission assembly supports all pylon components. The structural parts of the assembly consist of a spindle, pylon case, intermediate case, and a top (mast) case. The engine and pylon cowlings are also supported by the transmission.

Power is transmitted from the engine by an adapter shaft which picks up the female spline of the PT6C-40(VX) power turbine shaft, then through a combination power and torquemeter shaft which is splined to a herringbone pinion. The herringbone stage of reduction gears transmits the power through a one-way clutch to the two planetary reduction units. Power is supplied to the rotor masts by the planet carrier of the upper planetary stage.

The interconnect power train, linked to the main propotor drive side of the one-way clutch, consists of a spur gear set, an intermediate shaft (with torquemeter shaft), and a spiral bevel gear set.

The accessory gears provided for:

- Hydraulic pump
- Transmission oil pump
- Constant speed drive for an AC generator
- N_{II} governor

The center gearbox, with splash lubricated bevel gears, is mounted on the rear spar of the wing at the centerline of the fuselage. This gearbox accommodates the change in interconnect shaft angle due to wing sweep.

E. POWERPLANT

1. Engine

The Model 300 is powered by the Pratt and Whitney PT6C-40(VX) free turbine turboshaft engine. It is a version of the PT6A-41 turboshaft engine which is scheduled for certification in May 1972. The turboprop gearbox is removed and the lubrication system modified for vertical operation. The PT6A-41 engine is an advanced version of the PT6A-20 turboprop engine widely used in executive, third-level airline and utility turboprop aircraft. The PT6C-40(VX) is a direct-drive engine with an output speed of 30,000 rpm. The engine has takeoff and 30-minute ratings of 1150 horsepower and a maximum continuous power of 995 horsepower. The engine is rigidly mounted to the transmission case. Engine torque is measured on the transmission-input shaft utilizing the two-gear phase-displacement technique.

2. Induction System (300-960-003)

The engine induction system is designed to give maximum total pressure at the engine inlet screen, to provide anti-icing, and to protect the engine from dust and sand ingestion. Air enters through the nacelle inlet and diffuser duct. A 90-degree turn into the engine plenum provides an effective internal particle separator to remove dust and sand.

Moisture and debris then go through a by-pass duct and out through an injector. Part of the air in the by-pass duct makes a 90-degree turn and spills out into a plenum, where it is drawn across the engine and transmission oil coolers by a blower. The exhaust air from the blower is the power source for the ejector which emits the contaminated air remaining in the by-pass duct. The opening between the by-pass duct and plenum is only partially covered by a screen. During icing conditions, when this screen ices over, the efficiency of the separator increases.

3. Oil System

The engine is supplied with oil from a 2.3-gallon tank that is an integral part of the compressor inlet case on the engine. Oil flows from the tank to the accessory reduction gears, engine bearings and filter. Scavenge oil is directed through the oil cooler located behind (airplane mode) or below (helicopter mode) the accessory gear case. The oil cooler is equipped with a thermostatically regulated bypass to prevent high surge pressures during starts under cold weather conditions. Air for the coolers is provided by a mechanically driven blower. A shaft from the accessory drive pad on the engine provides power for the blower. The oil leaves the coolers and is returned to the tank forming a "cold tank" system. The tank is vented overboard. Continuous indication of system operation is provided by oil temperature and pressure instruments in the cockpit. Warning lights are

also provided to indicate low oil pressure and high oil temperature.

4. Fuel System

Fuel is supplied by two separate systems, one for each engine. Each system is composed of two cells interconnected to form a single tank in each wing. The total fuel capacity is 1600 pounds. The cells are constructed of a flexible rip-resistant material. Continuous support for each cell is provided by the structural honeycomb panels of the wing. Gravity refueling is accomplished through filler caps in each of the outboard cells. One fuel-booster pump is provided at each inboard cell.

Engine fuel passes from the booster pump discharge through a check valve, fuel filter, firewall shutoff and conversion swivel fitting before entering the fuel control. A pressure gage in the cockpit indicates the discharge pressure of the booster pump. An interconnect between the two discharge lines permits one pump to supply both engines if a pump fails. Opening the tank interconnect valve will allow inter-tank gravity transfer of fuel to the operative pump.

F. AIRFRAME

1. Wing (300-960-007)

The following specific objectives were established for the wing design.

- Place the elastic axis far forward to minimize the torsional deflections resulting from coupled proprotor/pylon/wing motions.
- Provide high torsional stiffness without undue weight penalty.
- Provide the maximum possible flap and flaperon area, and design them to deflect to a large angle, in order to minimize the projected wing area, and hence the aircraft download, during hover.
- Provide an unobstructed passageway to route controls, hydraulic, electrical and fuel lines, and transmission and conversion actuation interconnect shafts.
- Provide fuel space.

These objectives are accomplished by a forward location of the structural box and sweeping the wing forward 6.5 degrees to obtain the desired relationship between the wing center of pressure and the conversion axis. Fuel cells are located inside the structural box; the controls, lines and transmission

interconnect shaft are located aft of the rear spar. The conversion actuator interconnect shaft is located in the leading edge.

A lightweight, torsionally-efficient structure is obtained by using sandwich construction for the skins of the structural box. All of the skin is effective in both bending and torsion, whereas with a skin-stringer combination, the skins may be in a buckled state under load, and the stringers provide no torsional stiffness.

A significant factor in obtaining high torsional rigidity is the high wing-thickness ratio which provides a large wing-box cross-sectional area. Since the rigidity varies with the square of the area, high torsional stiffness results. The high thickness ratio also contributes to the bending stiffness and permits a minimum weight structure.

The front spar web and caps is a single extrusion. The rear spar web is a sandwich panel in the outer wing and is removable, in sections, for access to the fuel cells. In the center section, the rear web and stiffeners are integrally machined. The outboard two ribs of the wing support the pylon conversion spindle and the conversion-actuator spindle. The pylon down stop fitting is attached to the front spar and tip rib. Intermediate ribs form bulkheads for the extremities of the fuel cells and redistribute the loads from the flaperon and flap hinge ribs.

The leading-edge structure consists of an outer skin bonded to a beaded inner skin. It is removable for access to the conversion interconnect shaft. Short sections are provided at the bearing hangers to make inspection easier.

EI and GJ distribution and panel-point weights for the wing are shown in Figure III-3.

2. Fuselage (300-960-008)

The fuselage is a nonpressurized, semi-monocoque structure of 2024 and 7075 aluminum alloy. Four main longerons are located above and below the cutouts required for the doors, windows, and the landing gear. Stringers and frames break up the skin panels to the required size. Major bulkheads are provided for the ejection seat rails, at each side of the entrance door, at the front and rear wing spars, at both ends of the landing gear bay, and for attachment of the horizontal stabilizer spars. Longitudinal beams are located under the cabin and cockpit floor at BL 7.75, each side of BL 0. They extend forward to FS 131 and support the nose gear. Controls are routed between these beams.

The cabin extends between the canted bulkheads at Stations 219.8 and 347. The inside cross-sectional dimensions are 60 inches wide, 127 inches long, and 60 inches high (54 inches under the

wing). The entrance door opening, located at the forward right side, is 28 inches wide and 52 inches high. Emergency exits are provided on each side of the cockpit and in the cabin on the left side between Stations 315 and 347. The floor is aluminum honeycomb sandwich with a rigidized upper surface.

EI and GJ distribution and panel point weights for the fuselage are shown in Figure III-4.

3. Empennage

The empennage is made up of a horizontal stabilizer with two vertical stabilizers located at its outboard tips, forming an H-tail configuration.

The structural box of the horizontal stabilizer is a single-cell configuration consisting of two spars and skins. The two spars attach to bulkheads provided in the fuselage and to the vertical stabilizer at each tip. Bulkheads are provided at elevator hinge points and at the intersection of the vertical stabilizers. Ribs and chordwise stiffeners are provided to break up the skin panel.

Two spars of the vertical fins attach to the spars of the horizontal stabilizer. Bulkheads are provided at rudder hinge points and at intersection with the horizontal stabilizer. Ribs and chord-wise stiffeners, to break up the skin panel, are located between the two spars.

EI and GJ for the vertical and horizontal stabilizers are shown in Figures III-5 and III-6.

4. Landing Gear

A fuselage-mounted main gear was chosen because of the high-wing configuration. The gear retracts into the sides of the fuselage. Flush doors are provided between the bulkheads at Stations 347 and 410. The gear geometry was developed to permit the gear to clear the lower longerons when it retracts. A dual-wheel nose gear retracts into the compartment between Stations 131 and 169. The shock-absorption system is a conventional air-oil oleo.

G. AIRCRAFT SYSTEMS

1. Conversion System

The conversion system provides controlled rotation of the propulsion pod from the vertical to the horizontal position and return. It can safely restrain the pylon in either extreme, or in any intermediate position. The system also serves as a reference for the collective control system by providing a phasing control motion as a function of flight regime. The conversion actuator holds the pylon against the down stop on the front spar in airplane mode.

Conversion is controlled by a switch on the cyclic-stick grip. Forward movement of the switch rotates the pylons forward from helicopter to airplane flight position, and rearward switch movement returns them to the helicopter position. The conversion of the pylons may be stopped or reversed at any position. The normal conversion time is approximately eleven seconds.

Should one conversion actuator fail to function due to hydraulic or electrical failures, that unit is driven by the actuator motor on the opposite wingtip through the mechanical interconnect shaft. In the event of a complete dc power failure, a mechanical backup system, operated by pulling the emergency reconversion T-handle located in the cockpit, positions the hydraulic valves to cause the actuators to move the pylons to the helicopter position.

The major components of the conversion system include the double-extension ball-screw actuators with hydraulic motors and electrically powered servo-valve package, the interconnect shafting, and a control-phasing gear box located on the forward side of the front spar near the center of the fuselage. The hydraulic motors that power the conversion actuators are controlled by a series of valves, packaged in a single unit on each actuator, that control the rate and direction of flow to the motors. The directional valve is controlled by pilot-activated bidirectional solenoids. The rate of flow is controlled by a bidirectional solenoid that receives signals from the phasing actuator. This signal indicates the angular position of the propulsion pod and reduces flow at each extreme of the conversion and provides full flow during the conversion cycle. A dual activated conversion brake assembly is incorporated in the actuator gearbox which holds the pylon in position when hydraulic power is off.

The control-phasing gearbox provides a linear output, proportional to the pylon angle, that phases the collective and differential collective controls during conversion. This unit also provides protection from converting to aircraft mode while on the ground.

Asymmetry detection is provided by a signal picked up from synchronous motors at each main conversion spindle. This signal splits the needles on the pylon conversion-angle indicator in the cockpit, illuminates the master caution light, and stops flow through the control valve of the pylon actuators.

2. Hydraulic System

The hydraulic system is a MIL-H-5440 Type II (-65°F to +275°F) system utilizing MIL-H-5606 fluid at an operating pressure of 3000 psi. It has two independent transmission-driven hydraulic pumps. Since the pumps are driven by the transmission, they operate whenever the propellers are turning, and they are independent of engine power.

The primary hydraulic system, connected to one side of the dual flight-control actuators, is powered by the hydraulic pump in the left pylon. The utility system is powered by the pump in the right pylon. After retraction, the landing-gear portion of the utility system is separated from the flight-control portion by an isolation valve. The system powered by the right transmission pump, isolated from any utility function, then becomes a second primary system for one side of the dual flight-control actuators. Dual-concentric servo valve spools are provided for each valve body. A separate valve is provided for each half of the tandem cylinders. Refer to Figure III-13. Dual or single power is provided to the hydraulically-operated components as shown below:

Primary (Left Pump)	Utility (Right Pump)	Function
x	x	Cyclic
x	x	Collective
x	x	Flaperon (aileron)
x	x	Flaperon (flap) and Flaps
x	x	Proprotor Governor
x	x	SCAS
x		Conversion Actuator Left
	x	Conversion Actuator Right
	x	Proprotor Trim
	x	Landing Gear

3. Electrical System

The electrical system consists of two 200-ampere, 28-volt dc starter generators, and two 13-ampere-hour batteries, providing primary dc power. Two 250-v-a, 115/200-volt, single-phase 400-Hertz ac inverters provide the ac power. Two essential dc busses are connected in parallel through a bus-tie relay. Each 200-ampere starter generator supplies power to one of the essential dc busses. Each essential ac bus has a 250-v-a inverter with its essential ac bus. There are two essential ac and dc busses, and one nonessential dc bus.

The electrical system is designed to provide complete dual ac and dc power sources. These sources and their essential and nonessential busses are designed for complete isolation of the sources and their busses in the event of any failure.

H. AIRCRAFT CONTROLS

1. Proprotor Controls (300-960-002)

Proprotor controls consist of a rise-and-fall collective head assembly above the proprotor and a monocyclic (fore and aft) swashplate below the proprotor. A schematic of proprotor control geometry is shown in Figure III-14.

The collective head is attached to the proprotor mast. A non-rotating tube, extending inside the mast to the collective boost cylinder, gives vertical motion to the rotating collective head. A collective lever is attached to each of the three trunnions of the collective head. A control tube extends from one end of each collective lever to a pitch horn. At the other end of each collective lever a tube goes to the rotating swashplate.

The rotating swashplate (outer) is driven by the lower ring of the proprotor spinner. The nonrotating swashplate is attached to the top case of the transmission and is free to tilt about only one axis. The cyclic cylinder is attached to the non-rotating swashplate (300-960-003).

Collective control inputs, which increase or decrease the pitch of all blades at the same time, are introduced by means of a tandem hydraulic cylinder which is attached to the transmission case below the mast (300-960-003). The servo-valve linkage of the collective cylinder receives its input from the pilot through a swivel joint, on the conversion axis, which connects to the fixed controls in the wing (300-960-007). The input motion is introduced along the conversion axis so that the collective system functions in the same way in both airplane and helicopter modes of operation, though with different ranges of collective pitch.

The cyclic control cylinder tilts the swashplate, which causes one-per-rev variations in blade pitch. The servo valve of the cyclic cylinder is actuated by the pilot through a linkage (300-960-003) which is automatically phased out as the pylon converts from vertical to horizontal. This phase out is accomplished by having the cyclic controls in the wing (300-960-007) impart rotating motion to the end of the cyclic torque tube. Motion is introduced to the servo valve of the cyclic cylinder when the input tube is vertical (helicopter mode), and phases out until no axial motion occurs when the tube to the servo valve is horizontal (airplane mode).

The design of the hydraulic boost cylinder control linkages shown on (Figure III-13) permits the pilot to control the aircraft manually in the event of a dual hydraulic failure. A mechanical stop is placed between the servo lever pivot point and the pilot input. The stops react the pilot input force which allows him to move the boost cylinder piston tube and move the control system

linkages upstream of the boost cylinder to control the swash-plate angle.

2. Flight Control

The flight-control system combines the basic elements of conventional helicopter and airplane control systems. The cockpit controls for the proprotors and control surfaces are arranged so that a single pilot can maintain full control in all flight regimes, including conversion. Each of the two crew stations (300-960-009) has complete controls for pitch, roll, yaw, and thrust in all modes of flight. They consist of control sticks, rudder pedals with brakes, and collective levers, for both the pilot and copilot. A single set of power-management, rpm-select, flap, and landing gear controls is on the center pedestal. Dual-twist grips on the collective levers are electrically interconnected with the power-management controls on the center pedestal.

In helicopter mode, the controls apply blade-pitch changes to produce powerful control moments and forces. Fore-and-aft cyclic pitch provides longitudinal control, while differential-cyclic pitch produces directional control. Collective pitch is used for vertical flight and differential-collective pitch controls roll.

In airplane mode, the controls actuate conventional control surfaces which provide the control response characteristics of a conventional airplane. These control surfaces are also actuated in the helicopter flight mode, but they have minimal effectiveness because of the low dynamic pressures and high control moment capability of the proprotors.

Conversion or reconversion can be made within a wide range of variables such as airspeed, conversion angle, and fuselage attitude. Mechanical phasing of the proprotor control authority minimizes the need for control inputs during conversion. To provide the proper control authority during conversion (or reconversion), some controls are phased out, others are phased in, and the authority of others is altered. The automatic changes in controls as the pylon is converted from helicopter mode (95 degrees to 75 degrees conversion angle) to airplane mode (0 degrees conversion angle) is shown on Figures III-7 through III-11.

3. Stability and Control Augmentation System

A stabilization system is used to enhance the flying qualities in helicopter, conversion, and airplane modes. The three-axis stability and control augmentation system (SCAS) uses rate gyros to sense pitch, roll, and yaw. An electronic box receives signals from the rate gyros as well as signals from the conversion system and flight control system to differentiate the various

flight modes and amount of control input. This information is relayed to the SCAS units mounted on the hydraulic cylinders (Figure III-13). The SCAS actuates the controls, through servo actuators located on the hydraulic cylinders, in a direction to oppose the angular rate sensed by the rate gyros. In helicopter mode the collective SCAS introduces differential collective pitch to control roll rate and in airplane mode it introduces differential collective pitch to control yaw rate. The cyclic SCAS introduces differential cyclic to control yaw rate in helicopter mode and cyclic pitch in airplane mode, to serve as a flapping controller. Redundancy is provided by dual actuators which are operated individually by the two hydraulic systems.

4. Proprotor Governor System

The proprotor governor system is used to simplify power management and rpm control and to prevent engine-power adjustments and external disturbances from changing proprotor rpm. The system is a closed-loop control system that maintains a pilot-selected proprotor rpm by controlling collective blade-pitch in the airplane mode.

The proprotor governor system detects any error between the command rpm and the actual proprotor rpm. This error signal is amplified and is used to signal a hydraulic actuator in the collective control system. With a constant proprotor rpm setting, increasing power with the power management levers will increase the collective blade pitch to hold a constant rpm. This will result in increased aircraft velocity without changing proprotor rpm. Decreasing power will decrease the collective blade pitch and reduce aircraft velocity.

The proprotor governor is a fail-operate type system. Sufficient redundancy and monitoring circuitry is included so that a single failure will not result in loss of the proprotor governor. If a failure occurs, a warning light will be illuminated. If a second failure occurs, the proprotor governor system will automatically shut off and the pilot will control proprotor rpm manually with the collective lever.

5. Power Management

Power management is simple and is designed for straightforward cockpit procedures. Power control is provided by two control systems. For helicopter flight, the engine power-turbine governors maintain selected proprotor rpm by increasing or decreasing power as manual changes are made in collective pitch. In airplane flight, the proprotor-pitch governor maintains selected rpm by increasing or decreasing collective pitch as manual power changes are made. Thus, the Model 300 may be flown in helicopter mode in the same manner as a conventional helicopter, and in airplane mode in the same manner as a conventional turboprop airplane.

Throttle and prop rotor governor rpm-select levers are mounted on the pedestal (300-960-009), convenient to both the pilot and copilot. The pilot and copilot collective sticks have dual twist-grip throttles, and beeper switches for controlling turbine rpm through the governor.

Conventional helicopter rpm droop compensation is provided for each engine. The collective stick is connected through the droop-compensator linkage to a droop-cam on each engine. The droop-cam positions the load-signal shafts on the engine fuel control, which in turn schedule limited rpm changes to compensate for the engine droop characteristics.

Engine output power, for both helicopter and airplane flight, is regulated by the fuel control on each engine. Movement of the power-control shaft on each engine controls fuel flow. This shaft is positioned by the throttle levers. The throttle levers are controlled electrically by the twist grips during helicopter flight.

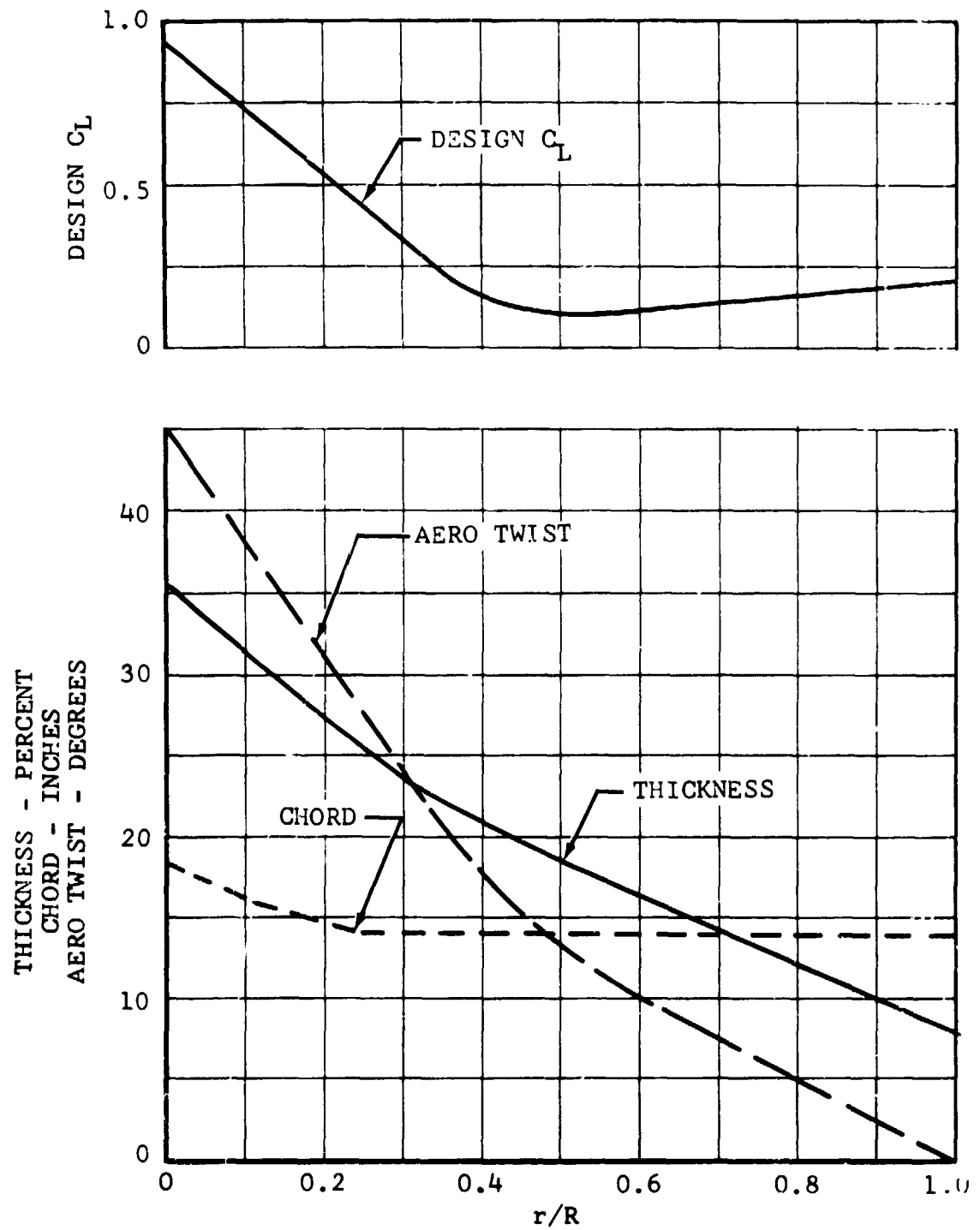


Figure III-1. Twenty-Foot Proprotor Parameters.

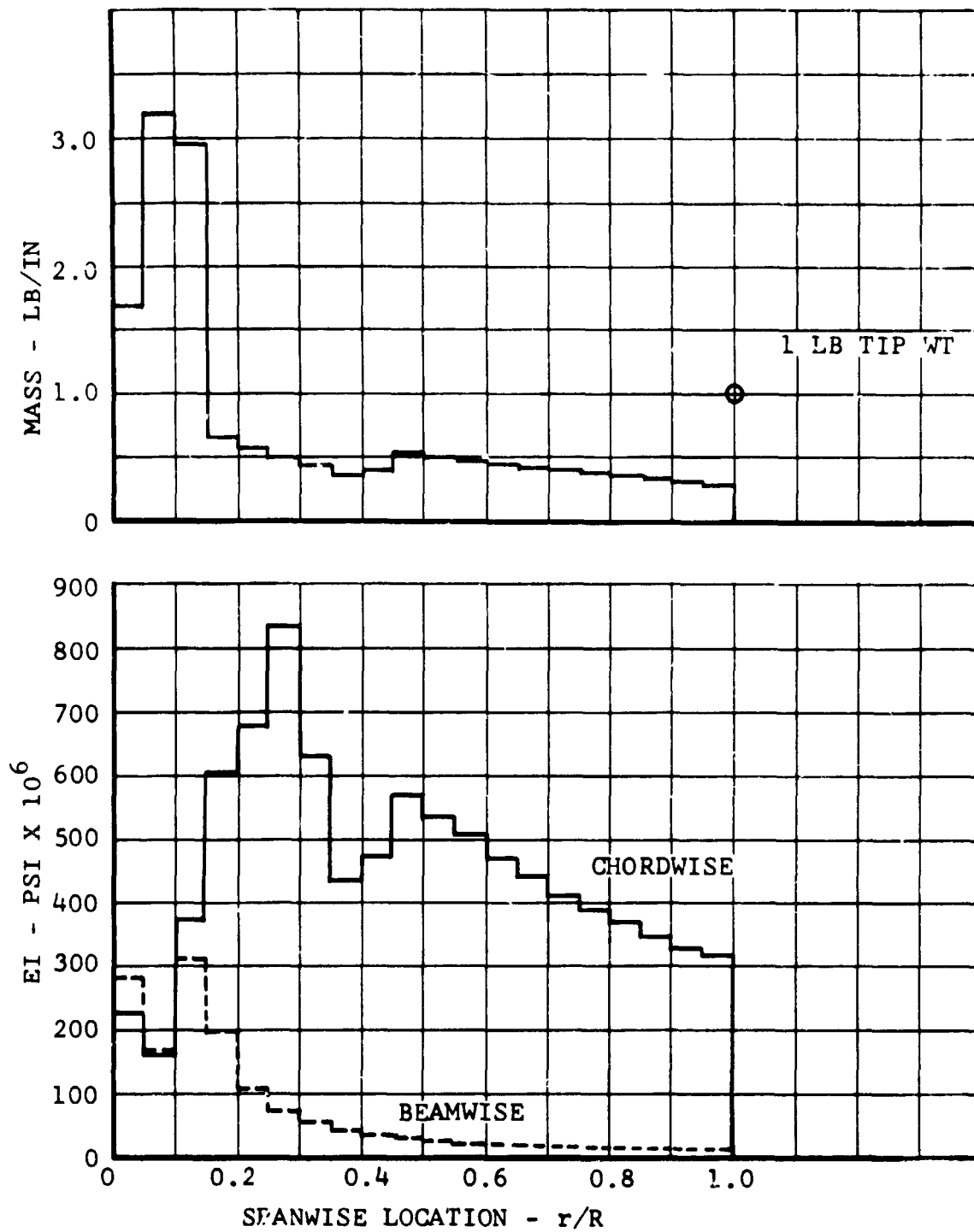


Figure III-2. Proprotor Stiffness and Mass Distribution.

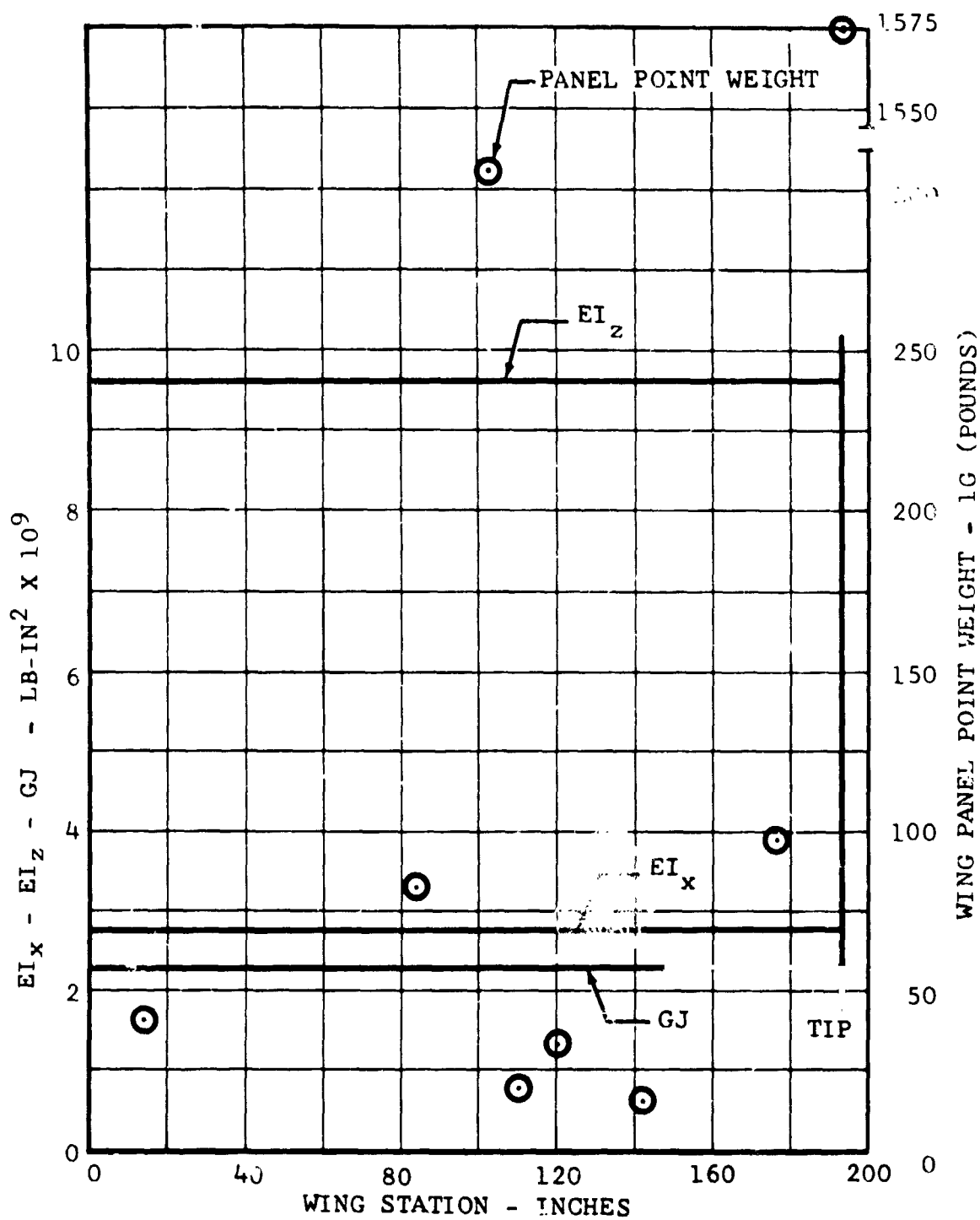


Figure III-3. Wing Stiffness and Panel Point Weight.

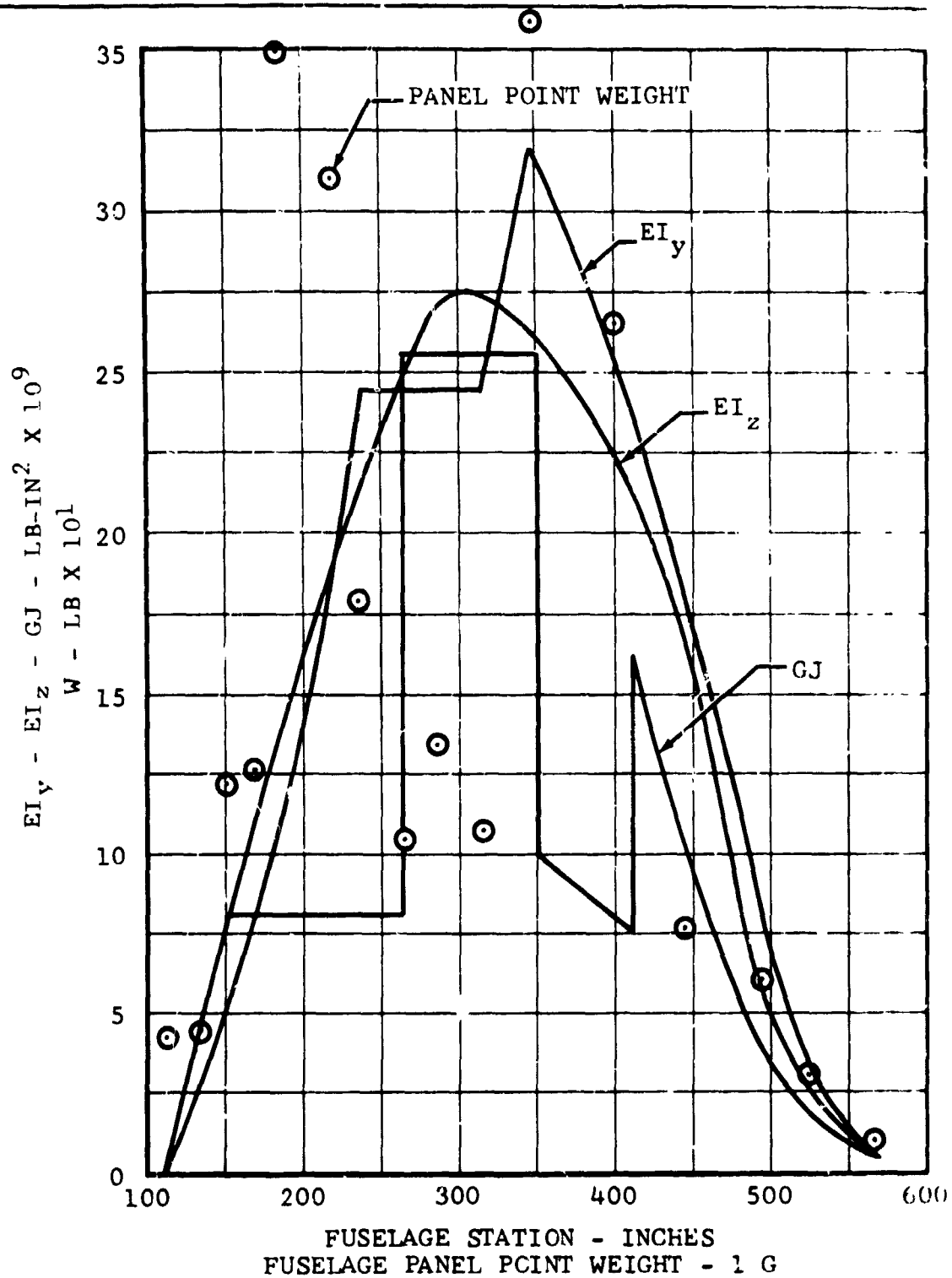


Figure III-4. Fuselage Stiffness and Panel Point Weight.

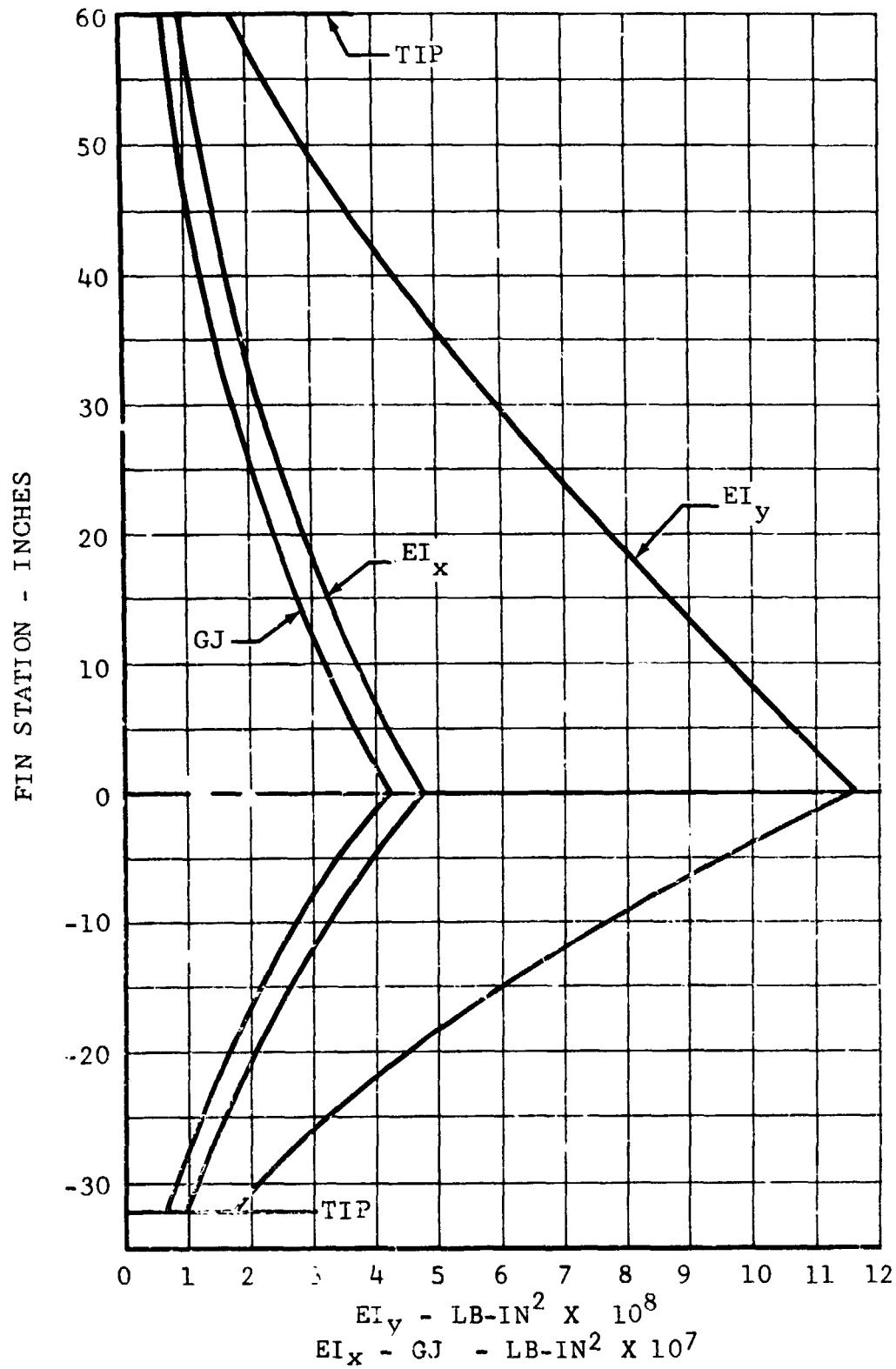


Figure III-5. Vertical Tail Stiffness.

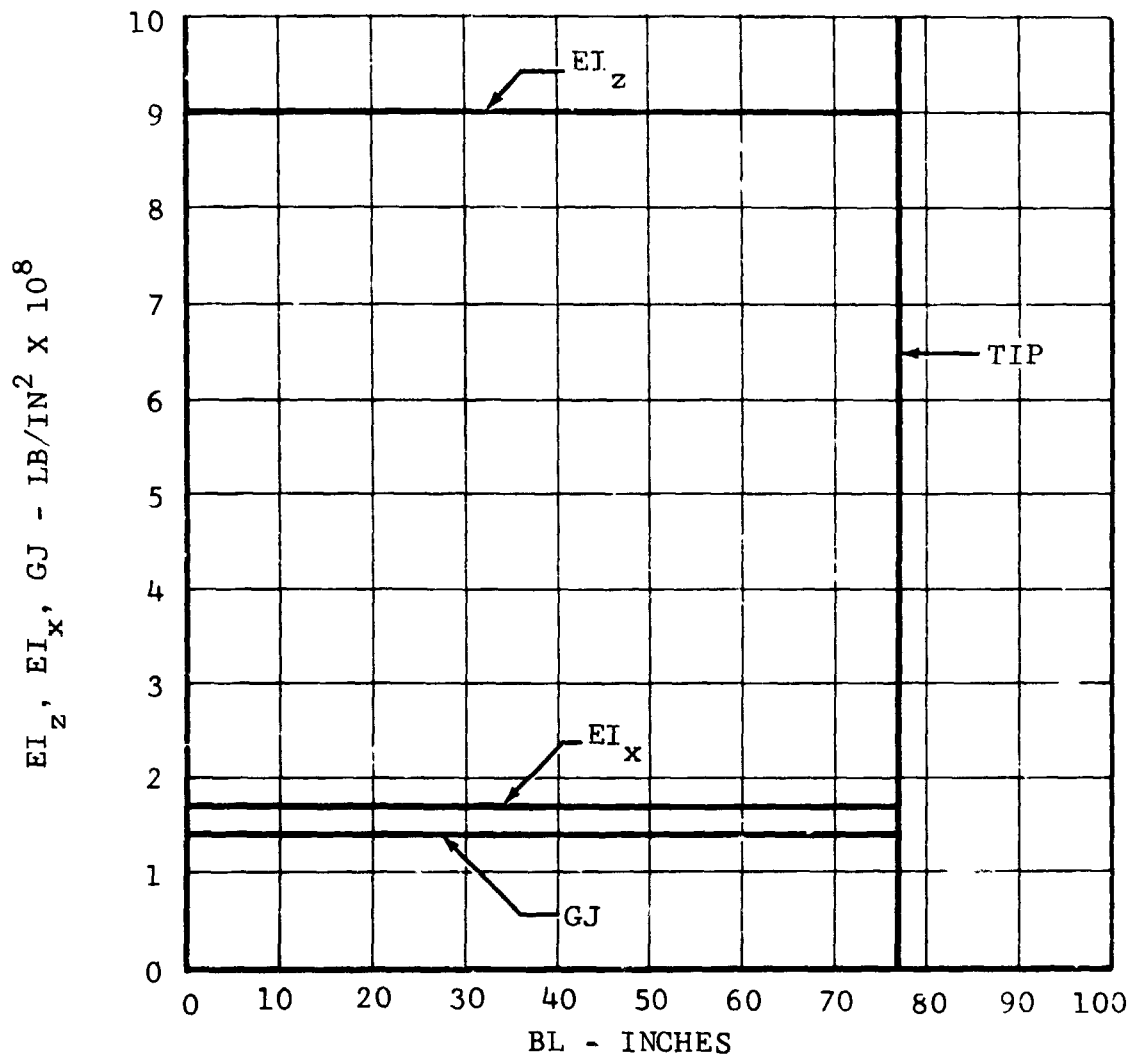


Figure III-6. Horizontal Tail Stiffness

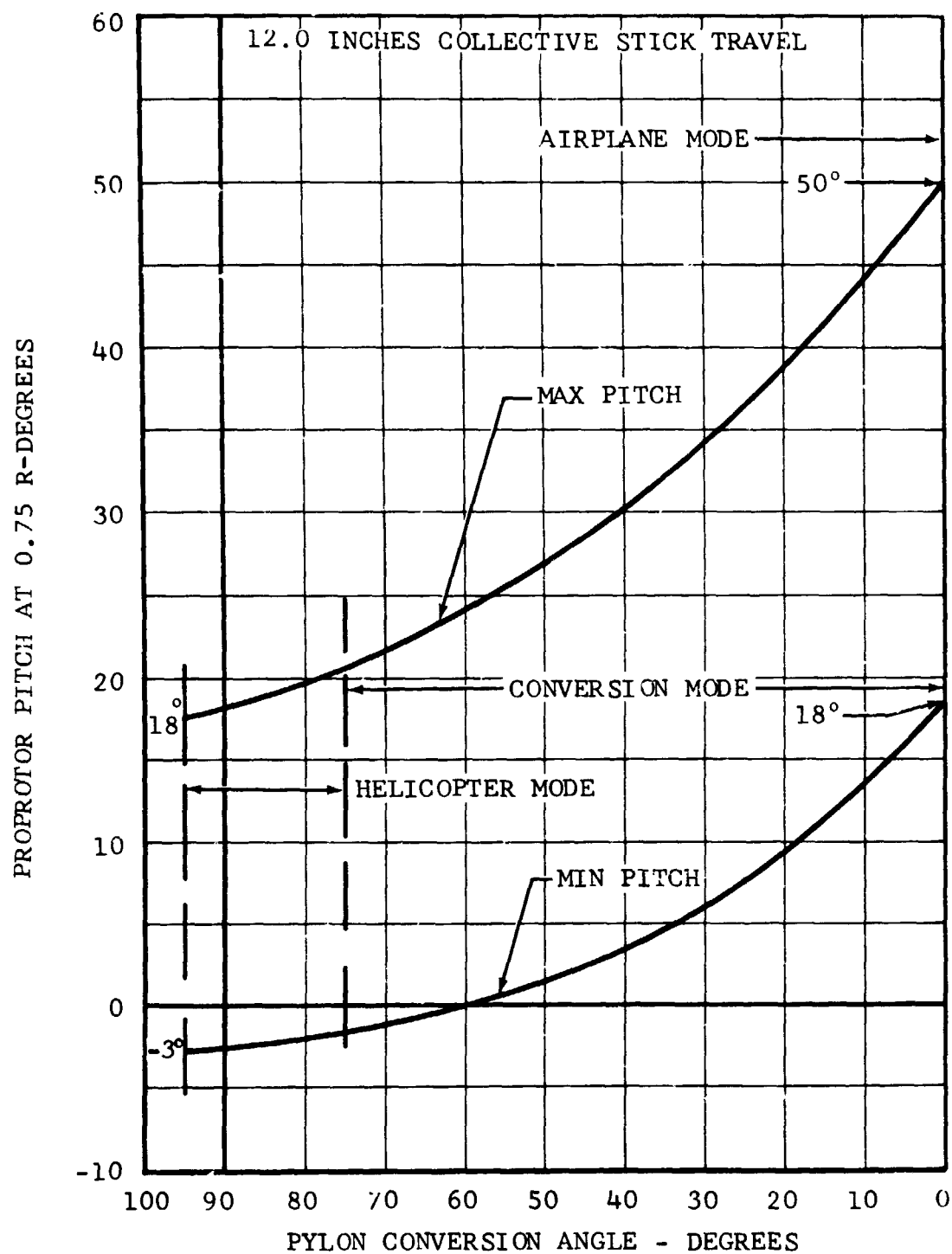


Figure III-7. Collective Pitch Versus Conversion Angle.

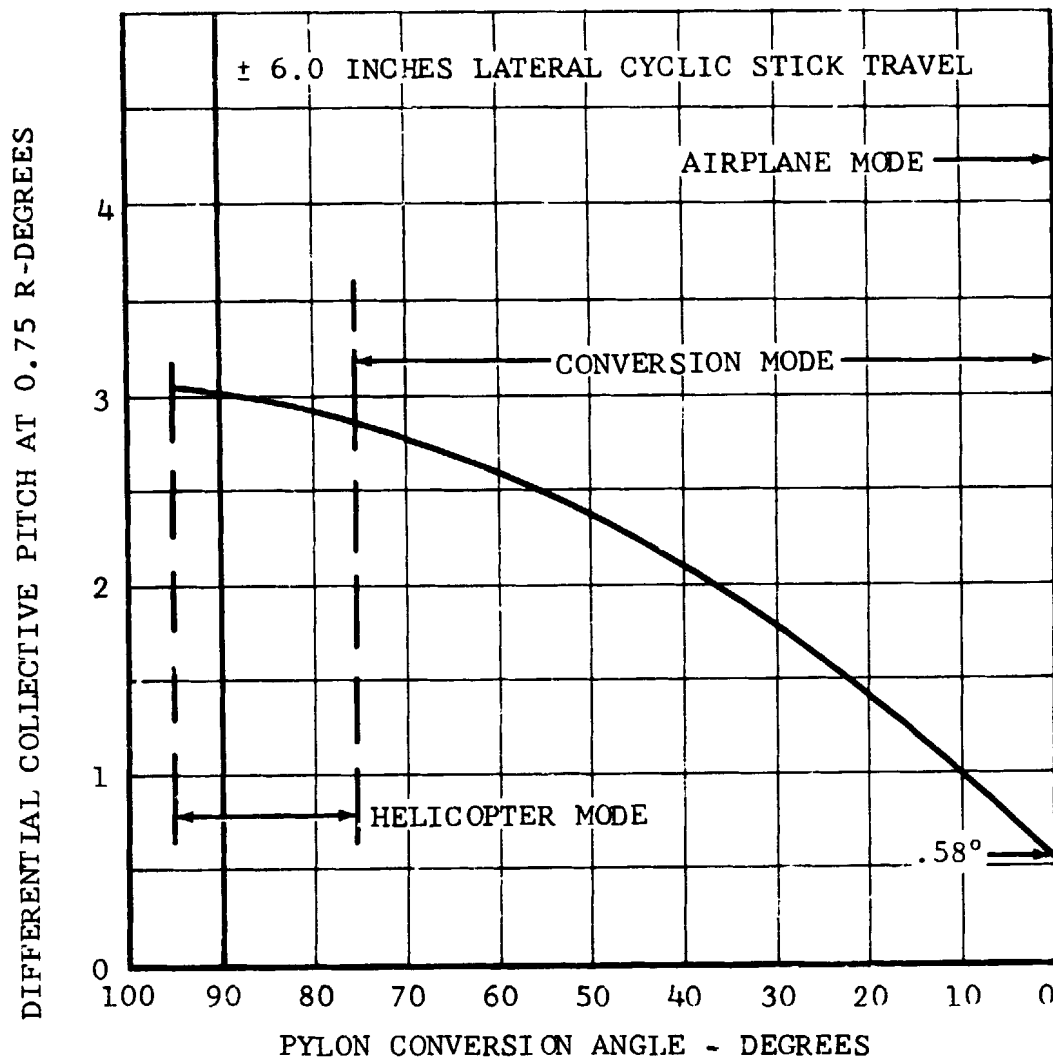


Figure III-8. Differential Collective Pitch Versus Conversion Angle.

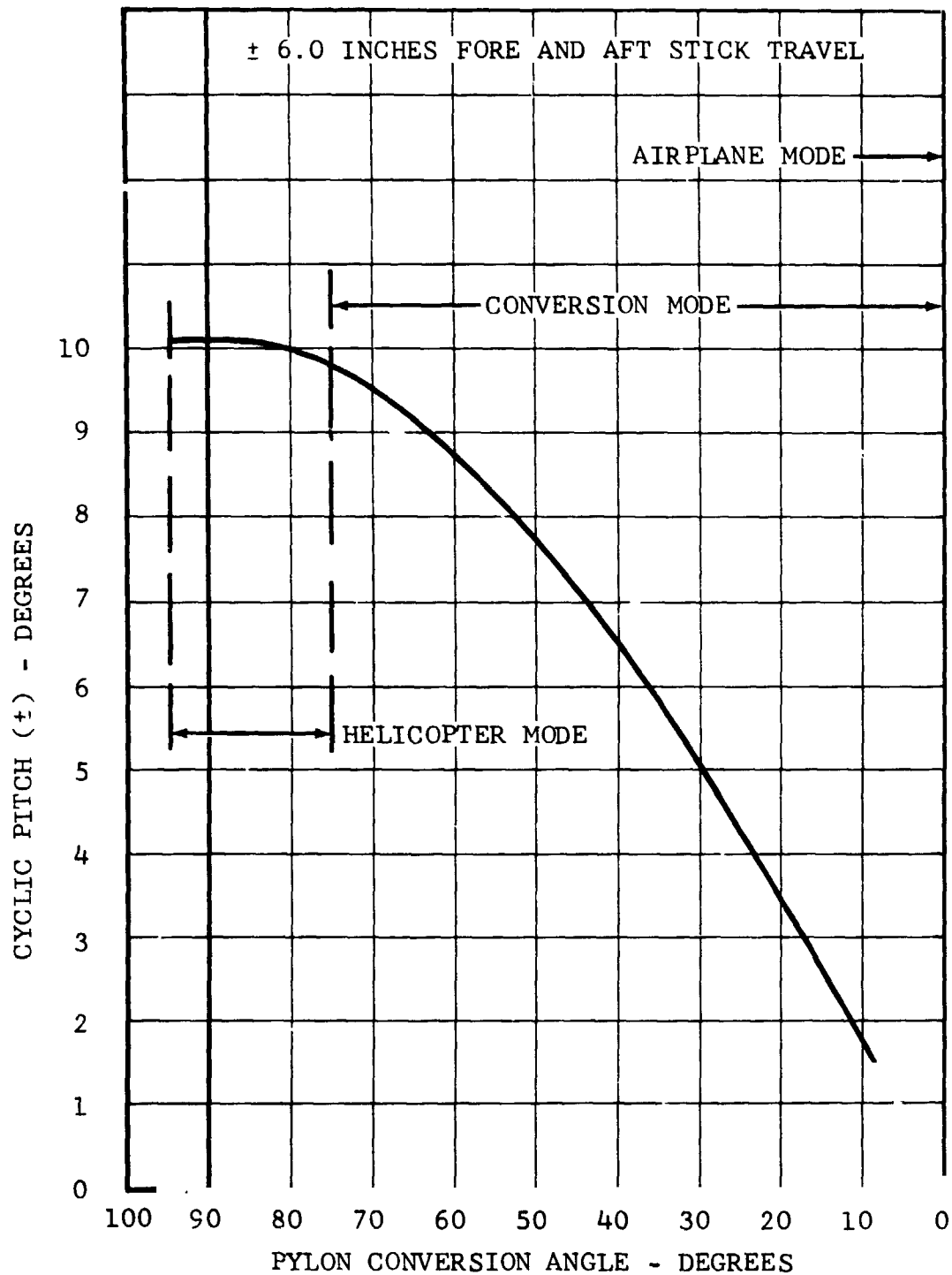


Figure III-9. Fore and Aft Cyclic Pitch Versus Conversion Angle

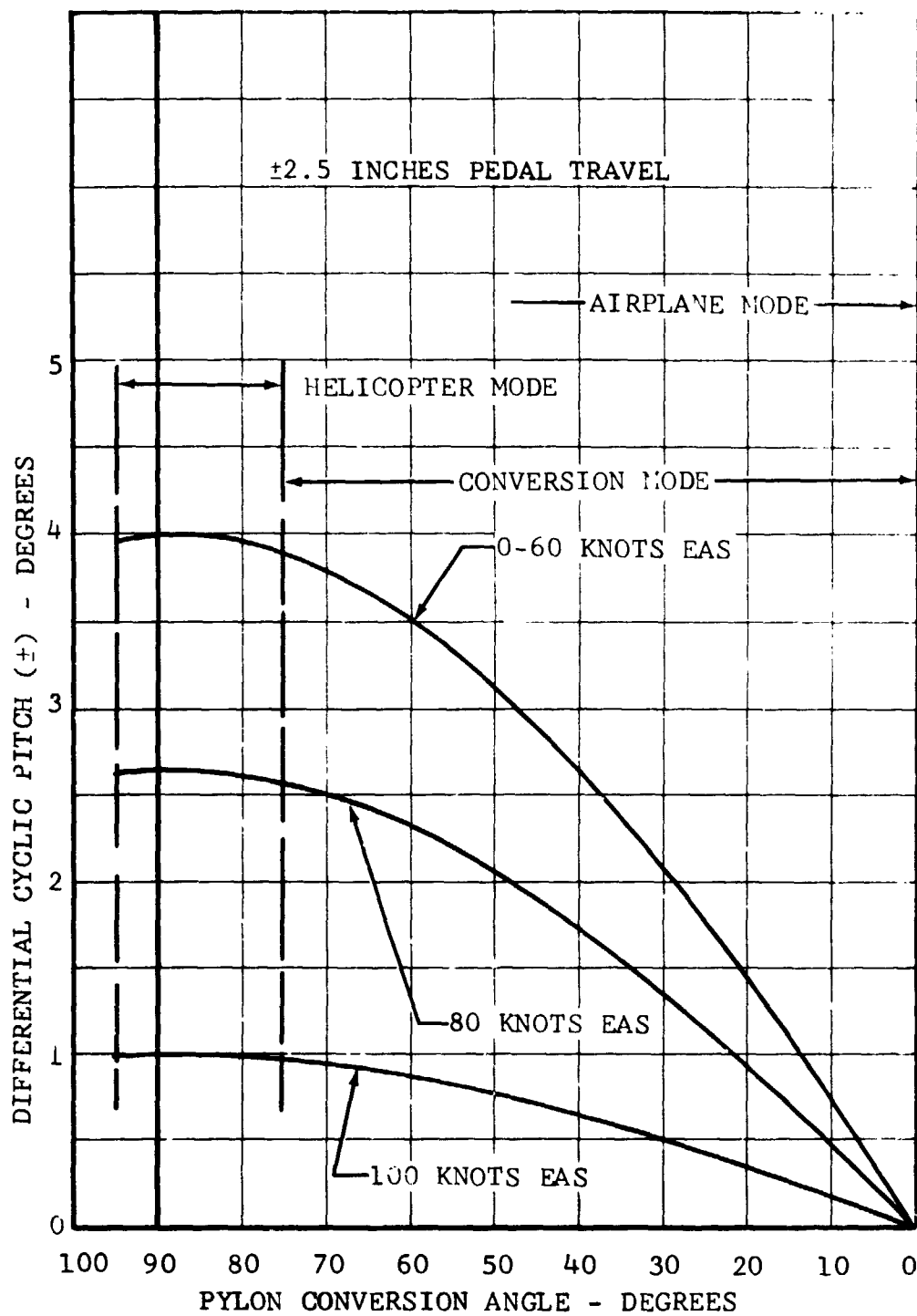


Figure III-10. Differential Cyclic Pitch Versus Conversion Angle.

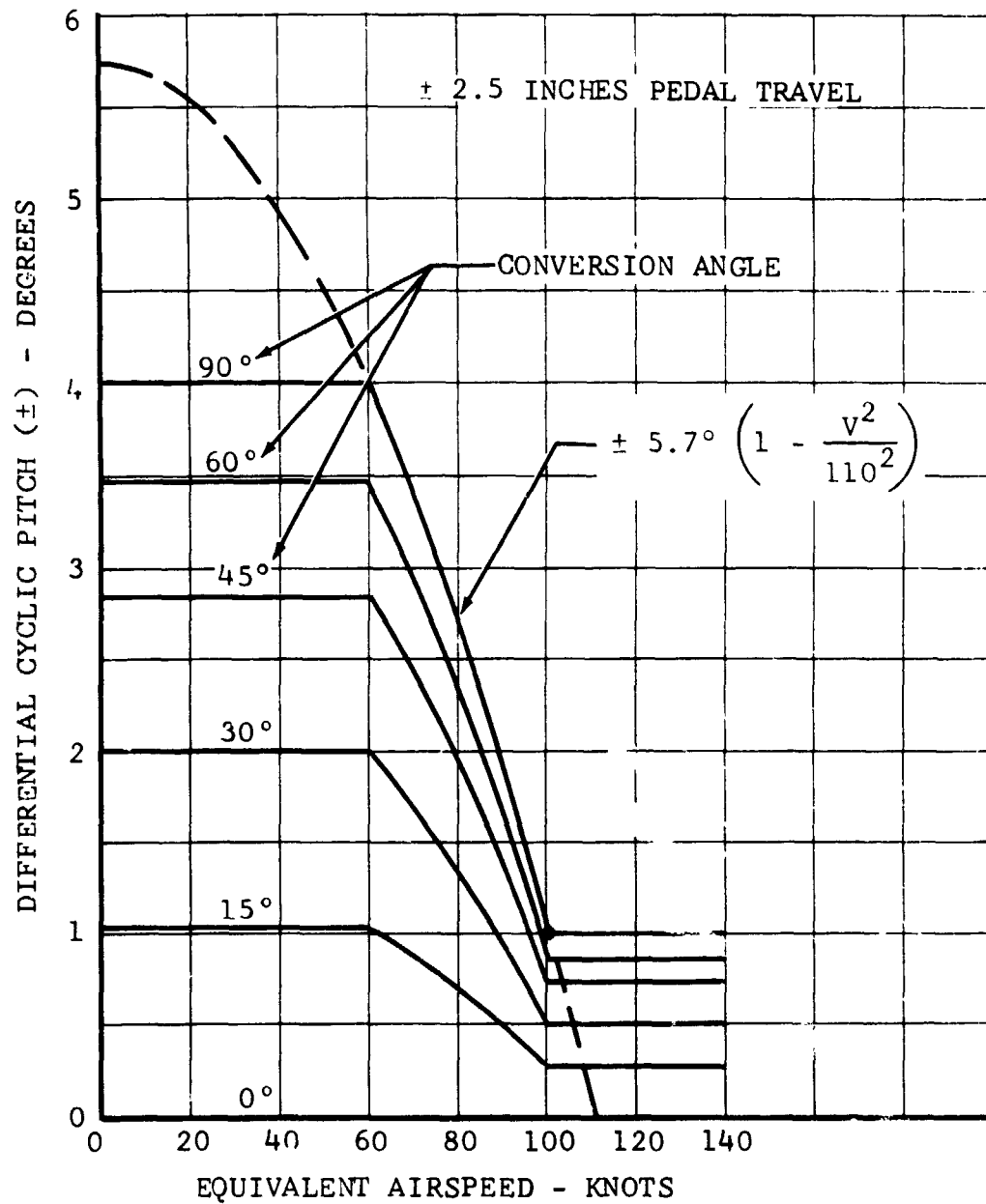


Figure III-11. Differential Cyclic Pitch Versus Airspeed.

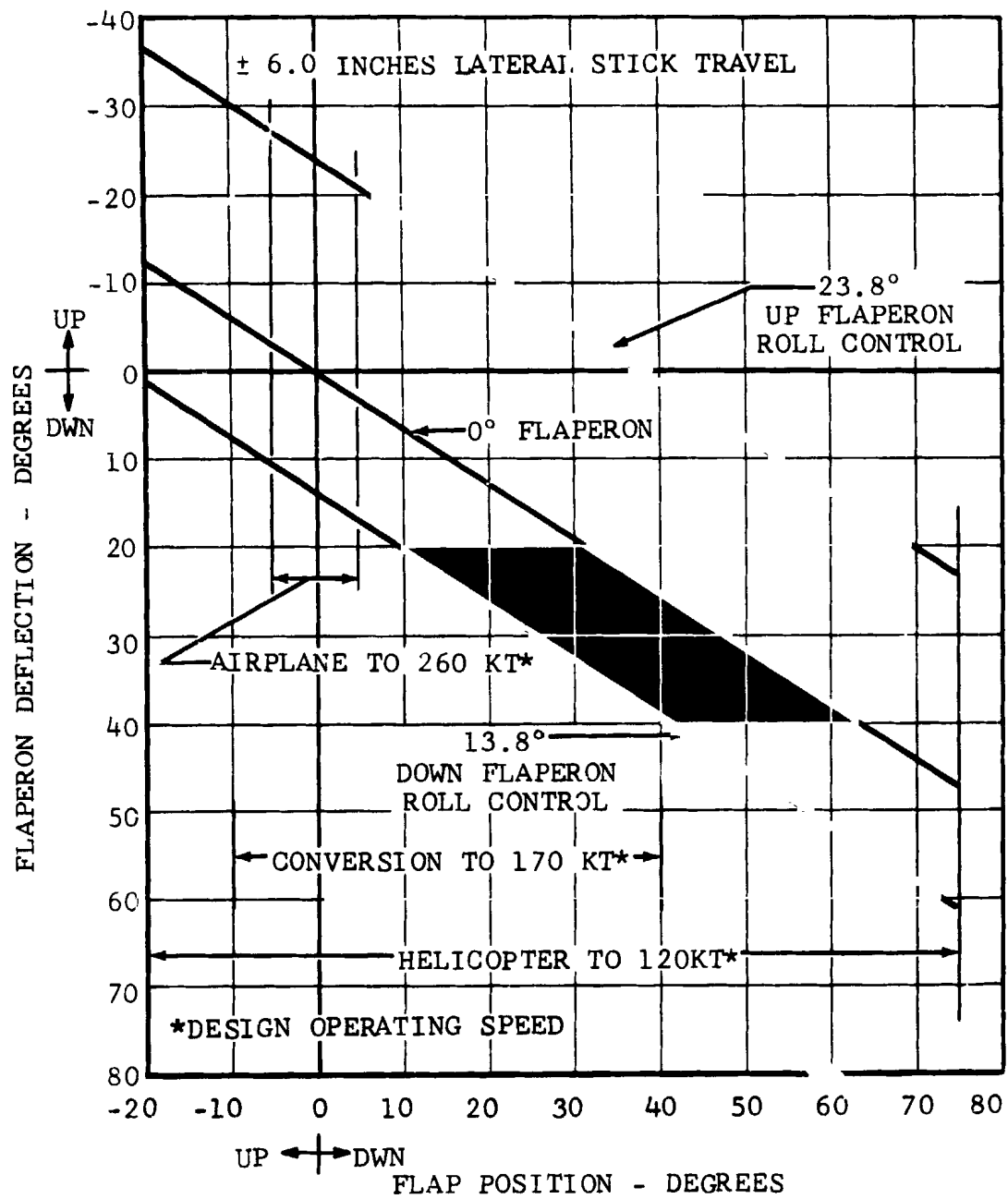


Figure III-12. Flaperon Deflection Versus Flap Position.

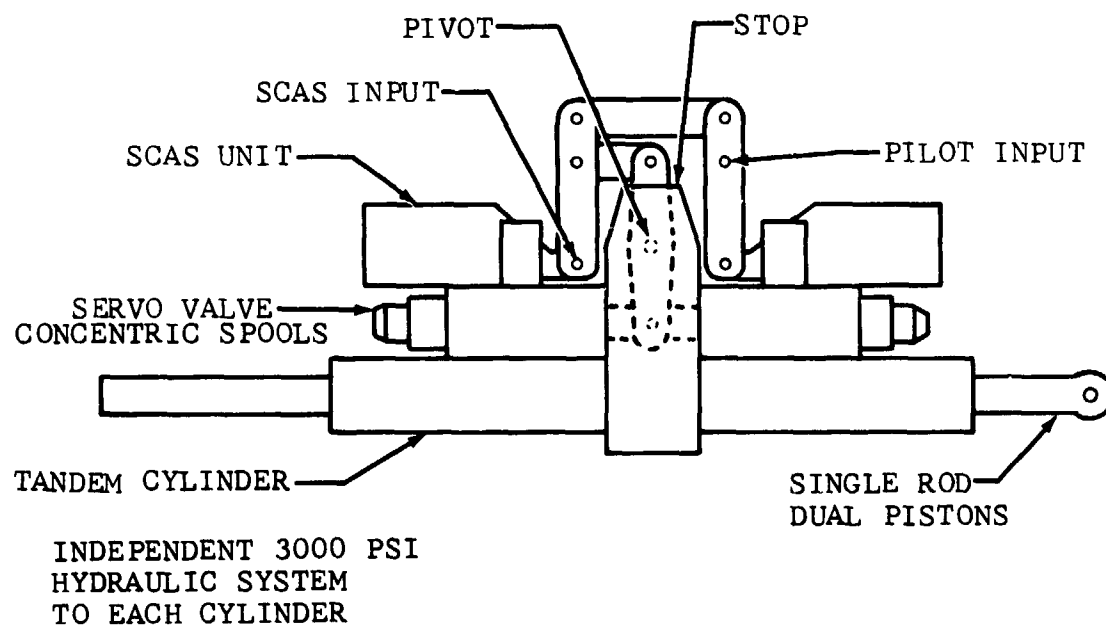


Figure III-13. Typical Hydraulic Boost Cylinder.

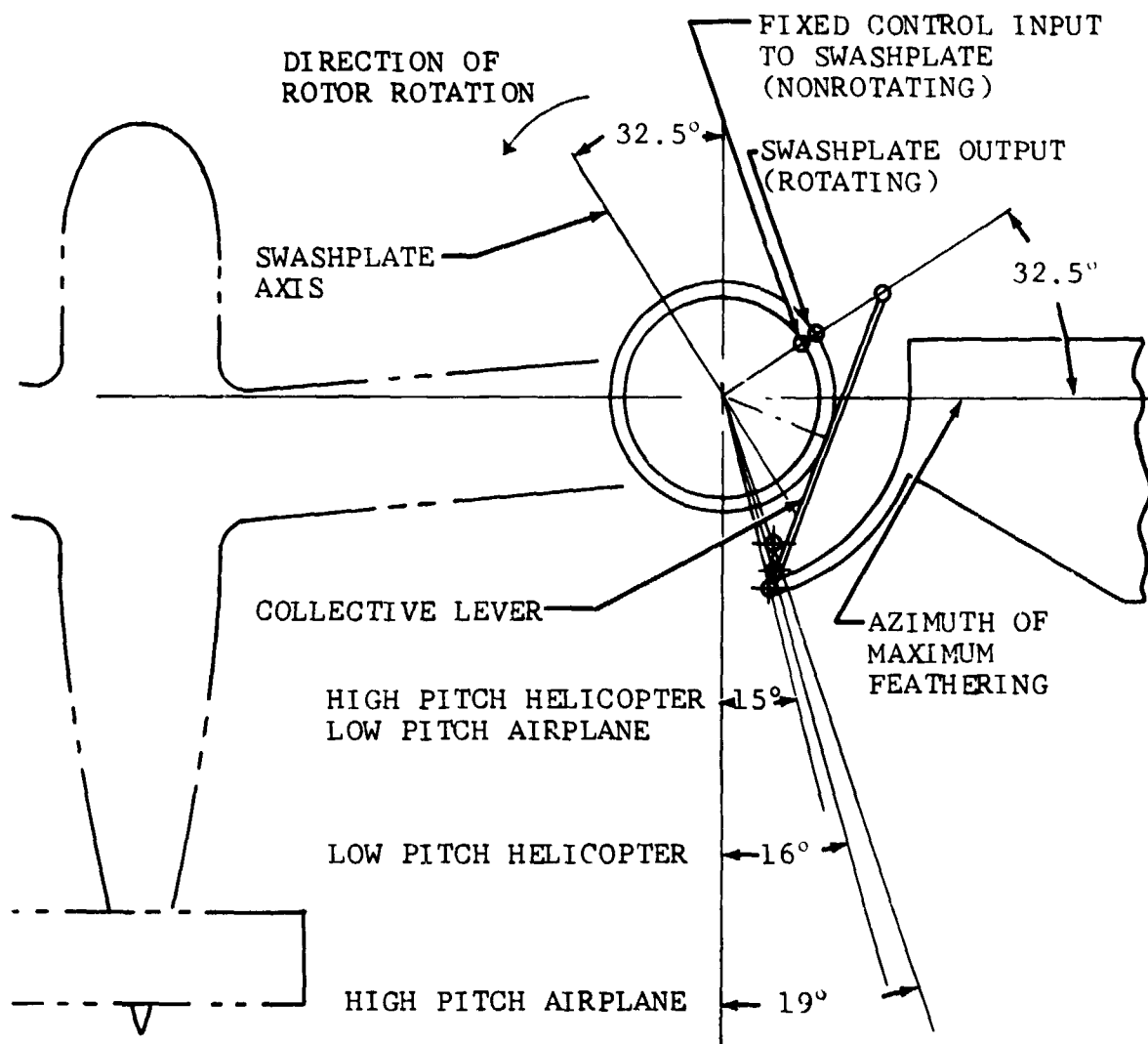


Figure III-14. Schematic of Proprotor Control Geometry.

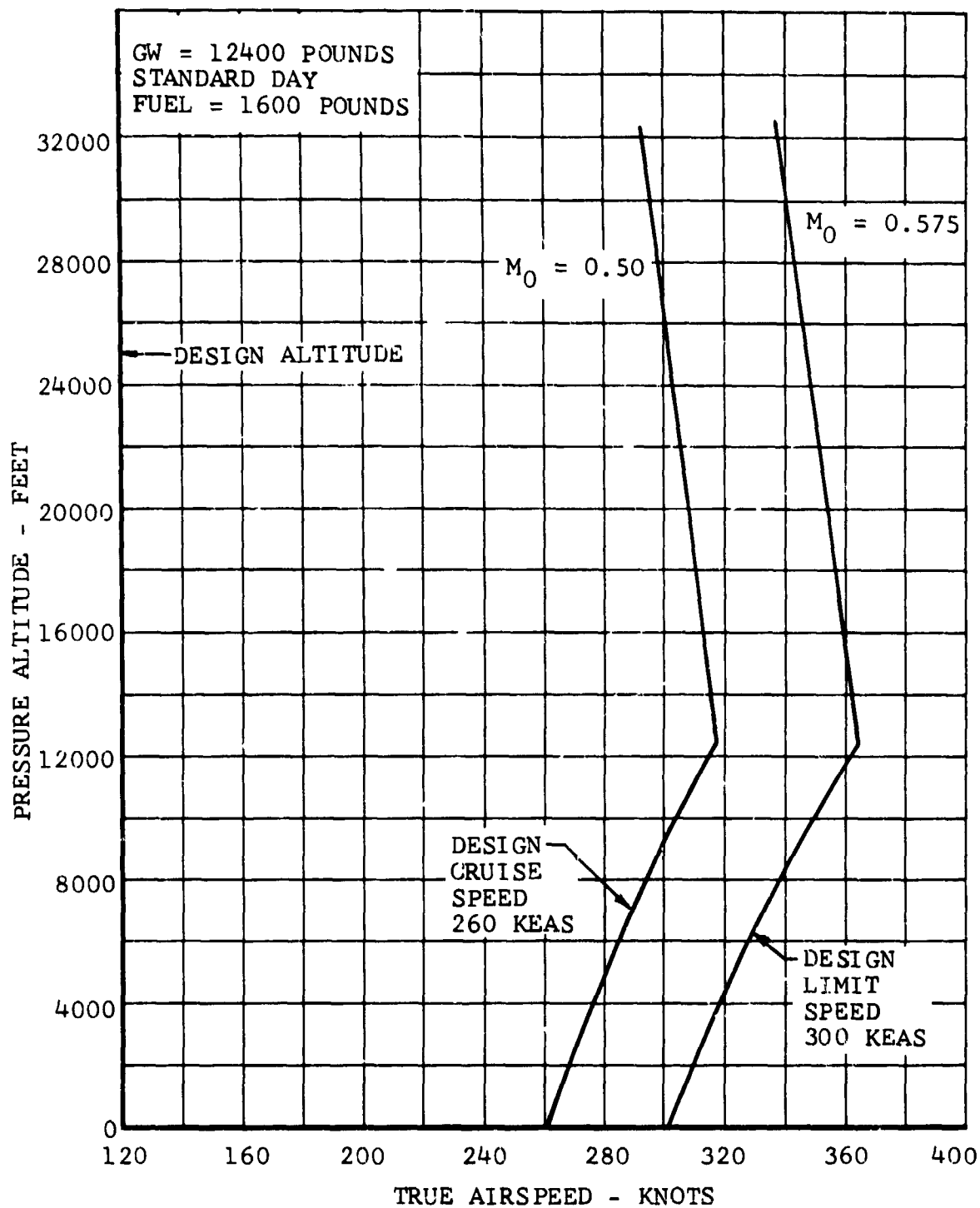


Figure III-15. Model 300 Design Airspeed Versus Altitude.

IV. WEIGHT ANALYSIS

The current estimated weight empty of the Model 300 is 7390 pounds. This weight is a combination of actual weights of most propotor and power transmission components, calculated weights of wing and control system components, and estimated weights of the remaining structure, systems, and equipment. A breakdown of this weight in MIL-STD-451 Group Weight Statement format is presented in Table IV-I, and the source of these group weights are subsequently discussed.

Useful load items included in each of the three evaluation mission gross weights are shown in Table IV-II. The payload weight includes necessary flight-test monitoring equipment and mission simulated weight.

TABLE IV-I. MODEL 300 GROUP WEIGHT STATEMENT

Proprotor Group		895
Blade Assembly	565	
Hub Assembly	270	
Spinner	60	
Wing Group		734
Tail Group		226
Horizontal	125	
Vertical Tail	101	
Body Group		1079
Alighting		350
Flight Controls Group		574
Cockpit Controls	53	
Proprotor, Nonrotating	247	
Proprotor, Rotating	171	
Fixed Wing	103	
Engine Section		316
Engine Mount	-	
Firewall	125	
Cowl	191	

TABLE IV-I. Concluded

Propulsion Group		2265
Engine Installation	732	
Conversion System	128	
Air Induction	66	
Exhaust System	11	
Lubrication System	35	
Fuel System	118	
Engine Controls	41	
Starting System	59	
Proprotor Governor	20	
Drive System	1055	
Gearboxes	933	
Transmission Drive	56	
Rotor Drive	66	
Instrument Group		111
Hydraulic and Pneumatic Group		105
Electrical Group		283
Electronics		34
Furnishings and Equipment		310
Personnel Accommodations	188	
Miscellaneous Equipment and Furnishings	64	
Emergency Equipment	58	
Air Conditioning Equipment		58
WEIGHT EMPTY, POUNDS		7390

A. PROPROTOR GROUP

The proprotor group weight is the sum of actual weights of the proprotor assemblies, including blades, hub, spinners, and associated linkages and hardware as shown on Bell Drawings 300-960-002, 300-010-001, and 300-010-100.

B. WING GROUP

Weights for the wing and associated control surfaces were calculated from detail drawings of structural components which were sized by a complete stress analysis. The wing arrangement is shown on Bell Drawing 300-960-007.

TABLE IV-II. MISSION GROSS WEIGHTS

	Typical Test Weight	Normal Gross Weight	STOL Gross Weight
Crew	400	400	400
Fuel - Usable	1600	1600	1600
- Trapped	14	14	14
Oil - Engine	35	35	35
- Trapped	12	12	12
- Transmission and Gearbox	58	58	58
Payload	1191	2591	5491
Useful Load	3310	5010	7610
Weight Empty	7390	7390	7390
Mission Gross Weight	10700	12400	15000

C. TAIL GROUP

Weights for the tail assemblies, shown on Bell Drawing 300-960-008 were estimated from layouts. The unit weights obtained compare favorably with those for similar designs operating in comparable flight regimes as shown in Table IV-III.

TABLE IV-III. TAIL SURFACE UNIT WEIGHTS

Model	Horizontal Tail (lb/sq ft)	Vertical Tail (lb/sq ft)
XV-5A	1.81	2.13
XC-142	2.31	2.21
AC-1	2.23	1.86
262	2.44	2.44
266 Bell	2.68	2.28
300 Bell	2.40	2.00

D. BODY GROUP

The fuselage of the Model 300 is a nonpressurized semi-monocoque structure shown on Drawing 300-960-008. The basic fuselage weight was estimated from Bell-developed equations with penalties added for the flooring, doors, windows, and windshields. The estimated method of Reference 3 was used to verify the fuselage weight. Inasmuch as this method is based on aircraft operating in a higher speed regime than the Model 300, it is felt that the results will be conservative.

The estimating method considers the total fuselage weight to be the sum of the basic weight required to provide minimum skins, stringers or longerons, and circumferential stiffeners to resist basic flight loads plus weight penalties incurred to support concentrated loads and redistribute around cutouts and through joints. Basic weight is F_B , as defined by the expression

$$F_B = 1.123 S + f (N_Z, Q, L, h)$$

The 1.123 constant is based on a minimum skin of 0.040-inch 7075 aluminum plus 0.038 equivalent gage to account for stiffeners (i.e., 0.078 inch x 0.10 pounds/cubic inch x 144 square inches/square foot equal 1.123 pounds/square foot). Because the Model 300 loadings and design permit use of minimum skin thickness of 0.020 aluminum, this factor was reduced to $(0.020 + 0.020) \times 0.10 \times 144 = 0.58$. Also, because the weight of the fuselage and contents is less than 4000 pounds, the function "f" is negligible. Therefore,

$$F_B = 0.58 S = 316 \text{ lb}$$

Penalties were then determined as shown in Table IV-IV.

TABLE IV-IV. FUSELAGE WEIGHT PENALTIES

Nose Gear Penalty	33
Bulkhead = $0.00025 W_L N_L$	5
Body Cutout = $0.4 \text{ lb/in} \times 38 \text{ in}$	15
Door = $2.0 \text{ lb/sq-ft} \times 4.1 \text{ sq-ft}$	8
Door Mechanism	5
Main Gear Penalty	196
Bulkhead = $0.001 W_L N_L$	21
Body Cutout = $0.8 \text{ lb/in} \times 58 \times 2$	93
Door = $2.0 \text{ lb/sq-ft} \times 12.5 \text{ sq-ft} \times 2$	50
Door Mechanism	32

TABLE IV-IV. Concluded

Canopy and Windshield Penalty (from Figure IV-1)	166
Cockpit Penalty	116
Bulkhead = 2 lb/sq-ft x 25 sq-ft	50
Body Cutout = 0.5 lb/in x 74 in	37
Flooring = 1.0 lb/sq-ft x 29 sq-ft	29
Tail Support Structural Penalty = $0.15 \times W_T$	34
Wing Attachment Structural Penalty = $0.0005 N_Z W$	30
Equipment Support Penalty = 0.5 lb/cu-ft x 20 cu-ft	10
Cargo Floor Penalty = 1.0 lb/sq-ft x 47 sq-ft	47
Door Penalty	31
Body Cutout = 0.4 lb/in x 28 in	11
Door = 2 lb/sq-ft x 10 sq-ft	20
Miscellaneous	
Penalty = $0.1 \times$ Total of Above Penalties	67
Total Fuselage Penalty Weight = F_P , Pounds	730
Total Fuselage Weight = $F_B + F_P$, Pounds	1046
Model 300 Fuselage Weight, Pounds	1079

Parameters and symbols used in the above equations are shown in Table IV-V.

E. ALIGHTING GEAR GROUP

Gear structure weight was taken from a gear design layout and stress analysis. Hydraulic system and control system weights were estimated from layout drawings. Rolling gear components and their associated weights, which were taken from vendor catalog data, are shown in Table IV-VI.

TABLE IV-V. FUSELAGE PARAMETERS AND SYMBOLS

Parameter or Symbol	Description	Value for Model 300
F_B	Fuselage Basic Weight	316 lb
S	Fuselage Wetted Area	544 sq-ft
f	Fuselage Size/Weight Function	Negligible
N_Z	Ultimate Flight Load Factor	4.75
Q	Weight of Fuselage and Contents	3483 lb
L	Fuselage Length	41.0 ft
h	Fuselage Depth	6.2 ft
F_P	Fuselage Penalty Weight	730 lb
N_L	Ultimate Landing Load Factor at 9500 Pounds	2.25
A_W	Windshield Area	56 sq-ft
W_T	Tail Group Weight	226 lb
W_L	Landing Gross Weight	9500 lb
W	Normal Gross Weight	12400 lb

TABLE IV-VI. ROLLING GEAR COMPONENT DATA

Item	Nose Gear			Main Gear		
	Number	Size	Weight (lb)	Number	Size	Weight (lb)
Tire and Tube	2	5.00 x 5	12	2	8.50 x 10	51
Wheel	2	5.00 x 5	7	2	8.50 x 10	26
Brake			-			14
Total			19			91

A comparison of the Model 300 gear weight as a percentage of design weight with similar data for current generation V/STOL aircraft is presented in Table IV-VII.

TABLE IV-VII. ALIGHTING GEAR GROUP WEIGHT COMPARISON

Model	Landing Gross Weight (lb)	Gear Group Weight (lb)	Percent
XC142	37474	1211	3.23
X22A	14500	432	2.94
XV-5A	9200	402	4.56
XV-4A	7200	291	4.04
300	9500	350	3.68

F. CONTROLS GROUP

This group includes the weights of cockpit controls, proprotor controls (both fixed and rotating), and wing and tail surface controls. Also included are the phasing mechanisms which interconnect the proprotor controls to the airplane controls in the helicopter flight mode and disconnect them in the airplane mode, and all linkages. All wing and proprotor control system weights were calculated from detail and installation drawings, and other system weights estimated from layouts.

G. ENGINE SECTION AND NACELLE GROUP

This group includes the firewalls and wingtip-mounted pylon cowl- ing; no engine mount weight is included because each engine bolts directly to a main transmission case.

Weights for the firewalls and cowl- ing were calculated from de- tailed drawings using gages determined by structural and FAA specification requirements. Although the firewall and cowl- ing weights of 125 and 191 pounds, respectively, are greater than those of comparable size contemporary aircraft, they reflect the recent, more stringent interpretation of the FAA requirements for fire containment. A lesser portion of the weight increase is due to an increase in access capability for ease of main- tenance and inspection.

H. PROPULSION GROUP

1. Engine Installation

The weights of the Bell-furnished input shaft assemblies, which are mounted directly to the engines, have been added to the

343-pound weights for each of the two PT6C-40(VX) engines and 20 pounds of residual fluids to make up the total engine installation weight.

2. Conversion System

This group weight includes vendor-furnished weights of the two conversion actuators, the hydraulic power systems and the inter-connect shafting which assures synchronization of the actuators and thereby the positions of the pylons.

3. Air Induction System

Weights for the air induction ducts, engine inlet screens, and ejector assemblies were calculated from detail drawings. Also included in this group are the weights of two blowers, taken from vendor data on similar units.

4. Exhaust System

The calculated weights of the exhaust stack installations and the exhaust ejector baffles total 11 pounds.

5. Lubrication System, Engine

Vendor weights for the oil coolers and valves were added to calculated weights of plumbing and ducting derived from installation drawings to give the current total weight of 35 pounds.

6. Fuel System

The fuel system weight was estimated from layout drawings of the four wing-located fuel cells and a distribution system schematic, using unit weights and component weights from similar equipment on existing aircraft.

7. Engine Controls

The engine control system consists of droop-compensator and power-lever controls for each engine. Weights for these components were calculated from detail drawings.

8. Starting System

Weights in this group consist of vendor-furnished weight for two starters (27.3 pounds each) and calculated weights of associated mounting and installation components.

9. Proprotor Pitch-Governor Control

The proprotor pitch-governor is an electro-hydraulic system which maintains selected proprotor rpm in airplane mode.

Electronic equipment, actuators and associated supports, and linkage weights were based on similar components used in existing systems.

10. Drive System

Bell Drawing 300-960-004 depicts the engine-to-proprotor power transmission system. The interconnect system which provides power to both proprotors from either engine, in case of failure of one of the engines, is presented in Drawing 300-960-007.

Actual weights of components comprise approximately 97 percent of the drive system weight of 1055 pounds.

Drive system component weights are given in Table IV-VIII.

TABLE IV-VIII DRIVE SYSTEM COMPONENT WEIGHTS

	Weight (lb)
Gearboxes	933
Main Transmission (both)	873
Gears, Bearings, Shafts	323
Housings (including case extension for engine support and spindle attachment)	365
Freewheeling Unit	8
Lube System	36
Accessory Drives	12
Spindle and Bearings	58
Liners, Hardware and Miscellaneous	71
Center Gearbox	60
Transmission Drive	56
Rotor Drive	66
TOTAL	1055

I. INSTRUMENT GROUP

The instrument group consists of engine, flight and navigation instruments, transmitters, and installations as shown in Table IV-IX. Weights for the instruments and transmitters were based on those currently in use on present day helicopters. Installation weights are assumed to be the same except for wiring, which has been increased to compensate for greater distance between the cockpit and propulsion group.

TABLE IV-IX. INSTRUMENT GROUP WEIGHTS

Instrument	No.	Indi- cators (lb)	Trans- mitters (lb)	Instal- lation (lb)	Total (lb)
Altimeter	1	1.5			1.5
Airspeed	2	1.7	0.9	0.9	3.5
Clock	2	1.0			1.0
Standby Compass	1	0.8			0.8
Angle of Attack	2	2.5			2.5
Vertical Speed	2	2.4			2.4
Turn and Slip	2	3.8			3.8
Attitude	1	2.8			2.8
Vertical Gyro	1	6.0	9.0	4.2	19.2
Gyro Compass	1	6.5	7.3	4.8	18.6
Outside Air Temperature	1	0.2			0.2
Fuel Flow	2	1.8			1.8
Transmission Oil Pressure	2	1.8	0.8		2.6
Engine Oil Temperature	2	1.8	0.4		2.2
Engine Oil Pressure	2	1.8	2.0		3.8
Fuel Pressure	1	0.6	1.2		1.8
Transmission Oil Temperature	2	1.8	0.4		2.2
Gas Producer Tachometer	2	1.8	1.6		3.4
Fuel Quantity	1	0.5	3.0		3.5
Dual Torquemeter	2	1.8	2.0	1.2	5.0
Triple Tachometer	1	4.4	2.4	1.2	8.0
Hydraulic Pressure	2	1.8	2.0	2.0	5.8
Turbine Inlet Temperature	2	1.8			1.8
Engine Output Torque	2		0.8		0.8
Interconnect Torque	2		2.0		2.0
RPM Warning	1	0.3	2.2		2.5
Position, Flap	2	2.2	0.1	0.5	2.8
Position, Main Gear	1	0.3	0.9	2.0	3.2
Conversion	2	1.1	0.1	0.5	1.7
TOTAL INSTRUMENT GROUP WEIGHT					111.2

J. HYDRAULICS GROUP

Hydraulic power is utilized to extend and retract the landing gear and flaps; to power the flaperons and pylon conversion actuators; and to provide boost capability in the prop rotor governor and cyclic and collective control systems. The Model 300 has a completely dual 300 psi hydraulic system. Only the weights of the pumps, reservoirs, filters, valves, and interconnecting plumbing are included in the main system weight. Weights of components and plumbing providing power to a specific system are carried in the weight of that system.

K. ELECTRICAL GROUP

The ac-dc electrical system on the Model 300 is powered by starter-generators attached to the engines. Two 13-ampere-hour batteries are provided to furnish power for the starter-generators. Weights of these and other major components are based on vendor data. Wiring and hardware weights were estimated from wiring diagrams and routing layouts. The weights of the components are listed in Table IV-X.

TABLE IV-X. ELECTRICAL GROUP WEIGHTS

	Weight (lb)
<u>DC System</u>	
Batteries	48
Battery Installation	2
Transformer	4
Voltage Regulator	6
Switches, Rheostats and Panels	4
Relays	19
Wiring and Miscellaneous	87
Equipment Supports	16
<u>AC System</u>	
Inverter	26
Ammeters and Voltmeters	2
Switches, Rheostats, and Panels	26
Circuit Breakers and Fuses	10
Junction and Distribution Boxes	3
Relays	1
Wiring and Miscellaneous	14
Lights	15
TOTAL ELECTRICAL GROUP WEIGHT	283

L. ELECTRONIC GROUP

Electronic equipment consists of AN/ARC-114 VHF-FM and AN/ARC-115 VHF radios, Collins 613L-2 transponder system and a four-station ICS, C-6533. Weights for these systems were taken from existing installations used in current aircraft.

M. FURNISHINGS AND EQUIPMENT GROUP

The furnishings and equipment group includes crew ejection seats, furnishings, miscellaneous equipment, and emergency equipment. The weights shown in Table IV-XI were based on similar equipment presently in use on existing aircraft.

TABLE IV-XI. FURNISHINGS AND EQUIPMENT GROUP WEIGHTS

	Weight (lb)
<u>Accommodations</u>	
Crew Seats	176
Crew Safety Belts	6
Crew Shoulder Harness and Inertia Reels	6
<u>Miscellaneous Equipment</u>	
Windshield Wiper	14
Instrument Panel	15
Consoles	20
<u>Furnishings</u>	
Soundproofing (cockpit)	15
<u>Emergency Equipment</u>	
First Aid Kit	4
Fire Detection System	5
Portable Fire Extinguisher	7
Engine Fire Extinguisher	42
TOTAL FURNISHINGS AND EQUIPMENT GROUP WEIGHT	310

N. AIR-CONDITIONING EQUIPMENT GROUP

The air-conditioning system of the Model 300 is used for forward window defogging and heating and cooling of the cockpit compartment. The environment control unit is included in this group.

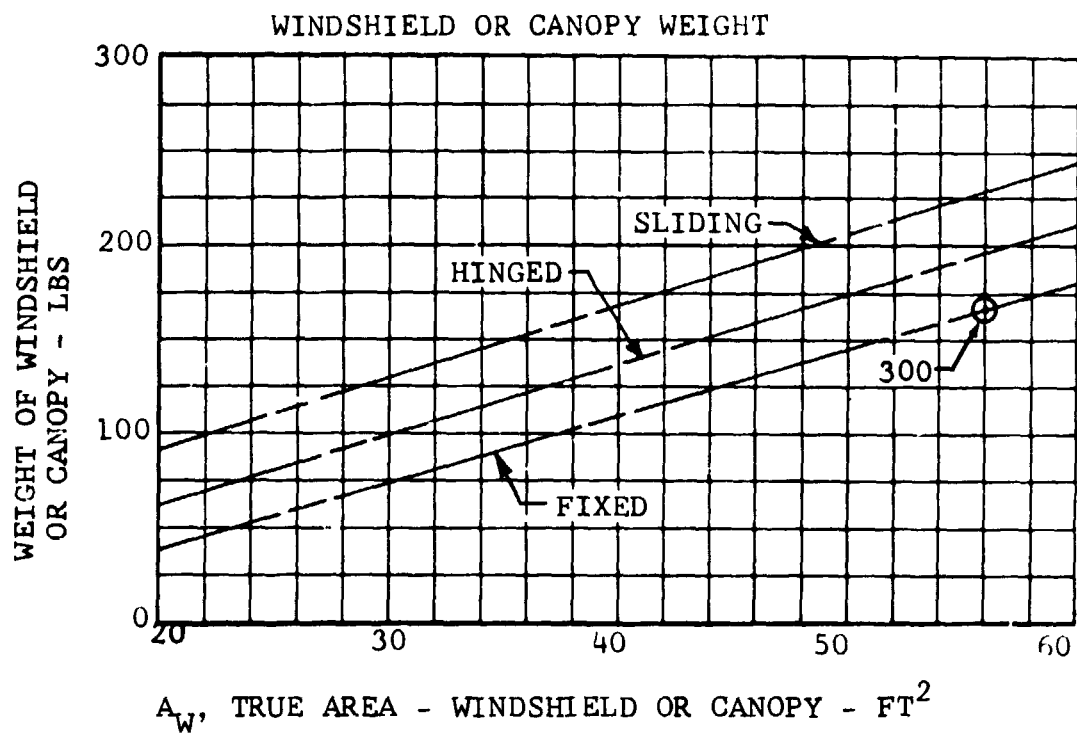


Figure IV-1. Fuselage Weight Estimation Parameters.

V. PERFORMANCE

A. SUMMARY

At 10,700 pounds gross weight, the Model 300 tilt proprotor aircraft hovers out of ground effect at 9600 feet on a standard day and 4000 feet on a 95°F day. Maximum speed at this weight is 314 knots at 8,000 feet. At the normal gross weight, 12,400 pounds, out-of-ground-effect hover ceiling is 4600 feet on a standard day. Making use of the running takeoff capability, a 50-foot obstacle can be cleared in 2750 feet on a 95°F day at 4000 feet elevation at a gross weight of 15,000 pounds. Payload for this condition can be up to 5491 pounds. The performance of the Model 300 tilt-proprotor aircraft provides research capabilities with useful loads from 3300 to 7600 pounds. Full-fuel payloads range up to 5491 pounds. Flight endurance in cruise can be up to 2.9 hours with takeoff at normal gross weight with a 2891-pound payload. Performance is summarized in Table V-I.

B. AIRFRAME AERODYNAMICS

The aerodynamic characteristics of the Model 300 tilt-proprotor airframe has been determined through extensive tests of a one-fifth-scale model. These tests have been conducted in the LTV low-speed 7- by 10-foot tunnel and the 16-Foot Transonic Dynamics Tunnel at NASA-Langley. A wide range of Reynolds numbers (0.8 to 7.8 million) and Mach numbers (up to 0.72) have been covered in these tests.

Vortex generators on the wing and several empennage configurations were tested. The "H-tail" empennage was selected and is used in the lift and drag analyses which follow.

1. Lift Analysis

Lift coefficient versus fuselage angle of attack is shown on Figure V-1 for two configurations. One is airplane mode with pods full down and flaps up. The other is for helicopter mode with pods vertical and flaps down 40 degrees. Both curves include the elevator lift required to trim the airframe moments to zero. Vortex generator effects are included.

Both the LTV and Langley tests included vortex generators. In these tests, 19 counter-rotating vortex generators per side were used. These were of the following full-scale dimensions:

Height = 1.5 inches

Root Chord = 4 inches

Tip Chord = 2 inches

Incidence was 20 degrees with respect to a buttline plane and extended inboard from 15 inches from the wing-pod junction at

TABLE V-I. PERFORMANCE SUMMARY

Mission	Units	Typical Test Weight	Normal Gross Weight	STOL Gross Weight
Takeoff Gross Weight	lb	10700	12400	15000
Crew	lb	400	400	400
Fuel Weight	lb	1600	1600	1600
Payload	lb	1191	2891	5491
<u>Helicopter Mode</u>				
Hovering Ceiling, OGE				
Standard Day	ft	9600	4600	--
95°F Day	ft	4000	--	--
Takeoff Distance 4000 Feet, 95°F Day	ft	--	930	2750
Maximum Speed, NRP				
Twin Engine, Sea Level	kt	131	130	124
Maximum Rate of Climb at Sea Level				
Twin Engine, NRP	ft/min	2890	2280	1450
Single Engine, 30 min power	ft/min	850	520	--
<u>Airplane Mode</u>				
Maximum Speed, 30 min power	kt	314	312	302
Altitude for Maximum Speed	ft	8000	8000	5000
Single Engine Maximum Speed at 10,000 Feet	kt	216	205	--
Maximum Rate of Climb				
Twin Engine, Sea Level	ft/min	3700	2900	2100
Single Engine, Sea Level	ft/min	1065	670	155
Service Ceiling				
Twin Engine	ft	29000	26800	22000
Range				
Sea Level	nm	403	394	376
10,000 Feet	nm	523	496	457
20,000 Feet	nm	618	567	494
Average Cruise Speed				
Sea Level	kt	226	228	237
10,000 Feet	kt	232	234	242
20,000 Feet	kt	237	242	248

25 percent chord with 7.5-inch spacing. It is recognized that the test vortex generators are probably too large. No attempt was made in the wind-tunnel tests to optimize on size or spacing.

2. Drag Analysis

The drag curves on Figure V-2 are for the same configurations as the lift curves discussed in the preceding section. Elevator drag is added to account for trimming the airframe moments to zero. Both LTV and Langley test data are used in the drag determination. The test results indicate a slightly higher minimum drag than shown in Figure V-2, but the minimum and low C_L drag on this figure are considered attainable with an optimized vortex generator configuration. The anticipated improvement from reducing the vortex generator size and/or number is ΔC_D value of about 0.003.

The drag curve from Reference 1 is shown on Figure V-3 for comparison purposes. The improvement at the higher lift coefficients is due to the vortex generators eliminating trailing edge separation. At lower lift coefficients the difference is primarily due to conservative correction of the low Reynolds number LTV data to full scale. The Langley tests were made at very nearly full-scale Reynolds numbers. Figure V-4 presents C_D versus Mach number for C_L values from 0 to 0.6. The drag rise begins at 0.5 Mach number and does not affect Model 300 standard day performance since the maximum attainable level flight speed at any altitude does not exceed 0.5.

3. Proprotor Power Required

a. General

An aerodynamic description of the proprotor and a discussion of analytical methods is given in Reference 2. Airplane mode performance computations use the standard airfoil data given in Figures IV-2 through IV-5 of Reference 2.

For hovering, helicopter, and conversion performance, modified airfoil data tables are used. The use of these tables yields a closer correlation with full-scale test results. A discussion of these modifications are found in Reference 2.

b. Helicopter Mode Hovering

Power required versus thrust for out-of-ground-effect hover is shown in Figure V-5. For calculation of hovering ceilings, this curve is entered at a thrust value 1.07 times gross weight to account for proprotor download on the wing.

Figure of merit curves are given in Figure V-6. The upper curve is for the isolated proprotor and the lower curve includes the seven-percent download.

c. Helicopter Mode - Forward Flight

Sea level, standard performance in helicopter mode is shown in Figure V-7. These data are for a configuration with a mast tilt angle of 75 degrees (15 degrees from the vertical), flaps down 40 degrees, and flaperons down 25 degrees. Rotor downwash effects on wing angle of attack are included (60 percent of the average downwash velocity at the rotor disc was applied in the determination of wing angle of attack). The "side-by-side" effect was included by reducing prop rotor power required by an amount equal to 15 percent of the isolate prop rotor induced power for each speed and thrust.

Helicopter power required is obtained through the use of programs C81 and F35. Program C81 is used to obtain trimmed level flight data from which prop rotor lift and propulsive force are obtained. These values of lift and propulsive force are entered into F35 to obtain power required data. Program C81 also computes power required, but F35 is a more refined aerodynamic analysis as far as rotor performance is concerned, and is, therefore, better suited to precise performance analysis.

A typical wing-rotor lift-sharing curve is shown on Figure V-8. The prop rotors are producing the majority of lift throughout the helicopter speed range.

d. Conversion Mode

Power required data in conversion mode are shown in Figure V-9. Mast tilt angles from 0 to 90 degrees are shown with flaps down for all except one of the zero degree mast tilt cases. Programs C81 and F35 are used for conversion mode performance as previously discussed for the helicopter mode.

e. Airplane Mode

Prop rotor efficiency curves are shown in Figures V-10 through V-12 for sea level, 10,000 and 20,000 feet for a standard day. A curve is given on each figure denoting trimmed level flight conditions for a 12,400-pound gross weight. Prop rotor shaft horsepower required curves are shown in Figures V-13 through V-15 for standard day conditions for sea level, 10,000- and 20,000-foot altitudes.

4. Powerplant Performance

Power available and fuel flow are identical to that given in Reference 1. Helicopter mode power available is shown on Figure V-16, and helicopter mode fuel flow on Figure V-17. Figures V-18 and V-19 show takeoff, 30-minute, and maximum-continuous power available in airplane mode versus airspeed and altitude for standard day conditions. Fuel flow in airplane mode is given in Figure V-20. Engine installation losses are shown in Table V-II.

TABLE V-II. ENGINE INSTALLATION LOSSES

Inlet Pressure Loss	5.8 in. H ₂ O SLS
Exhaust Pressure Loss	3.0 in. H ₂ O SLS
Inlet Temperature Rise	2.7°F
Ram Recovery Loss	$(1 - \eta_{\text{RAM}}) q$ in. H ₂ O SLS
RAM	$1.0 - 14.4 \left(\frac{W_a}{\sigma V} \right)^2$
Extracted Horsepower Loss	11.5 hp
Twin Engine Transmission Efficiency	0.98
Single Engine Transmission Efficiency	0.97

5. Hover Ceilings

The hover ceilings shown in Figure V-21 are constructed by use of the given power required and power available curves. Single- and twin-engine operation is covered for standard day and a 95°F day. The gross weight for out-of-ground-effect hover is 14,100 pounds at sea level, standard day.

6. Rate of Climb

Maximum rate of climb in conversion mode from helicopter flight to airplane flight is shown in Figure V-22 for a 12,400-pound gross weight at sea level on a standard day. Flaps are down and tip speed is 700 feet per second.

Rate of climb versus altitude and gross weight in airplane mode is shown on Figure V-23 for flaps up and a cruise tip speed of 600 feet per second.

7. Flight Envelope and Maximum Speeds

Figure V-24 shows the airplane mode maximum speeds versus altitude with maximum continuous and 30-minute power for standard day operation at a gross weight of 12,400 pounds. Single-engine operation is also shown on this figure. The minimum flight speed is 1.2 times the flaps-up stall speed.

8. Specific Range

Nautical miles per pound of fuel are shown in Figures V-25 through V-27 for airplane cruise flight at sea level, 10,000- and 20,000-foot altitudes. Torque and engine power limits are shown on the figures.

9. Payload Range and Endurance

Payload versus range for takeoff at 12,400 pounds is shown on Figure V-28. Curves are shown for 10,000 and 20,000-foot cruise altitudes, with and without auxiliary fuel. Allowances include two minutes at normal rated power for warmup and takeoff, climb to cruise, and 10 percent of initial fuel for reserve. Weight for auxiliary tankage is accounted for as required. Range credit is taken for climb to cruise altitude, but not for descent. Endurance versus airspeed for helicopter and airplane mode is shown on Figure V-29 for altitudes of sea level and 10,000 feet in helicopter mode, and sea level, 10,000 and 20,000 feet in airplane mode. The same fuel allowances are used in the payload-range computations discussed above.

10. STOL Performance

Takeoff distance to clear a 50-foot obstacle versus gross weight is shown in Figure V-30. These data are for acceleration and climbout with a 70-degree mast angle (20 degrees from vertical) at 4000 feet altitude on a 95°F day. Even at a gross weight of 15,000 pounds, the 50-foot obstacle can be cleared in 2750 feet.

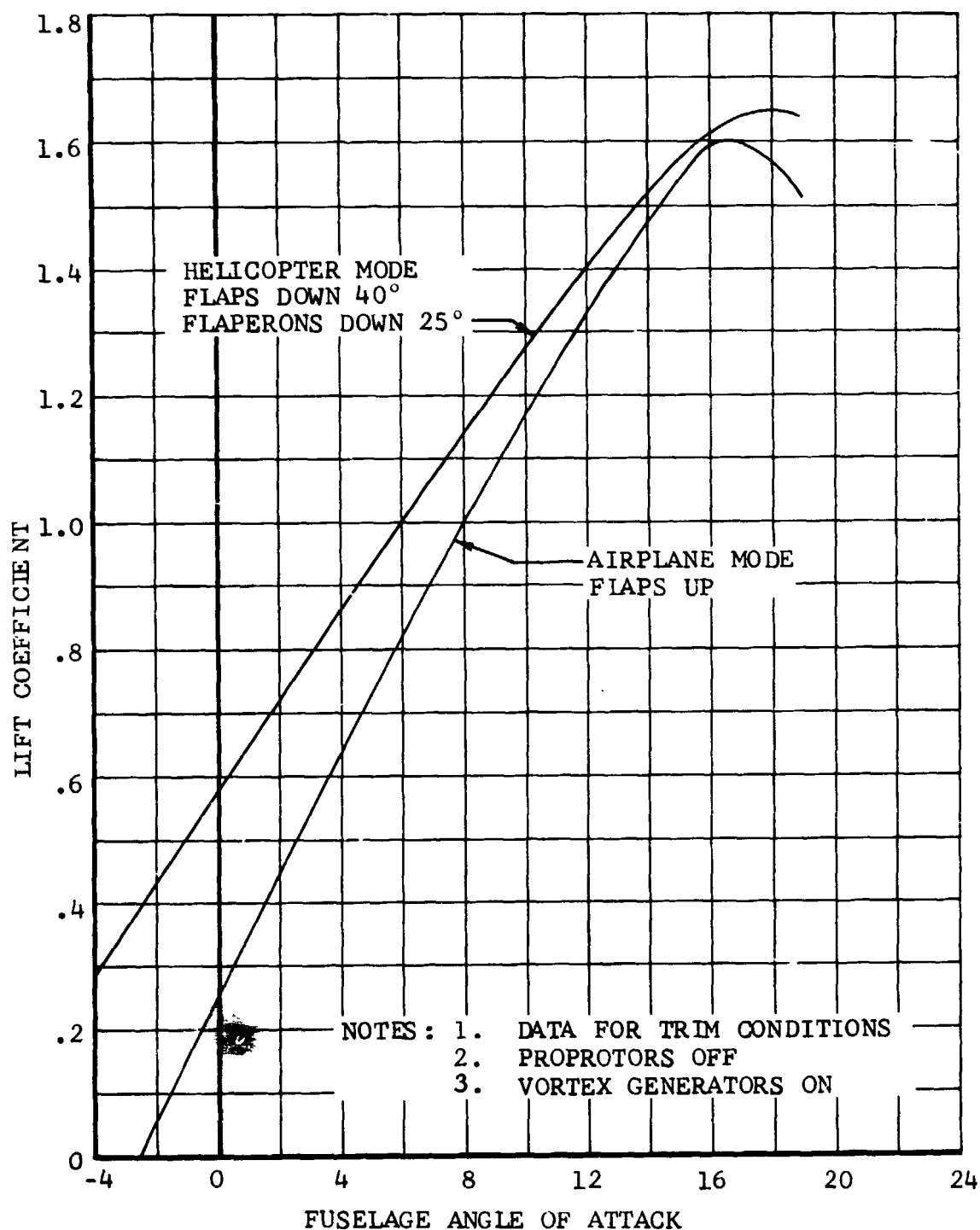


Figure V-1. Airframe Lift Coefficient Versus Fuselage Angle of Attack.

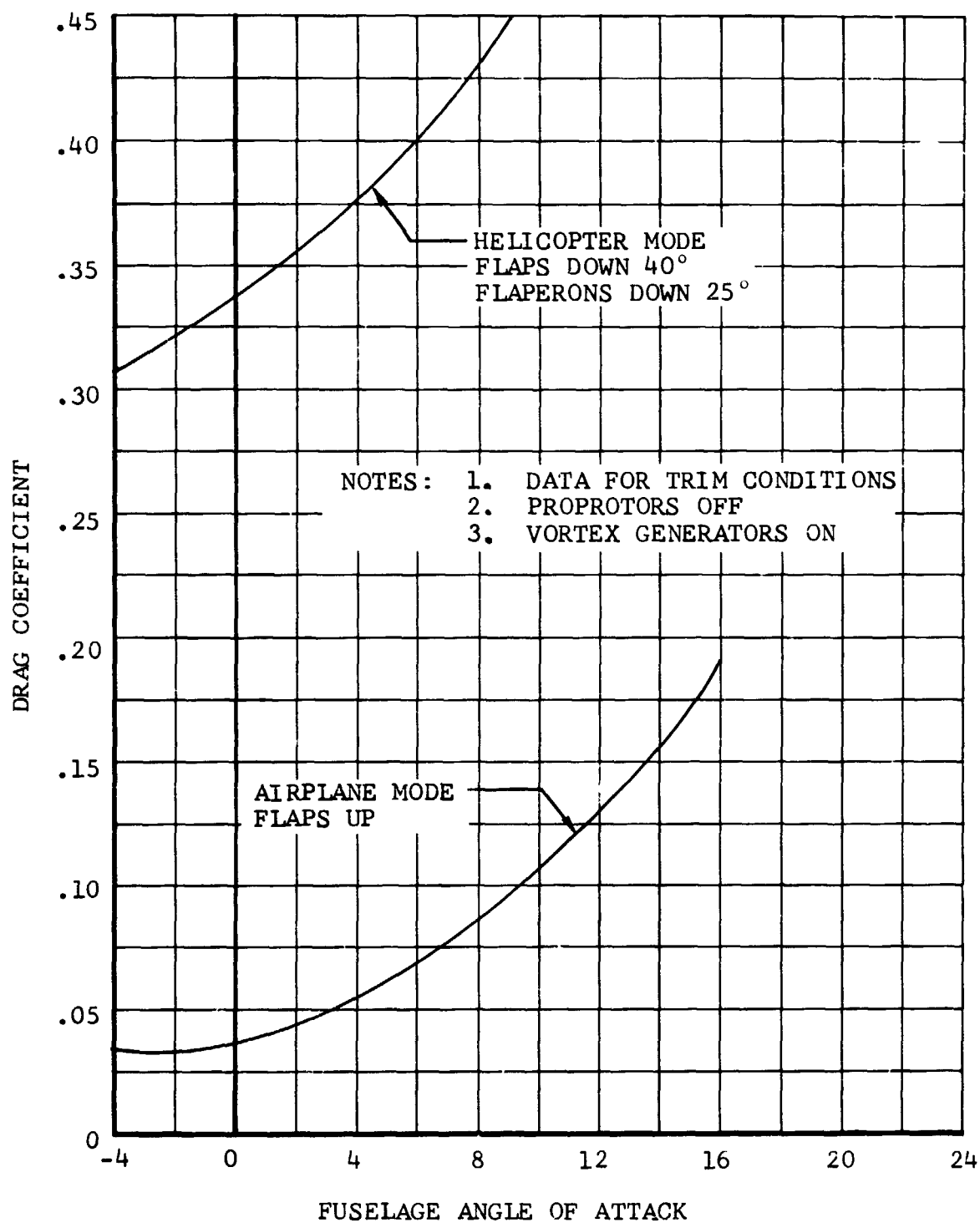


Figure V-2. Airframe Drag Coefficient Versus Fuselage Angle of Attack.

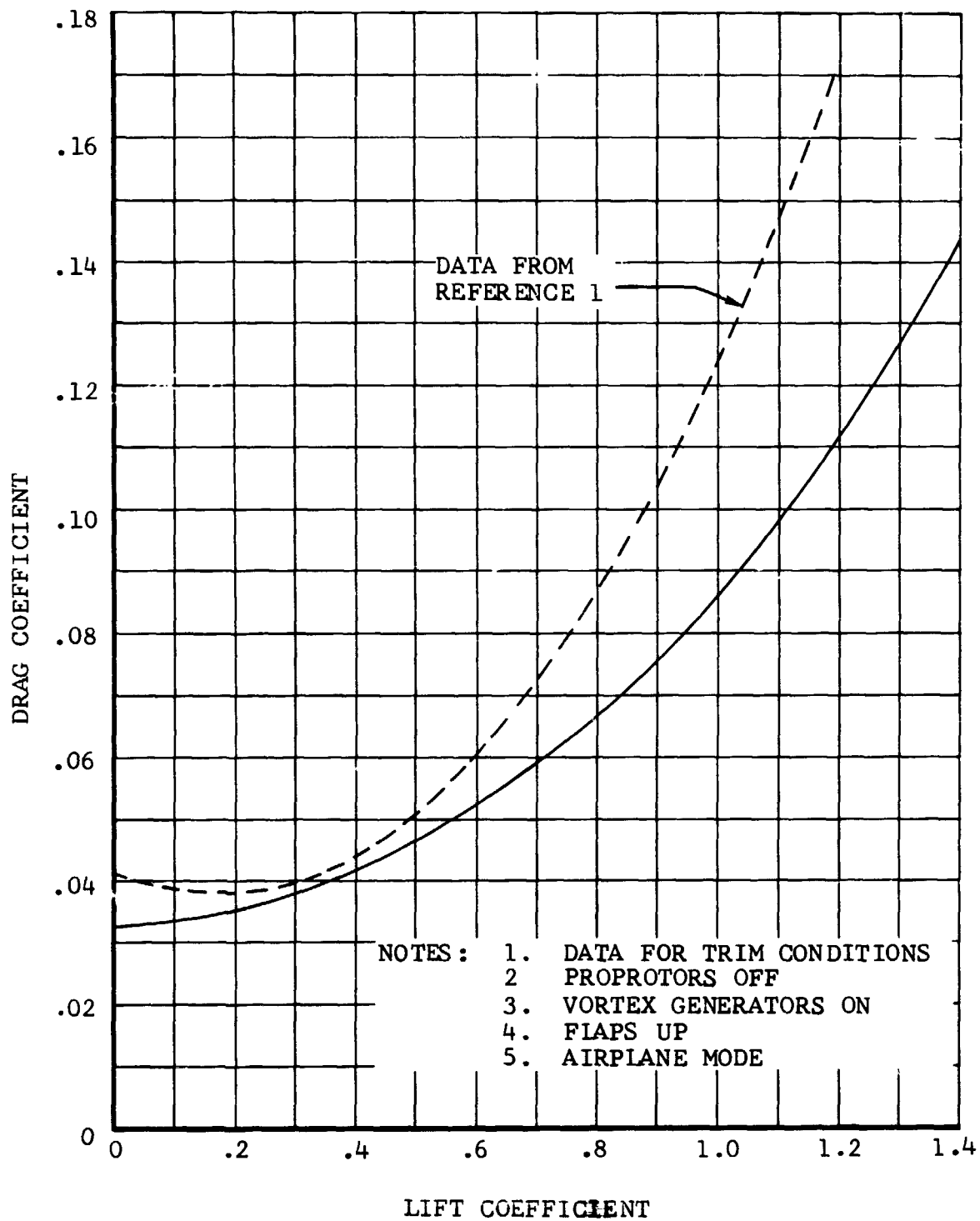


Figure V-3. Airframe Drag Coefficient Versus Lift Coefficient.

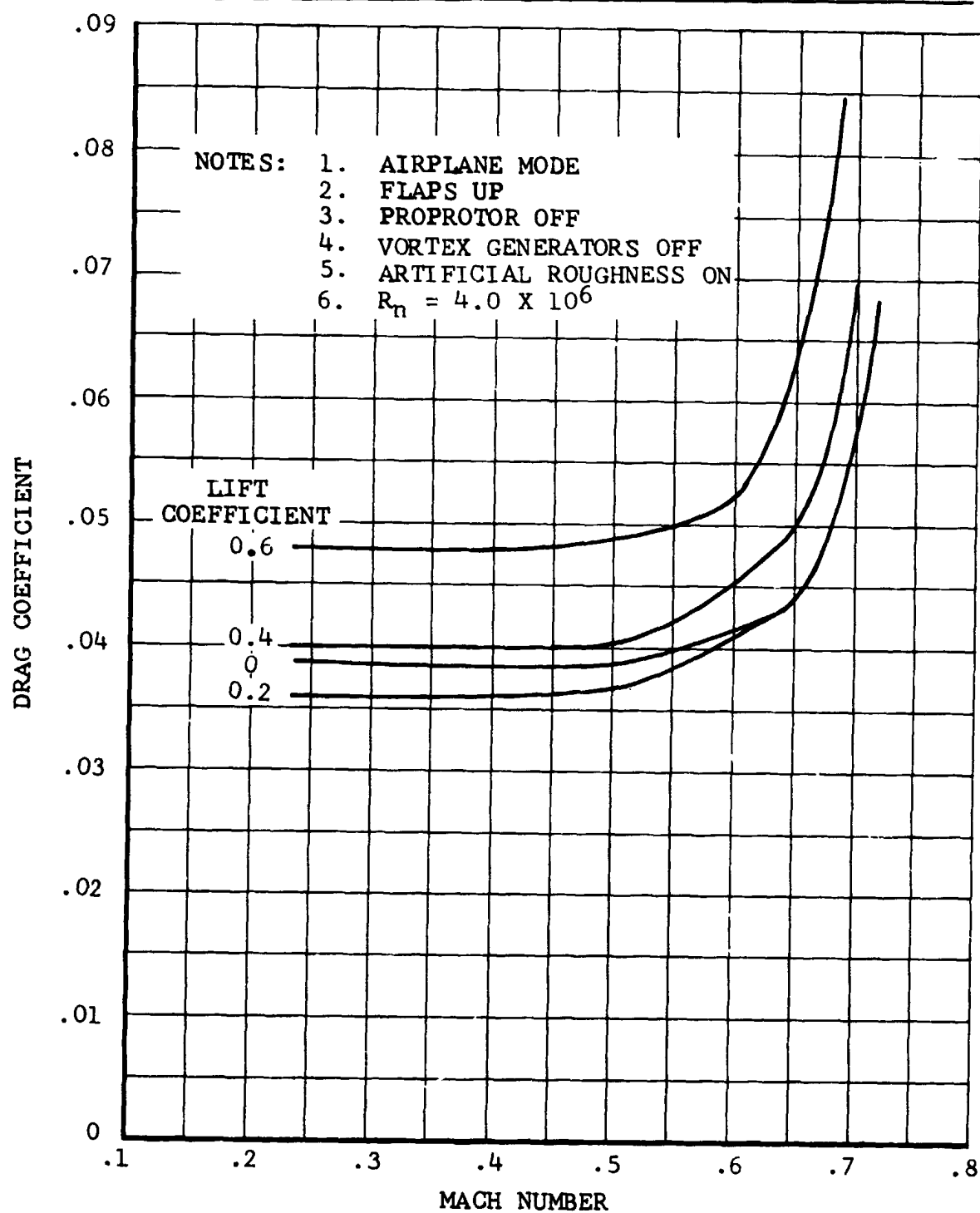


Figure V-4. Drag Coefficient Versus Mach Number.

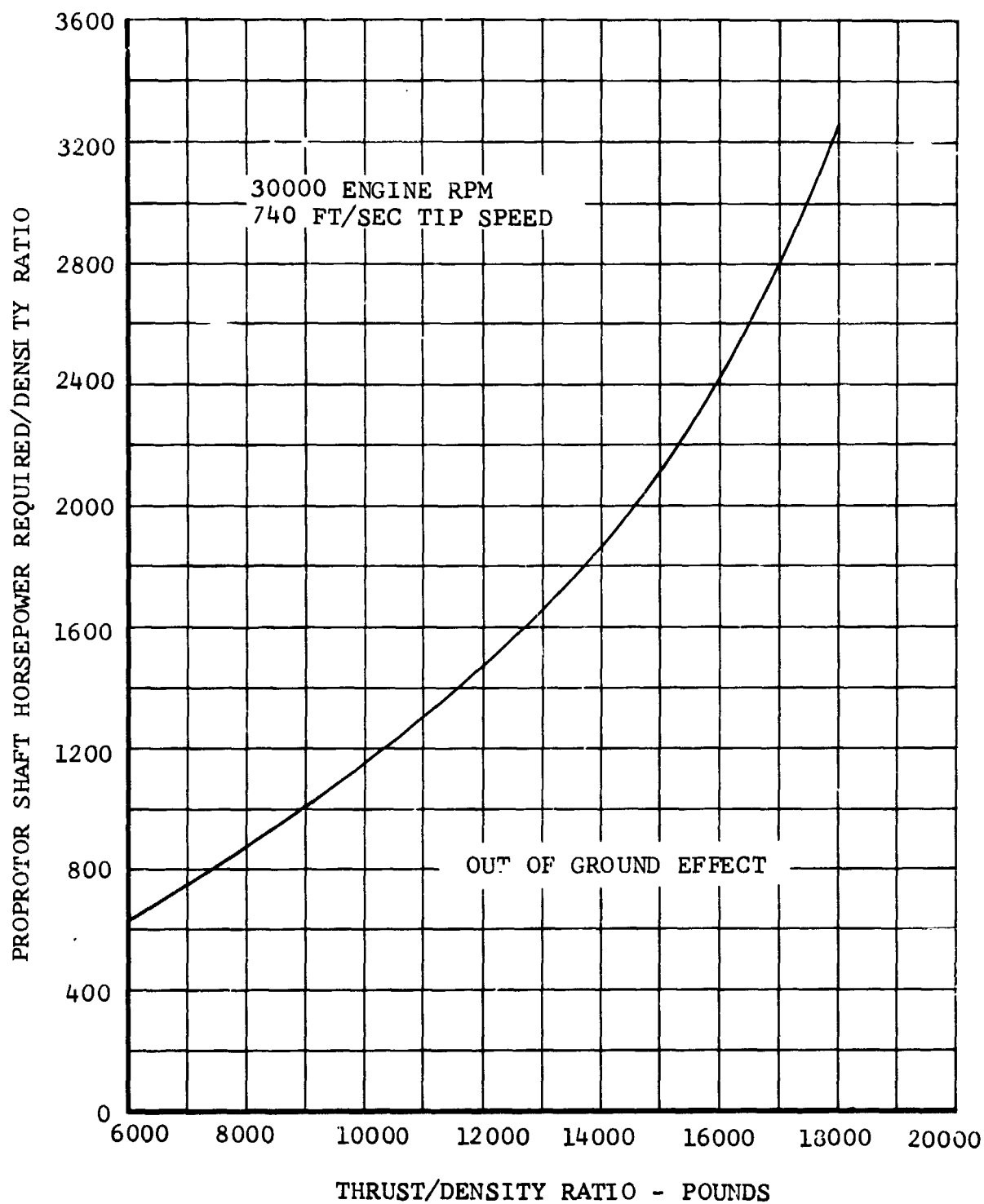


Figure V-5. Proprotor Hovering Power Required Versus Thrust.

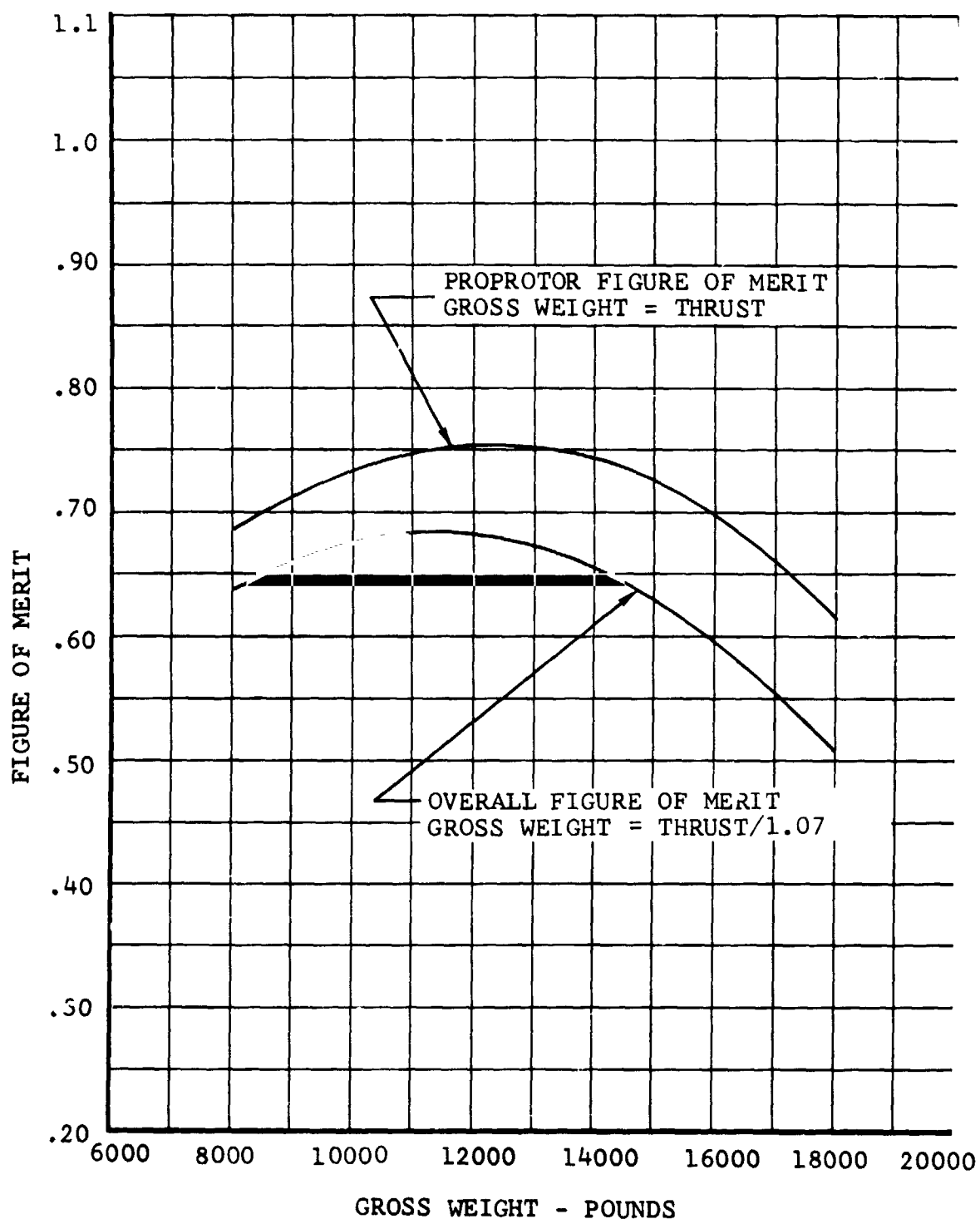


Figure V-6. Hovering Figure of Merit.

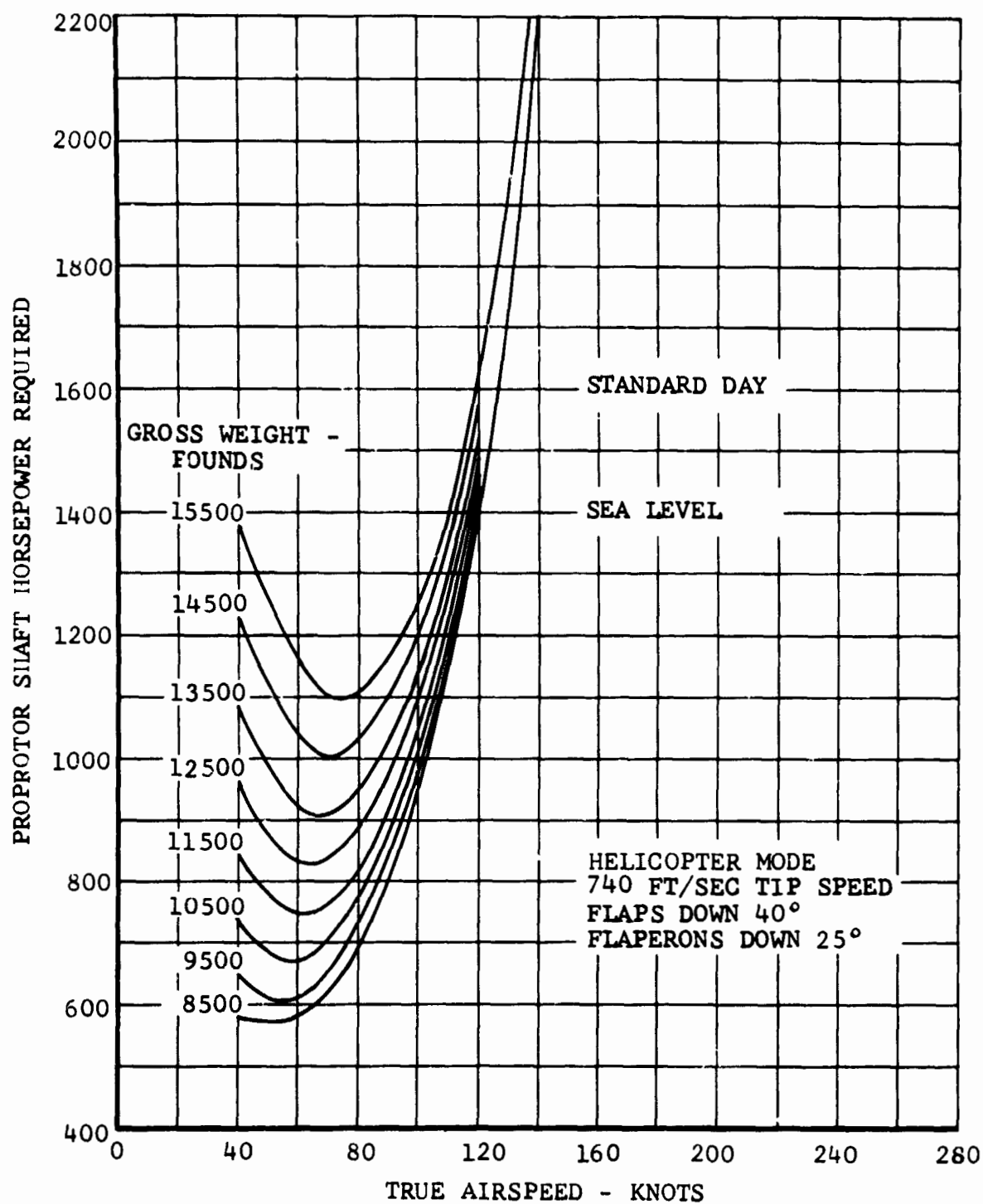


Figure V-7. Proprotor Shaft Horsepower Required Versus True Airspeed, Helicopter Mode.

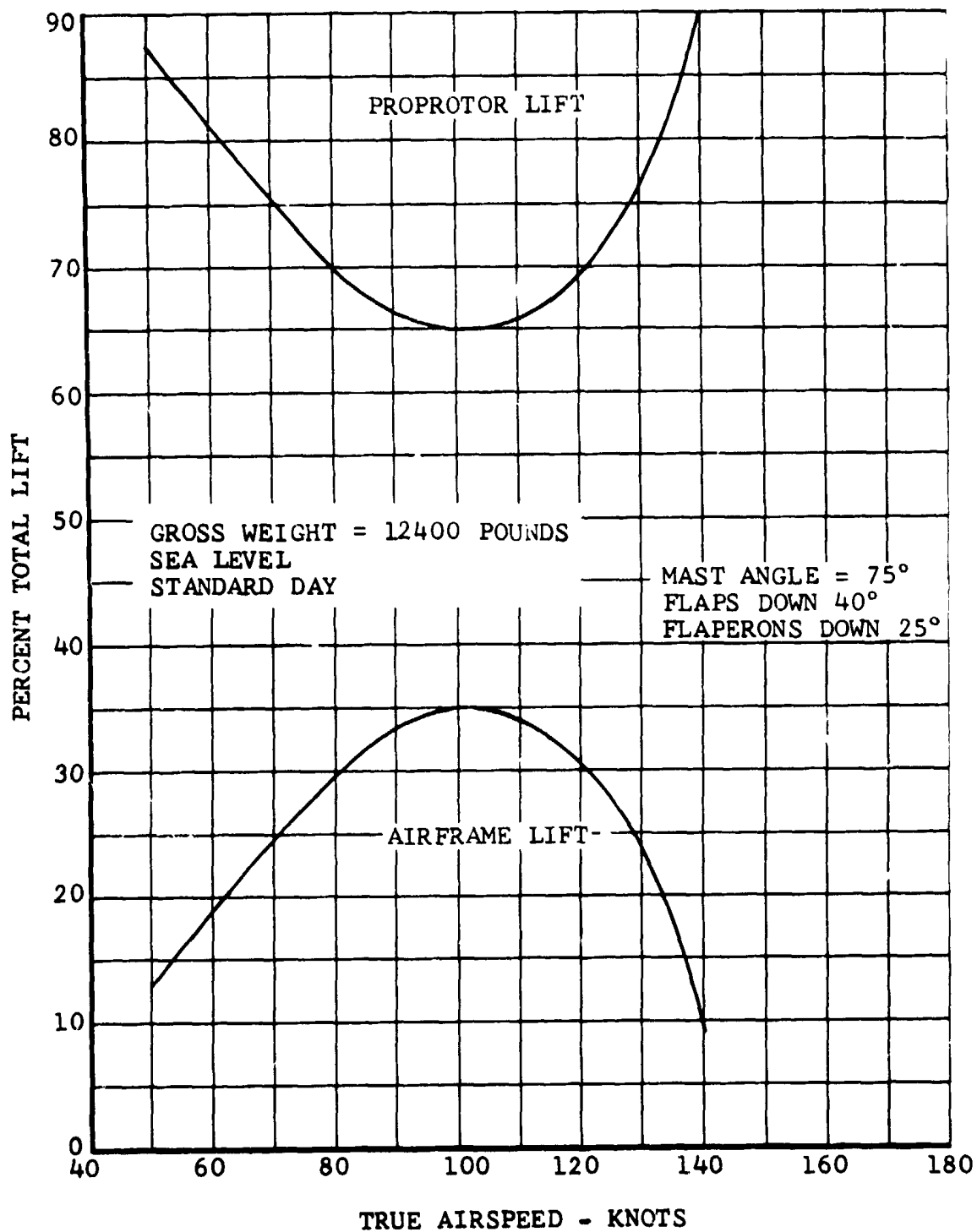


Figure V-8. Lift Distribution Between Proprotor and Airframe in Helicopter Level Flight.

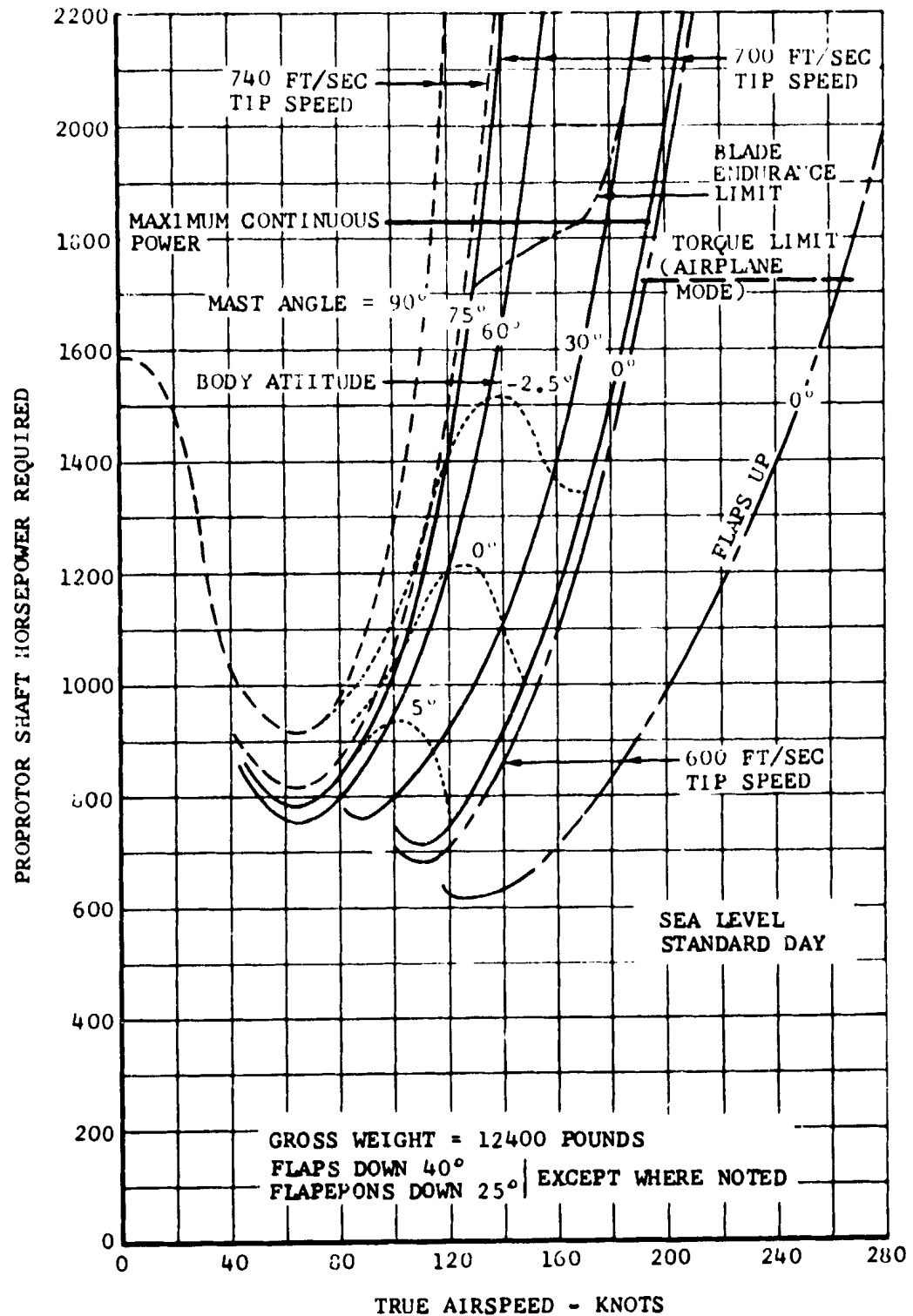


Figure V-9. Proprotor Shaft Horsepower Required Versus True Airspeed, Conversion Mode.

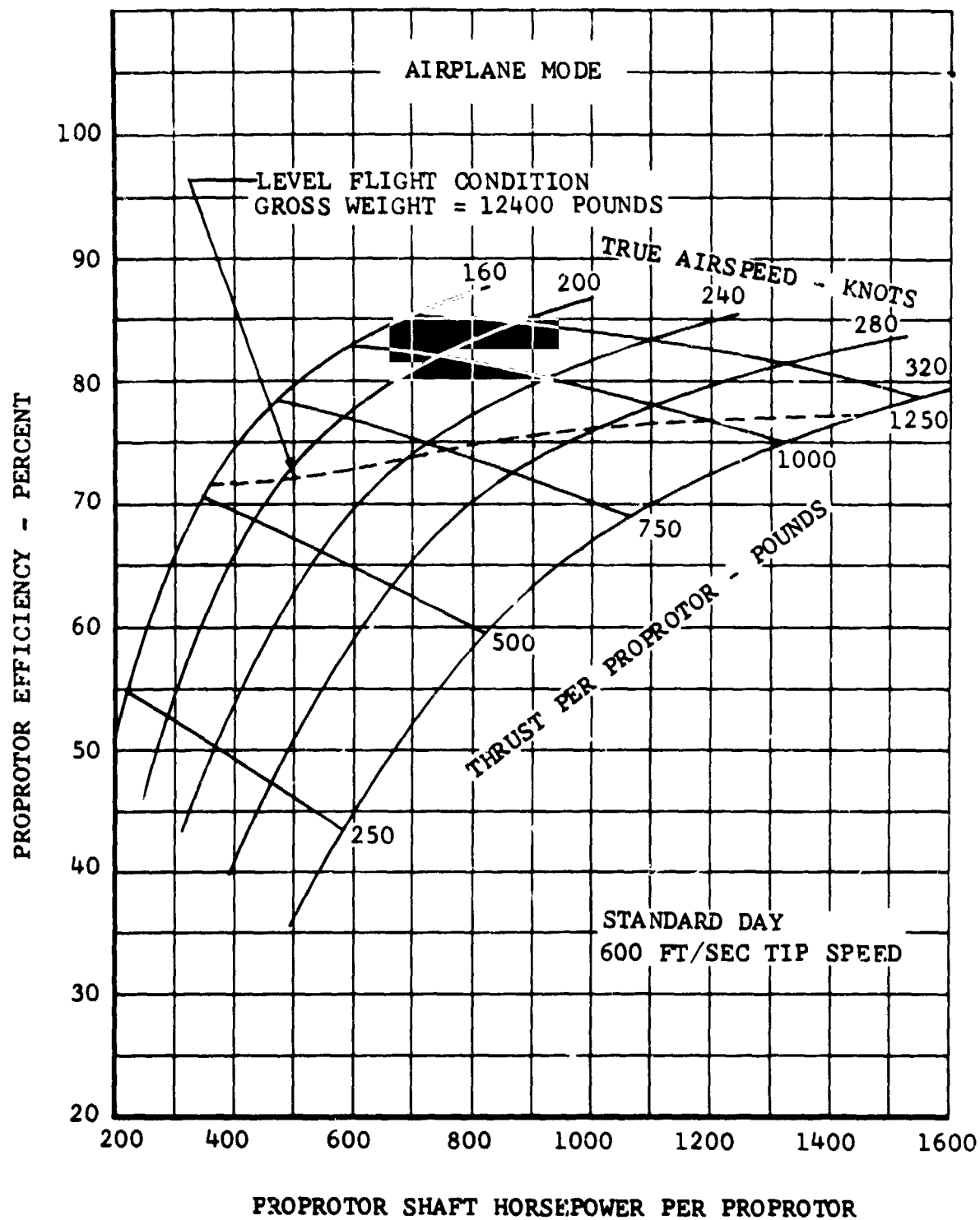


Figure V-10. Proprotor Efficiency Versus Shaft Horsepower, Sea Level.

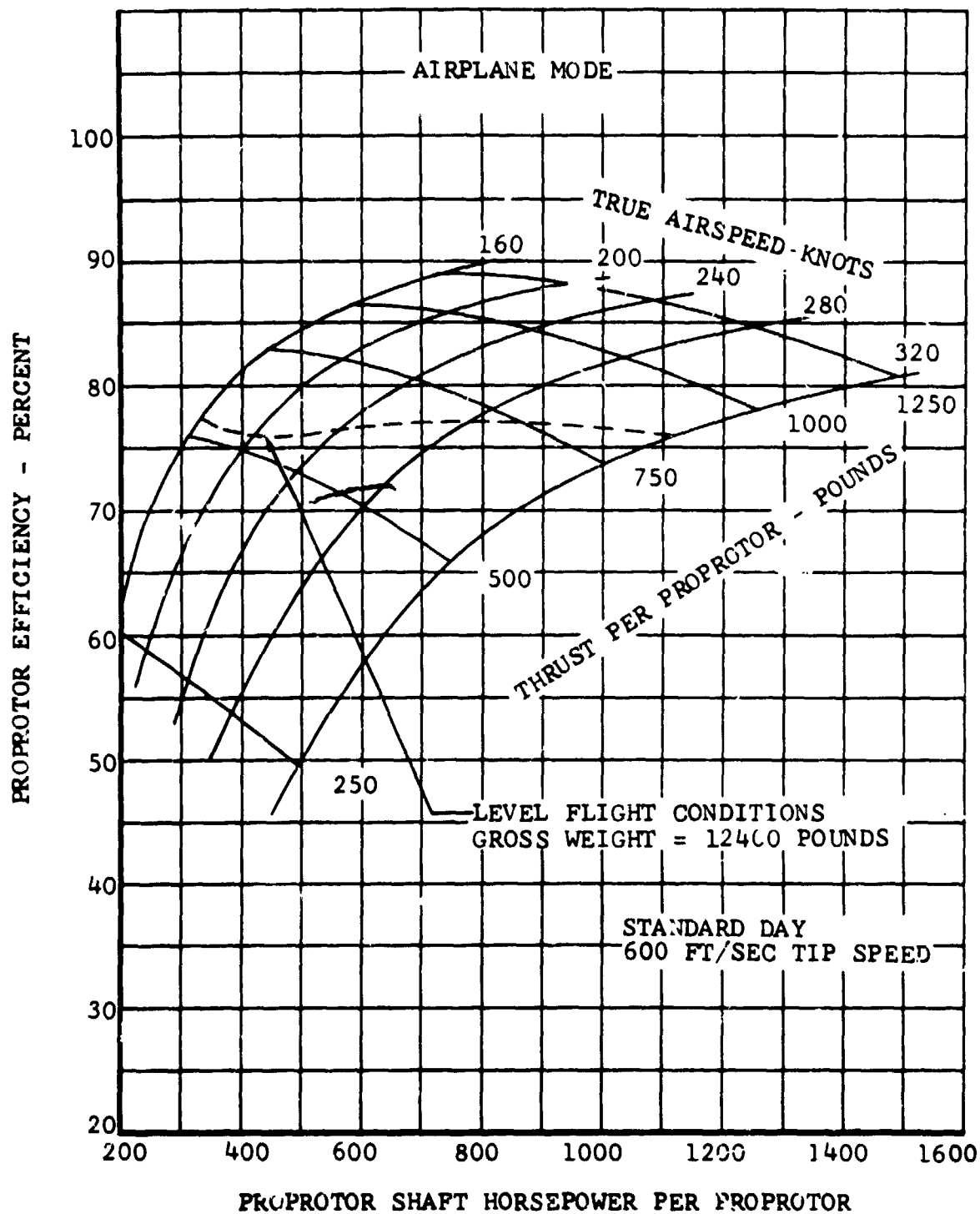


Figure V-11. Proprotor Efficiency Versus Shaft Horsepower, 10,000 Feet.

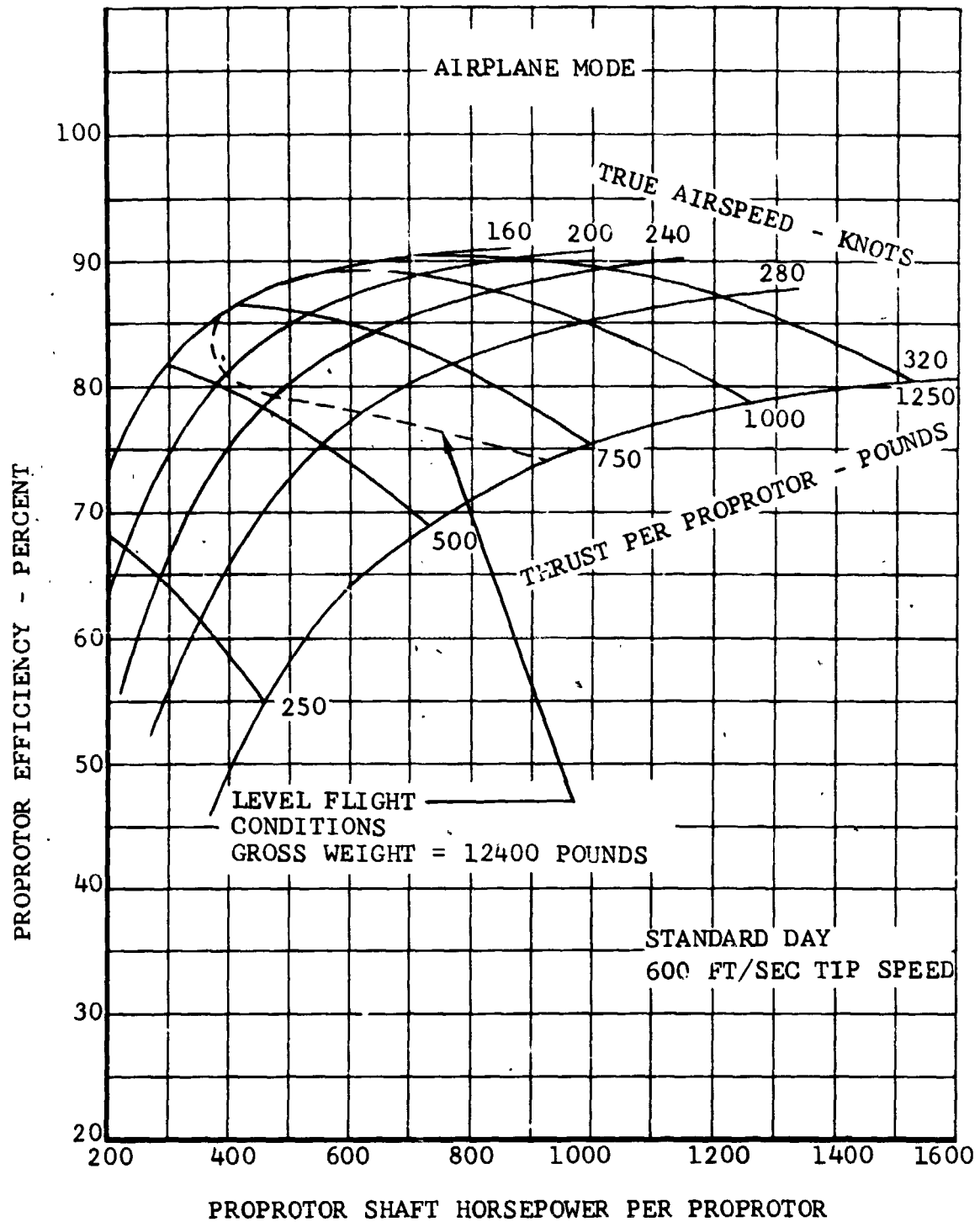


Figure V-12. Proprotor Efficiency Versus Shaft Horsepower, 20,000 Feet.

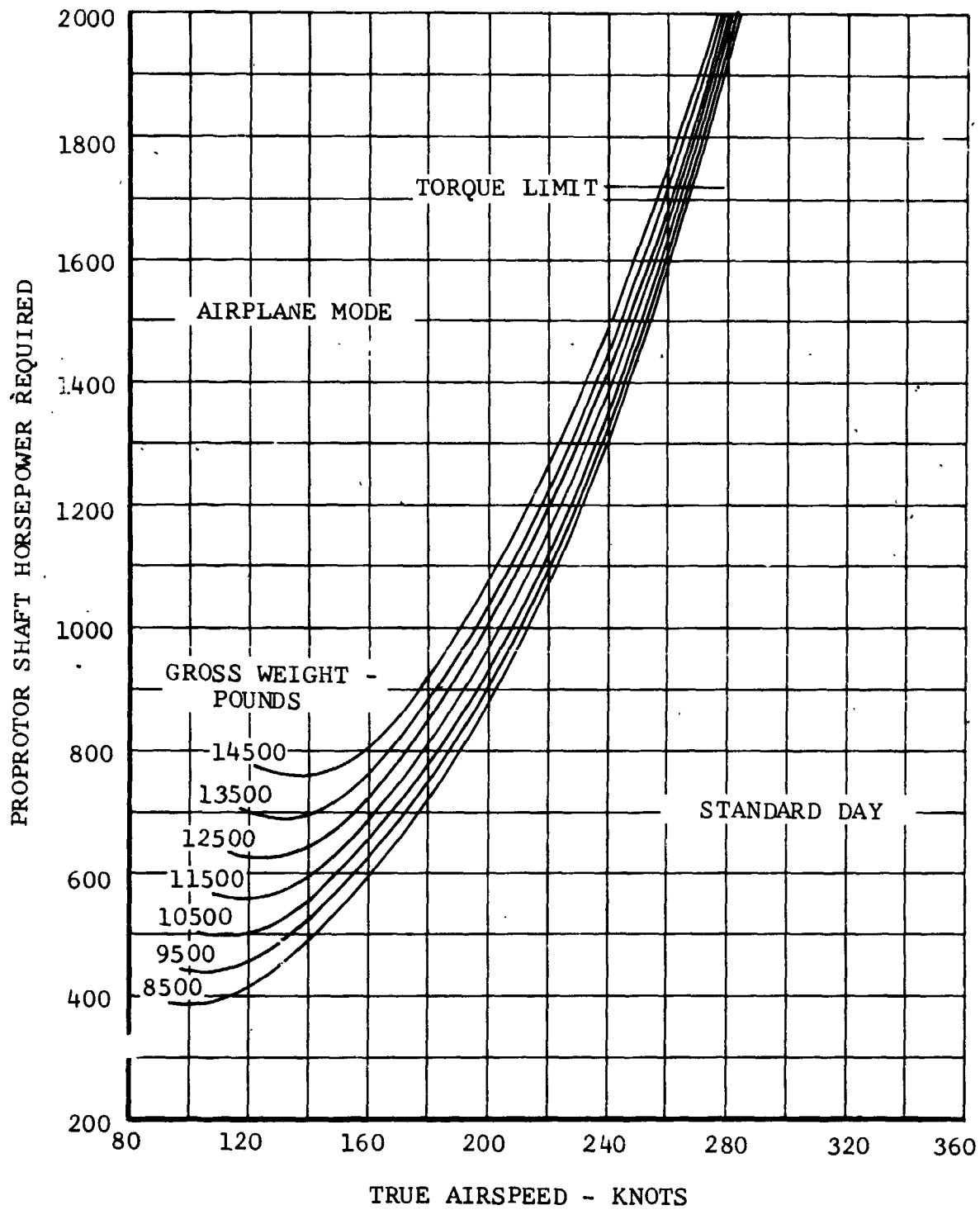


Figure V-13. Proprotor Shaft Horsepower Required Versus True Airspeed, Airplane Mode, Sea Level.

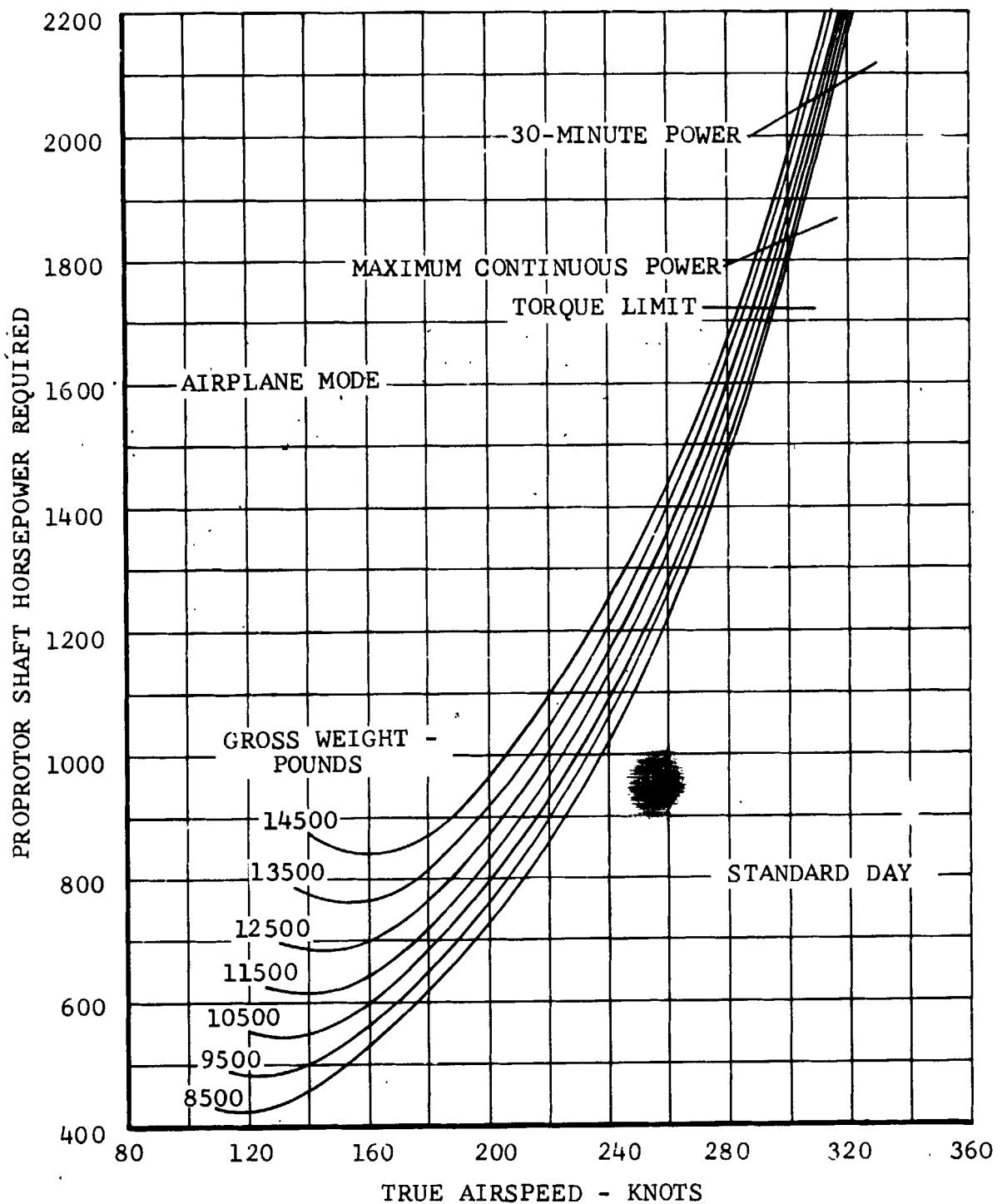


Figure V-14. Proprotor Shaft Horsepower Required Versus True Airspeed, Airplane Mode, 10,000 Feet.

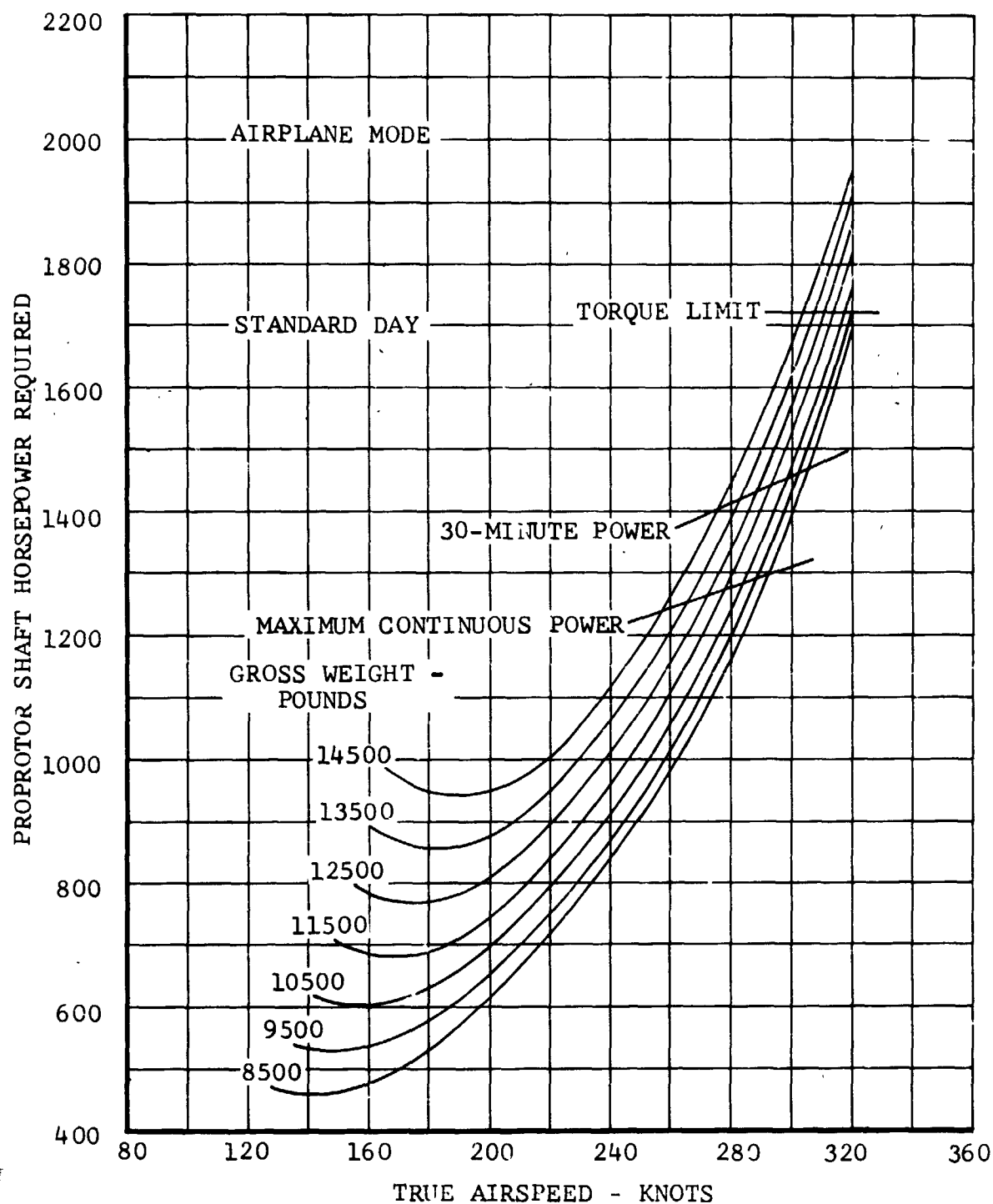


Figure V-15. Proprotor Shaft Horsepower Required Versus True Airspeed, Airplane Mode, 20,000 Feet.

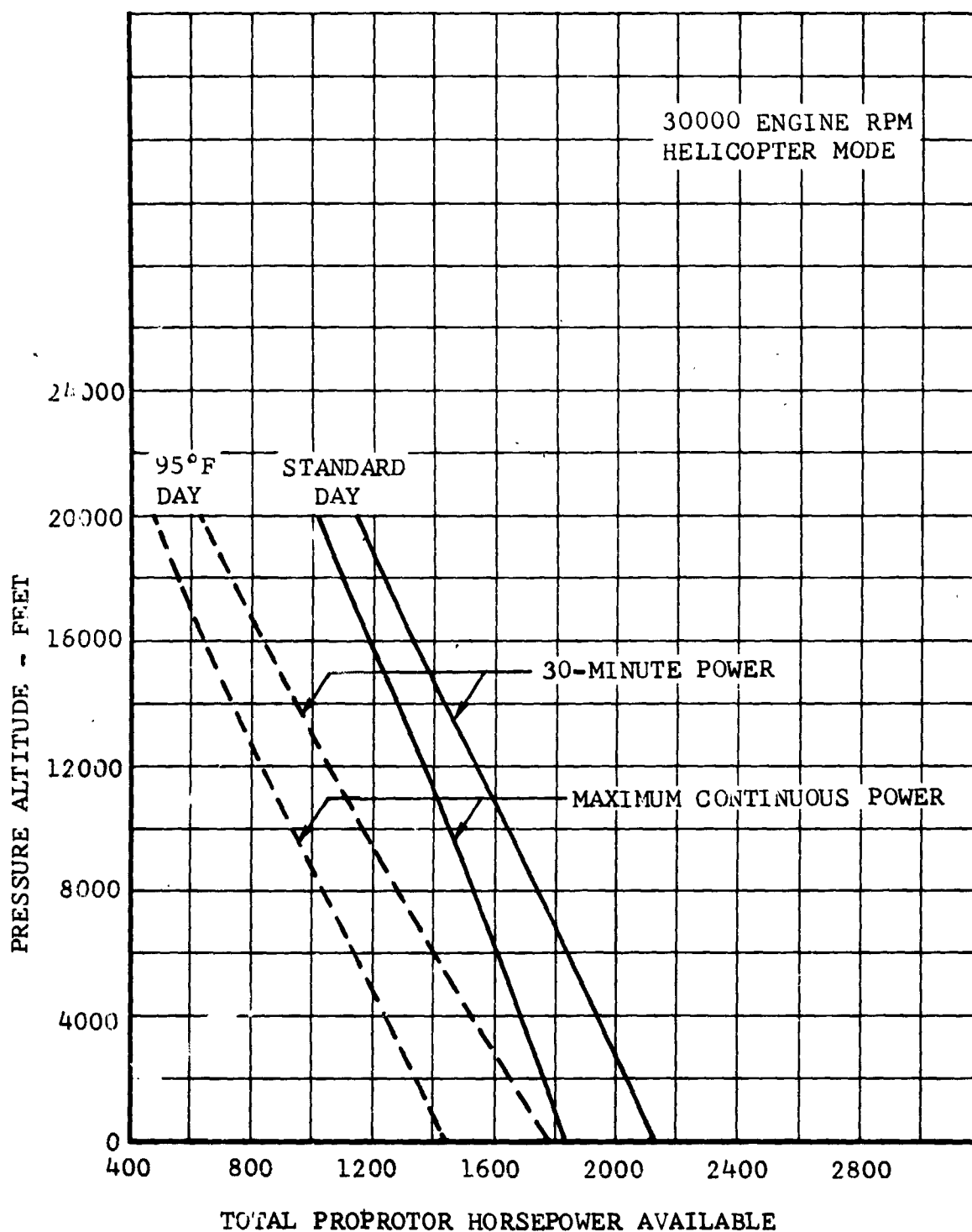


Figure V-16. Twin-Engine Proprotor, Shaft Horsepower Available, Helicopter Mode.

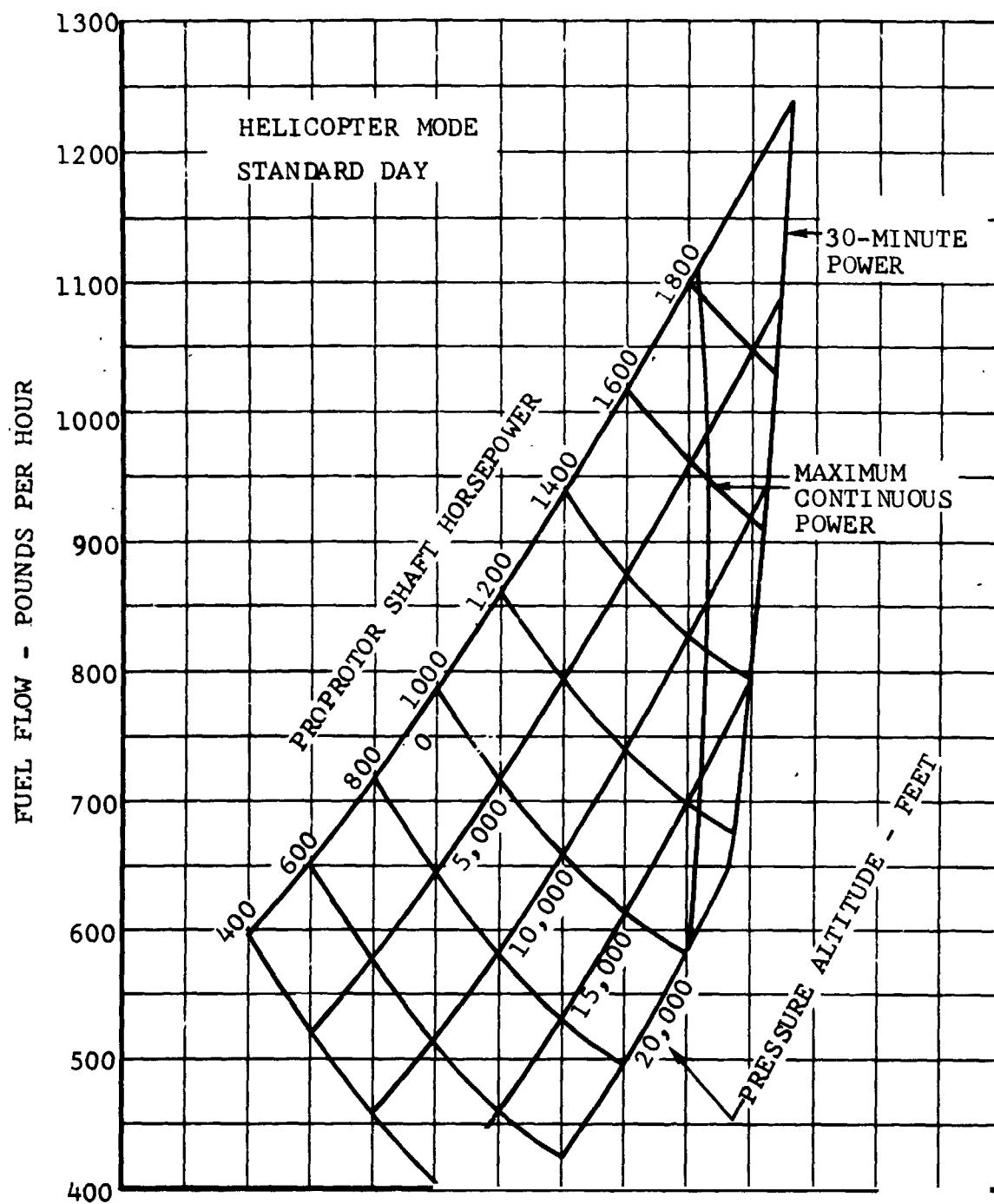


Figure V-17. Fuel Flow, Helicopter Mode.

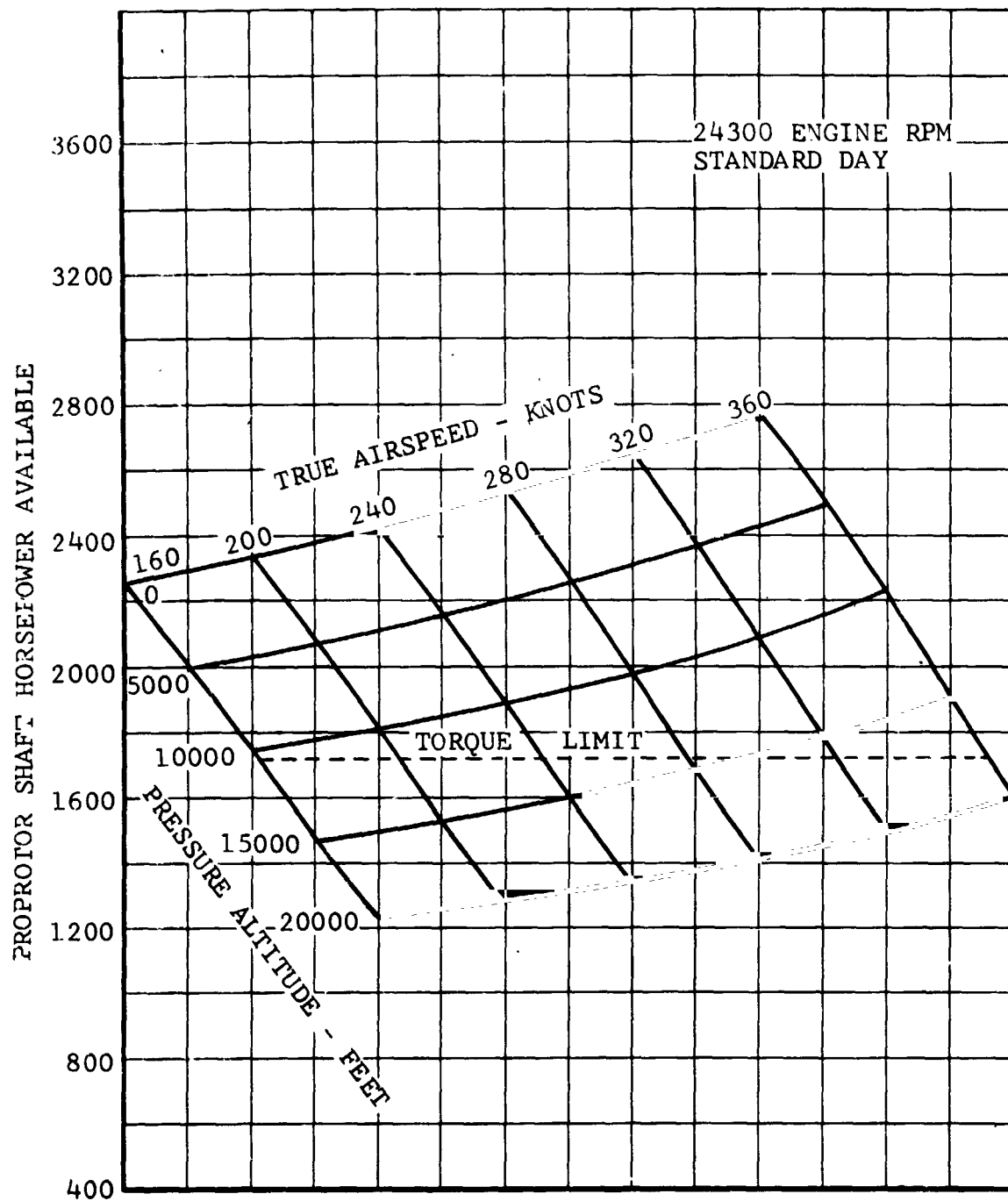


Figure V-18. Proprotor Shaft Horsepower Available, 30-Minute Power.

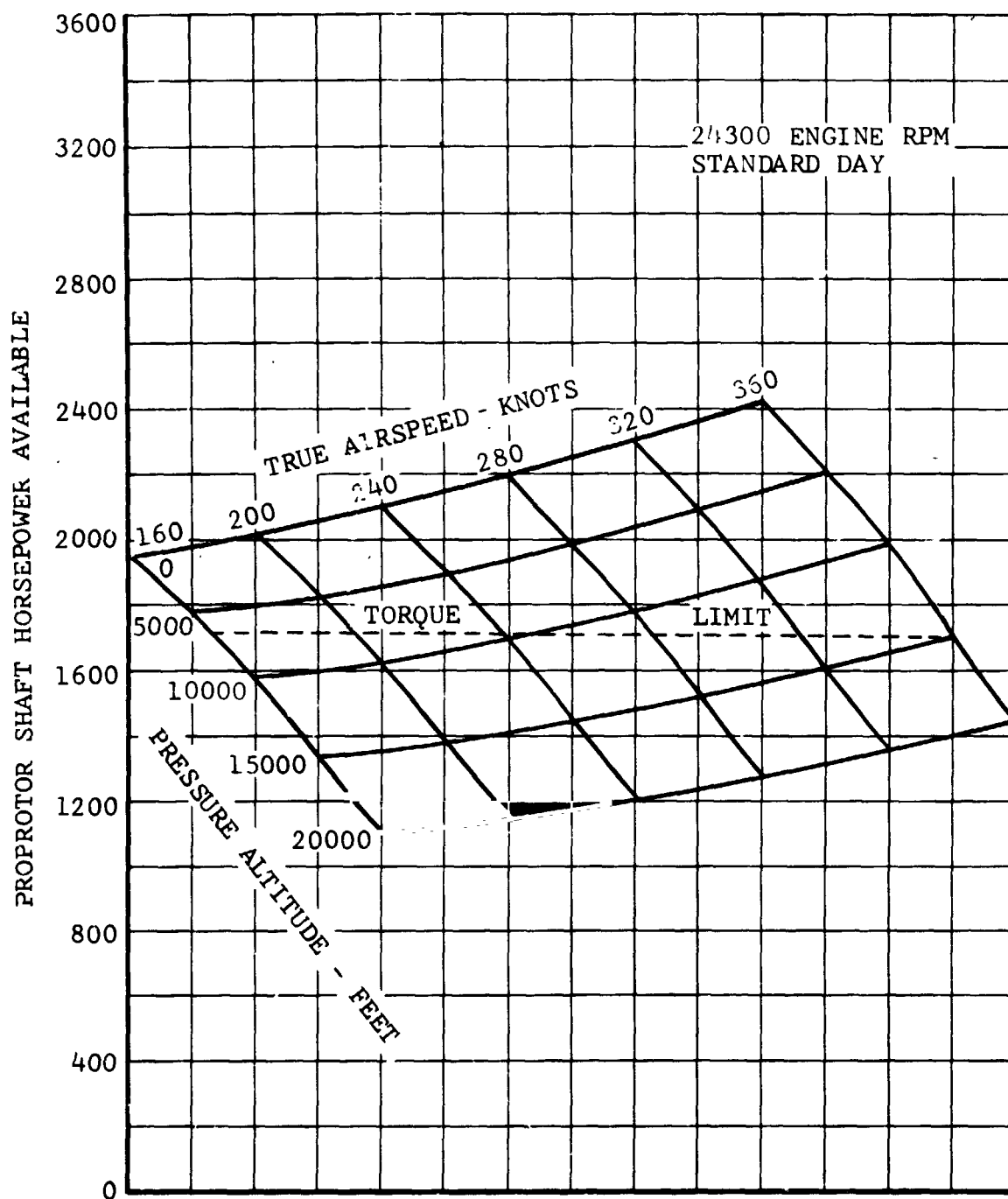


Figure V-19. Proprotor Shaft Horsepower Available, Maximum Continuous Power.

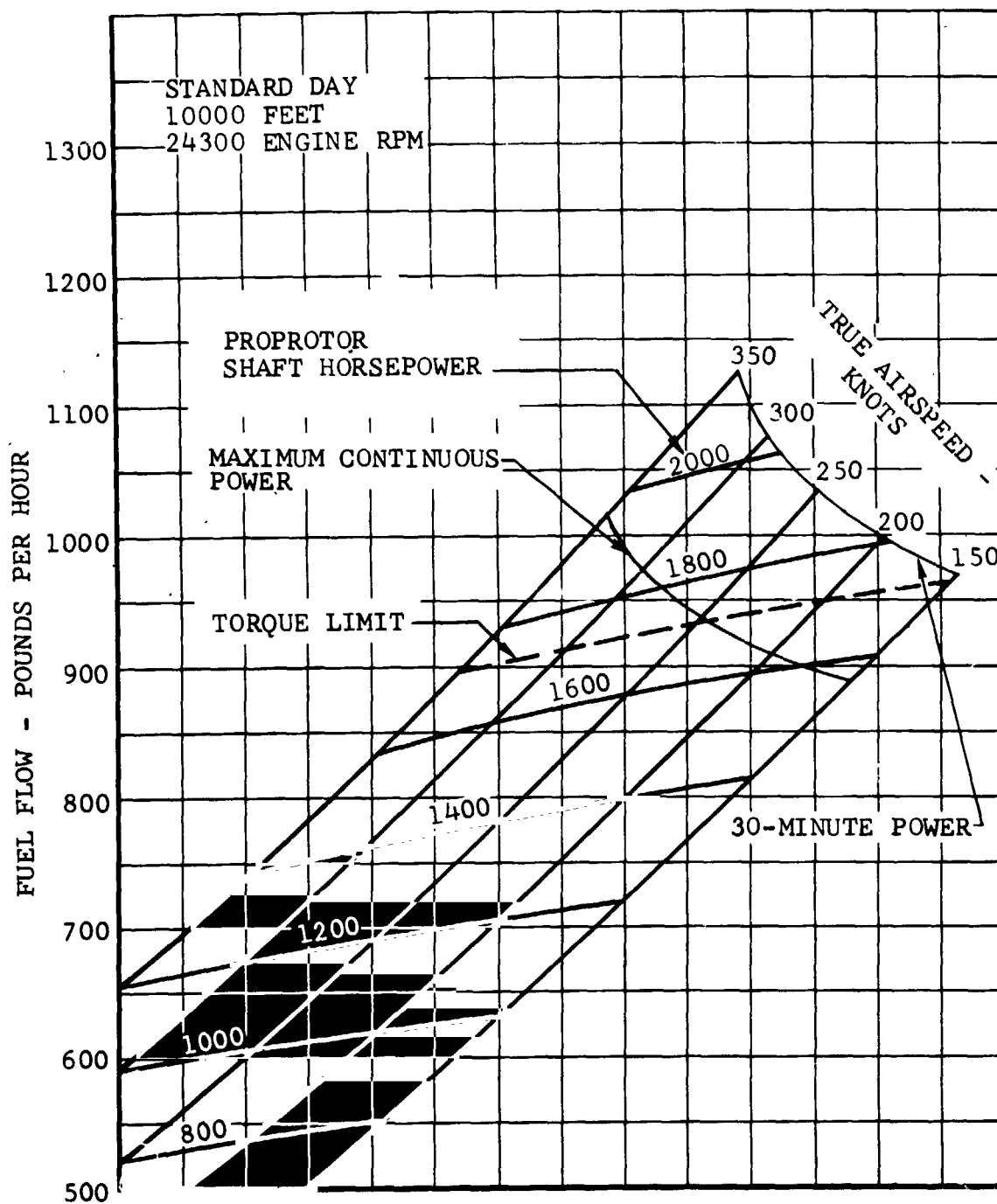


Figure V-20. Fuel Flow, Airplane Mode.

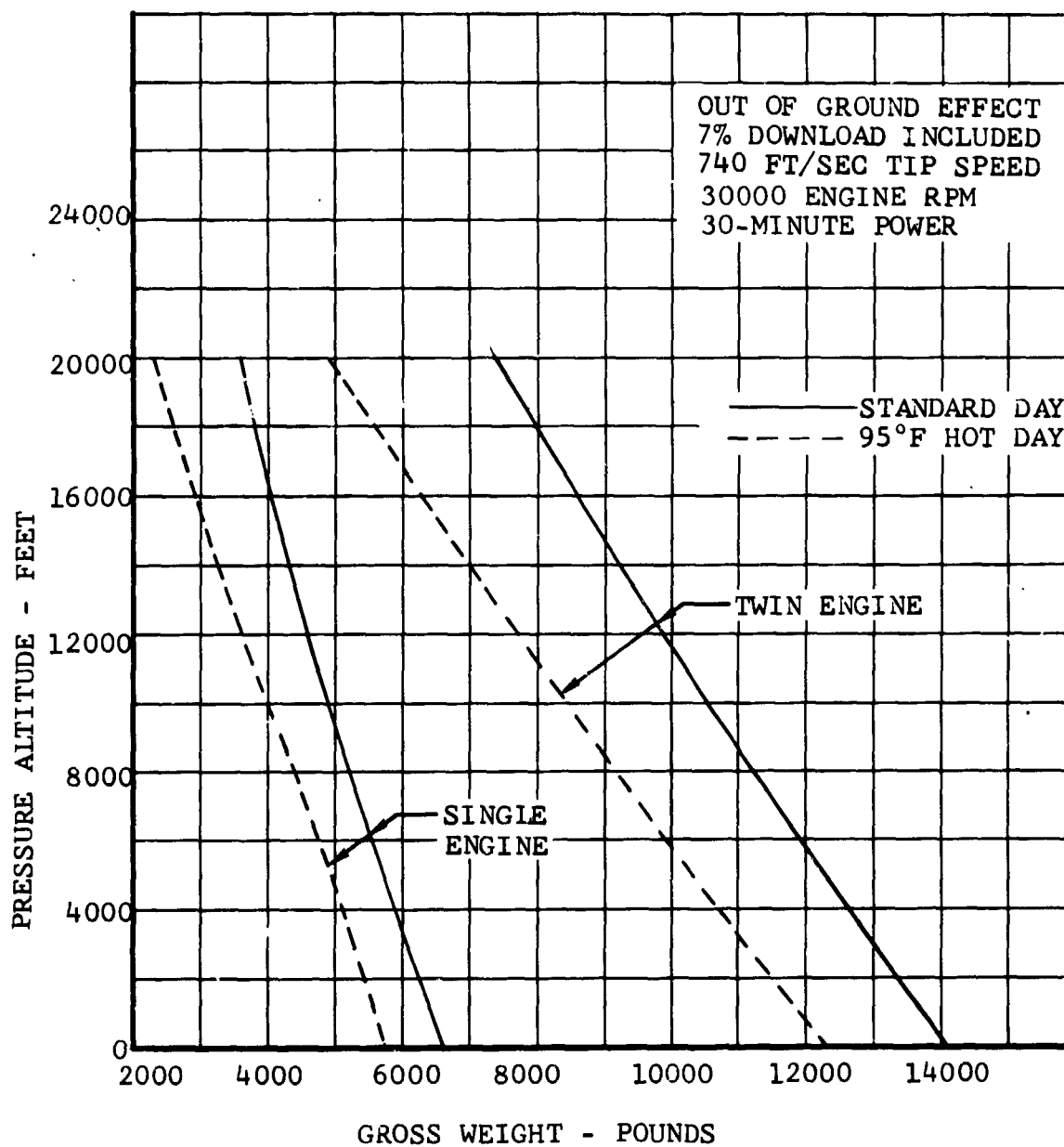


Figure V-21. Hover Ceilings.

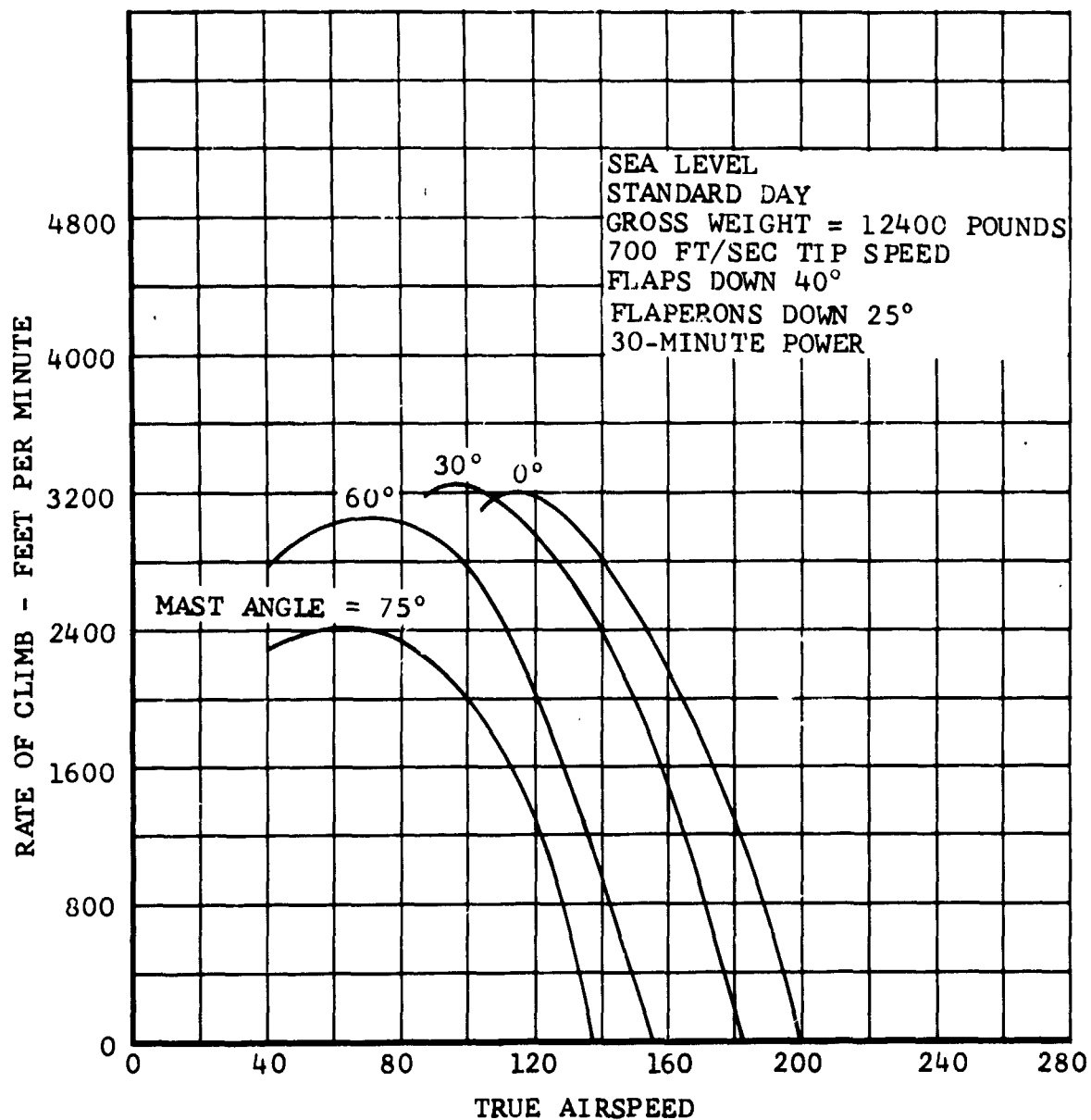


Figure V-22. Rate of Climb Versus True Airspeed, Conversion Mode.

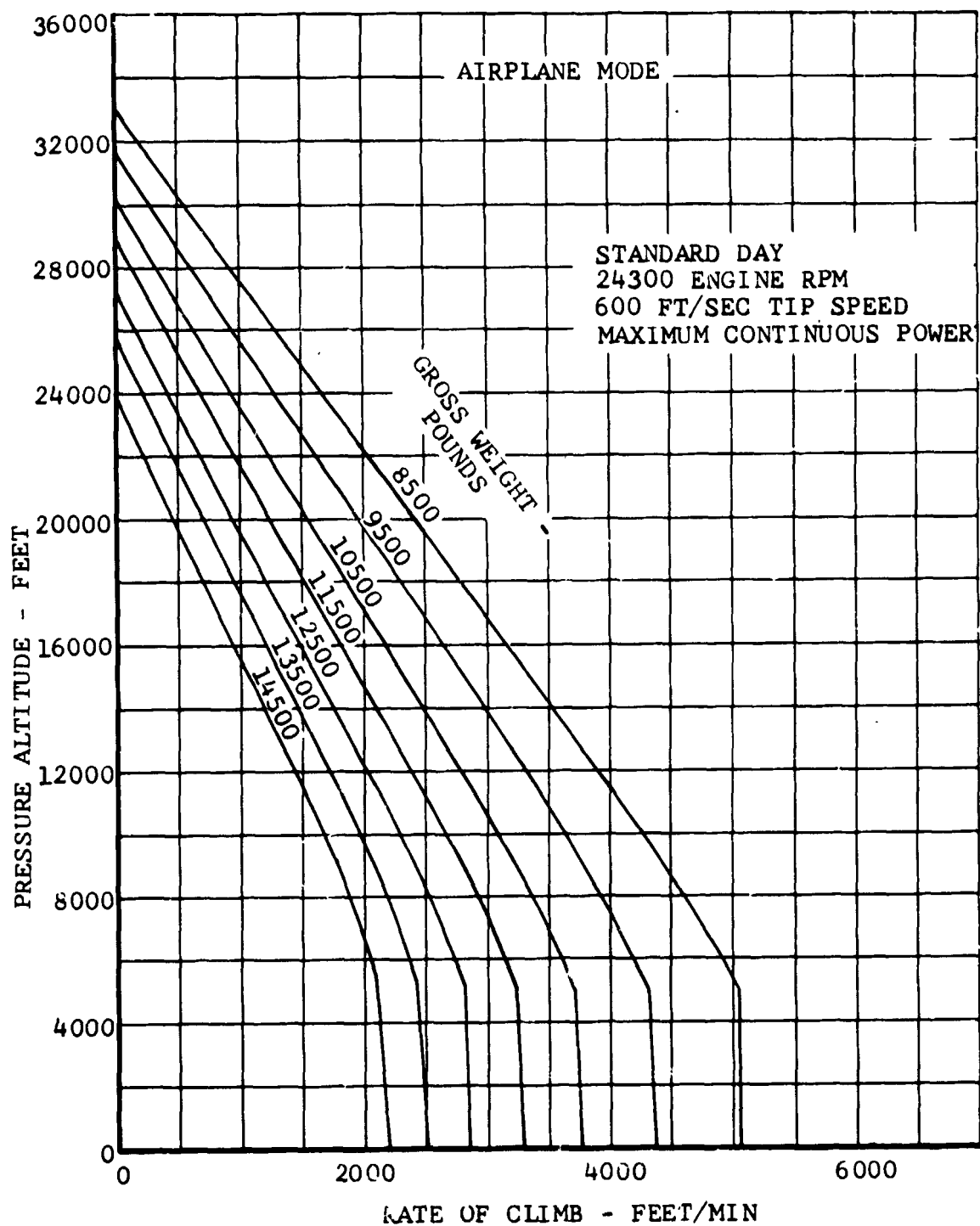


Figure V-23. Maximum Rate of Climb, Airplane Mode.

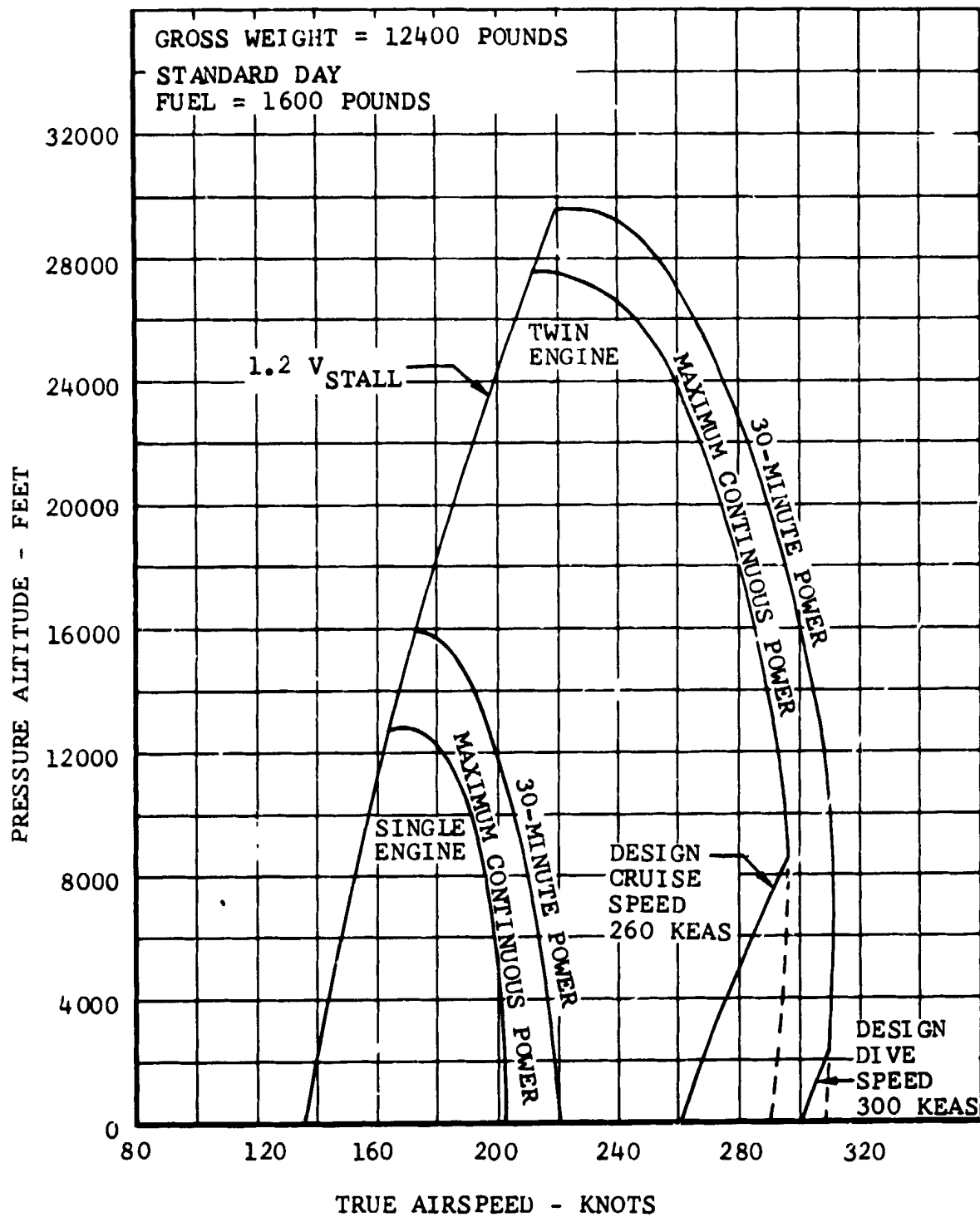


Figure V-24. Flight Envelope and Maximum Speed, Airplane Mode.

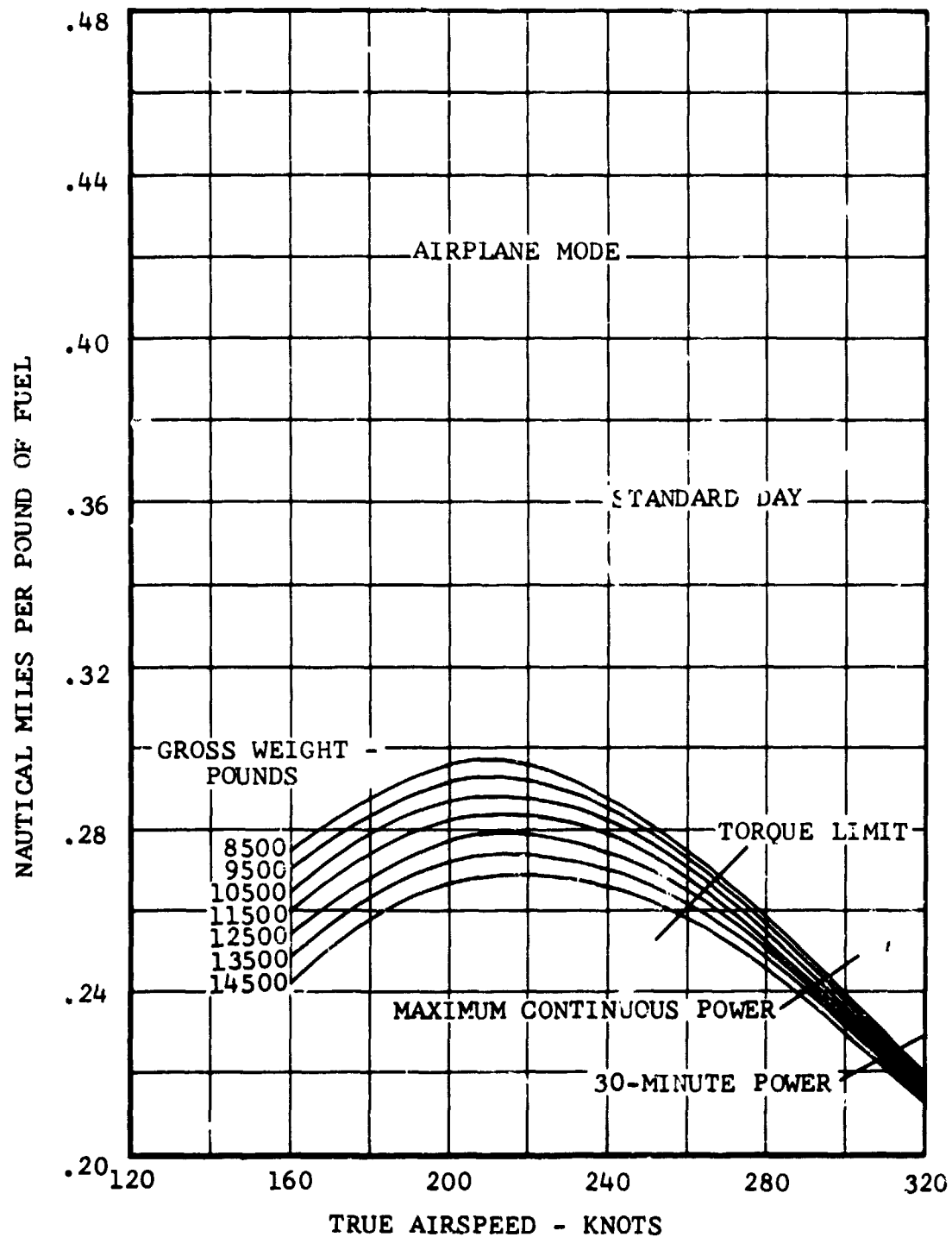


Figure V-25. Nautical Miles Per Pound of Fuel Versus True Airspeed, Airplane Mode, Sea Level.

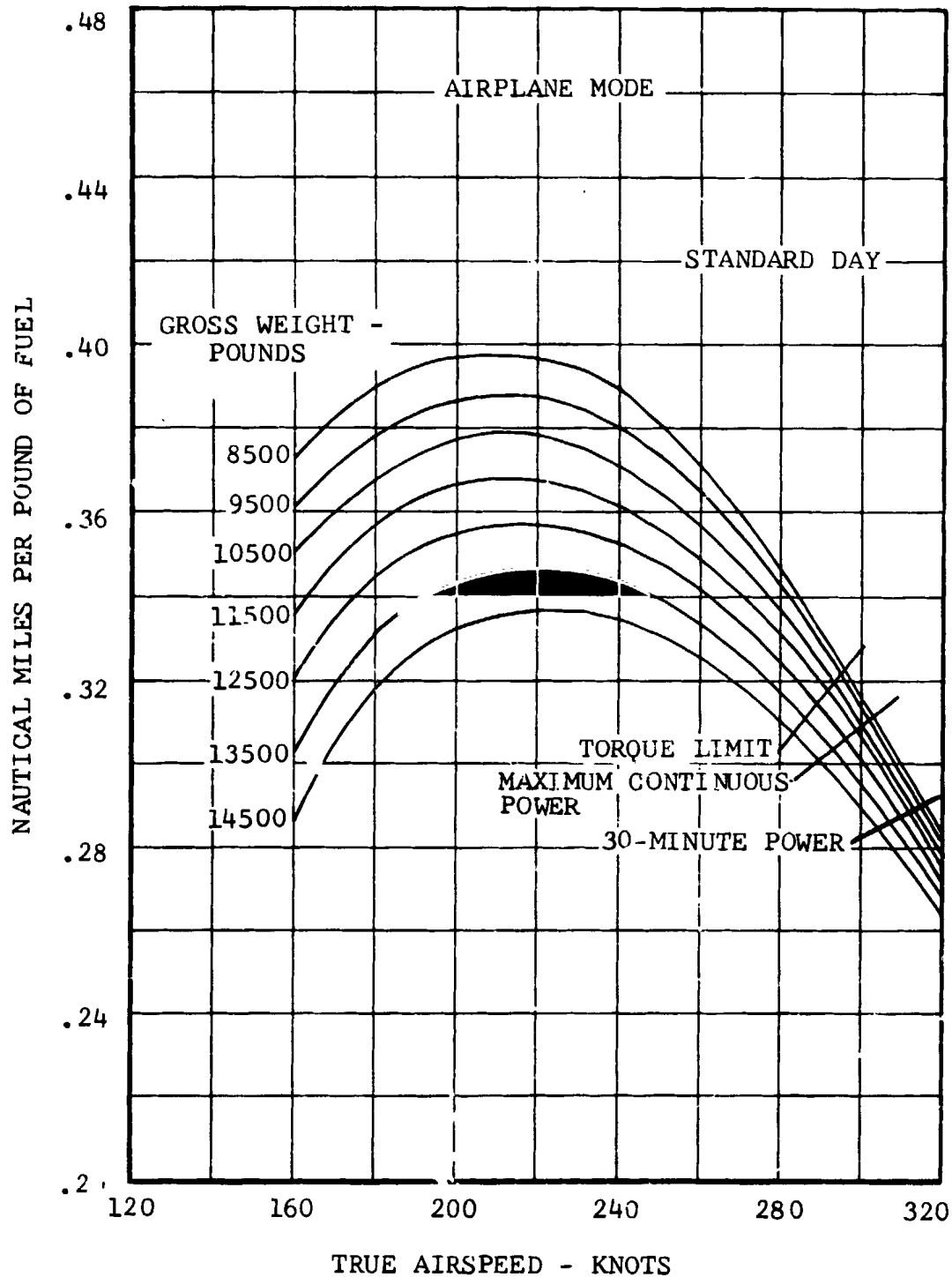


Figure V-26. Nautical Miles Per Pound of Fuel Versus True Airspeed, Airplane Mode, 10,000 Feet.

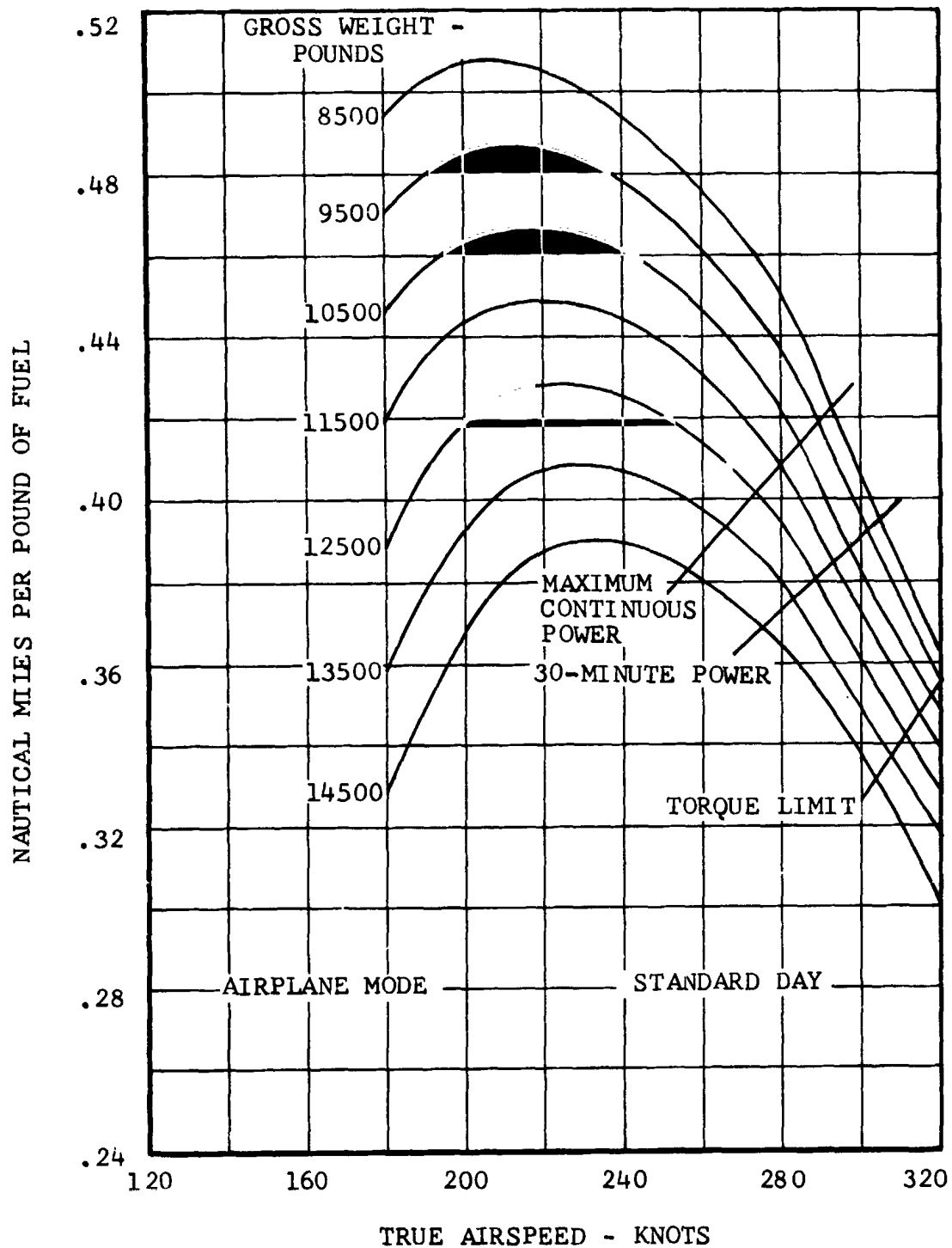


Figure V-27. Nautical Miles Per Pound of Fuel Versus True Airspeed, Airplane Mode, 20,000 Feet.

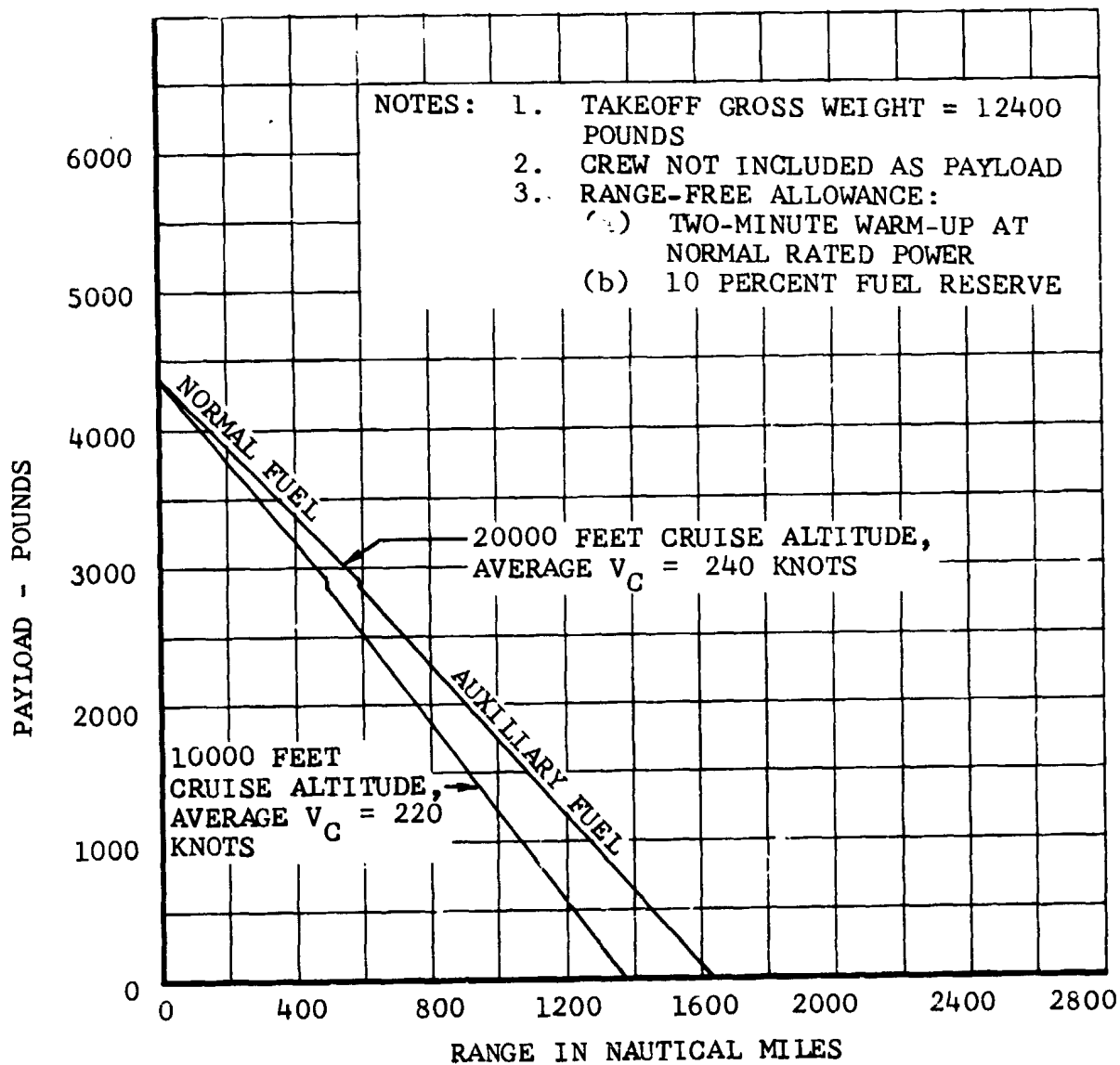


Figure V-28. Payload Range.

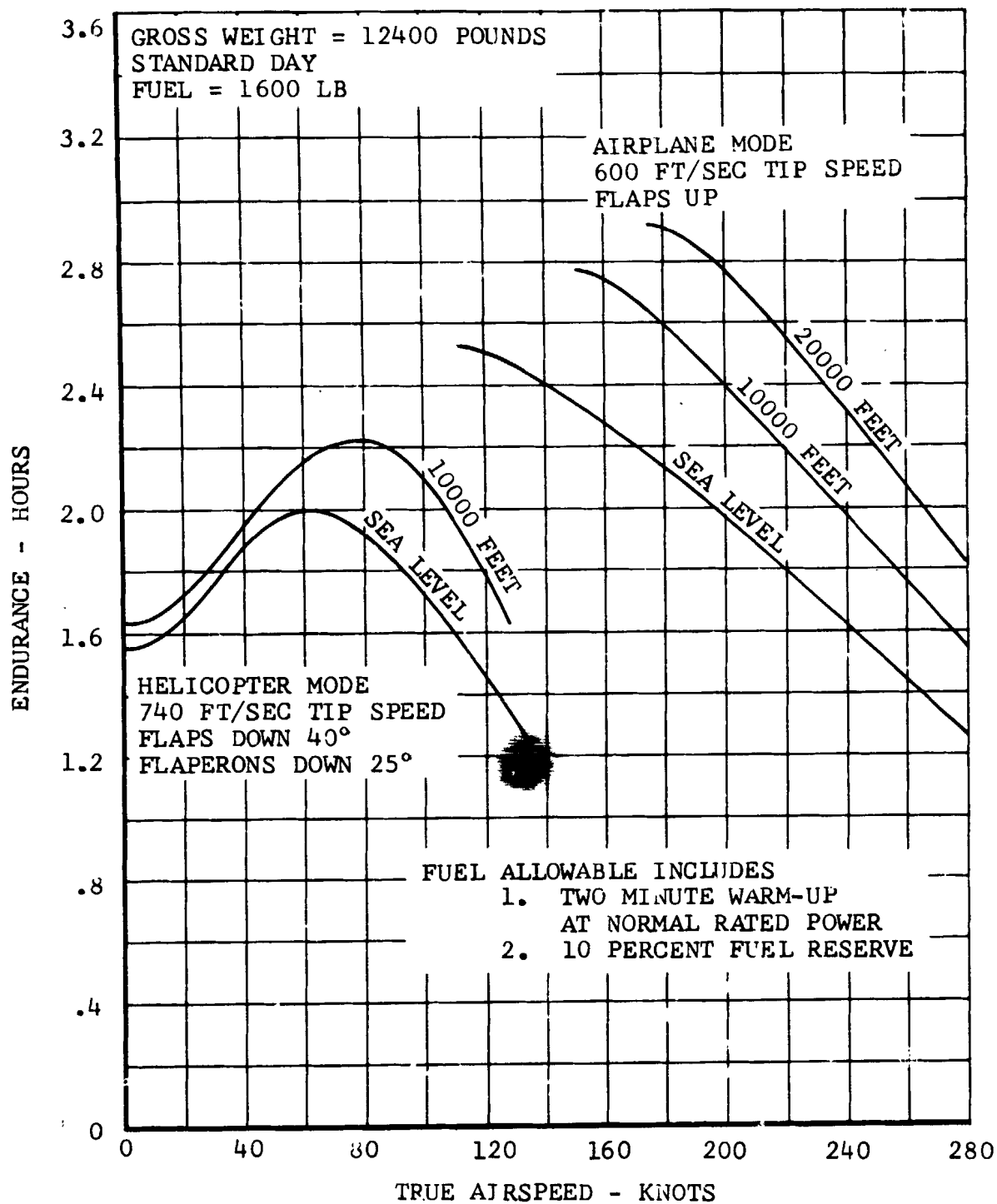


Figure V-29. Model 300 Endurance.

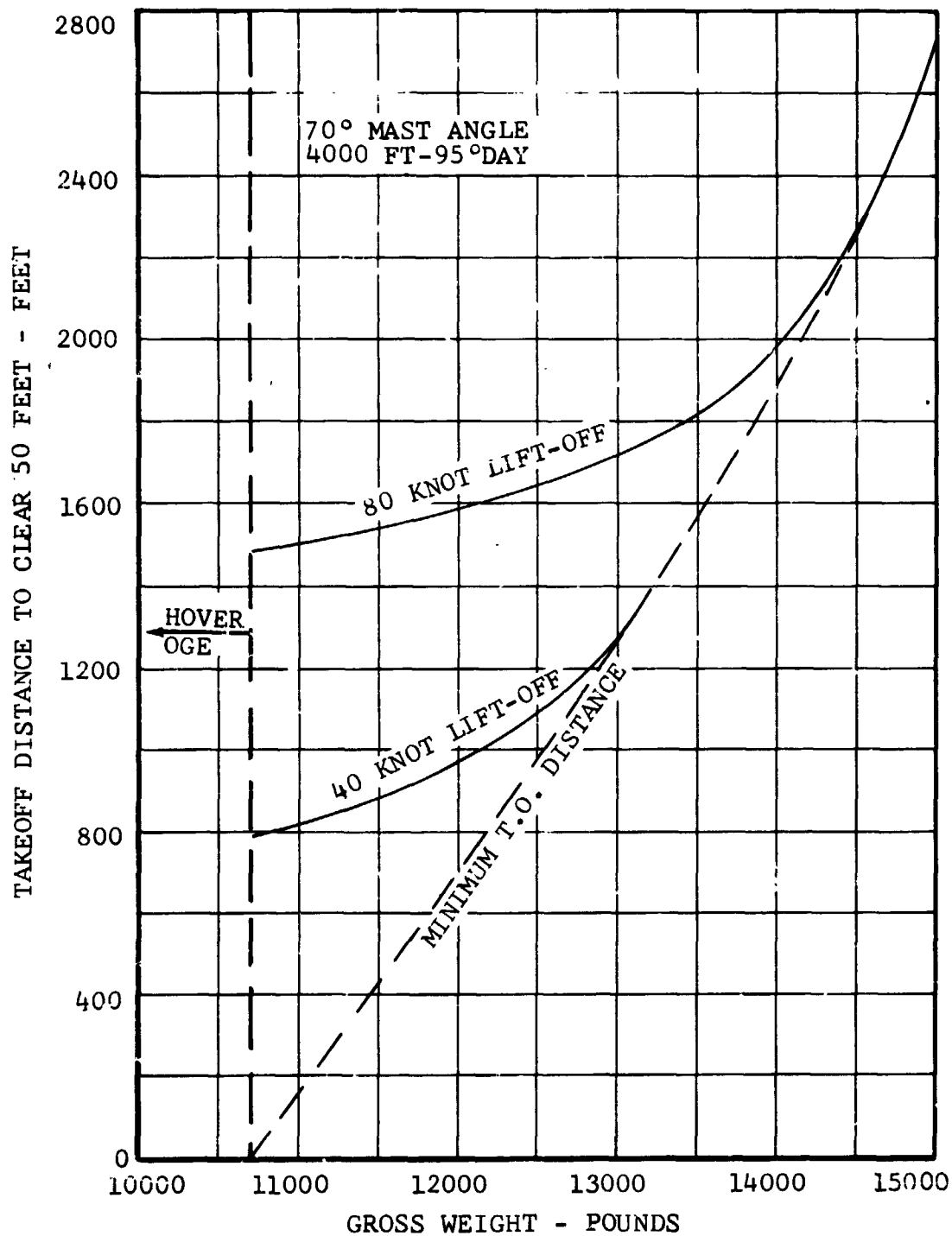


Figure V-30. Model 300 STOL Takeoff Distance.

VI. DYNAMICS

During this study, the system coupled natural frequency, blade flapping, and propotor stability calculations were updated and refined. The propotor blade passage frequency vibration levels at the crew station, at the aircraft center of gravity, and at the pylon center of gravity were calculated. Also, the response of the aircraft to atmospheric turbulence in airplane mode was investigated.

The results of these calculations confirm earlier predictions that the Model 300 has ample stability margins, adequate clearance for blade flapping, and low vibration levels. The results of the investigation of the response to atmospheric turbulence in airplane mode are encouraging. They indicate that earlier estimates of propotor VTOL ride comfort have probably been pessimistic.

A. COUPLED NATURAL FREQUENCIES

1. Propotor Natural Frequencies

The coupled natural frequencies of the Model 300 propotor are shown in Figures VI-1 and VI-2 in terms of collective modes and cyclic modes, respectively. The collective modes are the symmetric modes of the propotor, i.e., polar symmetric about the mast. The cyclic modes are the asymmetric modes. These rotor natural frequency fan plots were obtained by correcting calculated "fan plots" to reflect the natural frequencies measured in a nonrotating shake test of the propotor and during whirl tests and NASA wind-tunnel tests (Reference 2).

Note that several modes are indicated to be in or near resonance, namely the third collective mode and the second and third cyclic modes. These resonances were carefully monitored during the wind-tunnel tests, but were never a problem. Based on analysis of blade loads measured during the two wind-tunnel tests, it has been concluded that the placement of the Model 300 propotor natural frequencies is satisfactory.

2. Wing-Pylon-Fuselage Natural Frequencies

Placement of the Model 300 wing-pylon-fuselage natural frequencies such that the structure has low response to rotor harmonic excitation and at the same time achieves good dynamic stability characteristics has been a major design consideration. As a result, a number of components are designed to meet stiffness requirements. For example, the wing torsional stiffness is 60 percent greater than that required for strength considerations. At the pylon-to-wing interface, the stiffness of the conversion spindle and the actuator spindle are tailored to keep wing-pylon coupled modes out of one-per-rev resonance during conversion.

a. Analytical Method

The Model 300 structure has been modeled on the NASA structural analysis (NASTRAN), a finite element analysis. Several computer models with varying degrees of complexity, depending on purpose, have been developed. A detailed model of the wing-pylon interface, including details of the pylon assembly, has been developed to study the effect of pylon component stiffnesses on the coupled frequencies and response. Figure VI-3 shows this model and identifies the more significant components. Computer models of the complete vehicle, shown in Figure VI-4, have been used to calculate fuselage and empennage natural frequencies and study the influence of the wing-to-fuselage-junction stiffness on the wing-pylon natural frequencies.

b. Calculated Frequencies and Mode Shapes

The calculated natural frequencies of the wing-pylon-fuselage-empennage system as a function of pylon conversion angle are shown in Figures VI-5 and -6. The modes are separated into symmetric and asymmetric sets for convenience; Figures VI-5 and -6, respectively.

The natural frequency variation with pylon conversion angle is a result of the shift in location of the pylon mass as the pylon is converted. Since the pylons comprise over 40 percent of the empty weight, this effect is very significant. The sudden change in the natural frequencies at pylon conversion angle of zero degrees is caused by engagement of the pylon downstop. This downstop provides a direct load path between the transmission case and the wing front spar during airplane flight. The frequencies of modes which involve pylon pitching or yawing with respect to the wing are therefore significantly influenced by whether the pylon is on or off the downstop. (In airplane mode, the downstop reacts a load from the conversion actuator assuring positive engagement of the downstop.)

The natural frequencies shown in Figures VI-5 and -6 are based on the latest estimates of component masses and stiffnesses. Several modes are indicated to be near resonance. The most significant of these are the first symmetric wing torsion (one-per-rev resonance), the engine pitch modes (three-per-rev resonance), and the wing asymmetric beam and chord modes (one-per-rev resonance). However, the exact location of these frequencies is not yet certain. For example, the frequency of the engine pitch mode is highly dependent upon the stiffness of the transmission case extension from which the engine is cantilevered, and the engine exhaust frame. The case extension is an extremely complex structure containing gears and shafting. Estimates of its stiffness have a considerable range of uncertainty. The engine exhaust frame is a welded sheet metal structure with a large cut out for the exhaust port. Its stiffness is highly dependent on the effectiveness of stiffeners

around the cut out. Early in the research aircraft program, shake tests will be conducted with the engine mounted on the transmission, and the wing torque box stiffness will be measured to determine airframe natural frequencies more precisely.

The frequency of the wing asymmetric chord mode is dependent upon the stiffness of the wing-to-fuselage junction. For the data shown in Figure VI-6, the local flexibility at this junction has been neglected. In shake tests of the aeroelastic model, the frequency of the wing asymmetric chord mode was well below one per rev because of the flexibility of the fittings used to attach the wing spar to the fuselage spar. The flexibility in this area is presently under study for the full-scale design. Some flexibility may have to be designed in in order to place the asymmetric chord below one per rev.

The wing asymmetric beam mode is also indicated to be in one-per-rev resonance in airplane mode. This resonance has been present in the one-fifth-scale aeroelastic model, but has not caused a vibration problem. The resonances at six per rev are not expected to be problems because of the small amount of excitation and the inherent damping associated with the modes involved.

3. Drive System Natural Frequencies

Drive system natural frequencies were calculated using the analytical model shown in Figure VI-7. The major inertias and flexibilities of the drive system, as well as the pylon case torsional flexibility and the wing-tip mounting flexibility, are represented in the analysis.

The drive system undamped natural frequencies and normalized mode shapes are shown in Figure VI-8. The symmetric modes are those where the rotations of the left- and right-hand systems are opposite, e.g., there is no differential torque. The asymmetric modes are those where the right- and left-hand systems rotate in the same direction and thus apply torque to the inter-connect shafting.

The principal frequencies of torsional excitation are three per rev and six per rev. These n -per-rev and $2n$ -per-rev torques arise from oscillatory airloads. The proprotor's flapping gimbal (a Hooke's joint) causes two-per-rev torques, and some small amount of one-per-rev torque is normally present in a rotor. These bands of excitation are noted in Figure VI-8. The Model 300 drive system natural frequencies appear to be reasonably well located with regard to these excitation bands.

B. BLADE FLAPPING ENVELOPE IN AIRPLANE MODE

Proprotor flapping envelopes for sea level and 20,000-foot density altitude are shown in Figures VI-9 and -10, respectively. The sea-level flapping envelope differs from that shown earlier

in Report 300-099-003 because of configuration changes since the -003 report was submitted.

These envelopes were determined by calculating the mast angle of attack and pitch rate for a given flight condition and multiplying by the calculated flapping derivative. The sideslip line is based on full-pedal displacement up to the airspeed where a 300-pound pedal force is required. Above that airspeed, the rudder deflection for a 300-pound pedal force was used. The flapping excursion caused by gust encounters (a sudden gust was assumed) was added to the level flight flapping.

C. PROPROTOR STABILITY

A high level of proprotor/pylon stability is achieved by using a torsionally stiff wing in combination with a stiff pylon-to-wing mounting and modest values of pitch-flap coupling and hub restraint. Blade motion stability is obtained by using a gimbaled, stiff-inplane proprotor. The lowest inplane frequency is above operating speed which eliminates mechanical instability (ground resonance). The blade is mass balanced so that pitch-flap flutter is precluded. Blade-pitch axis precone, torsionally stiff blades, and a stiff control system effectively prevent pitch-lag instability. Positive pitch-flap coupling of 0.268 degree/degree ($\delta_3 = -15^\circ$) prevents flap-lag instability.

1. Analytical Method

BHC has developed two analyses to predict proprotor dynamic stability characteristics: a linear analysis and a nonlinear analysis. The linear analysis, BHC Proprotor Stability Analysis, DYN4 (Computer Program DRAL06) is based on small perturbation theory. The nonlinear analysis, BHC Proprotor Aeroelastic Analysis, DYN5 (Computer Program ARAP08), is based on nonlinear open form theory. A brief description of each analysis is given in the paragraphs below. More complete details, including equations of motion, are contained in References 4 and 5.

- Proprotor Stability Analysis, DYN4

Program DYN4 is a linear, twenty-one-degree-of-freedom proprotor stability analysis. It can determine the proprotor/pylon, blade motion, and flight mode stability characteristics of a tilt-rotor vehicle. A tip-path-plane representation is used for the proprotor, and linear aerodynamic functions are assumed. Details such as pitch-axis precone, underslinging, pitch-flap coupling, and flapping restraint are included. The first inplane blade mode is represented. Control system flexibility may also be simulated. Five coupled wing/pylon elastic modes are represented: wing beam, chord, and torsion; and pylon pitch and yaw. Six rigid-body degrees of

freedom are included to allow simulation of free-free body conditions and the aircraft short period flight modes.

Inputs to DYN4 are lumped parameters describing the dimensions, inertia, stiffness, and kinematics of the aircraft being simulated. Standard aircraft stability derivatives are used to study the influence of the propellers and the wing/pylon dynamics on the stability of the flight modes. Outputs are system eigenvalues and eigenvectors. Root loci can be plotted automatically.

- Proprotor Aeroelastic Analysis, DYN5

Program DYN5 is a nonlinear, open-form proprotor aeroelastic analysis that uses the same basic mathematical model as DYN4. This program calculates proprotor loads, vibration, and stability in helicopter, conversion, and high-speed modes. A special version of the program has been developed for the Air Force, Reference 5.

The dynamic equations of motion were derived using the Lagrangian method. Provisions for large flapping and feathering motion are included in DYN5. Small angle assumptions are made on the wing-pylon and blade elastic degrees of freedom. The aerodynamic functions used in DYN5 are the same as those used in the Bell Rotor Performance Analysis, F35. C_l , C_d , and C_m are input in tabular form for a 180-degree range of angle of attack and for Mach numbers up to 0.9. Tables for different profiles may be input to account for differences in the blade section from root to tip, thereby properly accounting for blade stall and compressibility effects.

DYN5 is programmed for solution by digital computer. A predictor-corrector integration technique is used in the solution of the simultaneous equations of motion. Input to the program consists of lumped parameters and the coupled normal modes of the wing, pylon, and proprotor. The output consists of a time history of the wing and pylon motions, and the blade flapping and elastic deflection. Generally, initial conditions are input to minimize the time required for convergence to steady-state trim. For stability investigations, the transient response to external inputs or to initial conditions can be calculated.

Both analyses have been shown to yield excellent correlation with measured proprotor stability characteristics. Examples of the correlation are published in References 2 and 6. For this study, the linear analysis, DYN4, was used exclusively since its use involves much less time (for the analyst as well as the computer) than the nonlinear analysis, and since it has been shown to give conservative results.

With program DYN4, the modes which are symmetric about the fuselage longitudinal centerline are treated separately from those asymmetric about the centerline. This assumption simplifies the analysis somewhat since only one propotor needs to be represented. The other propotor is treated in either a mirror image (for the symmetric modes) or a reverse mirror image (for the asymmetric modes). For the Model 300 analysis, the DYN4 math model for each set of modes, symmetric or asymmetric, consists of the following fifteen degrees of freedom:

- Two rigid-body flapping modes, one involving backward precession in the rotating system, the other, forward precession.
- Two blade inplane bending modes in the rotating system, a forward whirl and a backward whirl of the displaced blade's center of gravity.
- Three rigid-body airframe modes: plunging, pitching, and longitudinal translation in the symmetric case, and roll, yaw, and lateral translation in the asymmetric case.
- Five wing-pylon elastic degrees of freedom: wing beamwise bending, chordwise bending, and torsion; and pylon pitch and yaw with respect to the wing.
- Three drive system degrees of freedom: propotor rotation, powerplant power turbine rotation, and pylon roll with respect to the wing.

These degrees of freedom, which are completely coupled in the analysis, are necessary and sufficient to represent the coupled natural modes of the Model 300 adequately. With this math model, the short period rigid-body flight modes, the propotor blade motion stability, and the propotor pylon stability are treated simultaneously.

The influence of compressibility on the airframe and propotor has been included in the Model 300 dynamic stability analysis. Ideally, the airframe derivatives and propotor aerodynamic characteristics are varied with airspeed, taking into account compressibility, up to the instability airspeed. However, for the Model 300, instability is calculated to occur well above drag divergence of both the airframe and propotor where aerodynamic characteristics are not clearly definable. Therefore, the following procedure was followed: the airframe aerodynamic derivatives were varied appropriately for airspeeds up to V_{limit} . Above V_{limit} , the derivative was held constant at the values for V_{limit} . The propotor lift curve slope was varied with airspeed using the method suggested in Reference 7 up to the drag divergence airspeed. Above drag divergence, the maximum possible value of lift curve slope (9.2/radian) was used. The propotor profile drag was not varied with airspeed. Studies using the nonlinear program,

DYN5, show this method of accounting for the influence of compressibility is conservative.

2. Stability Characteristics of the Coupled Modes

The stability characteristics of the coupled proprotor-pylon-wing-fuselage system can conveniently be discussed using root locus plots. To illustrate the coupling between the various modes of the system, the stability of the proprotor uncoupled flapping modes will be discussed first and then other modes added in a stepwise manner.

Figure VI-11 shows the root locus of the proprotor rigid-body flapping modes as a function of airspeed. The two modes correspond to forward and backward precession of the proprotor disc in a rotating coordinate system. The frequency and damping decrease with airspeed because the inflow angle increases with airspeed. However, even at the maximum speed shown (600 knots) the damping of the uncoupled flapping modes is very high.

The blade first inplane bending mode is coupled with rigid-body flapping in Figure VI-12. The two inplane modes represent forward and backward whirling of the center of gravity of the displaced blades in a rotating coordinate system. The damping of the uncoupled inplane modes increases with airspeed because of the increase in inflow angle. However, when the blade flapping and inplane roots become close, strong coupling is evident and damping of the inplane modes decreases.

The wing beam and chord bending and torsion modes are added to the proprotor flapping and inplane modes in Figure VI-13. The wing-root end condition is treated as though it were cantilever mounted. Coupling with the proprotor modes causes the frequency and damping of the wing/pylon modes to first increase with airspeed and then decrease at airspeeds above 400 knots. The wing beam mode becomes unstable at speeds over 500 knots.

The aircraft rigid-body modes and the drive-system modes are added to the proprotor and wing-pylon modes in Figures VI-14 and -15. As noted earlier, the modes are separated into symmetric and asymmetric sets. The short-period and Dutch-roll modes are basically rigid-body aircraft motion, but are strongly coupled with the proprotor and wing/pylon modes. The interconnect and power turbine modes are the drive-system modes discussed earlier but include the rotor and power turbine aerodynamic damping and are coupled with the wing-pylon modes. The first symmetric mode to become unstable is the wing chord bending mode, at a speed of approximately 535 knots. The asymmetric beam mode also becomes unstable at that airspeed.

3. Model 300 Stability Boundaries

Stability boundaries in airplane mode were calculated as a function of proprotor rpm and as a function of altitude. The

boundaries were obtained by calculating root locus plots for each flight condition (such as those shown in Figures VI-14 and -15) and determining the airspeeds at which modes become unstable. Figures VI-16 and -17 show the symmetric and asymmetric boundaries versus rpm, respectively. Figures VI-18 and -19 show the boundaries versus altitude for the symmetric and asymmetric modes, respectively. In each plot, the boundaries for the modes which become unstable are identified.

Stability boundaries were also calculated for the conversion mode conditions where the lowest stability boundary is expected. This occurs when the pylon is almost completely converted but has not engaged the pylon downstop. In this condition, the flexibility of the conversion actuator and actuator spindle reduces the effective torsional stiffness to approximately one-half of the torsional stiffness with the pylon on the downstop. Conversion mode stability boundaries versus altitude for the symmetric and asymmetric modes are shown in Figures VI-20 and -21, respectively.

The airplane mode stability boundaries are compared to the flutter-free requirement and to aerodynamic limits in Figure VI-22. The stability boundary at sea level is in excess of 500 knots over the full range of rpm, and even at 20,000 feet altitude the boundary is at 456 knots (above 12,000 feet altitude, the boundary is defined by rigid body flight mode instability). It is seen that the Model 300 stability boundary is greatly in excess of the aircraft's aerodynamic limits and of the required flutter-free airspeed. The boundaries for conversion mode are also in excess of the aerodynamic limits and the flutter-free requirement.

4. Sensitivity to Loss of Stiffness

The Model 300 wing torsional stiffness is the primary structural factor influencing the proprotor stability boundary. The design value of torsional stiffness is considerably higher than the value needed to meet the stability margin requirement. This results from the torsional stiffness needed to avoid one-per-rev resonance of the wing torsion mode. Consequently, a large loss of torsional stiffness could occur without incurring proprotor instability.

Figure VI-23 shows the variation in the stability boundary with torsional stiffness. A very large reduction in torsional stiffness could occur before instability occurred in the flight envelope. Of course, resonance with one per rev would result, but the pilot could select a proprotor rpm to minimize the response.

D. RIDE COMFORT

1. Rotor Harmonic Induced Vibration

Cabin and crew station vibration at the blade passage frequency was calculated using the NASTRAN structural model discussed in section VI-A.2 and applying calculated propotor three-per-rev hub forces. The hub forces in helicopter and conversion mode were calculated using the BHC Rotorcraft Simulation Analysis, Program C81, Reference 8. For airplane mode, the BHC propotor aeroelastic analysis was employed, Reference 4. Aerodynamic interference between the propotor and the wing is included in the analysis.

The cabin and crew station vibration levels are shown in Figures VI-24 and -25. These meet the MIL-A-8870(ASG) requirement. In airplane mode, the level is very low--about at the level of perception.

The pylon center-of-gravity vibration level is shown in Figure VI-26. These levels are well below the design vibration level for the pylon-- ± 1 g at three per rev.

2. Response to Atmospheric Turbulence in Airplane Mode

An analytical method based on a statistical representation of turbulence was used to calculate the Model 300 acceleration response to atmospheric turbulence. This power spectral approach provides for a realistic representation of the nature of turbulence and accounts for aircraft response characteristics in a rational manner.

a. Analytical Method

The procedure adopted for calculating the response to turbulence spectra follows Reference 9 and is depicted in Figure VI-27. The aircraft is treated as a point insofar as the gust field is concerned; that is, every point on the aircraft experiences the same gust velocity. This assumption does result in attenuation of the higher frequency turbulence components but is considered reasonable since the power spectral density is very low at higher frequencies. The assumption of a one-dimensional gust field was made to simplify the calculations and assessment of the results.

The Model 300 frequency response to turbulence was calculated by modifying the BHC Propotor Stability Analysis, Program DYN4 (see Section VI-C for a description of DYN4). Frequency response to vertical, lateral, and head-on sinusoidal fields of unit magnitude, i.e., one foot per second, is calculated separately for each airspeed and rpm of interest. Correlation of this method with measured response of a cantilever wing propotor model is reasonably good. Figure VI-28 shows the Model 300 frequency response to vertical and head-on gusts at 200 knots.

The Von Karman turbulence shown in Figure VI-29 with a scale of 1000 feet was used. (The scale refers to the wavelength below which there is less probability of encountering a gust of a shorter wavelength. Thus, the choice of scale determines the relative density of low-frequency and higher frequency gusts.) According to Reference 10, this spectrum is a reasonable analytic representation for atmospheric turbulence.

The Model 300 response spectral density to the assumed turbulence field is shown in Figure VI-30. When this response spectrum is compared to the unit gust frequency response (Figure VI-28), the weighting effect of the turbulence field is evident. Note that the highest response is at the frequencies of the aircraft rigid-body modes rather than the wing/pylon modes. This is due to the lower power spectral density of the turbulence at the higher frequencies.

To obtain a meaningful indication of the ride comfort, the mean square value of the response spectrum, Figure VI-30, is calculated. This rms acceleration response can be multiplied by the rms value of the turbulence to obtain an rms acceleration level.

b. Model 300 Response Levels

Figure VI-31 shows the rms acceleration response to vertical and head-on turbulence at the crew station. The response at the aircraft center of gravity is shown in Figure VI-32. The response to lateral turbulence is shown in Figure VI-33. Note that both the vertical acceleration response (σ_{g_z}) and the longitudinal acceleration response (σ_{g_x}) are shown for the vertical and head-on turbulence.

For perspective, a turbulence intensity value of less than one foot-per-second rms is considered smooth air; a five foot-per-second rms intensity is considered rough air. In rough air ($\sigma = 5$ feet per second), the rms acceleration value at the crew station at a true airspeed of 260 knots would be: 0.29g vertical, 0.105g longitudinally, and 0.0035g laterally (based on superimposing the response to five feet-per-second rms vertical, head-on, and lateral fields).

The contribution of the proprotors to the response in turbulence is shown in Figure VI-34. The influence on the vertical response is small; apparently, the proprotor damping of the wing modes offsets the increased short period mode response. Of course, the proprotors greatly increase the longitudinal response to head-on turbulence.

Figure VI-35 shows the contribution of the wing/pylon elastic degrees of freedom to the response in turbulence. The elastic modes increase the response by about 15 percent for vertical turbulence, and 20 percent for head-on turbulence.

c. Comparison with Conventional Aircraft

The aerodynamic and mass properties for a Beech 99 propeller-driven commuter transport were input to the same analysis used for the Model 300 response calculations. The airframe was assumed rigid and the cruise configuration flight aerodynamic derivatives were used. The propeller contribution was included in the airframe aerodynamic derivatives rather than treated separately as with the Model 300 proprotor.

The calculated response of the Model 300 to turbulence is compared with that for the Beech 99 in Figure VI-36. These show the Model 300 at the same airspeed to have a lower response to vertical turbulence than the Beech 99. (However, the Beech 99 wing loading is 43 psf compared to the 68.5 psf of the Model 300. On an equal wing loading basis, the aircraft would have about the same response.)

The longitudinal acceleration response of the Model 300 to head-on turbulence is three times that of the Beech 99 because of the proprotors. The vertical acceleration response to head-on turbulence is about the same.

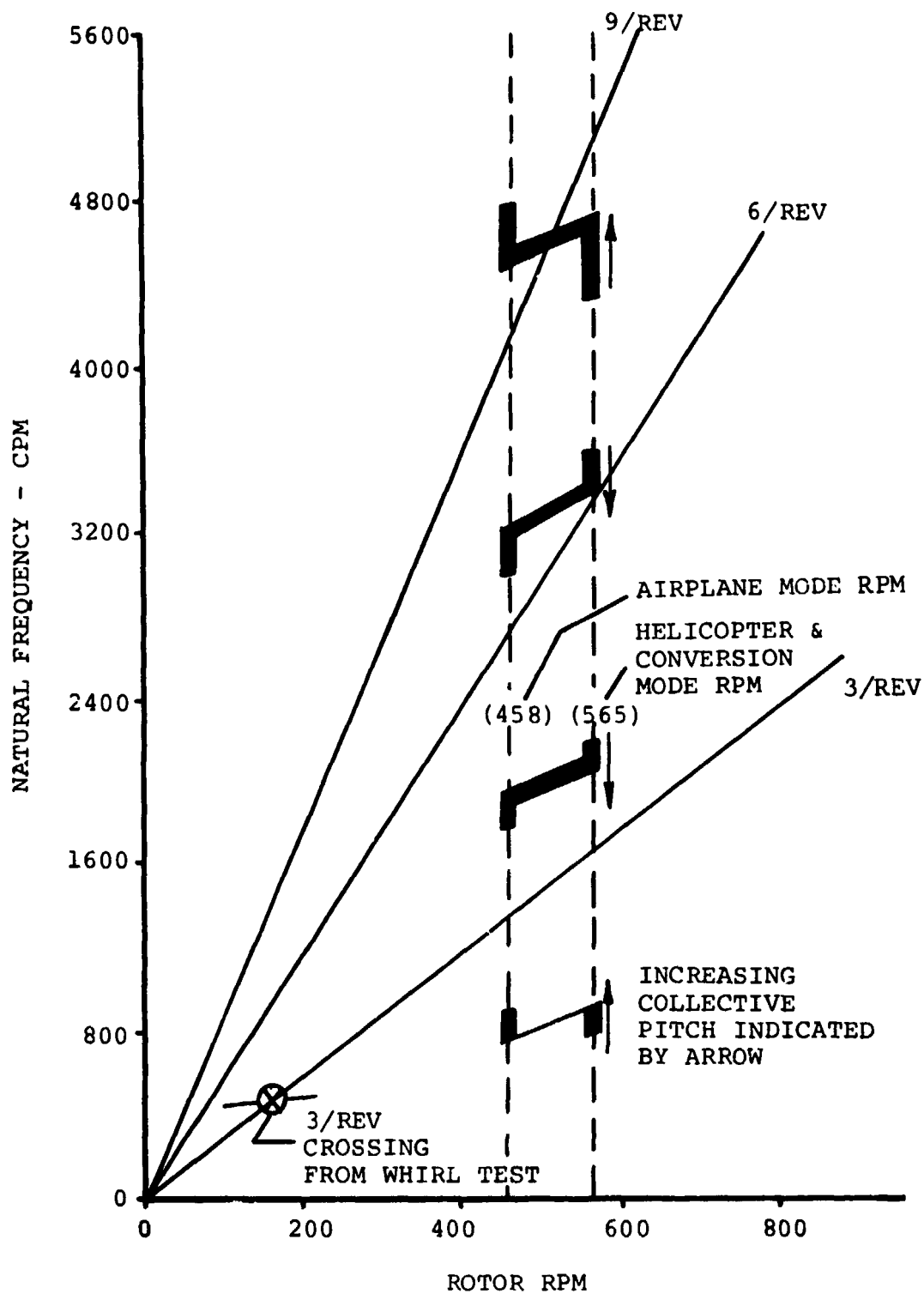


Figure VI-1. Model 300 Proprotor Collective Mode Natural Frequencies.

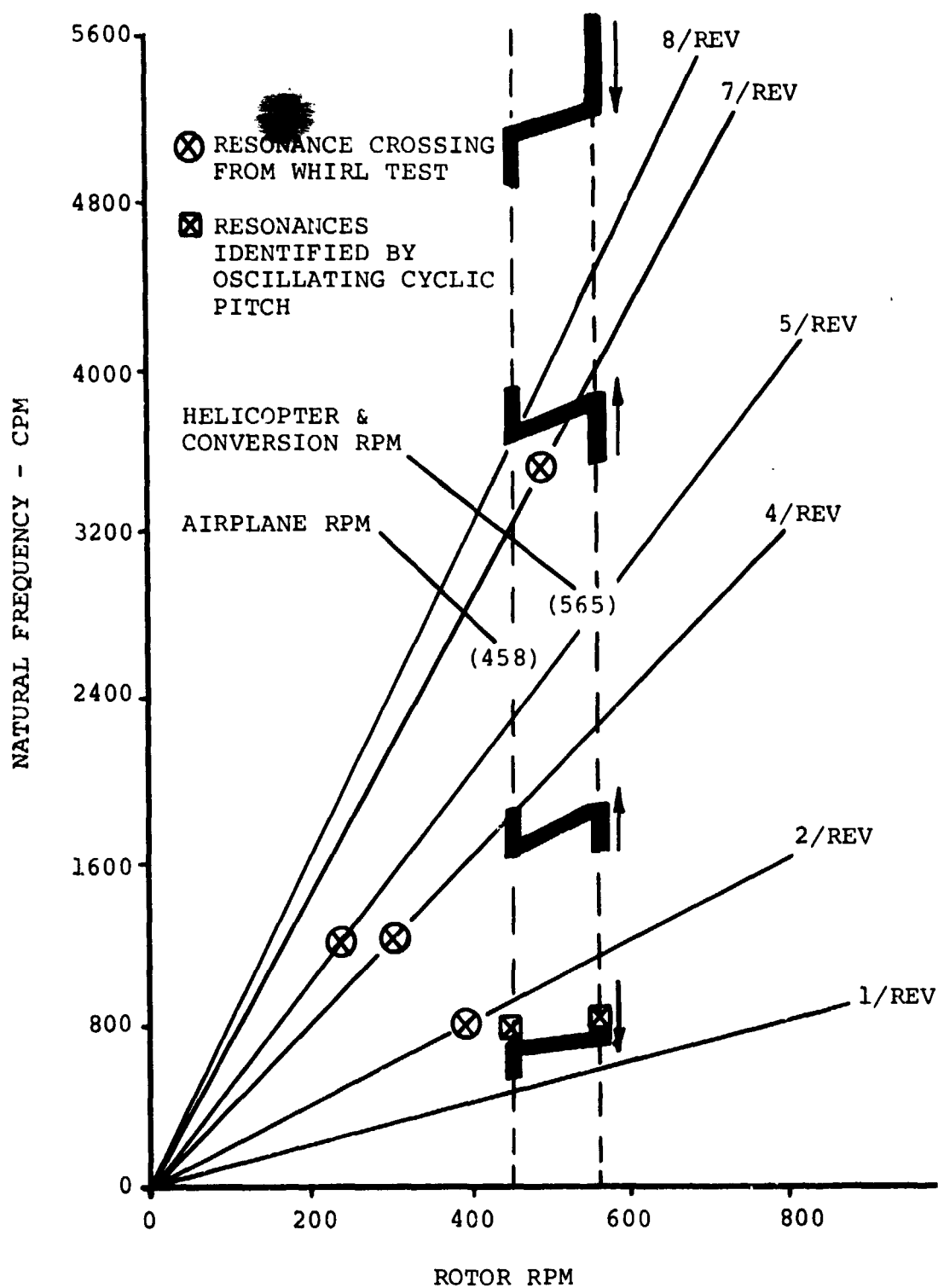


Figure VI-2. Model 300 Proprotor Cyclic Mode Natural Frequencies.

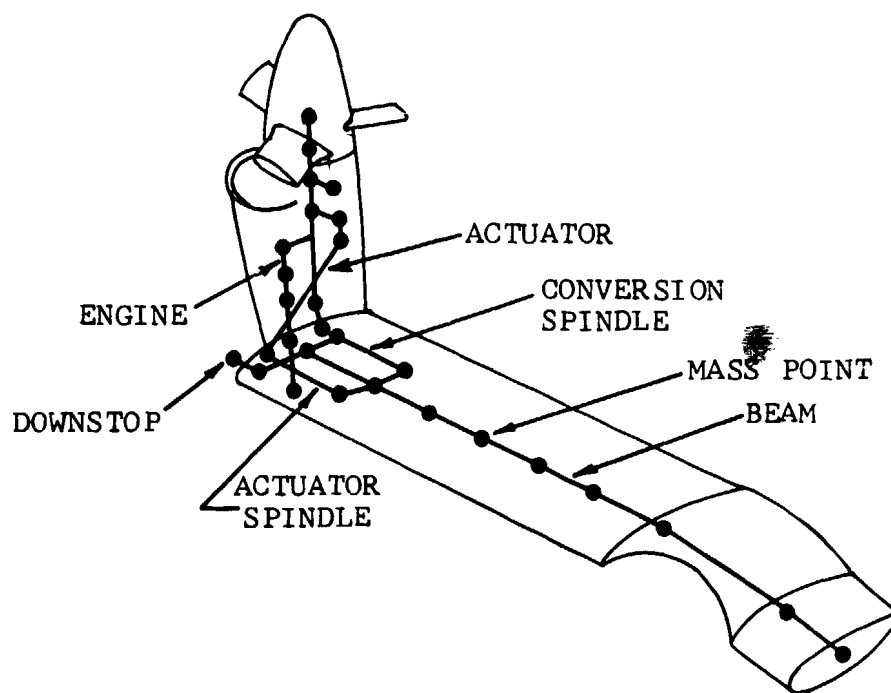
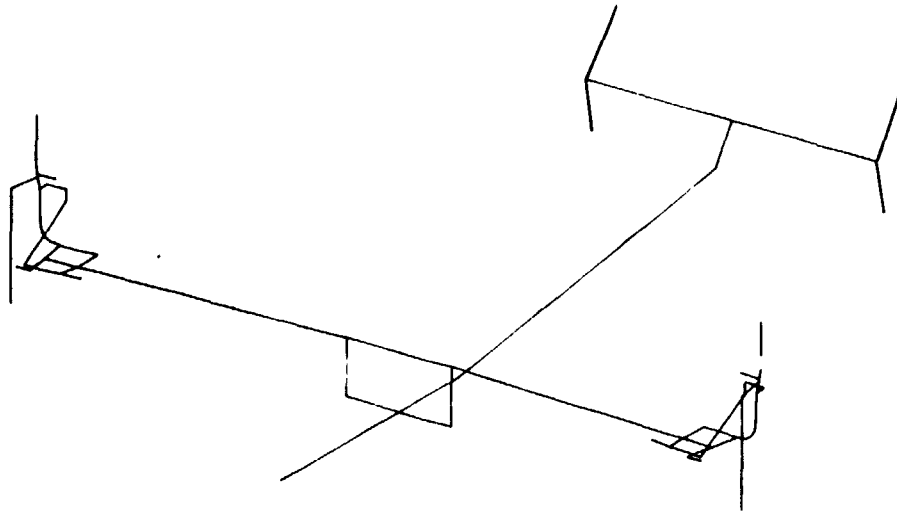
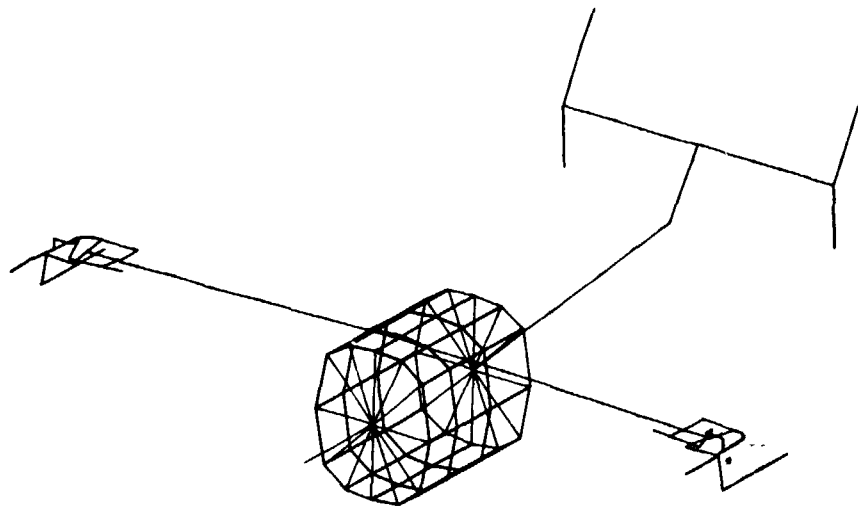


Figure VI-3. Structural Model of Wing-Pylon System.

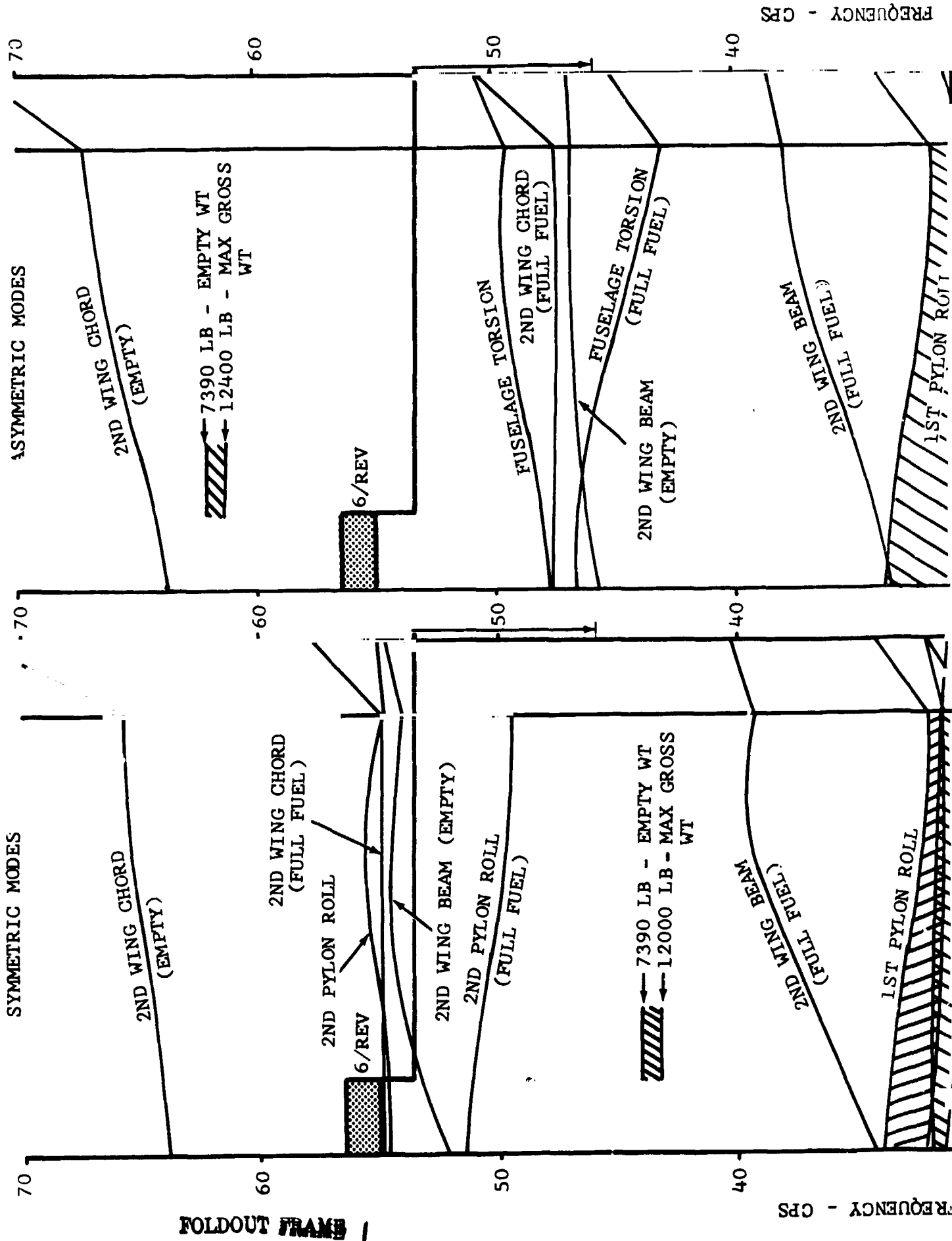


a. Full Span Wing with Simple Fuselage.



b. Full Span Wing with Detailed Fuselage
Center Section.

Figure VI-4. Structural Models of Wing-Pylon-Fuselage
System.



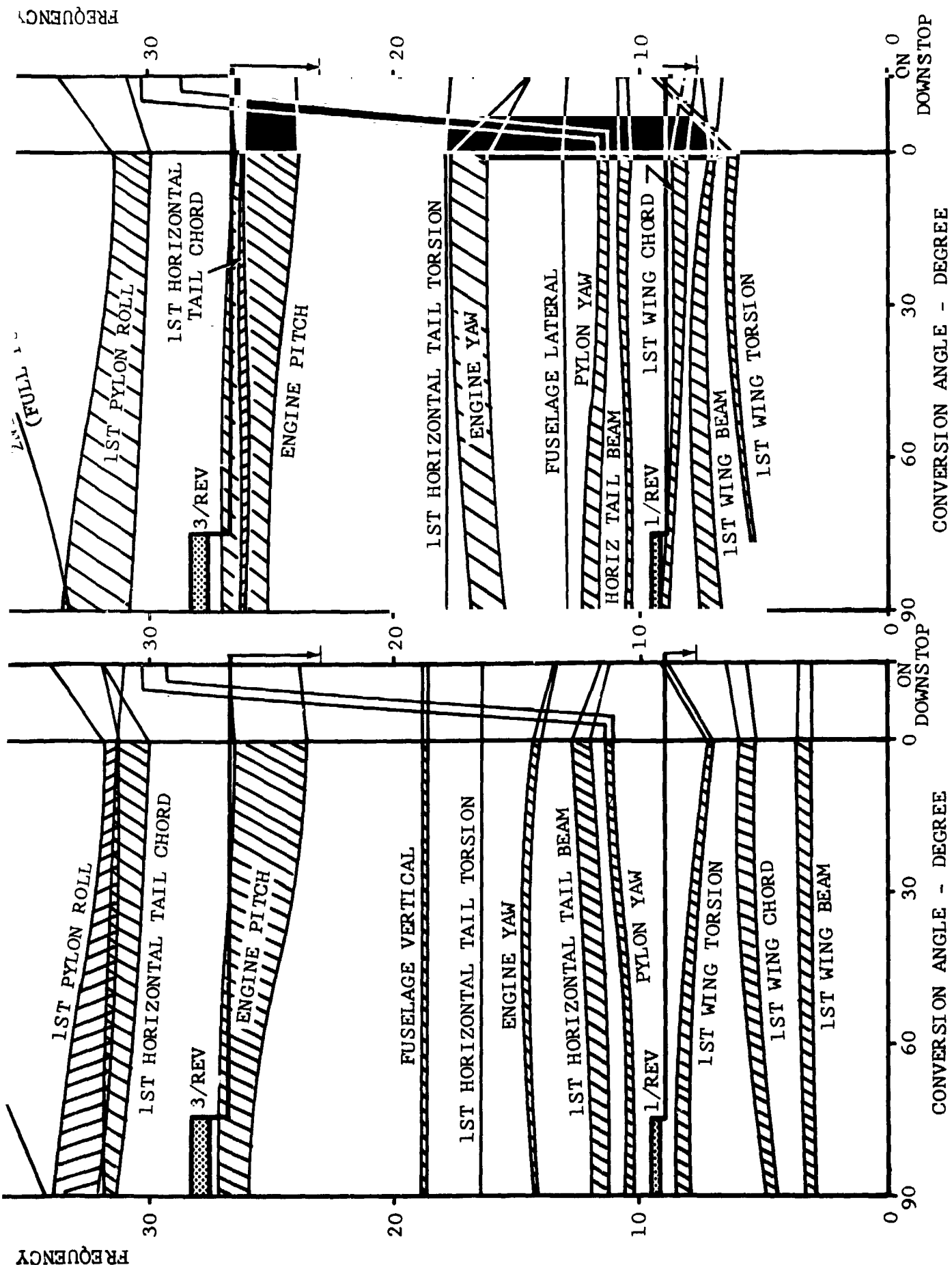


Figure VI-5. Model 300 Airframe Natural Frequencies, Symmetric.

Figure VI-6. Model 300 Airframe Natural Frequencies. Asymmetric.

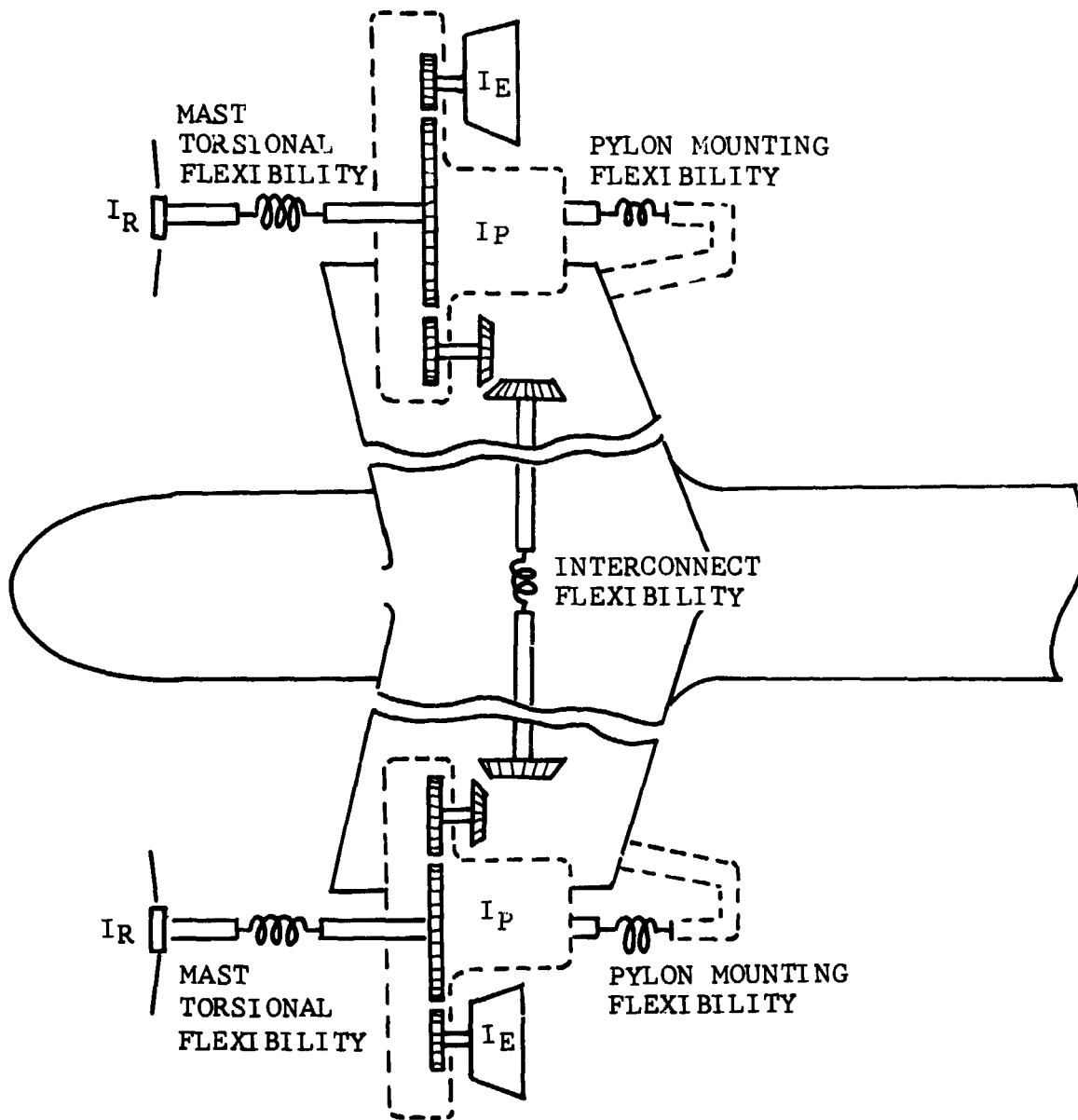


Figure VI-7. Analytical Model of Model 300 Drive System.

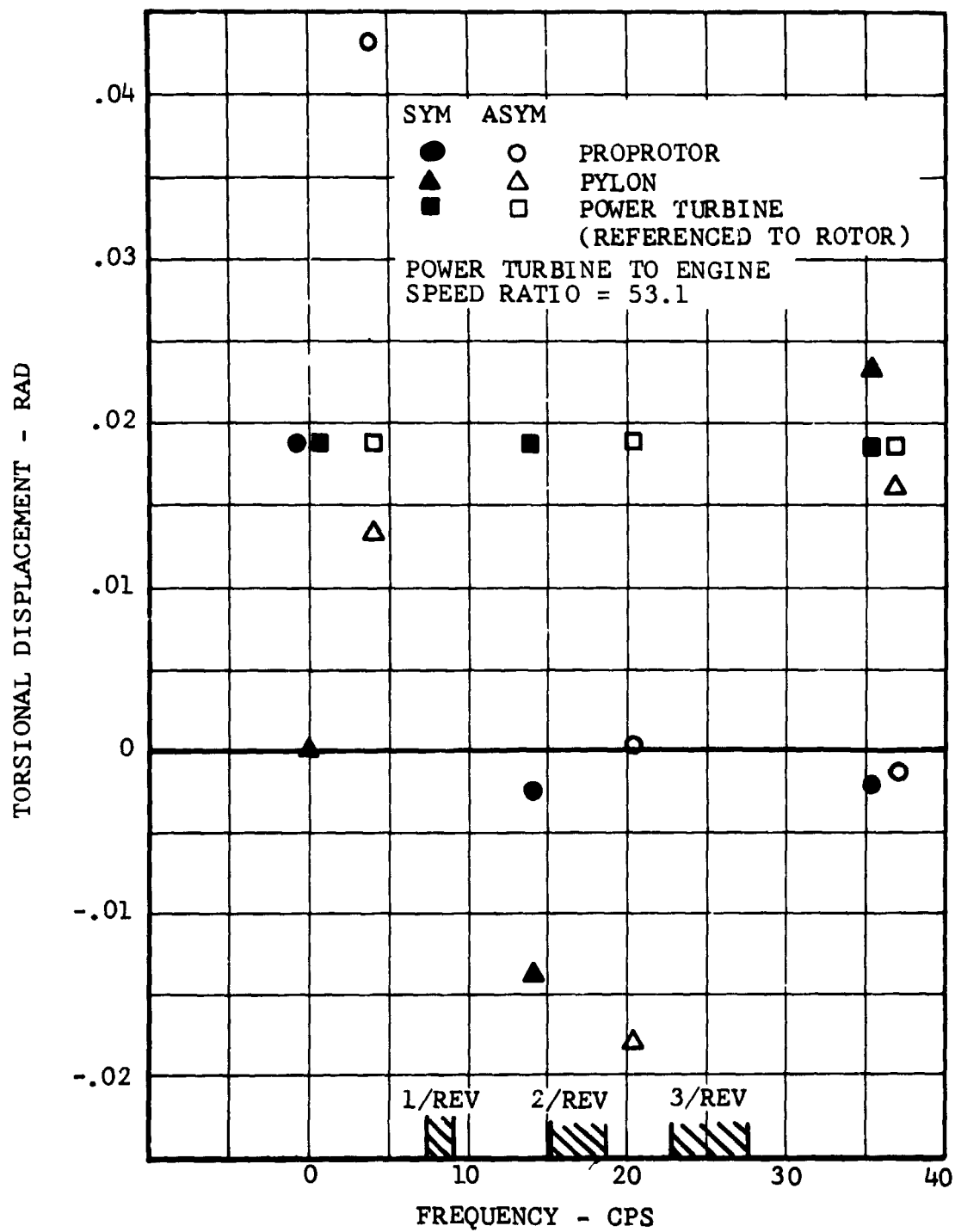


Figure VI-8. Model 300 Drive System Natural Frequencies and Modes.

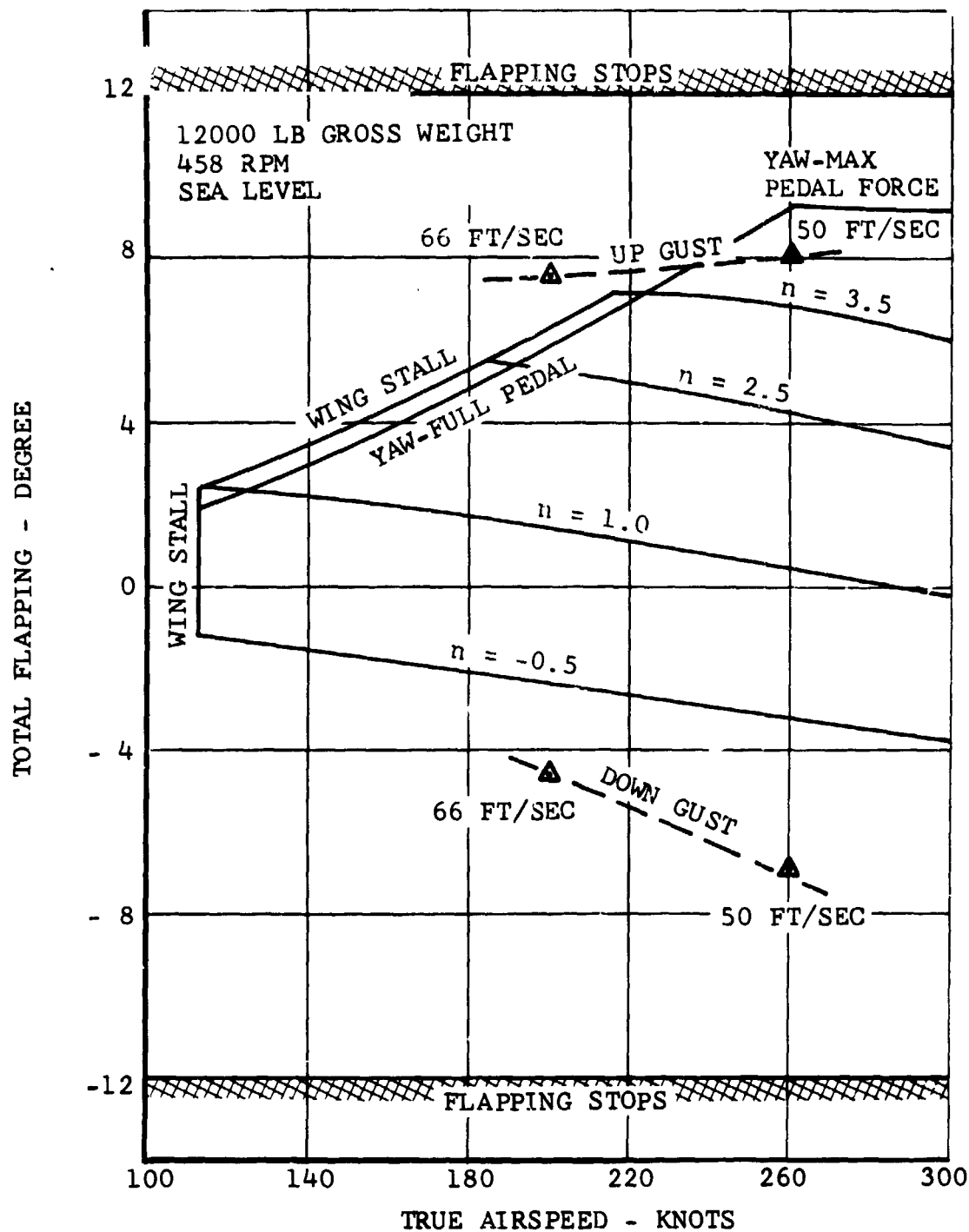


Figure VI-9. Airplane Mode Flapping Envelope, Sea Level.

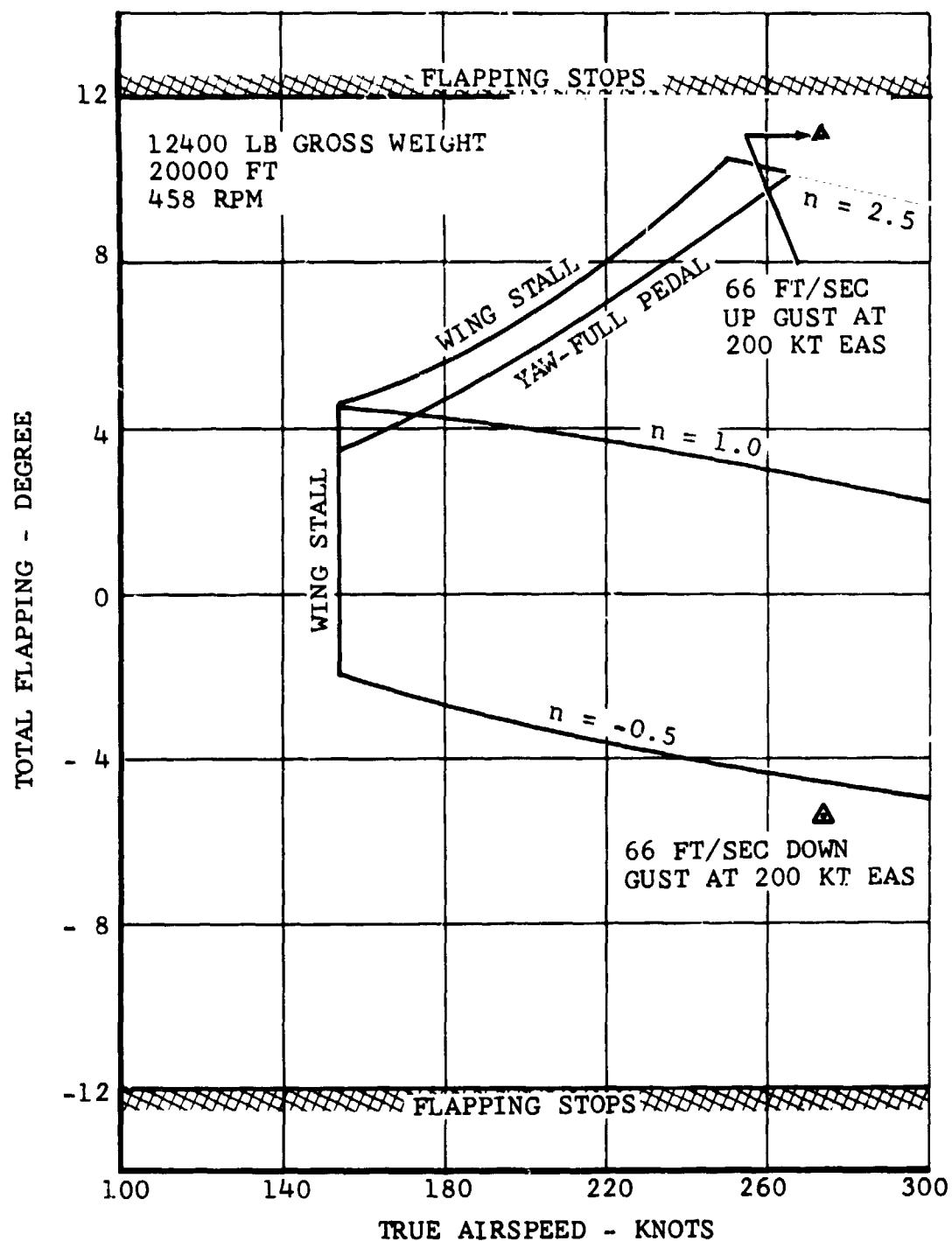


Figure VI-10. Airplane Mode Flapping Envelope, 20,000 Feet.

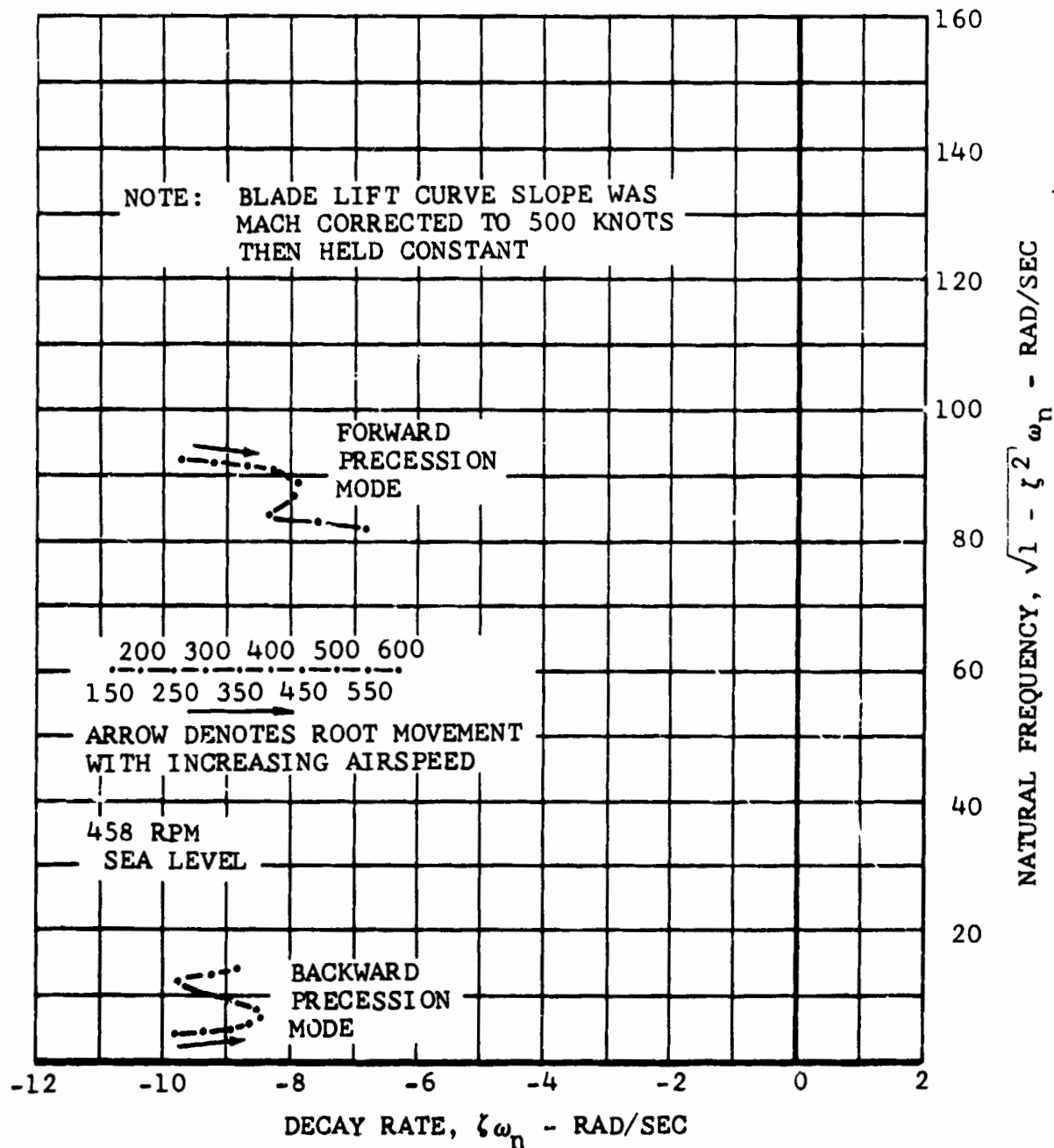


Figure VI-11. Model 300 Blade Flapping Modes, Root Variation with Airspeed.

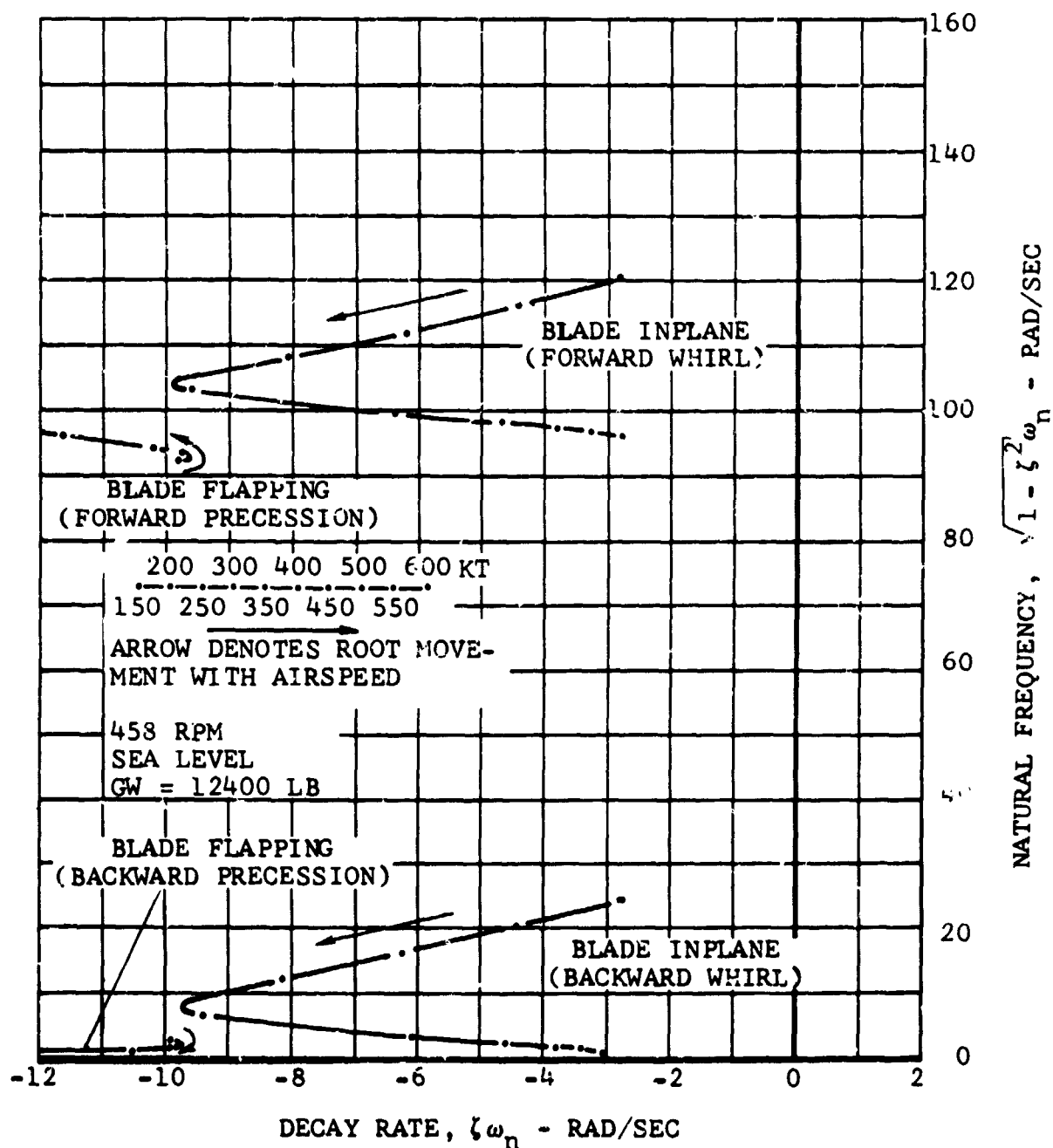


Figure VI-12. Model 300 Proprotor Coupled Flapping and Inplane Bending Modes, Root Variation with Airspeed.

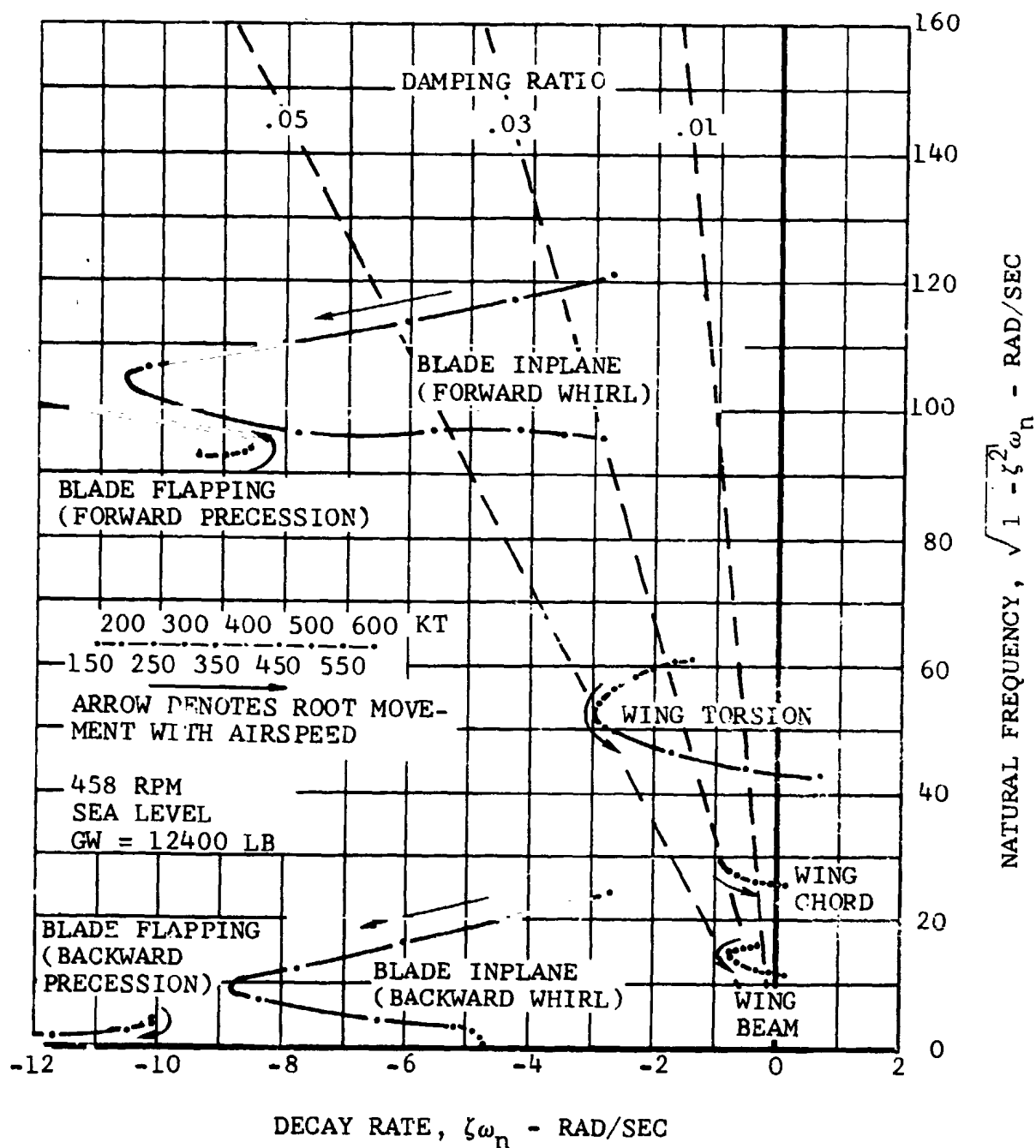


Figure VI-13. Model 300 Cantilevered Wing, Root Variation With Airspeed.

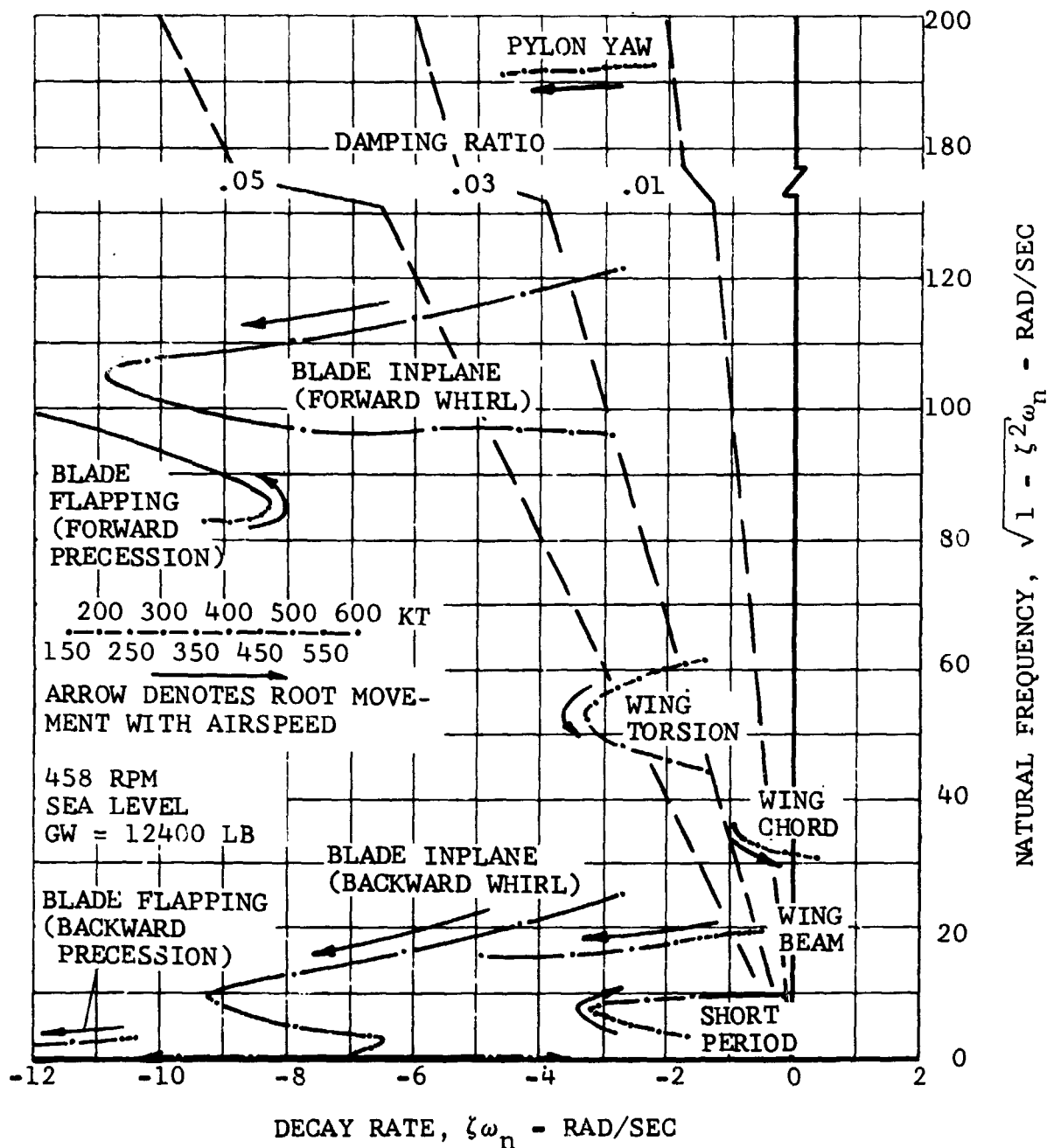


Figure VI-14. Model 300 Symmetric Modes, Root Variation with Airspeed.

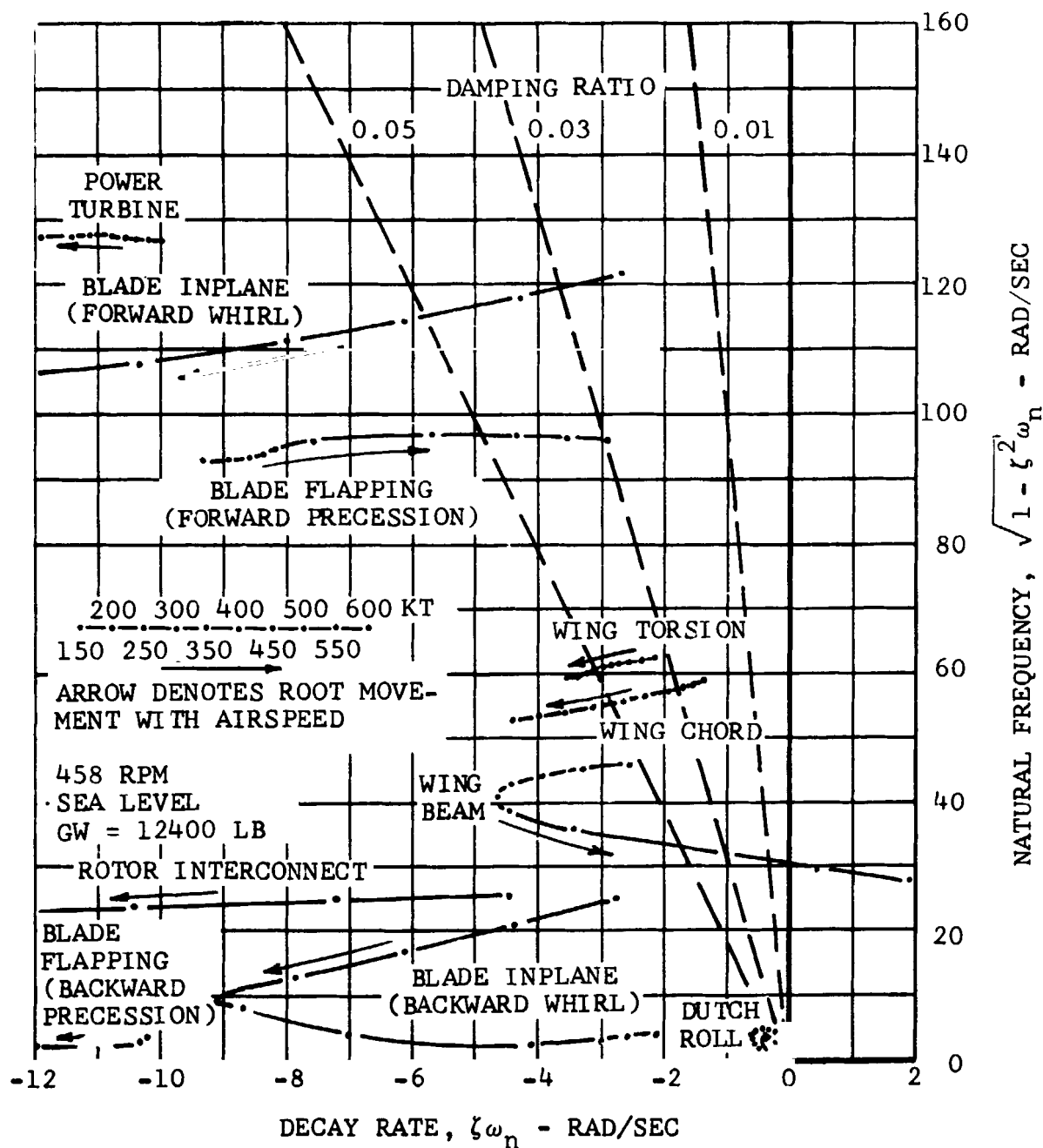


Figure VI-15. Model 300 Asymmetric Modes, Root Variation with Airspeed.

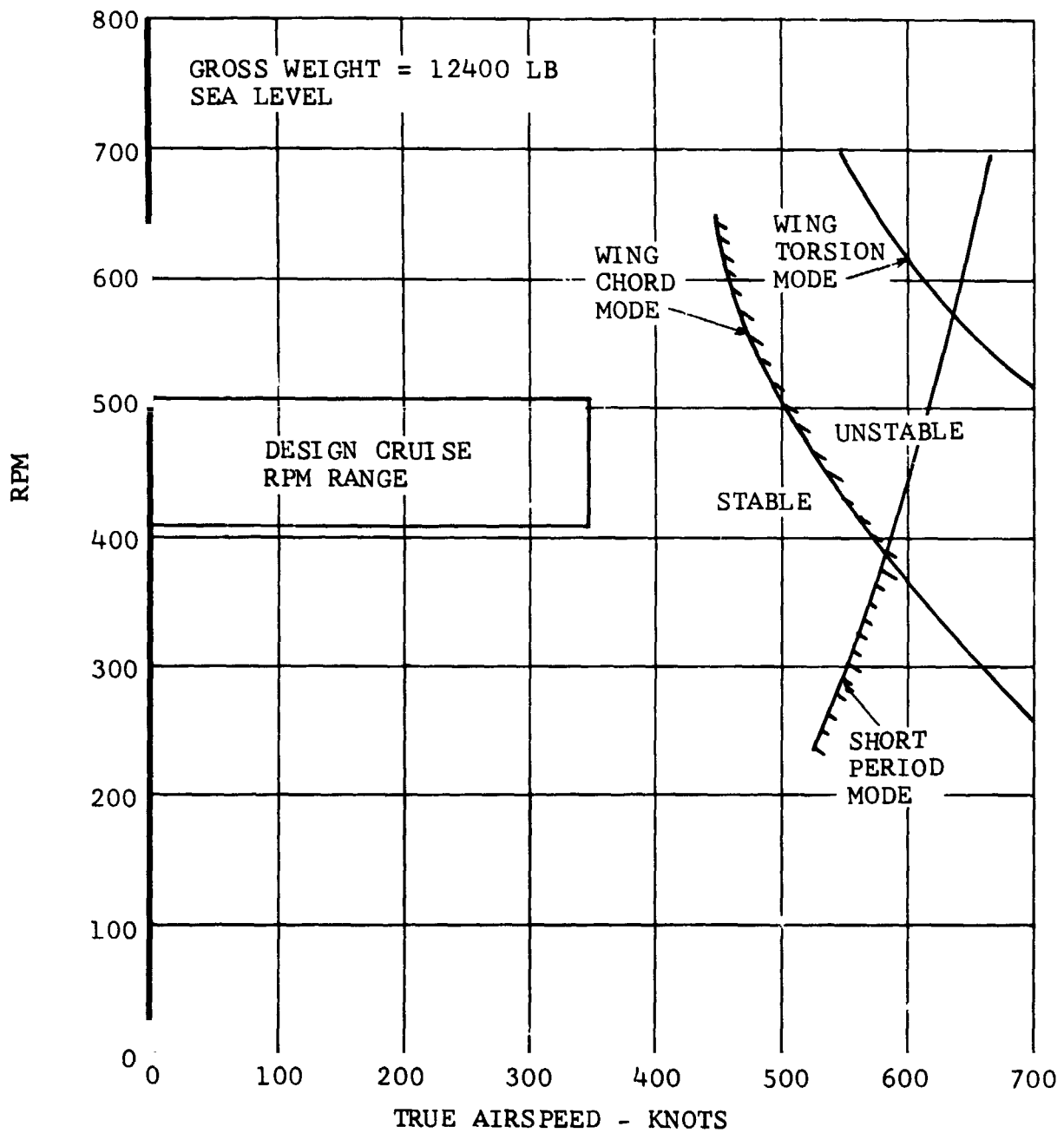


Figure VI-16. Model 300 Airplane Mode Stability Boundary Versus Proprotor RPM, Symmetric Modes.

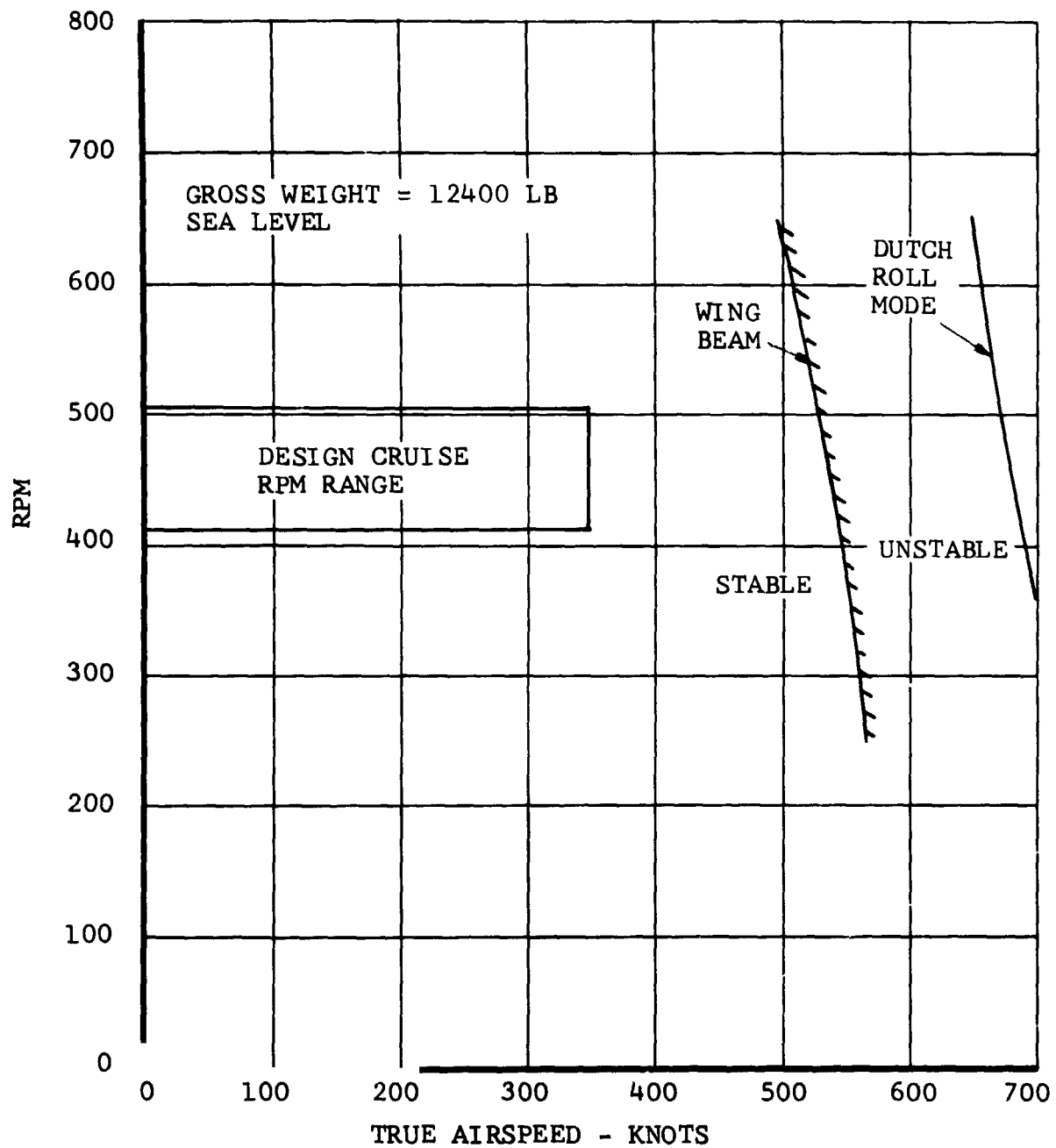


Figure VI-17. Model 300 Airplane Mode Stability Boundary Versus RPM, Asymmetric Free-Free Modes.

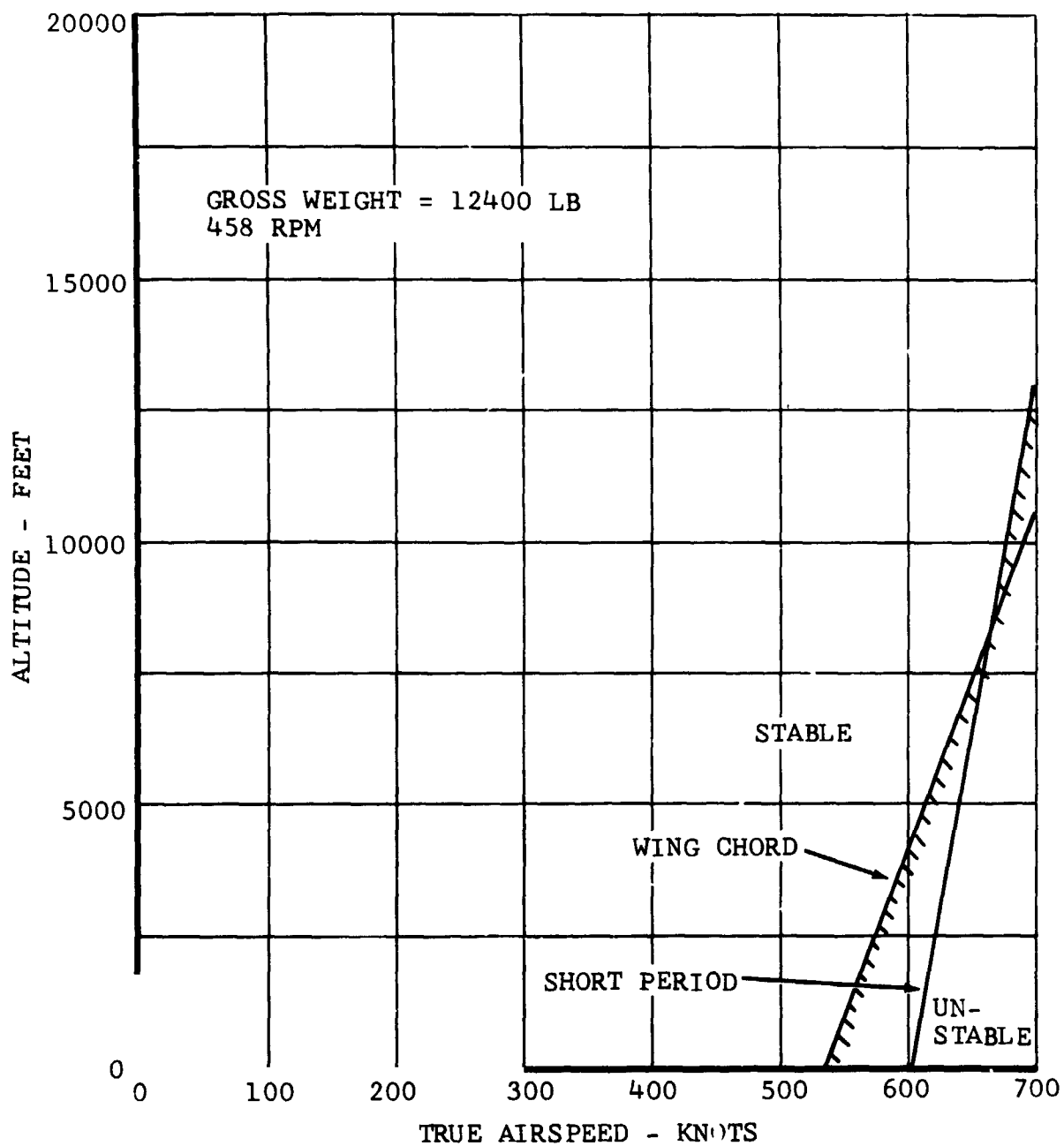


Figure VI-18. Model 300 Airplane Mode Stability Boundary Versus Altitude, Symmetric Modes.

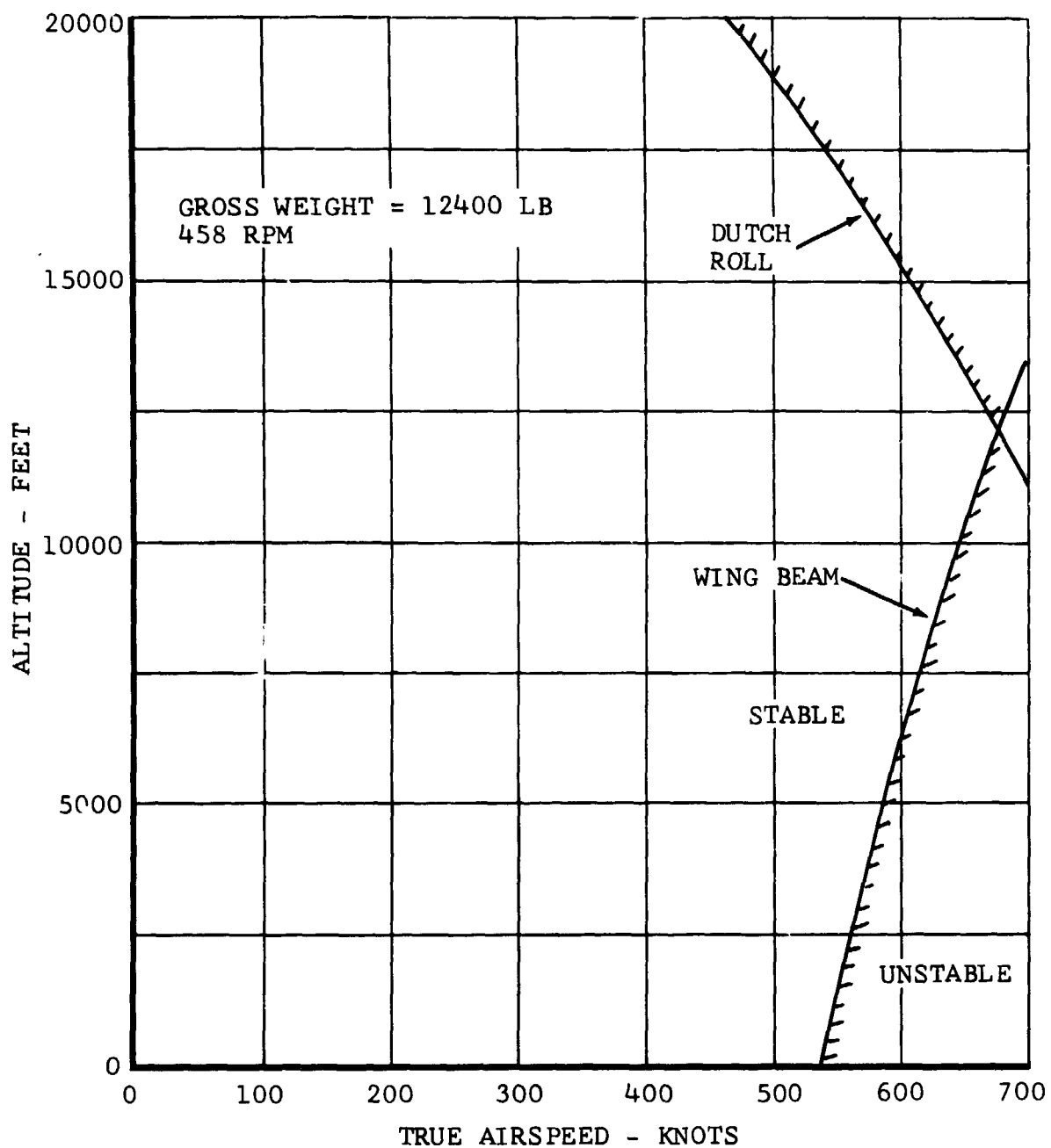


Figure VI-19. Model 300 Airplane Mode Stability Boundary Versus Altitude, Asymmetric Modes.

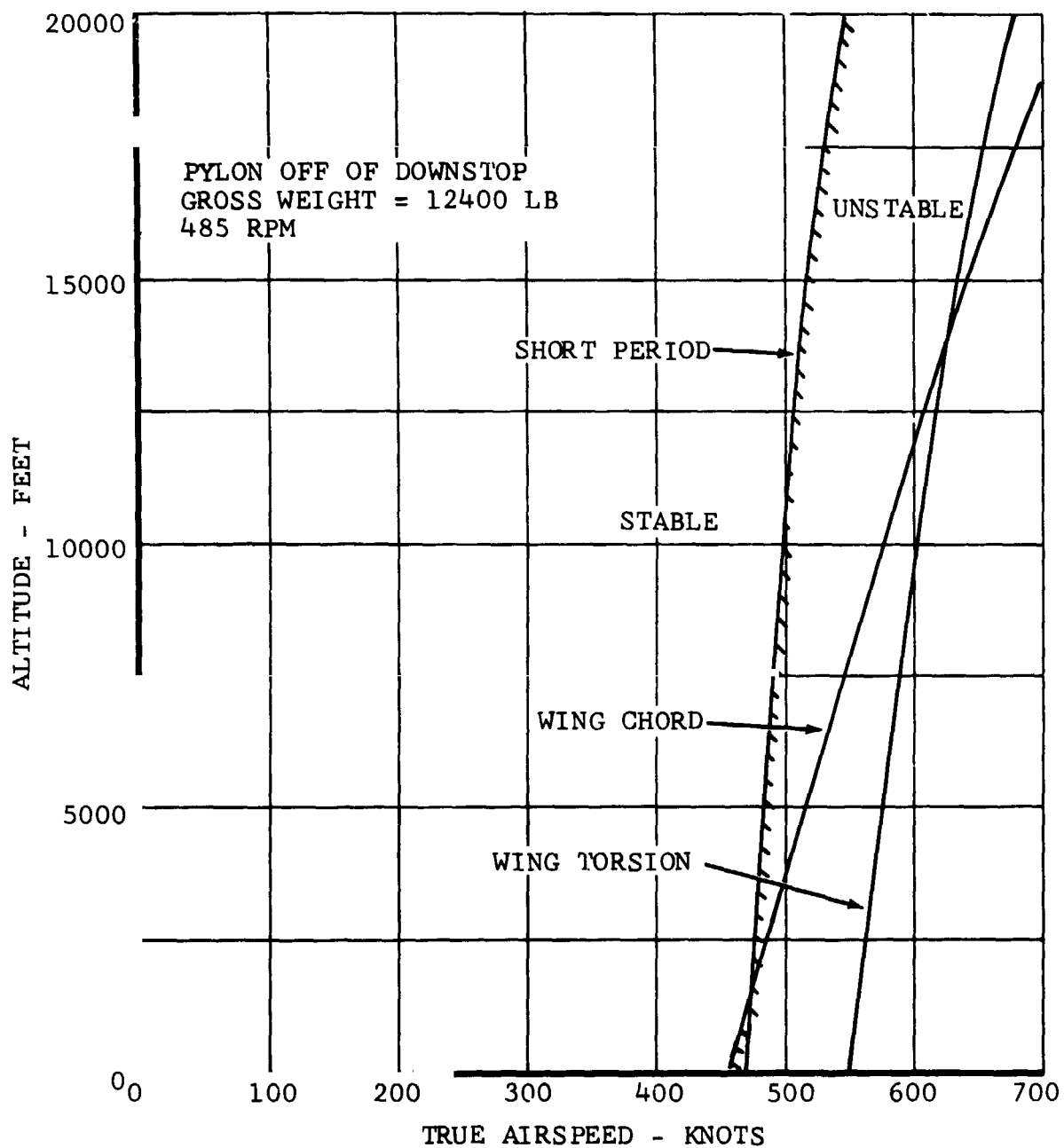


Figure VI-20. Model 300 Conversion Mode Stability Boundary Versus Altitude, Symmetric Modes.

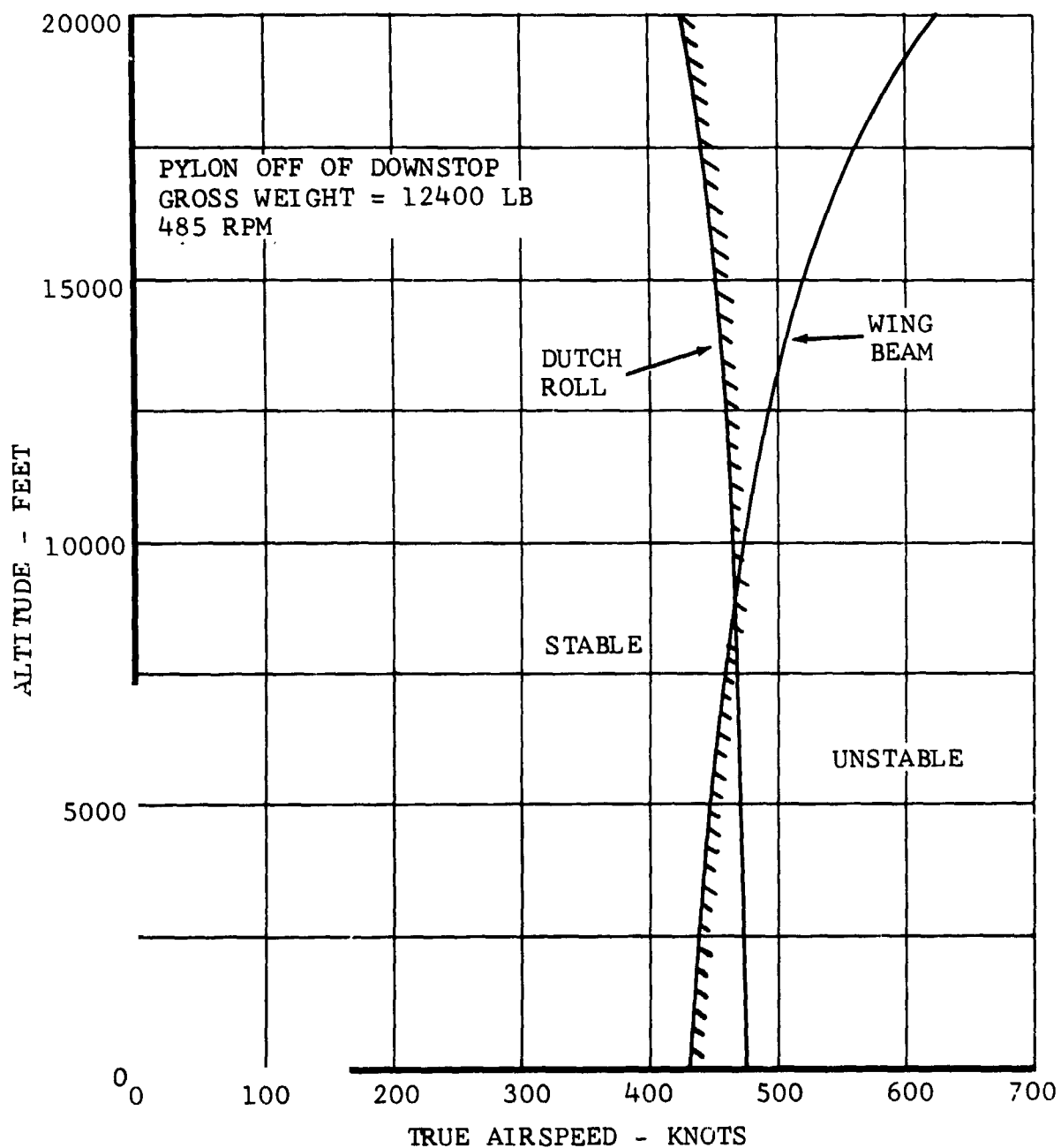


Figure VI-21. Model 300 Conversion Mode Stability Boundary Versus Altitude, Asymmetric Modes.

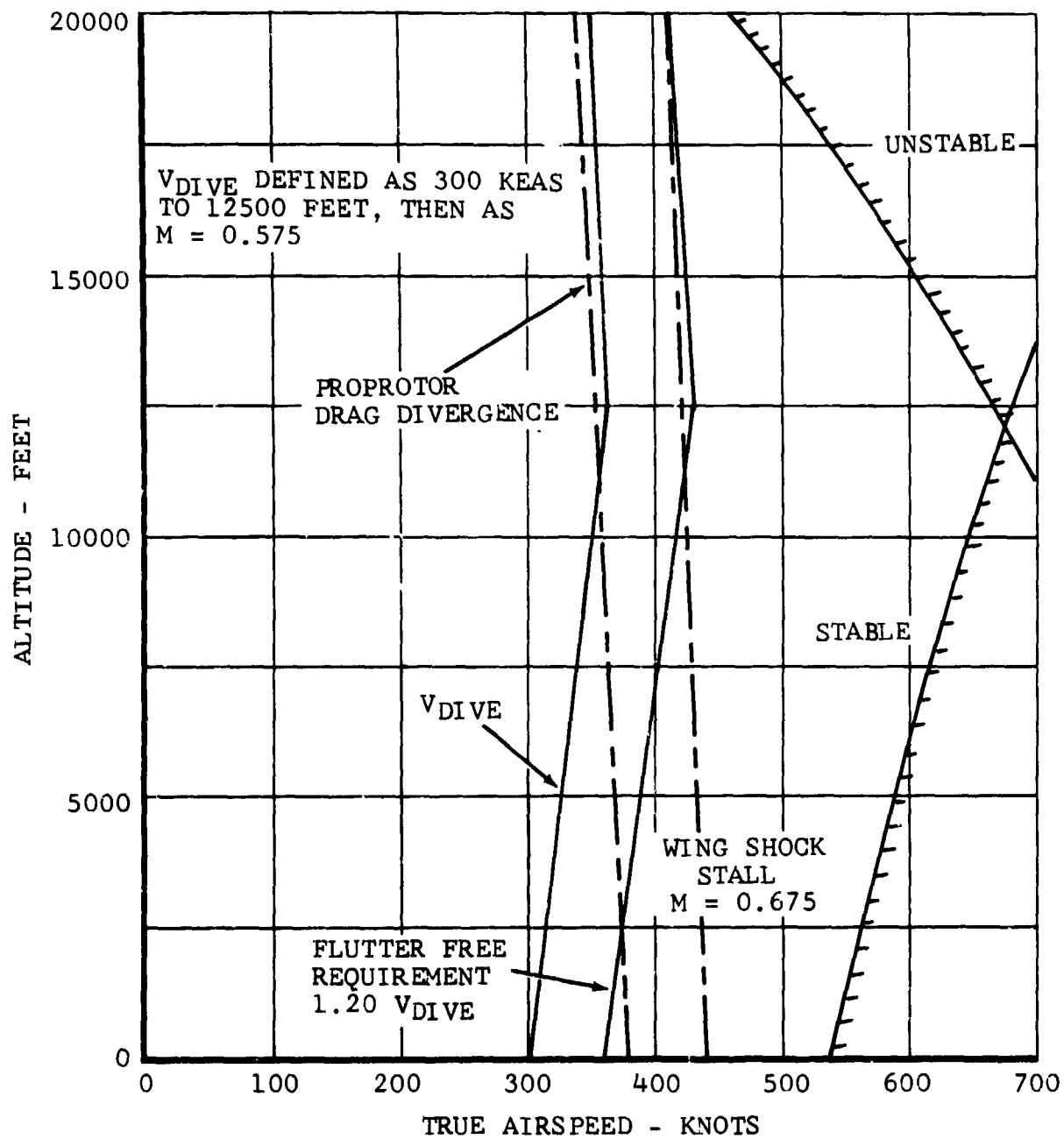


Figure VI-22. Model 300 Dynamic Stability Margin in Airplane Mode.

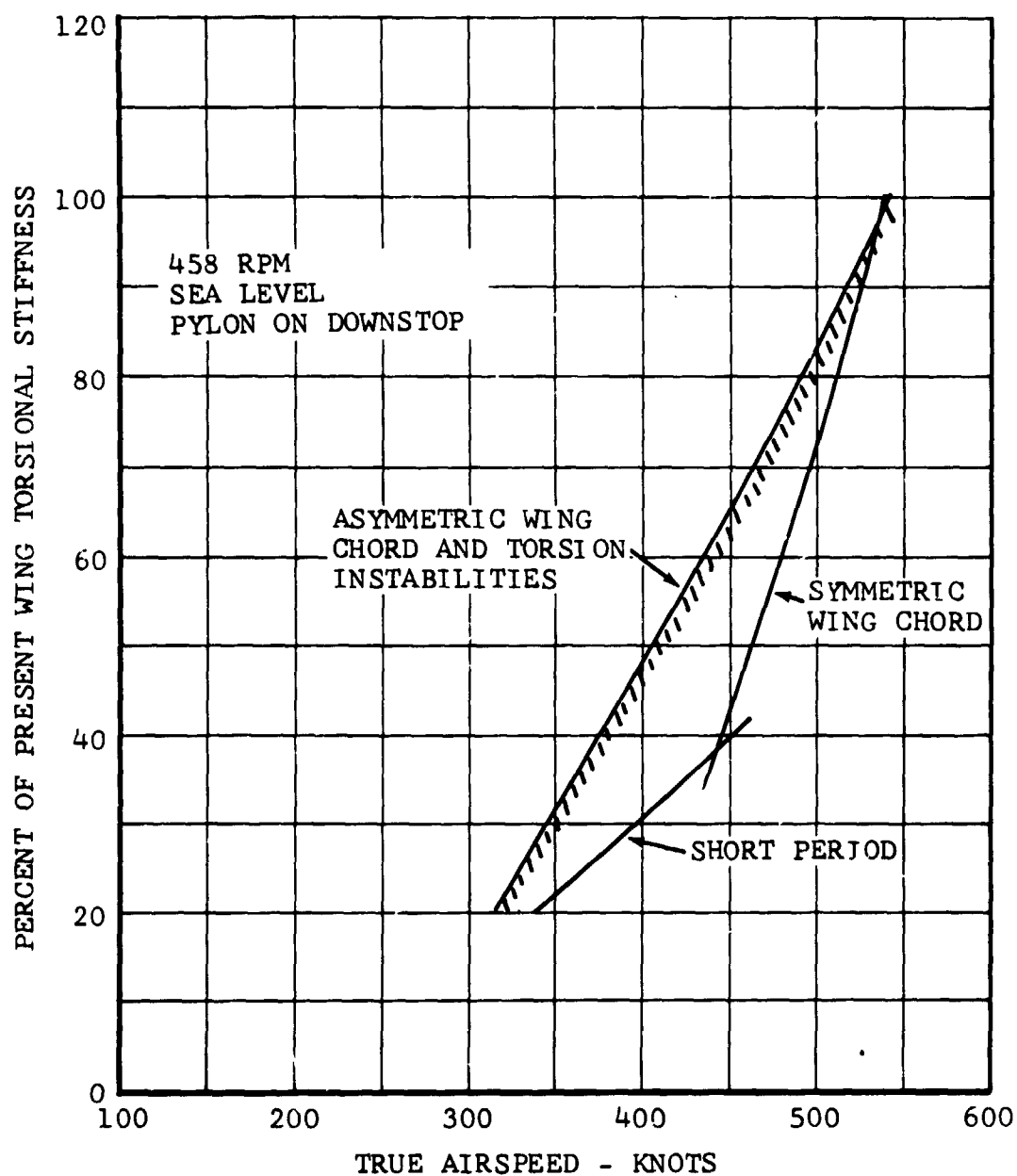


Figure VI-23. Effect of Loss of Wing Torsional Stiffness on Stability Boundary.

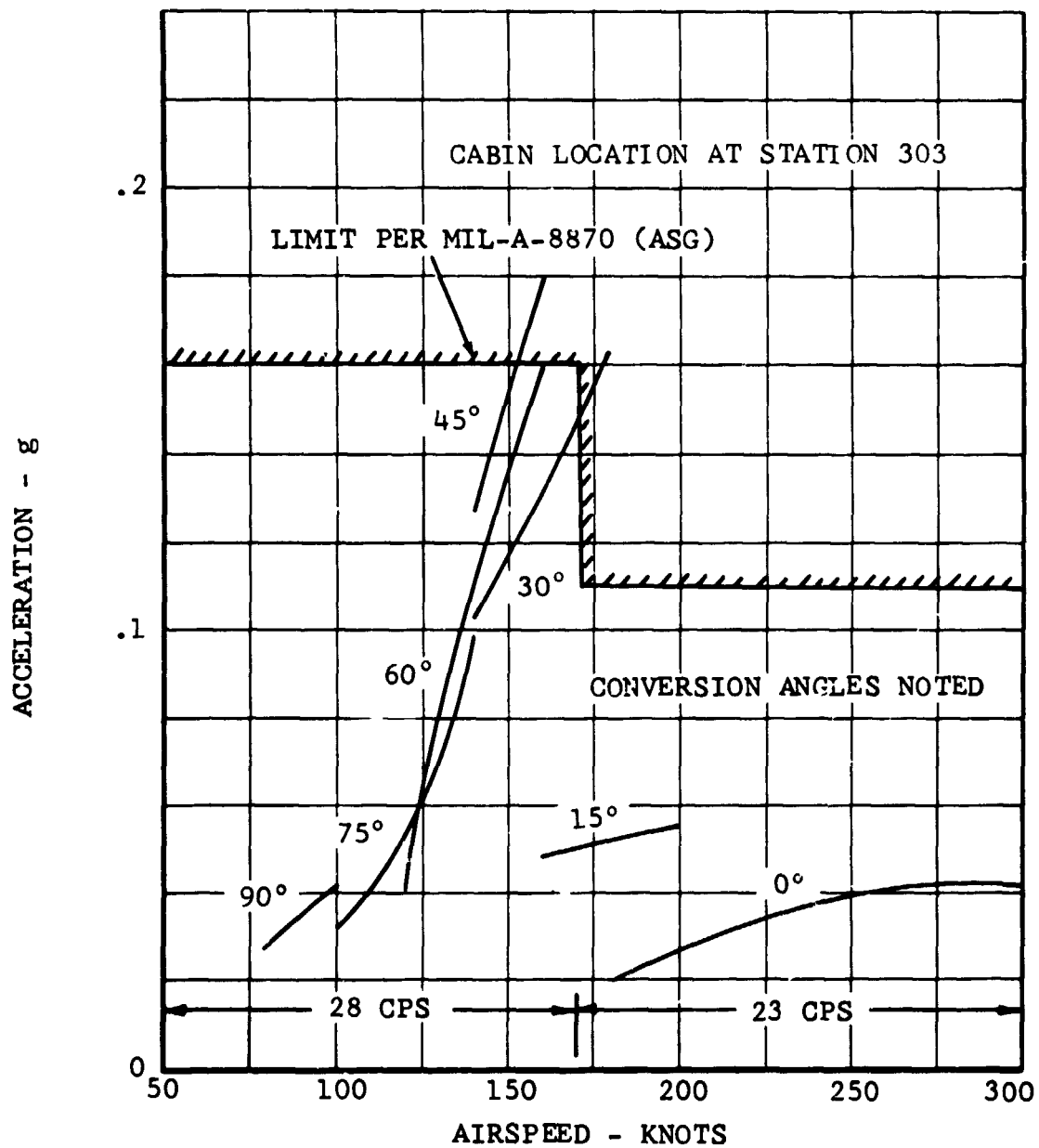


Figure VI-24. Cabin Vibration Level Versus Conversion Angle and Airspeed.

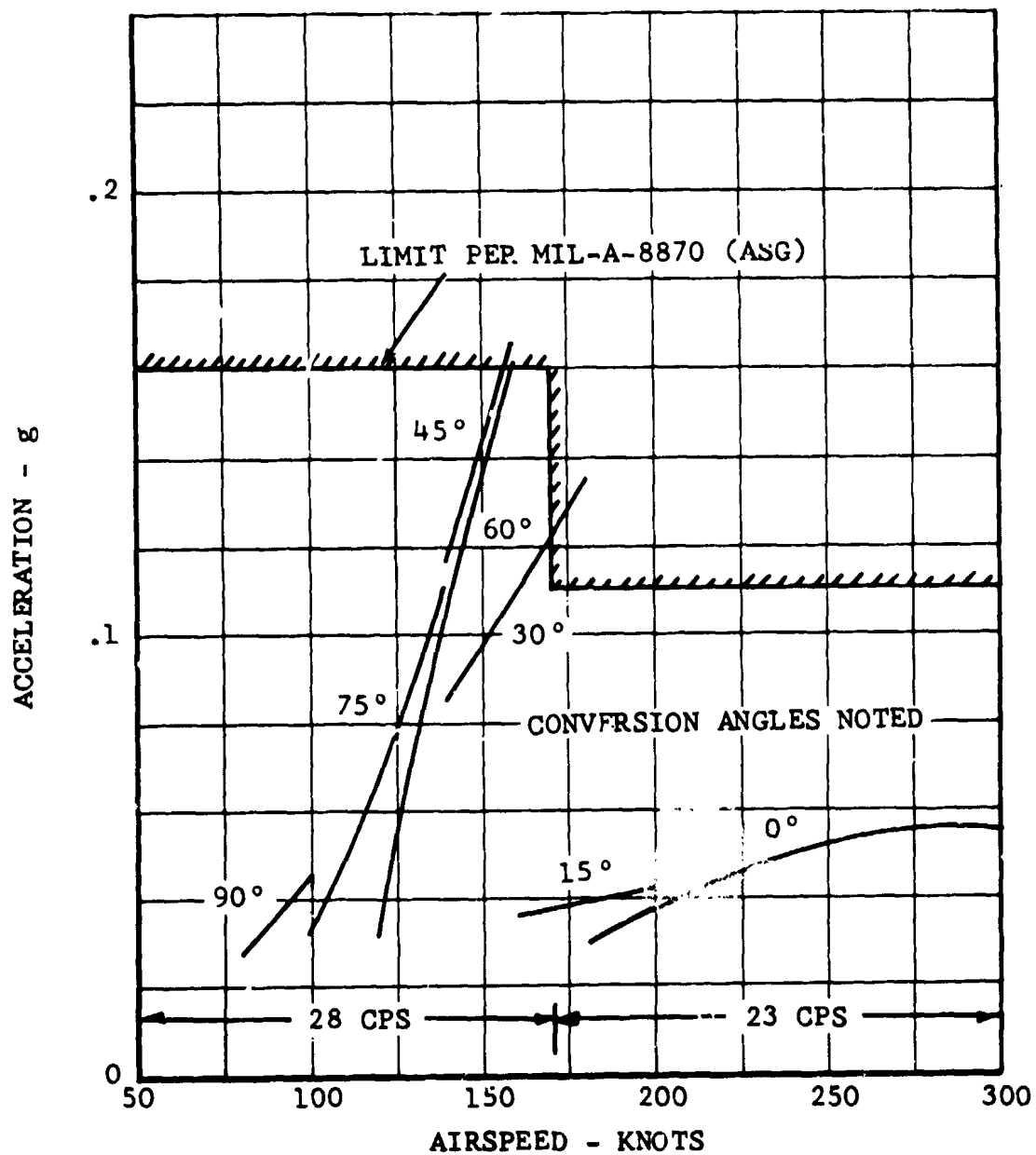


Figure VI-25. Crew Station Vibration Level Versus Conversion Angle and Airspeed.

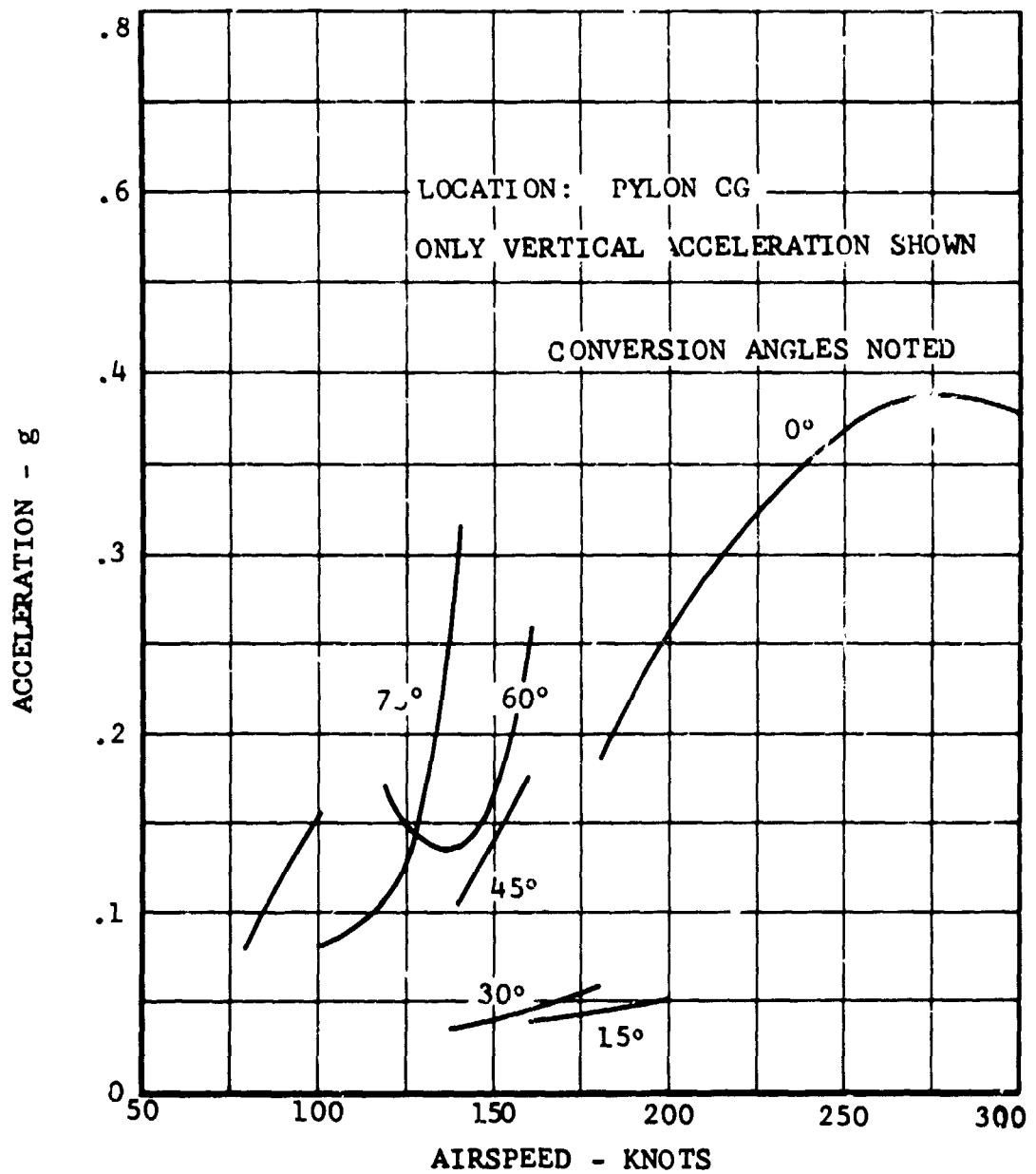
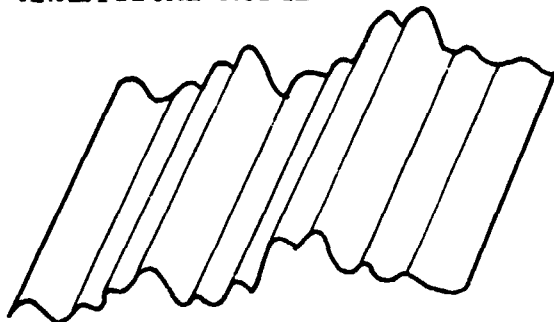
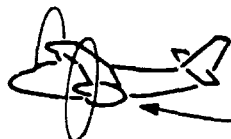


Figure VI-26. Pylon Vibration Level Versus Conversion Angle and Airspeed.

ANALYTICAL MODEL:



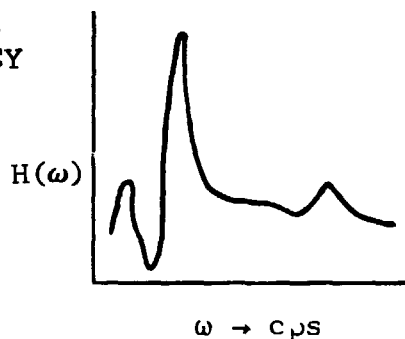
ONE-DIMENSIONAL GUST FIELD
(CAN BE VERTICAL, LATERAL,
OR HEAD-ON)



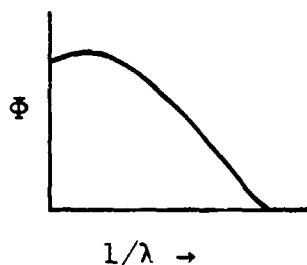
AIRCRAFT TREATED AS
A POINT

PROCEDURE:

- (1) CALCULATE AIR-
CRAFT FREQUENCY
RESPONSE TO
UNIT GUST

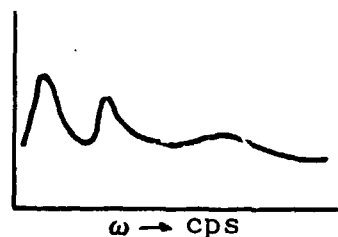


- (2) CHOOSE TURBU-
LENCE SPECTRAL
DENSITY



- (3) CALCULATE RE-
SPONSE SPECTRAL
DENSITY

$$\beta = H(\omega)\Phi$$



- (4) INTEGRATE OVER ω TO OBTAIN
RMS ACCELERATION RESPONSE

Figure VI-27. Procedure for Calculating Response to Atmospheric Turbulence.

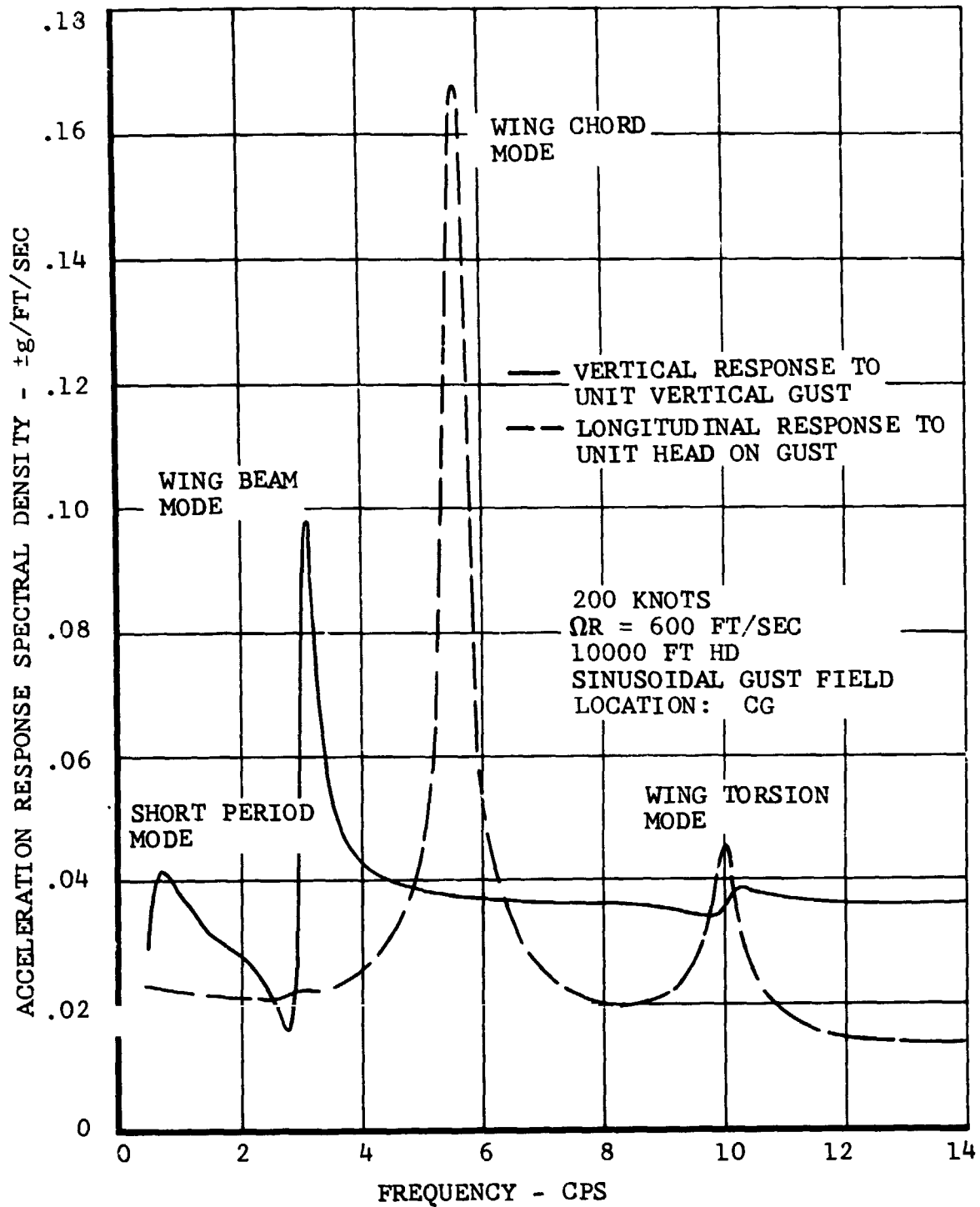


Figure VI-28. Model 300 Frequency Response to Unit Sinusoidal Gust Field.

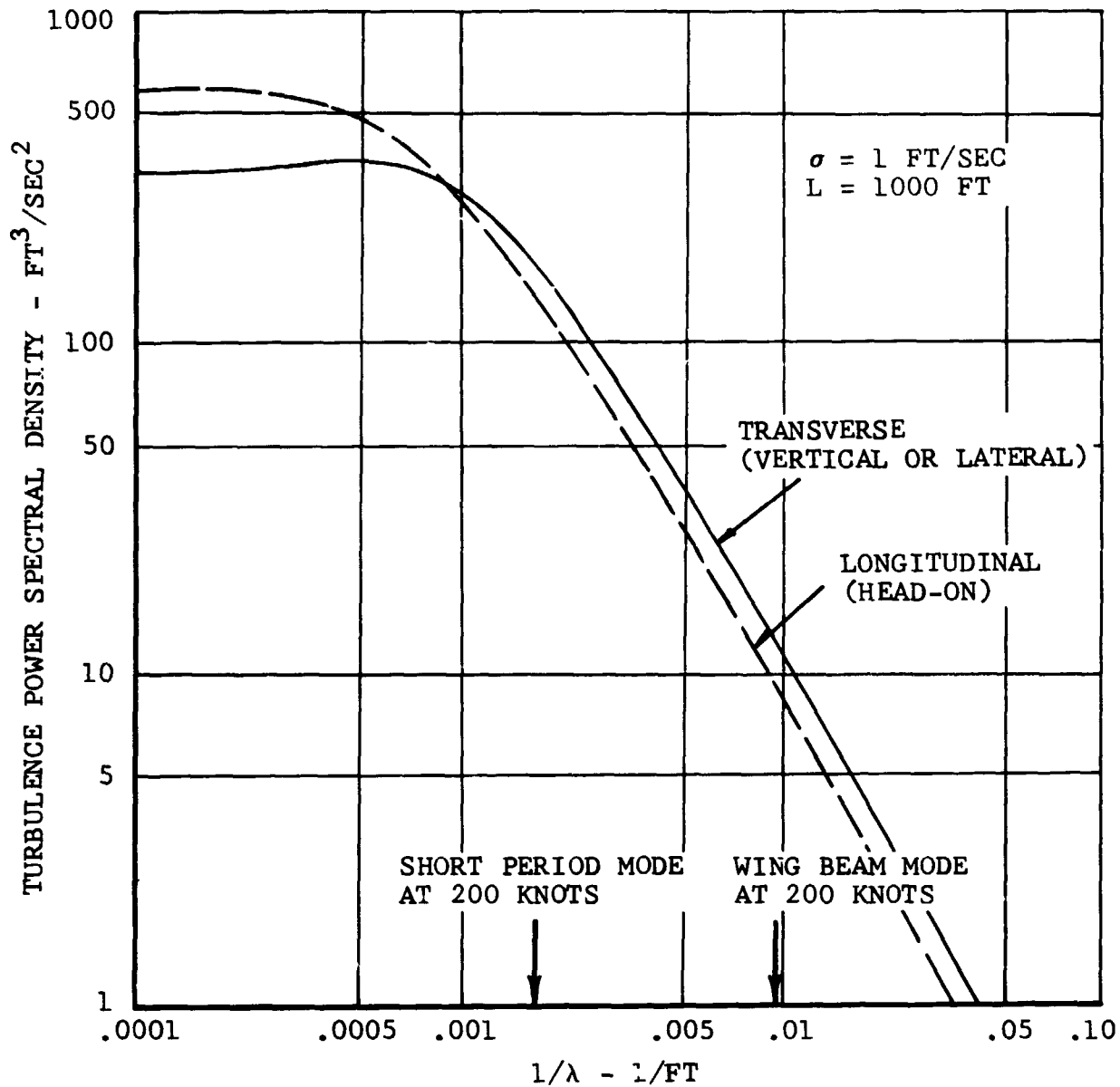


Figure VI-29. Turbulence Field Power Spectral Density (Von Karman Type).

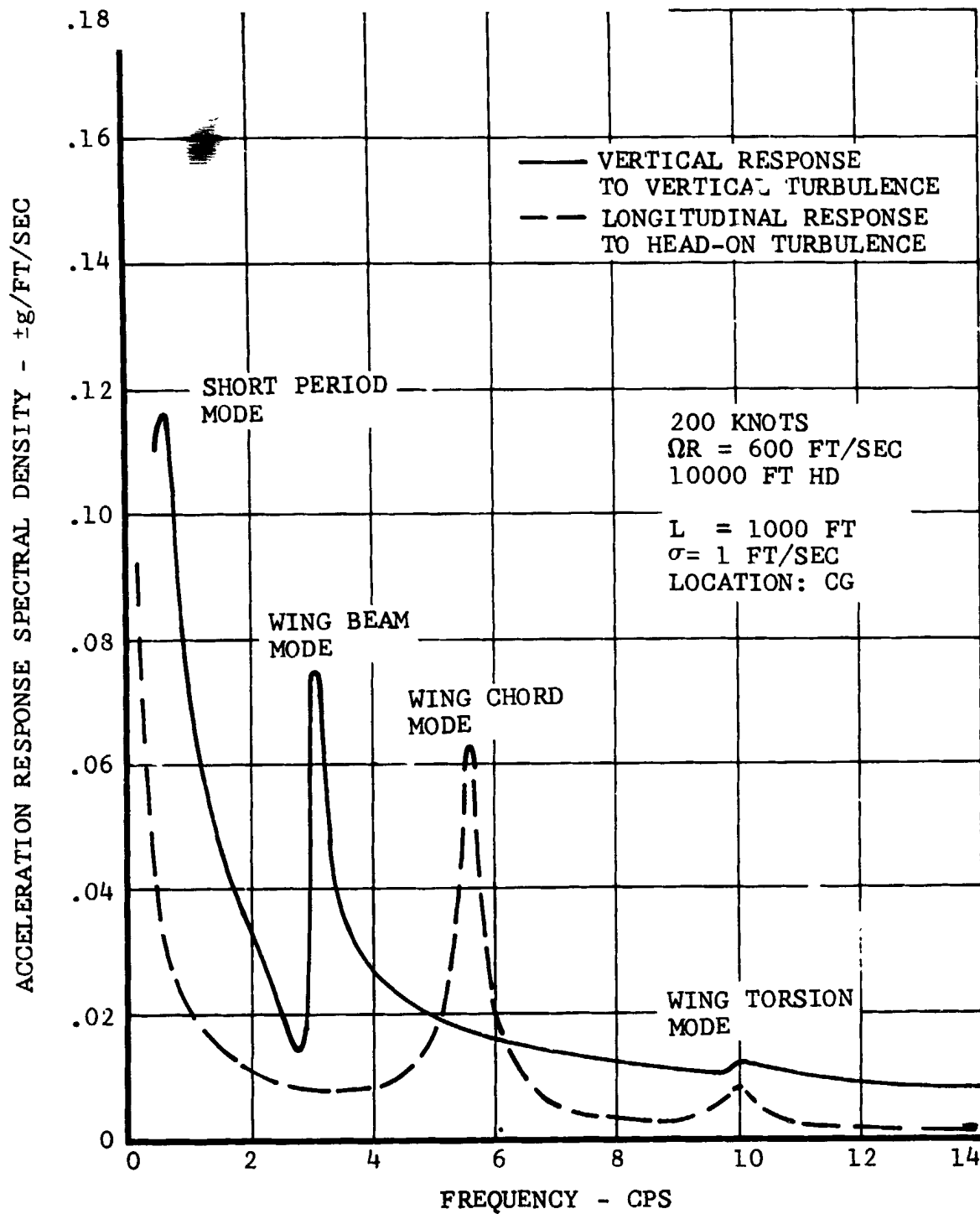


Figure VI-30. Model 300 Center of Gravity Acceleration Response Spectral Density.

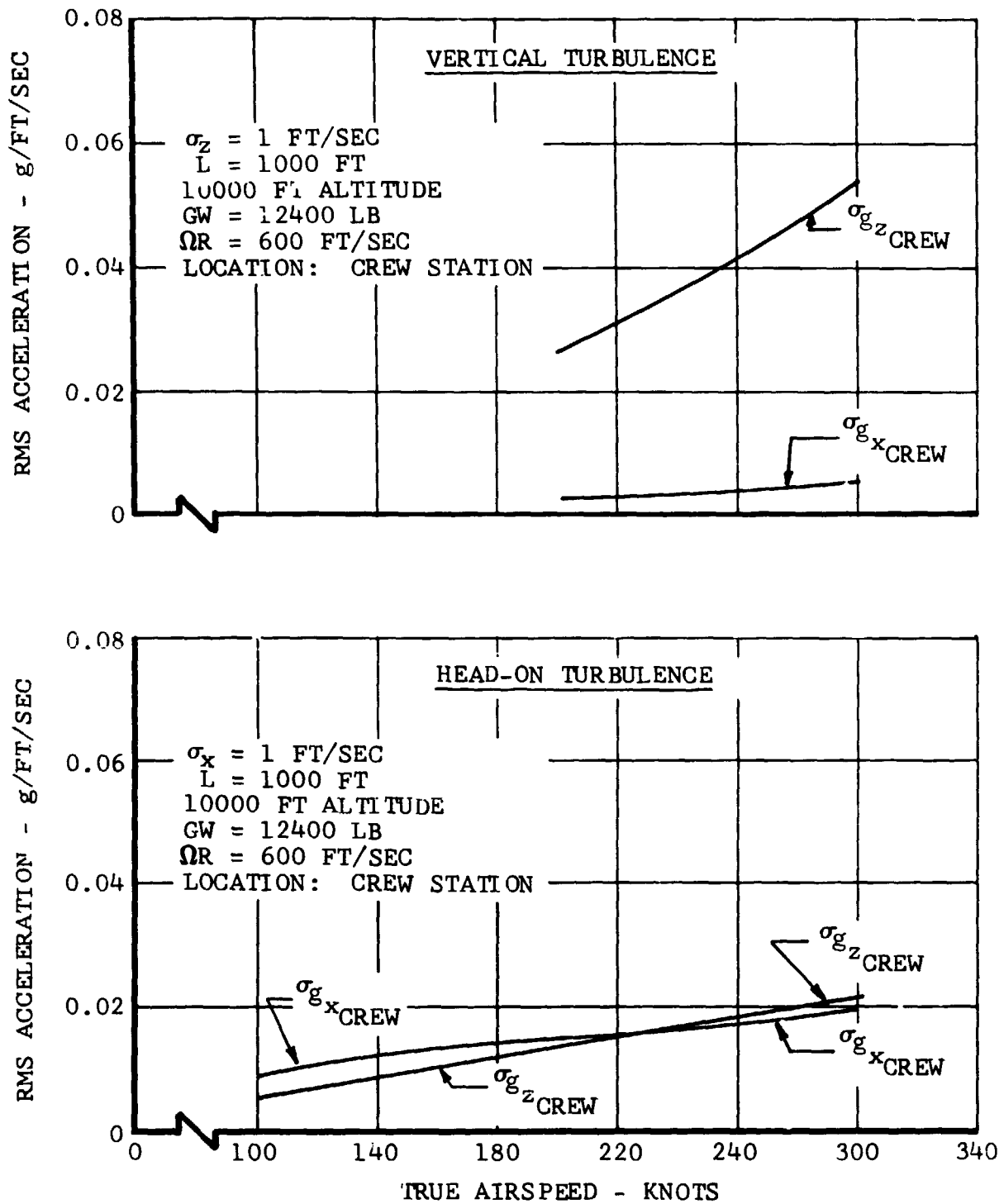


Figure VI-31. Model 300 Crew Station RMS Acceleration Response to One Foot Per Second RMS Turbulence.

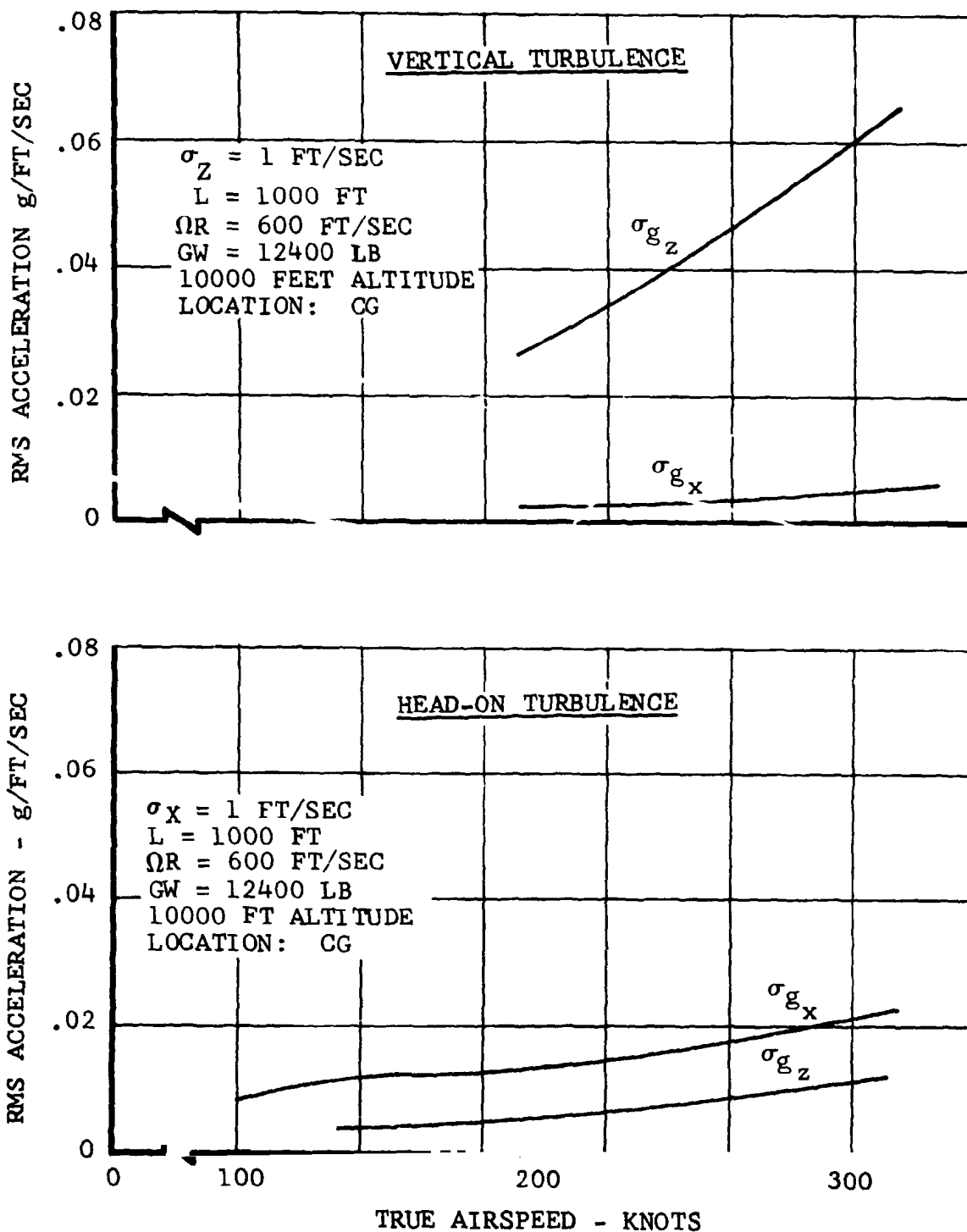


Figure VI-32. Model 300 Center of Gravity RMS Acceleration Response to One Foot Per Second RMS Turbulence.

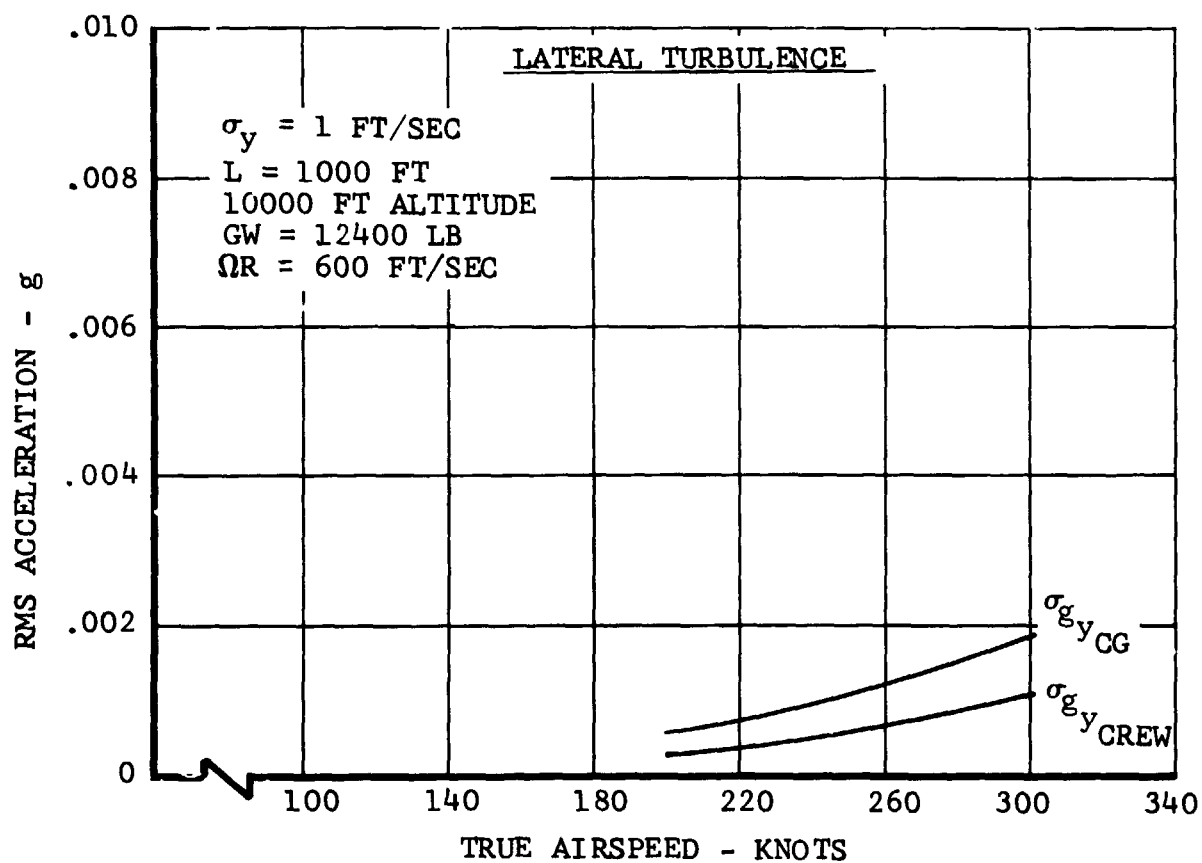


Figure VI-33. Model 300 RMS Lateral Acceleration Response to One-Foot-Per-Second RMS Lateral Turbulence.

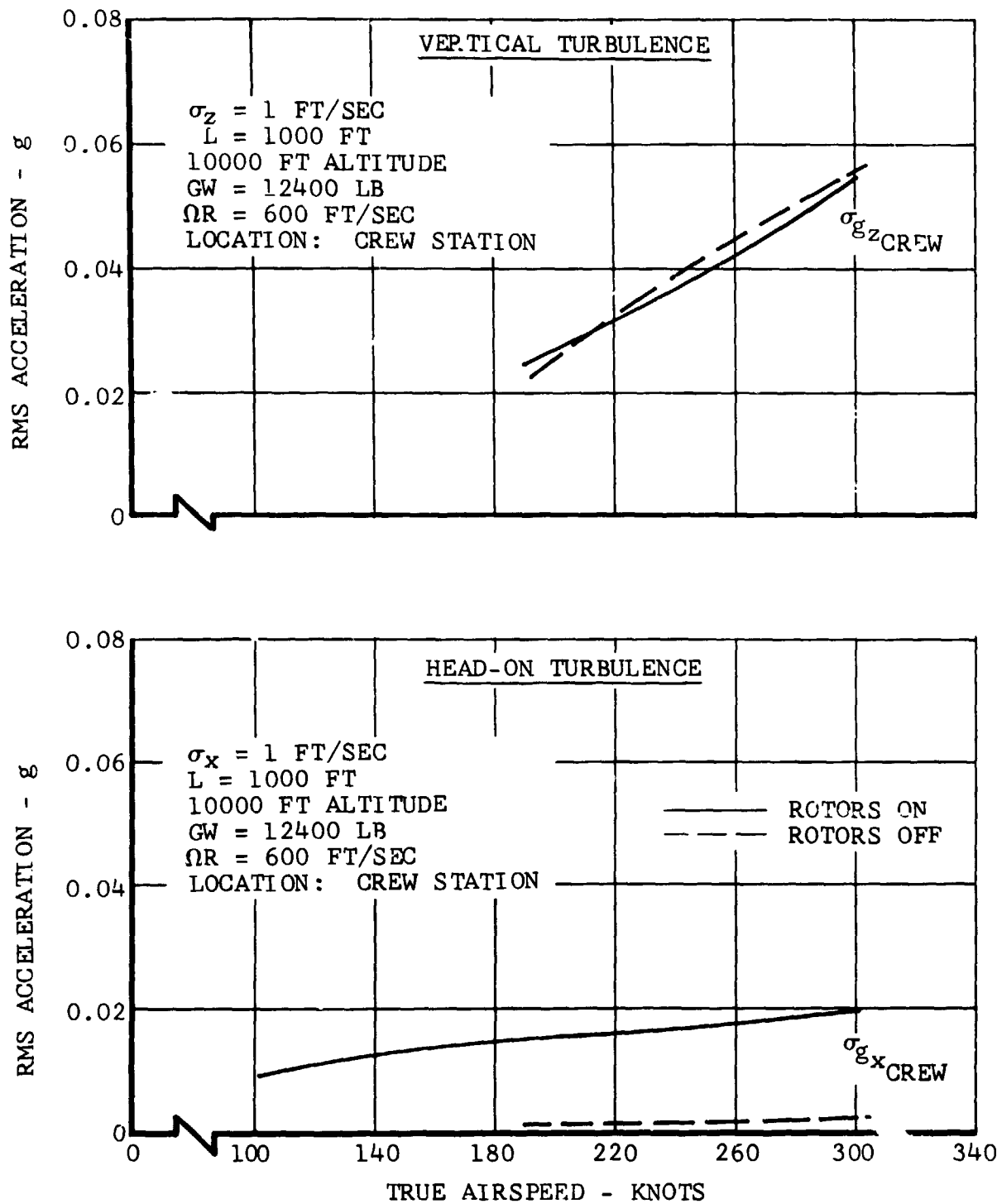


Figure VI-34. Model 300 Proprotor Contribution to Acceleration Response to Turbulence, Crew Station RMS.

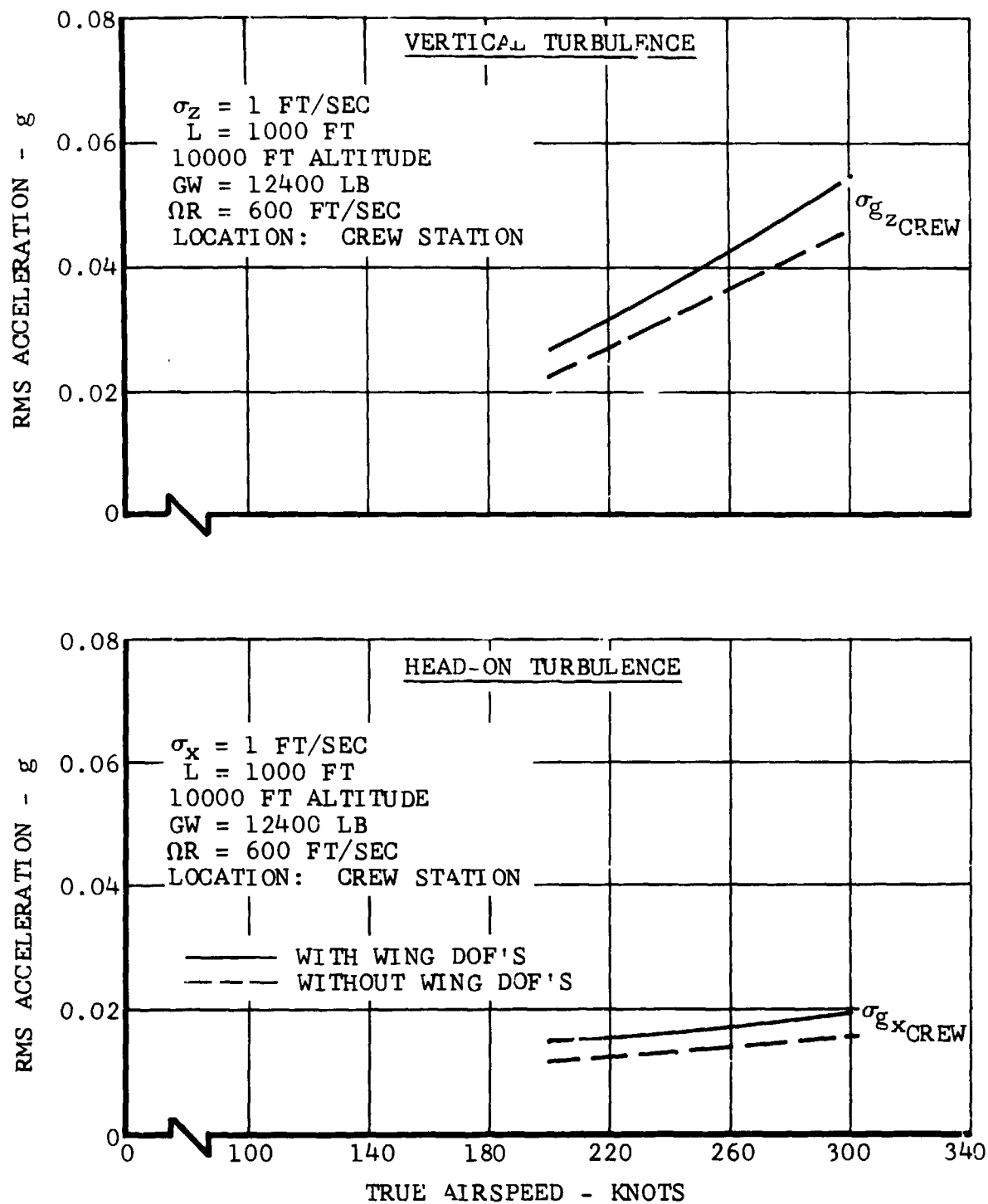


Figure VI-35. Wing Elasticity Contribution to Model 300 Acceleration Response to Turbulence.

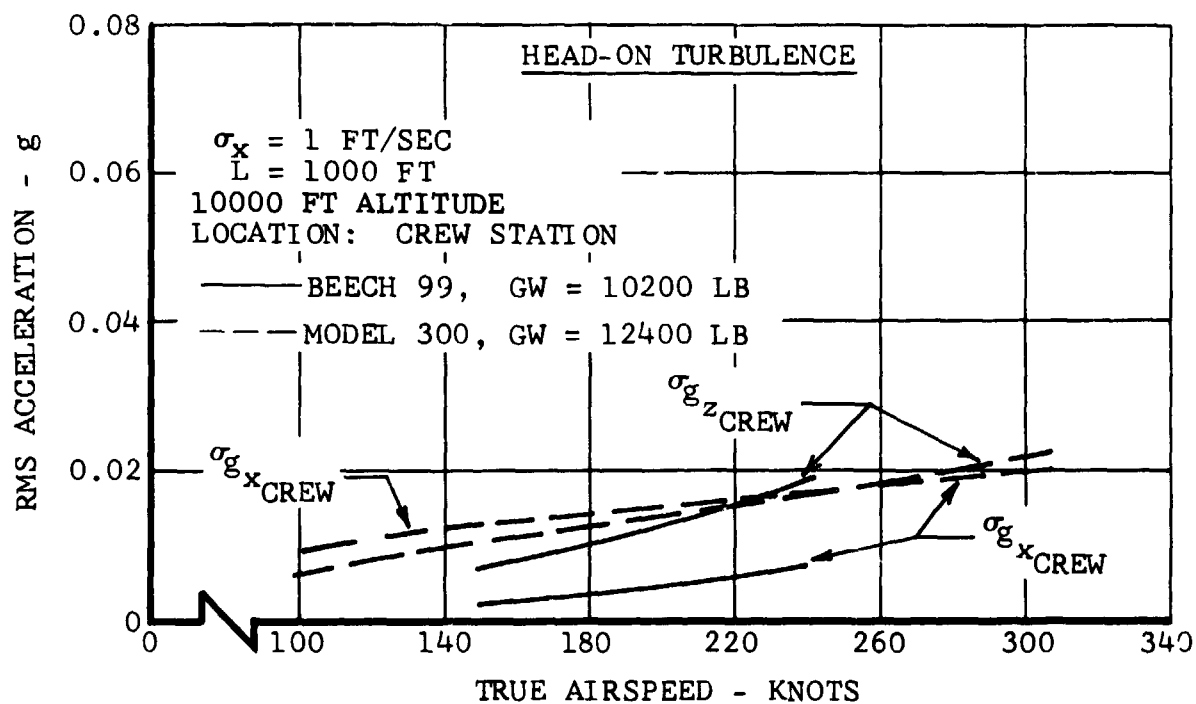
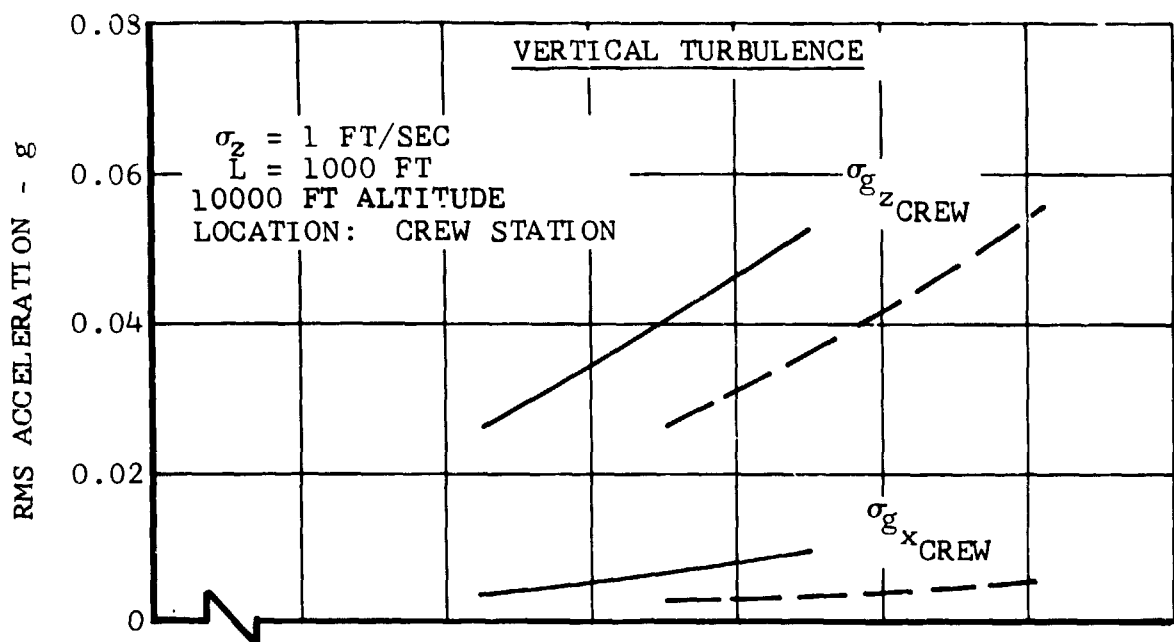


Figure VI-36. Comparison of Acceleration Response of Model 300 and a CTOL Airplane (Beech 99) to Turbulence.

VII. STABILITY AND CONTROL

This section presents the stability and control characteristics for helicopter, conversion, and airplane flight configurations. The Model 300 is equipped with a stability and control augmentation system (SCAS) which enhances the flying qualities about all three axes. Only SCAS-off flight conditions have been investigated. The analysis as presented here was concentrated on evaluating controllability for each flight configuration and dynamic stability in airplane flight.

Control power and damping requirements of MIL-H-8501A and MIL-F-83300 were used to compare the results of the analysis in low speed and conversion flight. Stability and control requirements of MIL-F-8785 were used in evaluating airplane flight.

In helicopter mode, roll control is provided by differential collective pitch, pitch control by proprotor cyclic pitch, and yaw control by differential cyclic pitch. Flaperons, rudder, and elevator are used for control in airplane mode. Conversion mode flight uses a combination of helicopter and airplane controls. Control travels and control phasing with conversion angle are shown in Figures III-7 through III-12.

Stability and control characteristics were determined with the aid of digital computer programs C81 and DYN4. Where possible, the results were checked with closed-form expressions derived for tilt-proprotor aircraft. Rotor analysis in the computer program C81 is based on blade element theory and includes an accurate representation of compressibility and blade stall effects. Program C81 contains the six conventional equations describing the aircraft and determines the control positions, angular orientation of the aircraft, power required, and flapping angles. Details of C81 can be found in Reference 11.

Program DYN4 is a linear, twenty-one degree-of-freedom proprotor stability analysis computer program used for determining the proprotor/pylon, blade motion, and flight mode stability characteristics.

Aerodynamic data which were used to configure the mathematical model of the aircraft were obtained from several wind-tunnel tests of a one-fifth-scale model, References 12 through 16. Effects of rotor downwash on the wing and horizontal stabilizer in hover and low-speed flight are also included. This is represented by changing dynamic pressure and angle of attack over only those portions of the surfaces that are in the slipstream region of the rotors. The downwash acting on that portion of the wing swept by the rotors is assumed to be 0.60 of the mean induced velocity at the rotor disc. Proprotor downwash acting on the horizontal stabilizer is assumed to be zero at speeds

below 40 knots, then increasing linearly to a value of 0.8 of the mean induced velocity at 80 knots and above.

A. HOVER AND LOW-SPEED FLIGHT

Stability and control in helicopter flight were analyzed for flight conditions ranging from a rearward flight speed of 35 knots to a forward speed of 120 knots at sea level on a NASA standard day. Stability and control requirements of MIL-H-8501A and MIL-F-83300 were used in evaluating flight characteristics in this flight mode.

1. Stick-Fixed Static Stability

The variation of longitudinal stick position in trimmed level flight is presented as a function of airspeed in Figures VII-1 and VII-2 for aft and forward center-of-gravity positions, respectively. The pitch control gradient with airspeed is positive throughout the speed range. A stable pitch control gradient is defined as requiring forward stick motion for an increase in speed and a rearward motion for a decrease in speed.

The change in fore-and-aft stick position required to maintain trim flight between 40 and 60 knots is caused by the proprotor slipstream moving onto the horizontal stabilizer. At forward speed, rotor downwash on the wing is assumed to be 0.60 of the mean induced velocity at the rotor disc.

2. Control Power and Damping

a. Hover

The estimated control power and damping about roll, yaw, and pitch axes are compared to the VFR requirements of MIL-H-8501A in Figure VII-3. Control power about the roll and pitch axis meet the requirements. Yaw control is slightly below the requirement, but can be increased for small control displacements with SCAS which has a control lead to assist the pilot input as well as rate damping.

Damping in pitch and yaw with SCAS-off is below the requirements. Damping of several other types of VTOL aircraft with SCAS-off is also shown for comparison purposes. Although the Model 300 does not meet the requirements, it has about the same level of damping as other aircraft that are considered satisfactory. This is shown more clearly in Figure VII-4 when the effects of inertia are considered in defining damping requirements.

b. Low Speed Flight

Elevator, ailerons, and rudder augment the rotor control power with increasing airspeed. The increase in control power with

increasing airspeed is shown in Figure VII-5 and roll performance is shown in Figure VII-6. The roll angle after one second per inch of lateral stick is shown. Control power remains satisfactory throughout the speed range.

The magnitude of the change in differential fore-and-aft cyclic pitch due to pedal displacement is designed for hover flight and causes adverse roll coupling in forward flight. For this reason, the ratio of the change in differential fore-and-aft cyclic pitch to pedal displacement is decreased by a dynamic pressure sensitive device from 1.60-degree per inch at hover to 0.40-degree per inch at 100 knots, as shown in Figure III-11.

B. CONVERSION FLIGHT

Conversion from helicopter to airplane flight is achieved by tilting the pylon forward at any mast angle between 75 and 0 degrees within the wide range of airspeed indicated in Figure VII-7. The lower limit is determined by wing stall and the upper limit is set by maximum continuous power. For continuous flight, airspeed must not exceed the blade endurance limit. Shaft horsepower required during conversions is shown in Figure V-9.

Power in conversion is managed by the throttle control and a propotor collective governor. Any throttle change causes the governor to change the propotor collective pitch thereby maintaining a constant rotor speed of 95 percent hover rpm.

Conversion flight was analyzed for fuselage pitch attitude between -2.5 degrees and +5 degrees as shown in Figure VII-7. The range of fuselage pitch attitude was assumed to reflect the pilot's likely preference for trim flight. Conversion within this range will result in flight between 1.2 V_{stall} and flap extension speed of 170 knots when fully converted.

Flight conditions ranging from an airspeed of 80 to 170 knots with mast angles ranging from 75 to 0 degrees at sea level on a NASA standard day were evaluated. Results are checked against the requirements of MIL-F-83300 which states that when operating about fixed points (such as trim) the same requirements as the forward flight configurations shall apply.

1. Stick-Fixed Static Stability

The variation of stick position at various mast angles and airspeeds for most aft and most forward center-of-gravity loadings is shown in Figures VII-1 and VII-2. Control gradient is stable for each conversion angle. The control position variation is gradual and requires a maximum of 3.8 inches of fore-and-aft stick movement. However, in a continuous conversion, where aircraft pitch attitude is held nearly constant, the stick displacement is even smaller.

2 Control Phasing and Control Power

The helicopter-type rotor controls are phased out as a sine function of pylon tilt angle. Controls phasing is designed to minimize coupling of one set of controls about the other axes. Thus, in the pylon mid-tilt range, the control movements are obtained by a combination of rotor and airplane type controls. Only a small amount of rotor controls are retained in fully-converted flight for trimming. As shown in Figure VII-5, the control power about roll and pitch axes meet the MIL-F-88300 requirements for Level 1 and Level 2 for yaw.

C. AIRPLANE FLIGHT

In airplane-flight configuration, the flaps are up and the mast is at 0 degrees. Flight in this configuration ranges from 135 KEAS ($1.4 V_{stall}$) to maximum cruise speed, sea level to 20,000 feet. Pilot controls in this configuration are similar to those of conventional twin-engine propeller-driven aircraft. Level flight characteristics were investigated and checked against the requirements for Class II Vehicles, Category B flight phase of MIL-F-8785.

1. Stick-Fixed Static Stability

The variation of longitudinal stick position in trimmed level flight is also stable as shown in Figures VII-1 and VII-2 at aft and forward center of gravity positions. Trim changes during flap changes require 2.4 inches of fore-and-aft stick movement to maintain level flight. This trim change is due to a change in pitch attitude with flaps. The attainment of any speed throughout the flight envelope is not limited by longitudinal control effectiveness as shown in Figures VII-1 and VII-2.

2. Control Power

Control sensitivity as shown in Figure VII-5 continually increases with increasing airspeed. Roll performance in airplane flight is shown in Figure VII-6. The requirements state that a 45-degree of bank angle change be obtained in 1.9 seconds. As shown, this can be obtained with only 70 percent lateral stick during low speed airplane flight.

3. Dynamic Stability

a. Short Period Characteristics

The effect of airspeed and altitude on short period natural frequency and damping ratio is shown in Figure VII-8. Figure VII-9 shows that the short period frequency characteristics are within the Level 1 requirements of MIL-F-8785.

b. Dutch Roll Characteristics

The Dutch roll frequency and damping ratio is shown in Figure VII-10 at varying airspeeds and altitudes and compared with MII F-8785. The aircraft is stable throughout the flight range and meets Level 1 requirements. The reduction in damping with airspeed and altitude is due to a decrease in the thrust damping contribution of the rotors.

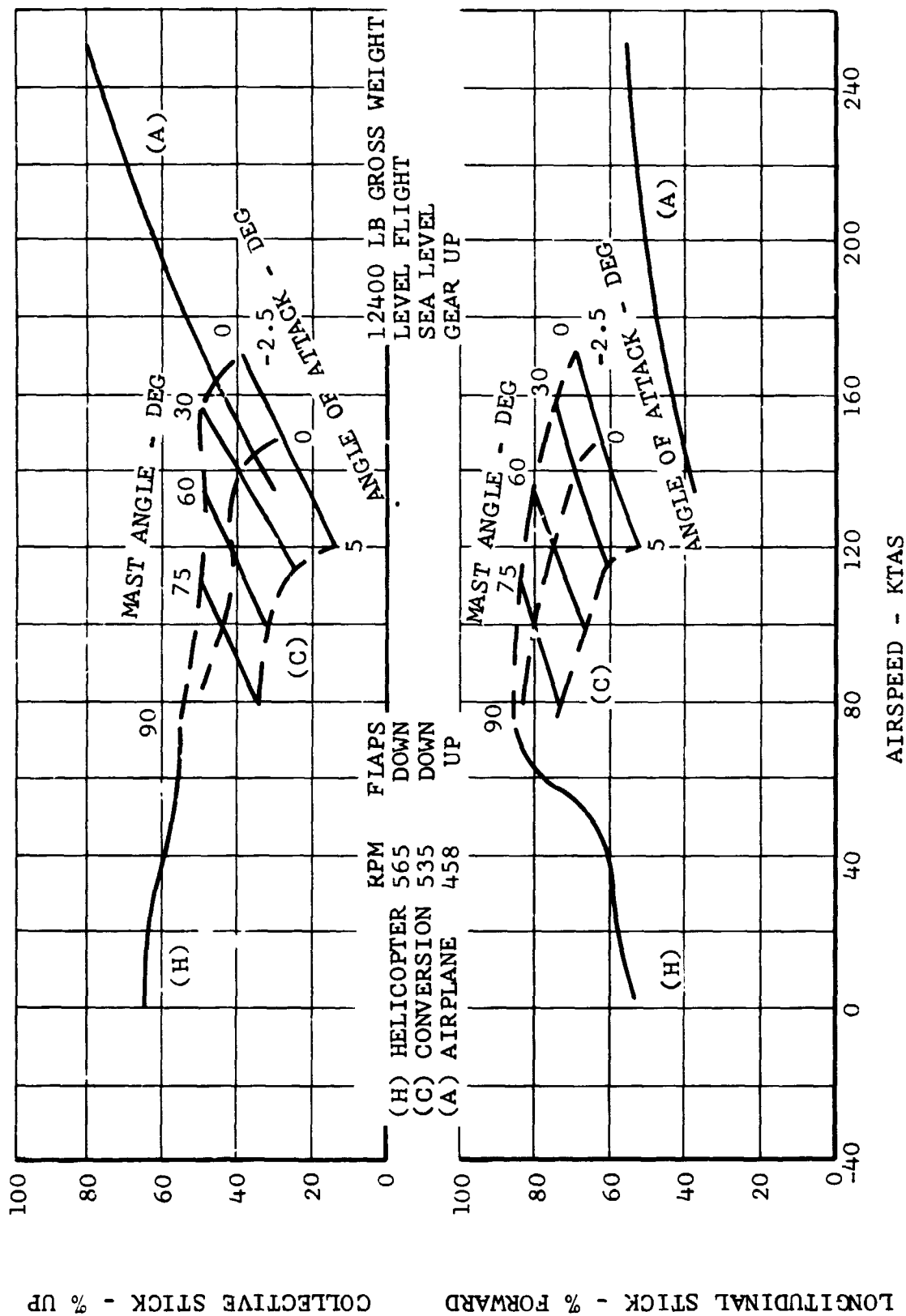


Figure VII-1. Model 300 Conversion Angle and Stick Position Versus Airspeed, Aft Center of Gravity.

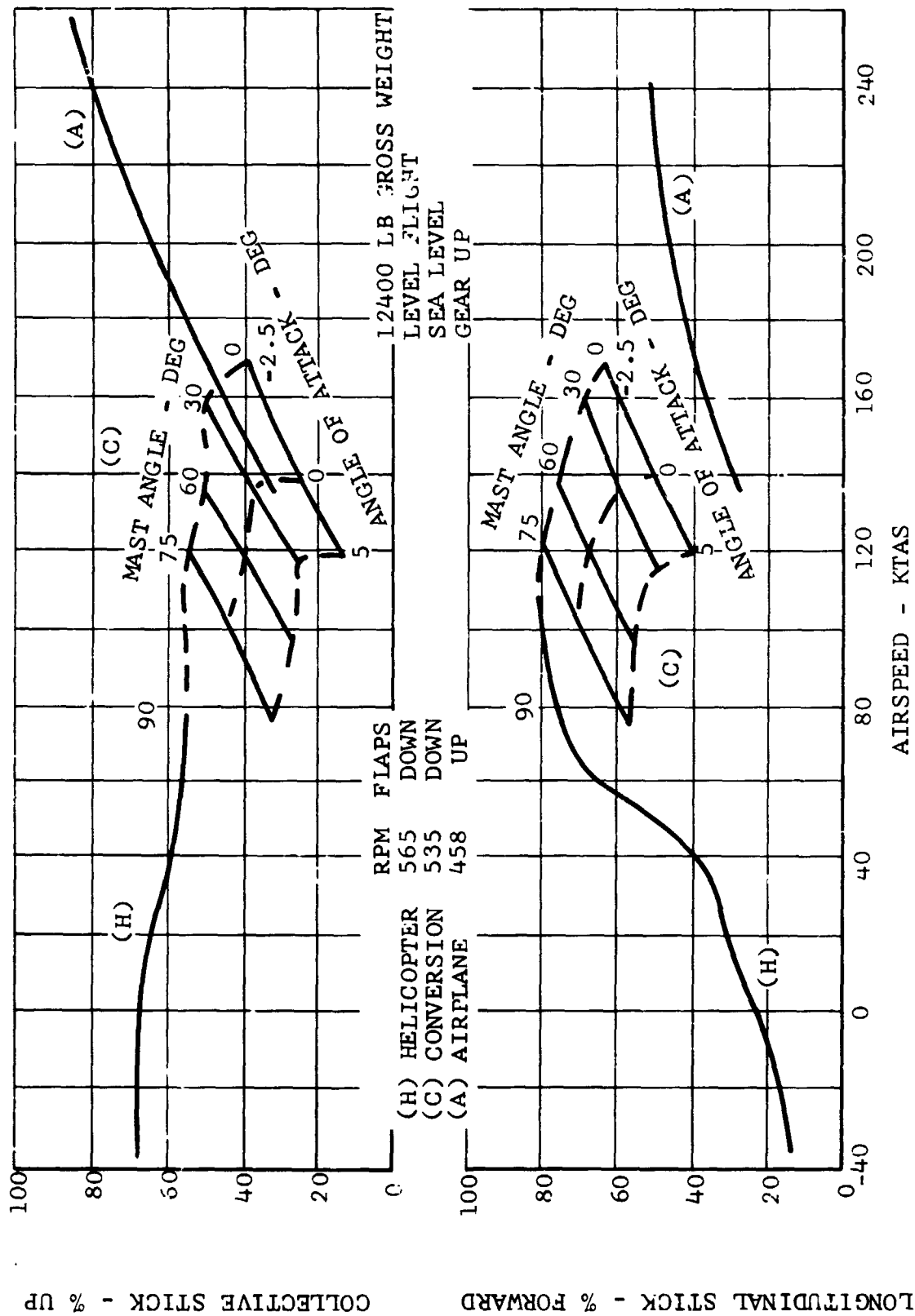


Figure VII-2. Model 300 Conversion Angle and Stick Position Versus Airspeed, Forward Center of Gravity.

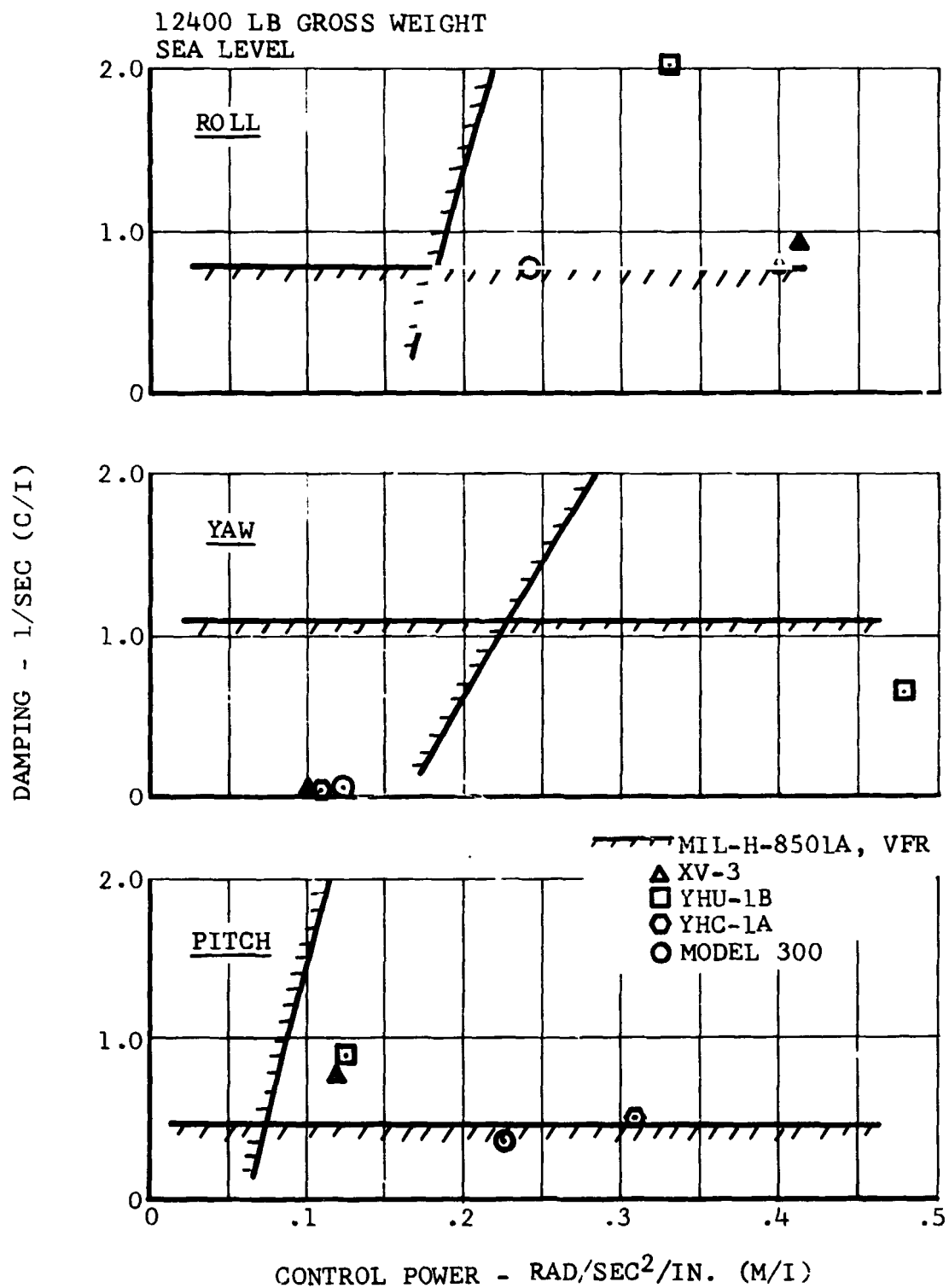


Figure VII-3. Model 300 Hover Control Power and Damping, SCAS Off.

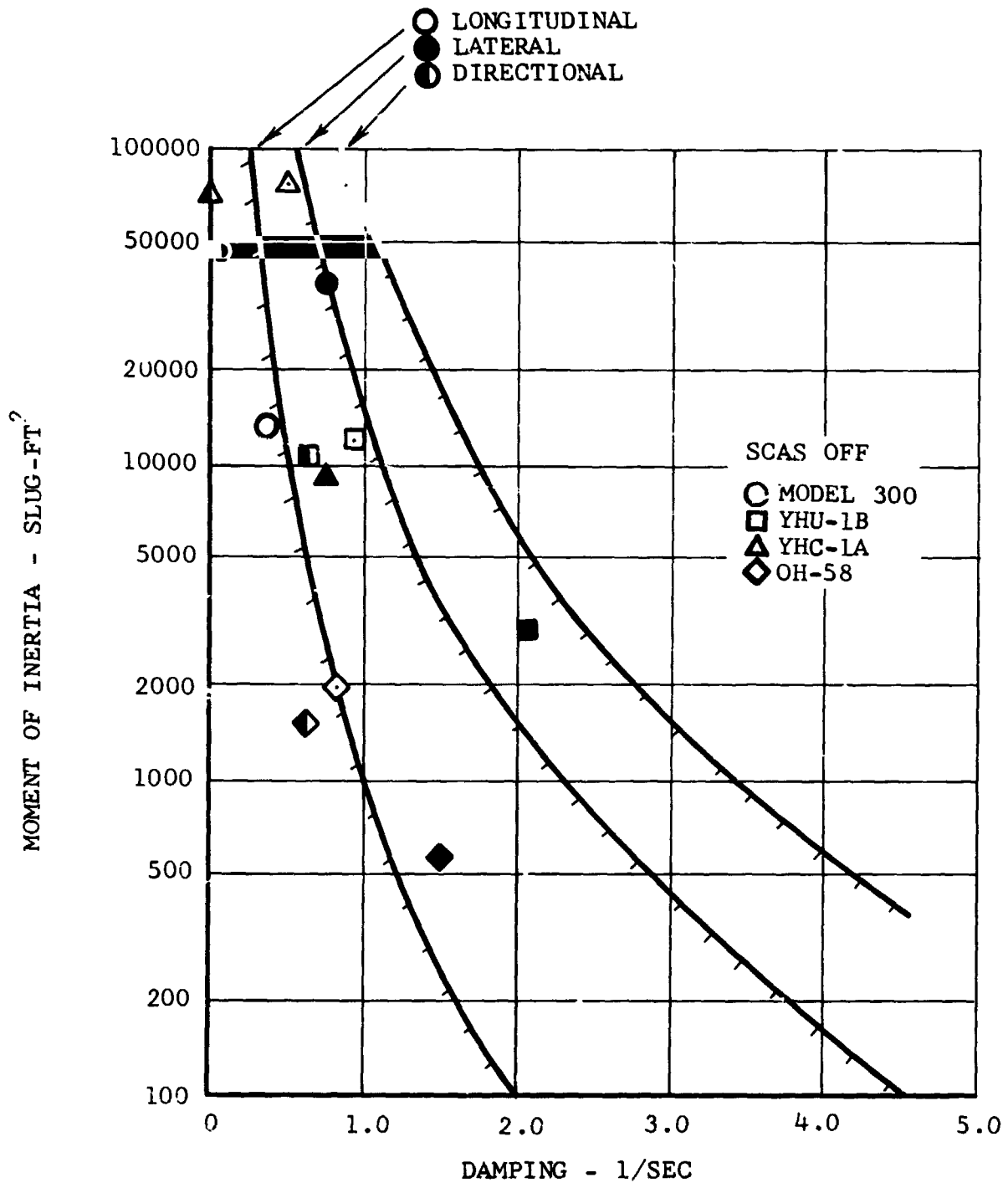


Figure VII-4. Model 300 Damping Comparison with Other Aircraft and MIL-H-8501A, VFR Requirements.

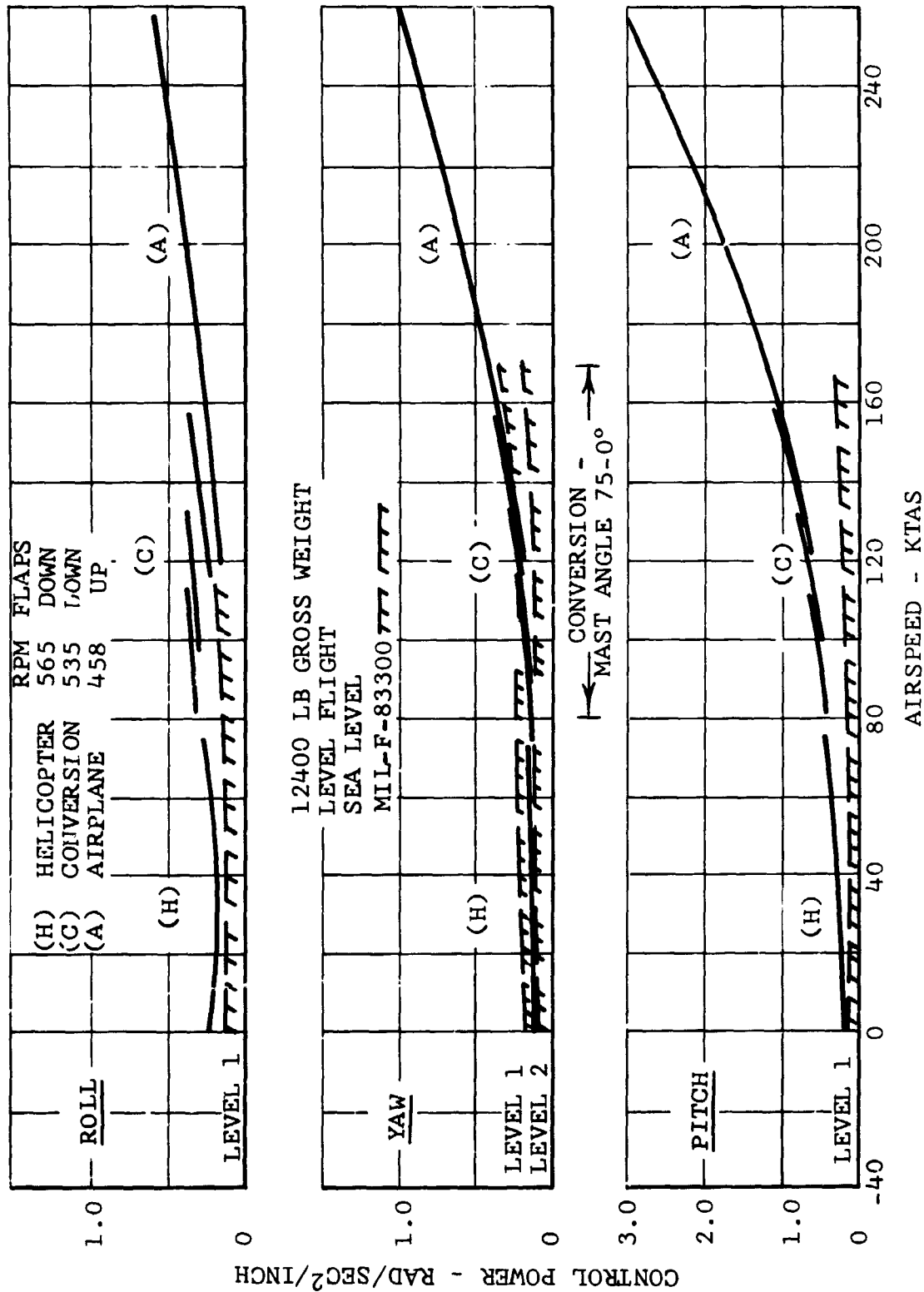


Figure VII-5. Model 300 Control Power Versus Airspeed.

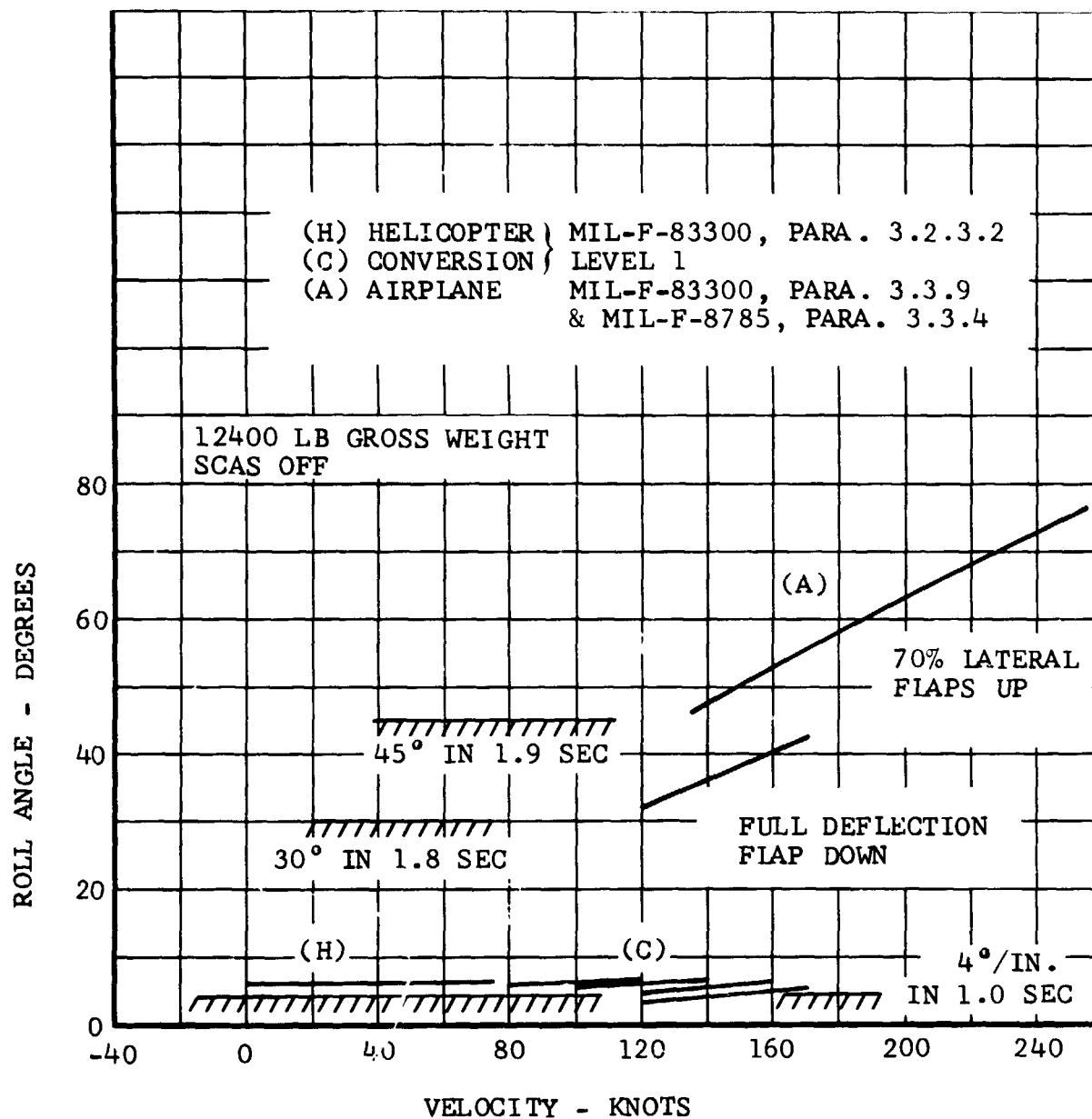


Figure VII-6. Model 300 Roll Performance Versus Airspeed, SCAS Off.

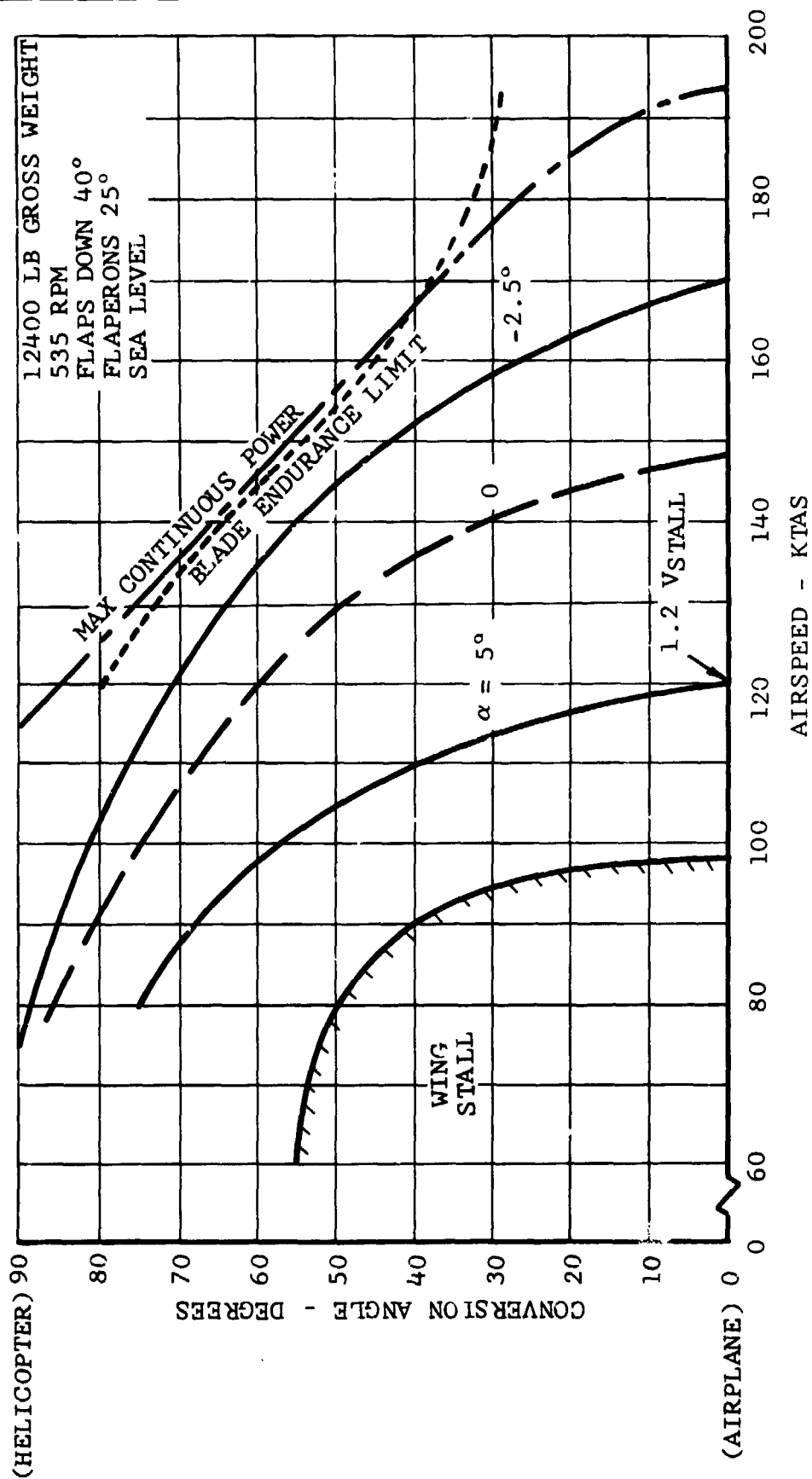


Figure VII-7. Model 300 Conversion Corridor.

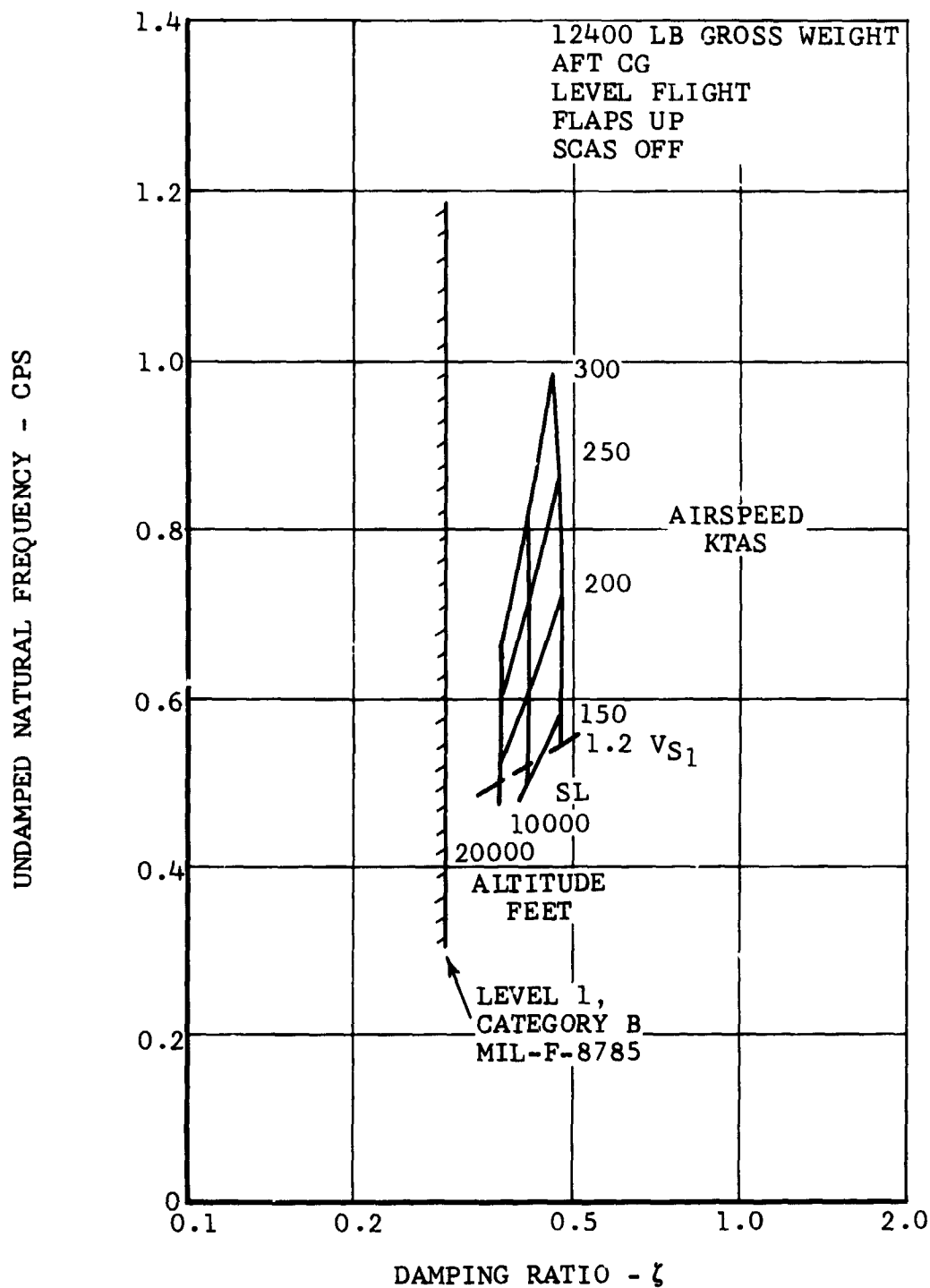


Figure VII-8. Model 300 Short Period Characteristics - Airplane Mode.

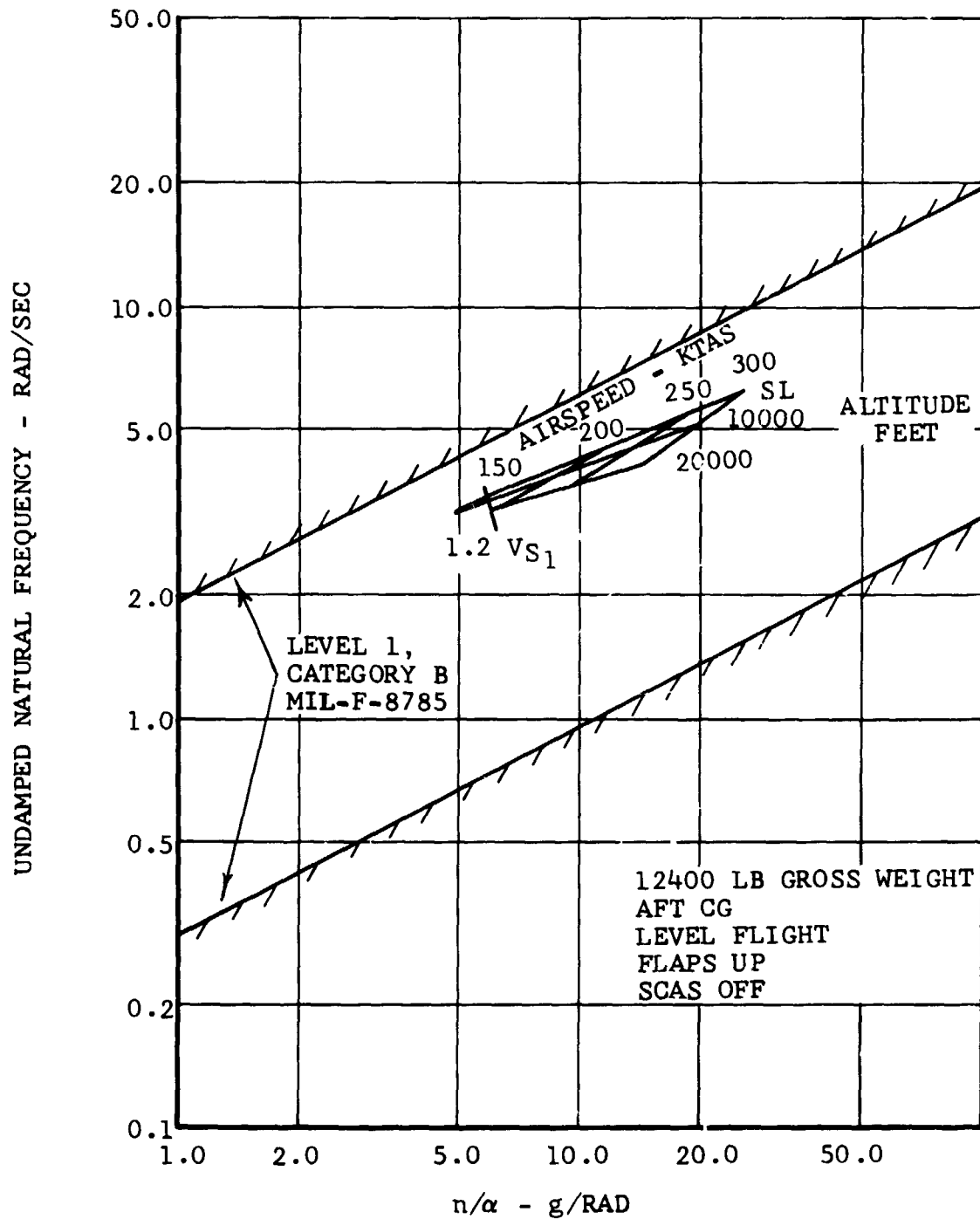


Figure VII-9. Model 300 Longitudinal Short Period Frequency Characteristics, Airplane Mode.

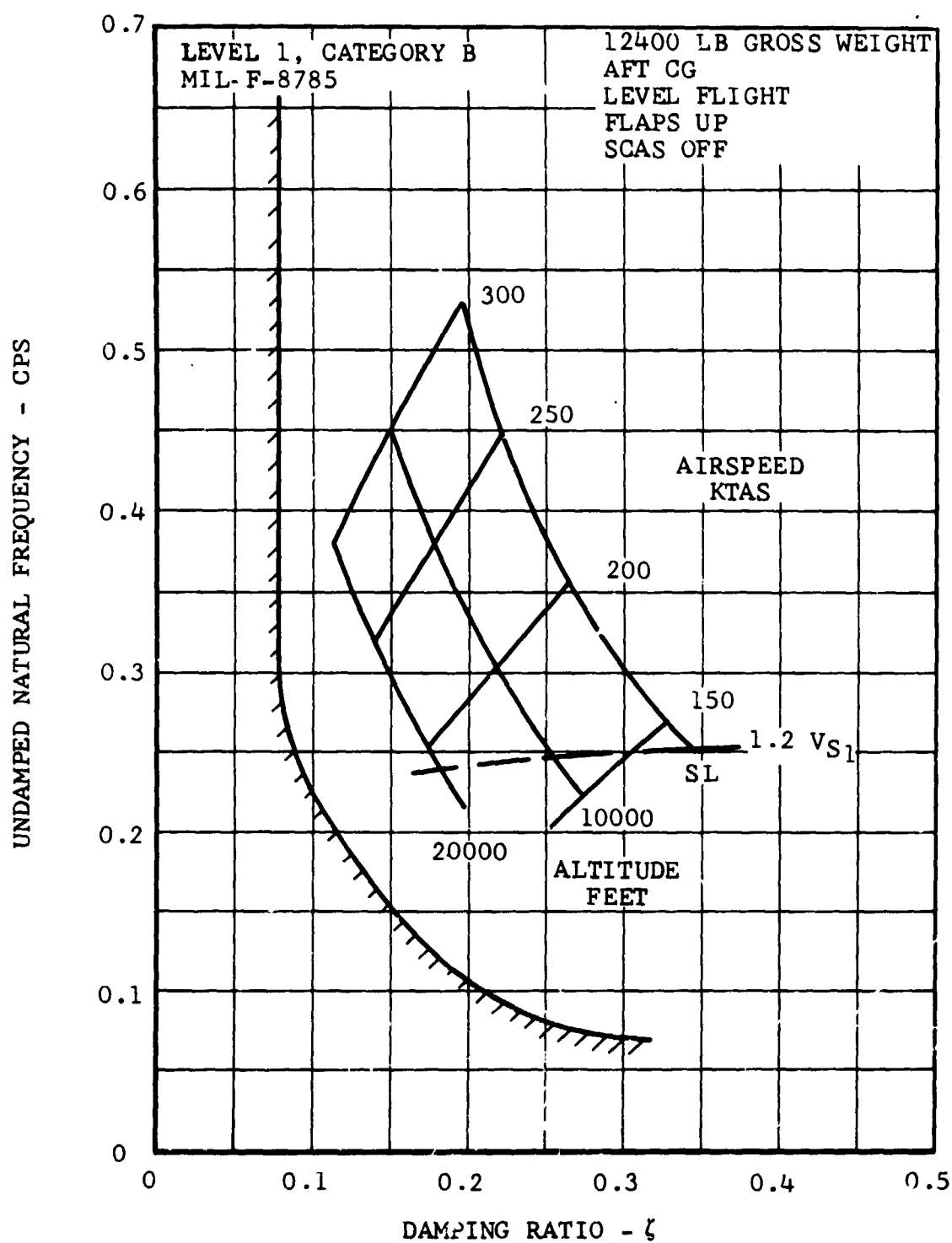


Figure VII-10. Model 300 Dutch Roll Characteristics
Airplane Mode.

VIII. NOISE

The noise of the research vehicle and its impact on a populated area's acoustical environment were assessed. Proprotor noise levels, frequency spectra, and sound directionality were predicted as functions of mode of operation, distance between vehicle and a listener, and viewing angle to the proprotors. A correlation study was performed using experimental proprotor noise data measured during wind-tunnel testing to verify the analysis method. Ground noise-footprints and noise-exposure time histories were then estimated by taking into account the vehicle's takeoff and approach operational profiles. Finally, the research vehicle's noise was compared with that of present-day modes of transportation.

A. WIND-TUNNEL EXPERIMENTAL DATA

The noise levels of the Model 300 proprotor were measured during the Ames 40- by 80-foot wind-tunnel powered testing (NASA Contract NAS2-5386). A microphone was located 68 feet upstream of the model and 5 feet above the floor on the centerline of the tunnel. This location is the same as that used to measure the noise of helicopter rotors (References 17 and 18). Proprotor noise data were recorded for mast tilt-angles from 0 to 75 degrees, for several tip speeds, and at various thrust and power settings. Figure VIII-1 shows the comparison between proprotor and helicopter rotor noise. For tunnel velocities above about 80 knots, the noise of the proprotor in takeoff mode is lower than that of a square-tip rotor. Also, the rate of increase in proprotor noise, as tunnel velocity increases, is somewhat less than for rotors. Qualitatively, the proprotor sounds much like a propeller and does not emit the easily distinguished blade slap which is characteristic of helicopters at high speeds.

In cruise mode, the noise of the proprotor decreases significantly, as predicted. The reduction was so great that the proprotor noise was masked by tunnel noise. These data show that the proprotor's noise in cruise mode, at tilt angles between 15 and 30 degrees, is at least 7 to 10 db lower than that in takeoff mode. Predictions show a reduction on the order of 20 db.

B. COMPARISON BETWEEN THEORY AND EXPERIMENTAL DATA

Propeller and rotor noise theories (References 19 through 21) are used to estimate the external noise of the vehicle's proprotors. The prediction method includes estimates of the rotational noise harmonics and their sound directionality, and of the peak level, center frequency, spectral distribution, and directivity of the broadband component.

Predicted noise levels are compared in Figures VIII-2 and -3 with wind-tunnel noise data measured during hover and 80 knots,

respectively. For the hover condition, theory accurately predicts the noise level of the first four harmonics of rotational noise but underestimates, by about 6 PNdb, the higher harmonics and the broadband noise component. As expected, theory becomes increasingly inaccurate as the airspeed increases, underestimating the noise level at 80 knots by approximately 9 PNdb.

Several qualifying factors must be considered before wind-tunnel acoustic data can be used to correct the theory's deficiencies. The tunnel enclosure amplifies the noise and has resonant characteristics peculiar to its size and construction. Amplification correction factors for the Ames 40 by 80-foot wind tunnel are available (Reference 22). However, their application is limited in this instance because of the following reasons:

- The sound source used to calibrate the tunnel is artificially generated and is a continuous wideband signal. The actual noise produced by rotors consists of discrete frequency harmonics and repetitive broadband pulses.
- The correction factors are only for the zero wind condition. Sound-wave propagation and tunnel-resonant characteristics will be different during normal tunnel operation. While tunnel noise measurements provide useful trends and parameter effects, comparisons of theoretical and experimental absolute levels must await more extensive tunnel calibrations.

C. PREDICTED NOISE CHARACTERISTICS

The Model 300 noise characteristics for various modes of operation are presented in Figure VIII-4. Predicted noise levels for the takeoff and cruise modes are shown for observer distances of 500 and 1000 feet, respectively. The estimated range of noise levels produced during conversion is also shown; the range being based on the aircraft's representative conversion corridor, i.e., pylon conversion angle and airspeed combinations. It can be seen that the Model 300 can be flown in all modes of operation such that its noise level does not exceed 95 PNdb (nearest distance is taken at 500 feet). Additionally, the pilot can assure minimum noise generation by entering the conversion corridor at the lowest practical airspeed, especially when operating over or near noise-sensitive areas.

D. GROUND NOISE EXPOSURE

Noise contours were calculated as functions of the operational flight-path profiles, the viewing angle of the observer to the rotor, the distance to the aircraft and Doppler effects. Sound-transmission losses caused by spherical spreading (-6 db per doubling of distance) and atmospheric absorption (Reference 23)

were taken into account. The operational flight paths for takeoff and landing operations are presented in Figure VIII-5. The glide slope, airspeed, climb/descent angle, and the altitude at various ranges from liftoff/touchdown are shown.

Noise exposure footprints, based on the takeoff and approach profile of Figure VIII-5, are shown in Figure VIII-6. Steep gradient profiles, particularly the noise abatement combinations of airspeed and rate of descent which avoid noisy blade wake interactions, result in a small noise footprint. The level for a 50-foot hover is estimated to be no more than 90 PNdb at 500 feet. The 90 PNdb contour takeoff extends only 2900 feet from the center of the landing pad. A 95 PNdb contour, although not shown, extends only about 1500 feet downrange of liftoff.

Noise time histories for various modes of operation are plotted in Figure VIII-7. The exposure time experienced by an observer located one nautical mile from the liftoff/touchdown spot is shown for typical takeoff/departure and approach/landing operations. Also shown is the observer's noise exposure for a 200-knot cruise-mode flyover. Takeoff/departure operations produce the maximum noise exposure; however, the peak level at the observer is only 82 PNdb. Approach/landing operations result in even less noise exposure, provided the pilot follows noise-abatement procedures during the descent stage. These procedures are embodied in the approach profile of Figure VIII-5 and consist of safe combinations of airspeed and descent glide path angle. Cruise-mode operations produce the minimum ground noise exposure.

E. COMPARISON WITH OTHER MODES OF TRANSPORTATION

The noise of the Model 300 is compared in Figure VIII-8 with measured levels of present-day helicopters and common surface-transportation vehicles. The noise of the Model 300 in takeoff mode will be slightly less than that of medium helicopters operating today at airspeeds below about 80 knots and will be no greater, at typical distances to each, than that generated by heavy commercial surface vehicles. In cruise mode, the flyover noise of the Model 300 will be lower than those produced by the smallest helicopters, and at typical flyover altitudes, will be comparable to ambients measured in areas with passenger car traffic. The Model 300 will not be loud enough to be heard in busier areas and will be socially acceptable when operating in and over populated areas.

CHANGE IN NOISE LEVEL IN 75-150 HERTZ OCTAVE - DECIBELS
(ARBITRARY COMMON REFERENCE LEVEL)

○ — ○ MODEL 300 PROPROTOR, $T = 4000-5000$ LB

□ — — □ SQUARE TIP 48-FT DIA ROTOR, $\theta_C = 80-85$ DEG,
 $T = 8000-9000$ LB

△ — — △ THIN-TIP 48-FT DIA ROTOR, $\theta_C = 70-85$ DEG,
 $T = 4250-5900$ LB

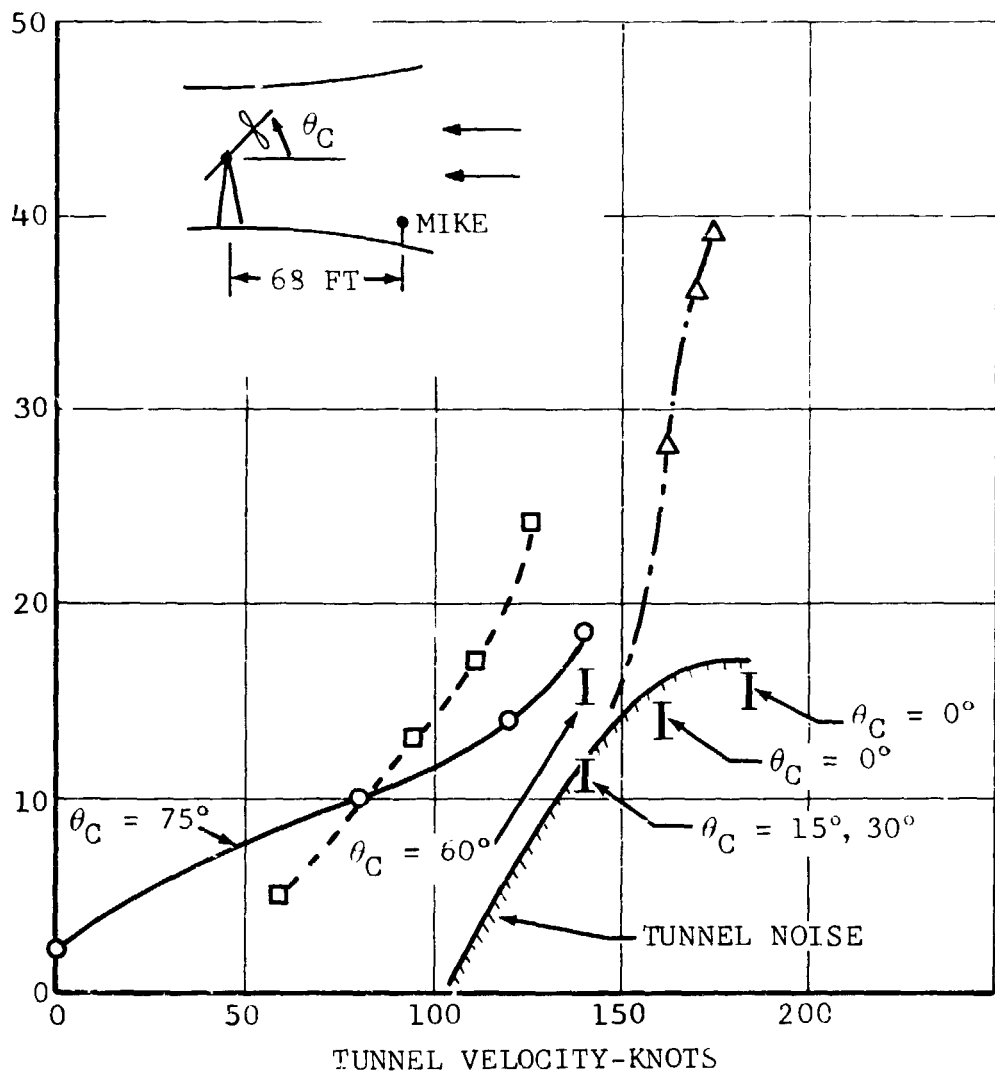


Figure VIII-1. Comparison of Model 300 Proprotor and Conventional Rotor Noise Levels Measured in Ames 40- by 80-Foot Wind Tunnel.

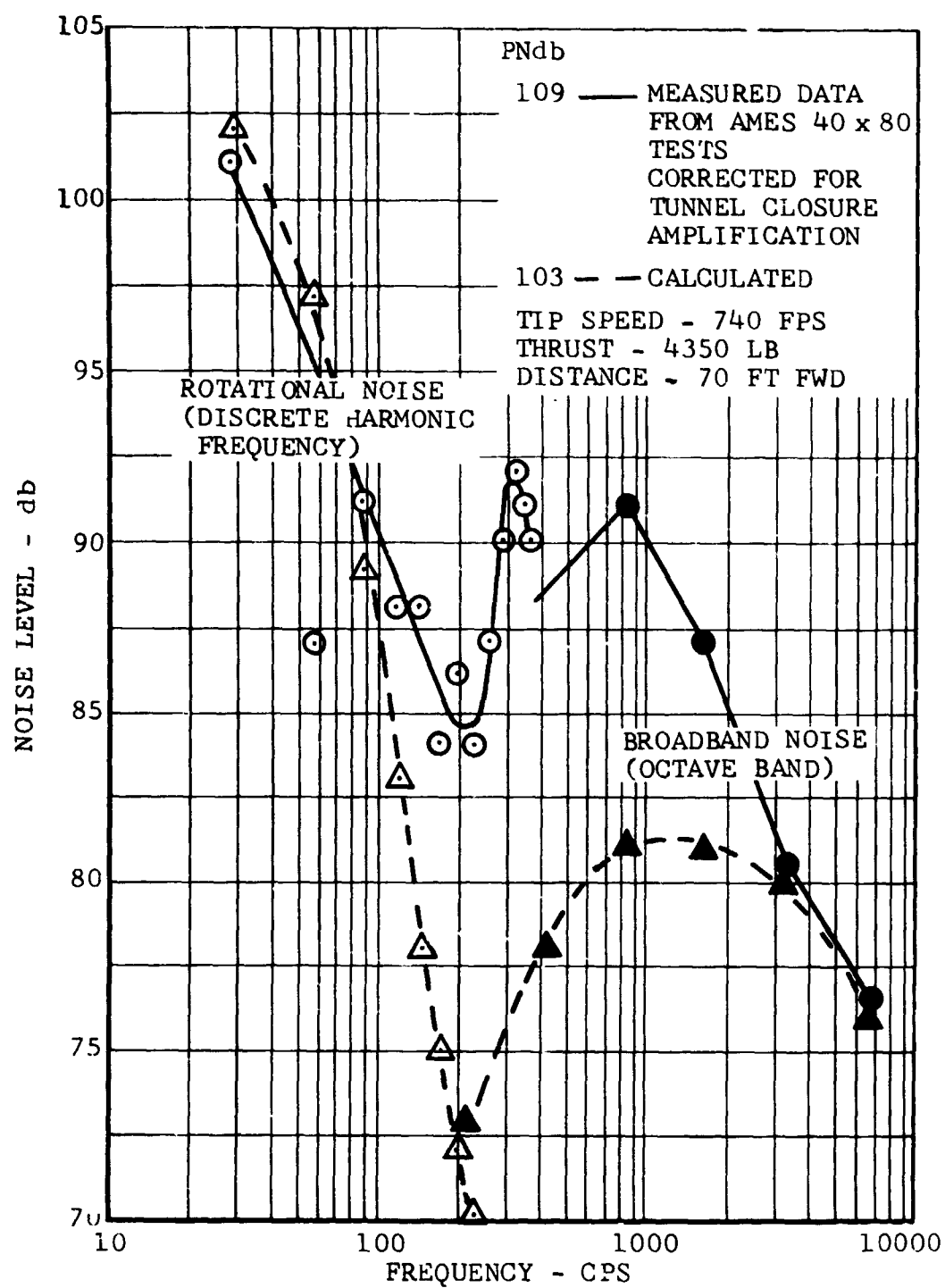


Figure VIII-2. Comparison of Calculated and Measured Propotor Noise Hover.

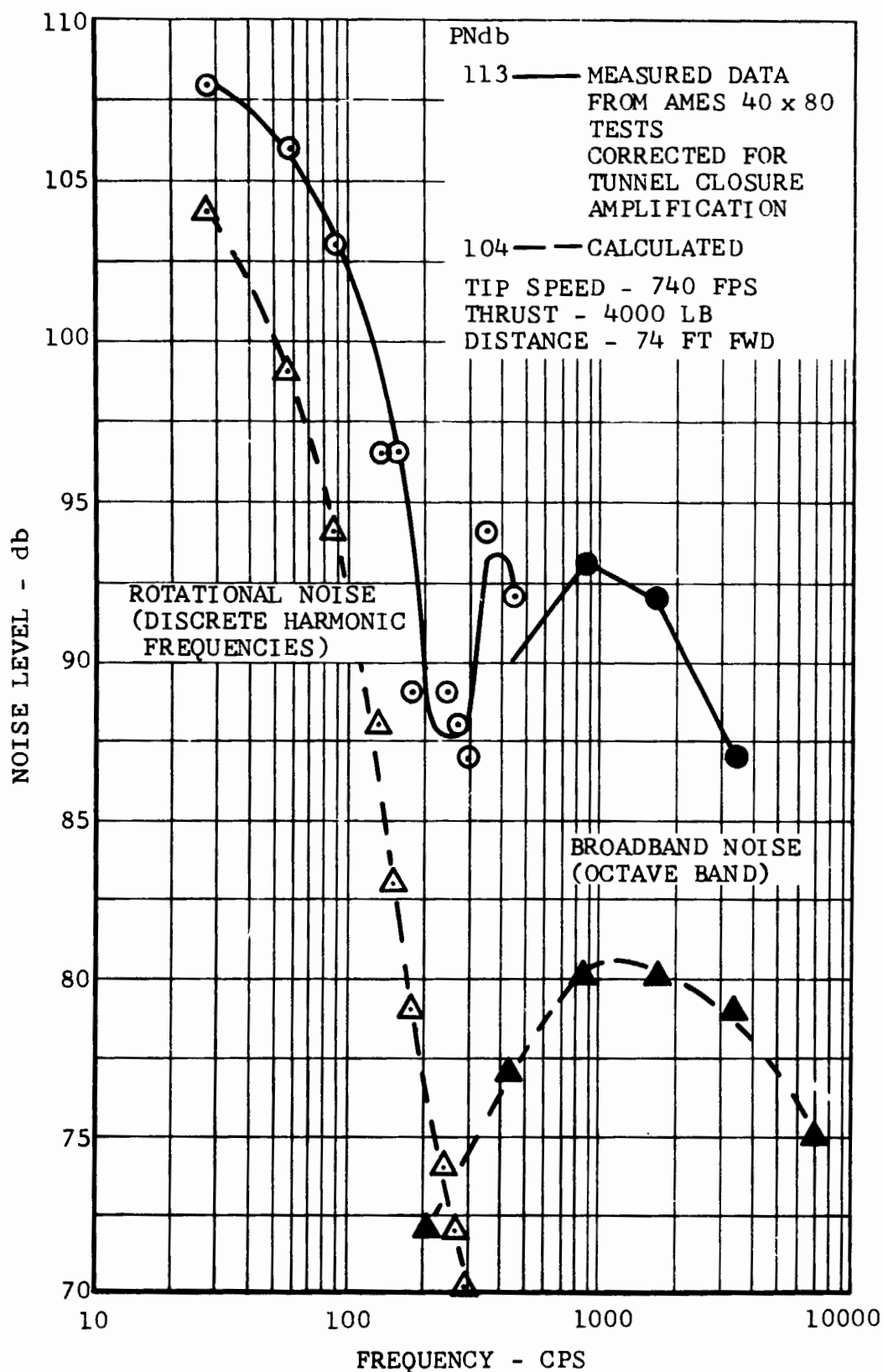


Figure VIII-3. Comparison of Calculated and Measured Propotor Noise 80 Knots.

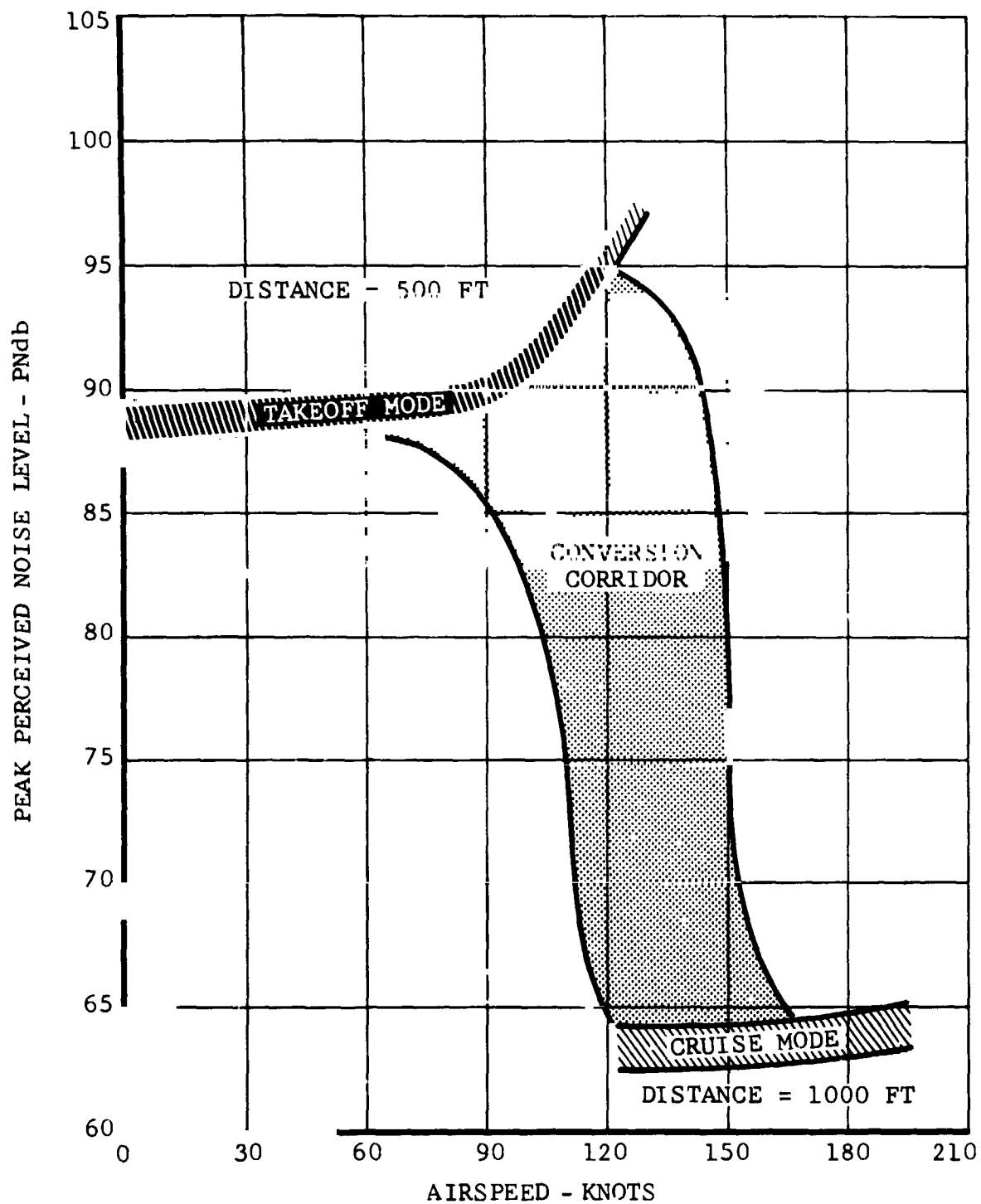


Figure VIII-4. Model 300 External Noise as a Function of Mode of Operation.

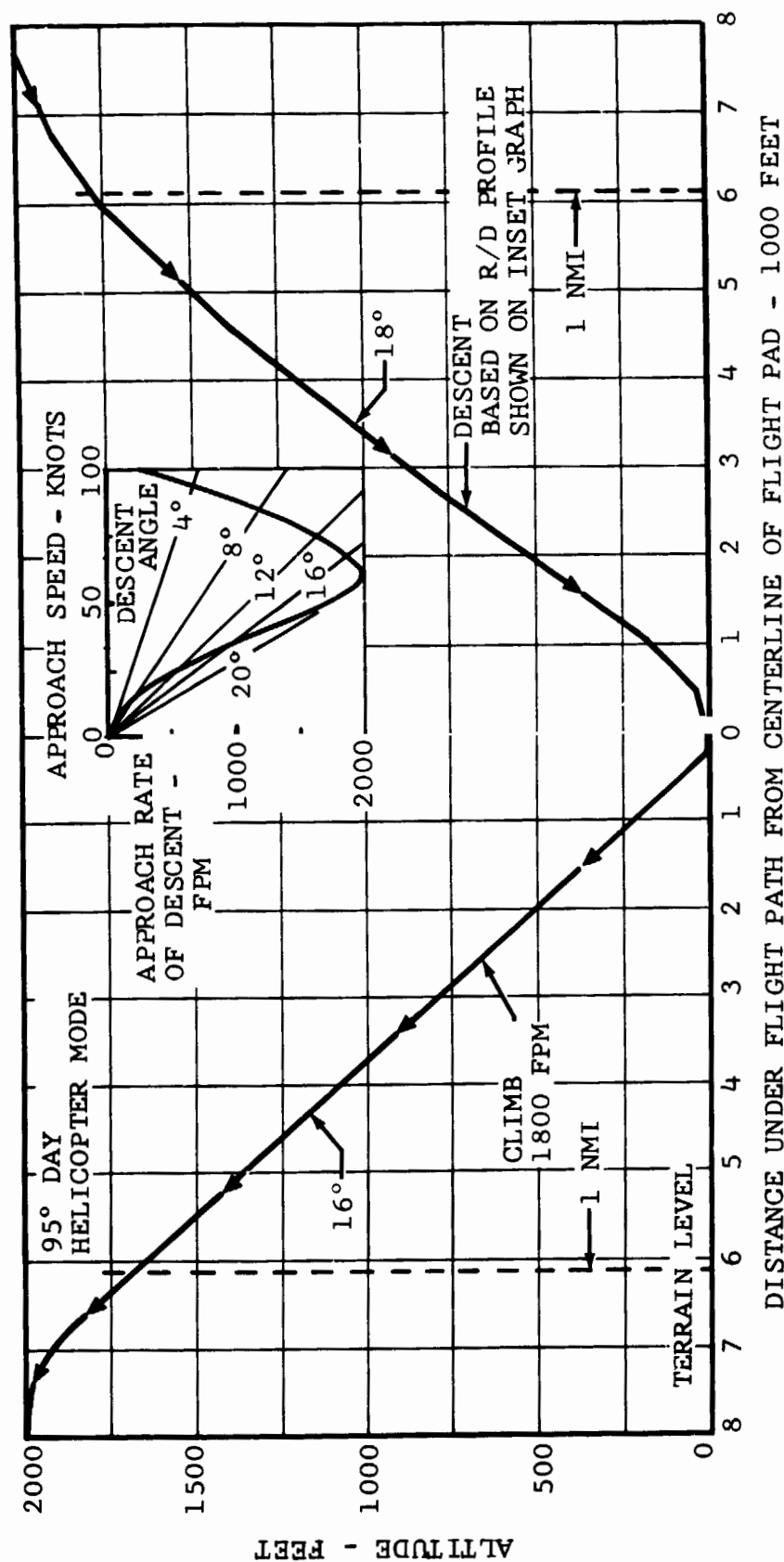


Figure VIII-5. Takeoff and Approach Profiles.

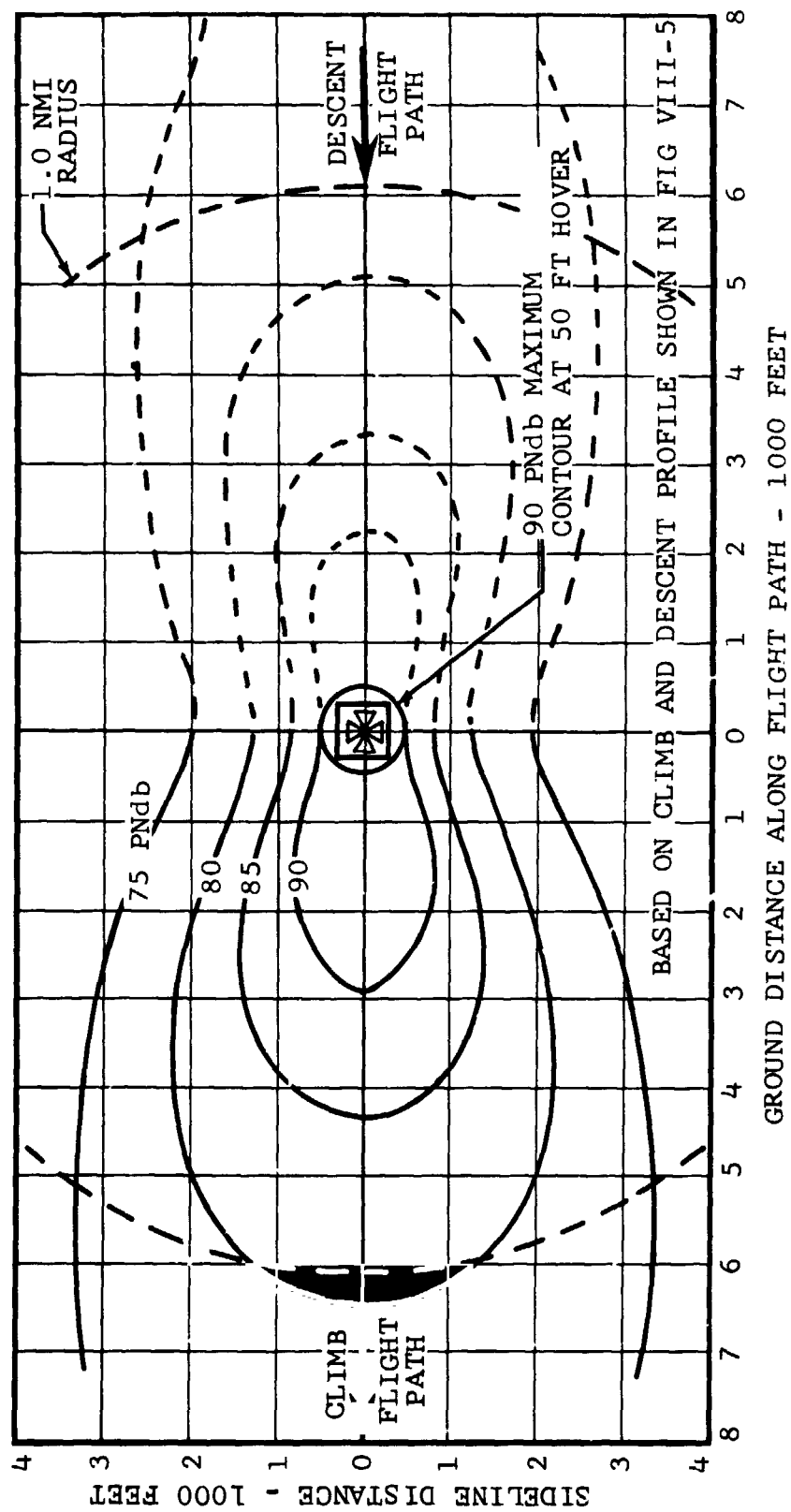


Figure VIII-6. Model 300 Noise Exposure Footprints

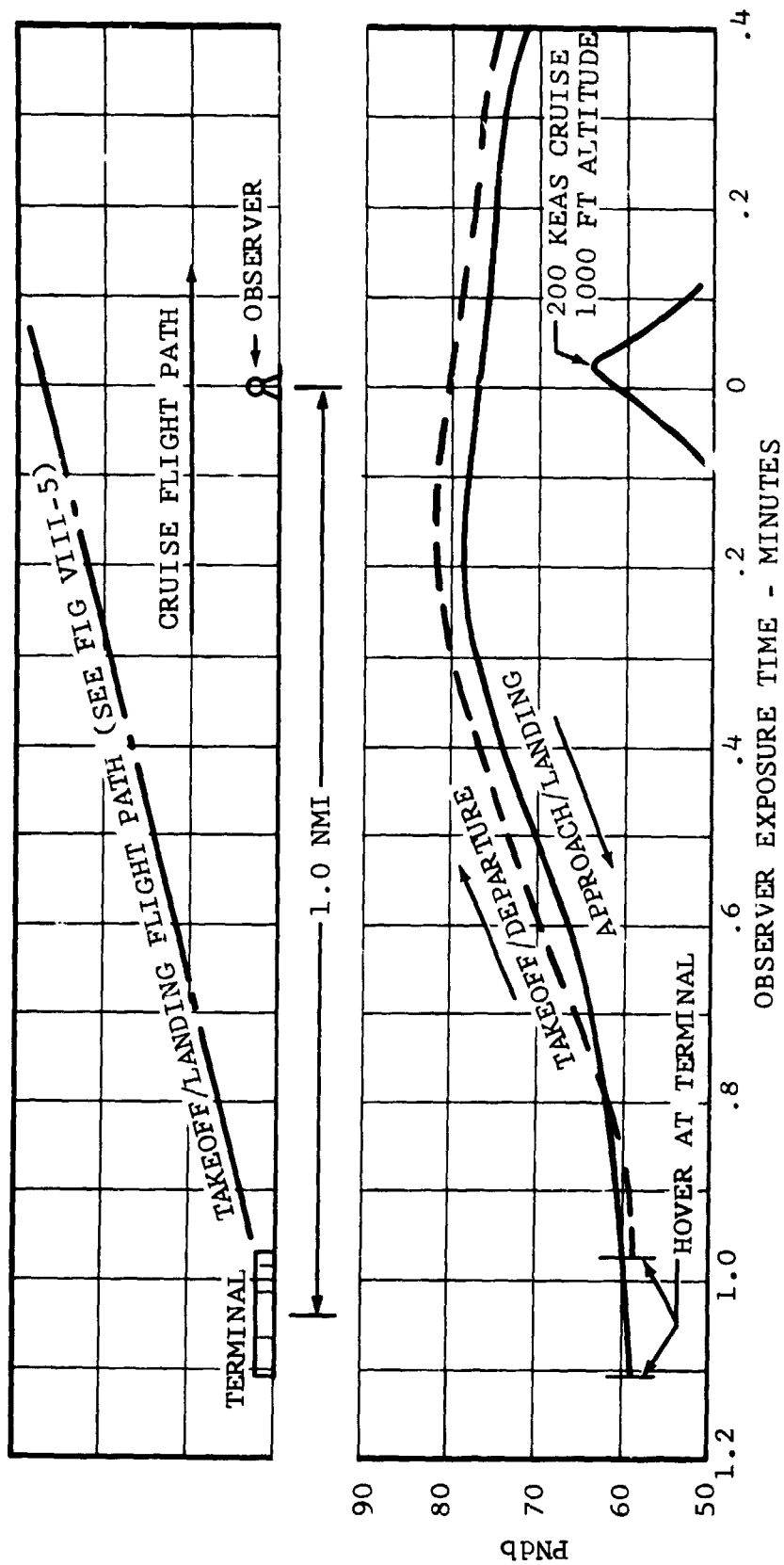


Figure VIII-7. Model 300 Noise-Time Histories for Various Modes of Operation

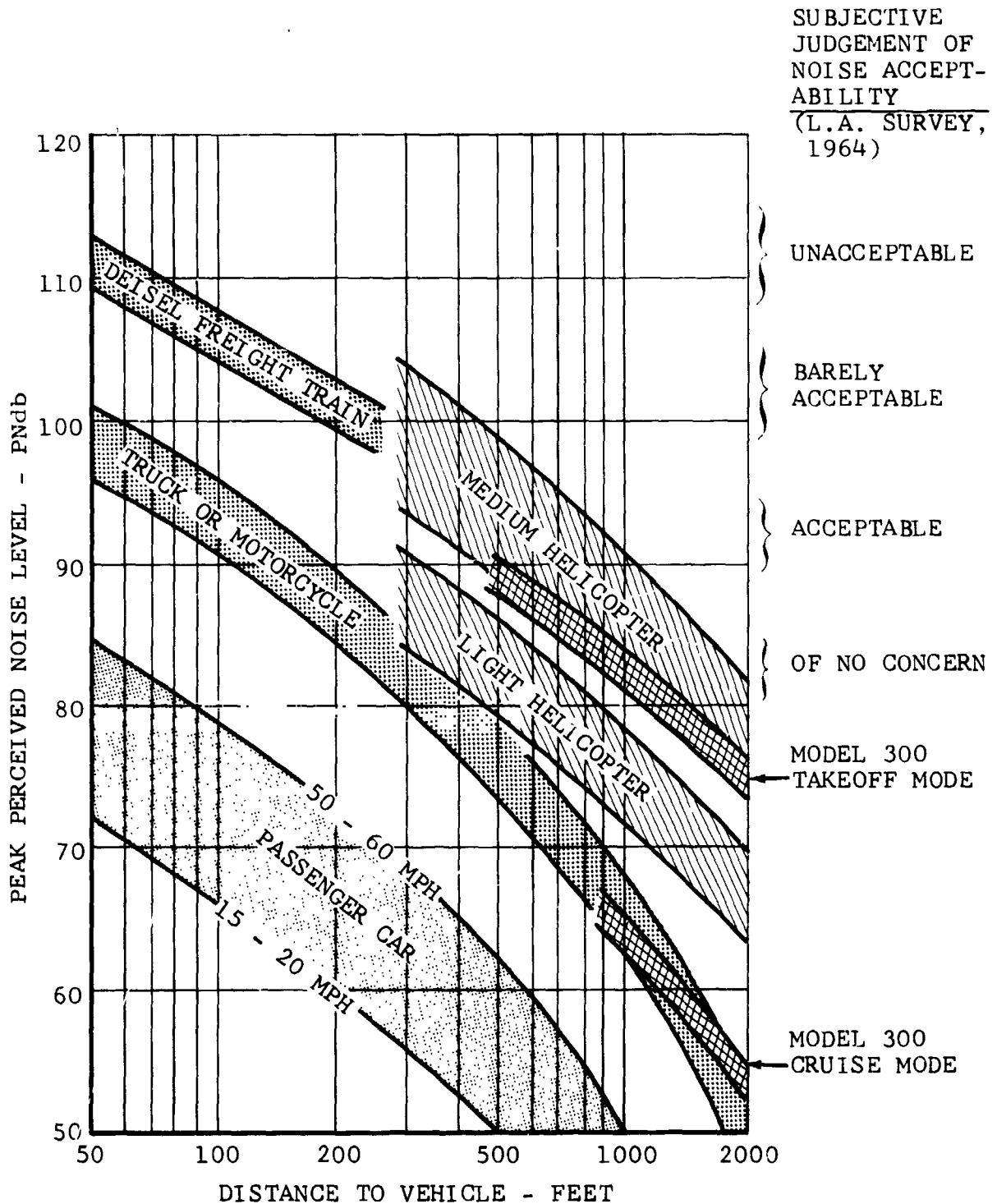


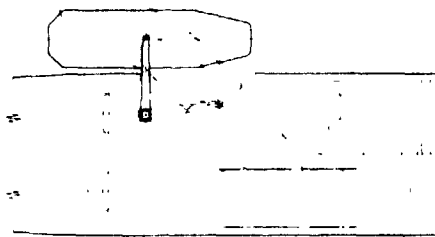
Figure VIII-8. Comparison of Noise of Model 300 and Other Modes of Transportation.

IX. REFERENCES

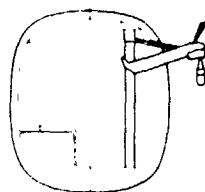
1. "Advancement of Proprotor Technology, Task I - Design Study Summary," NASA Contractor Report CR 114363, September 1969.
2. "Advancement of Proprotor Technology, Task II - Wind Tunnel Test Results," NASA Contractor Report CR 114363, September 1971.
3. "Fuselage Weight Estimation by Weight Penalty Evaluation Method," Chance Vought Aircraft Report 10043, November 1955.
4. Neal, G. T., "Proprotor Dynamic Stability Analysis - Program DYN4," Bell Helicopter Company Report 599-099-011 to be published.
5. Yen, J. G., et al, "A Study of Folding Proprotor VTOL Dynamics," AFFDL-TR-71-1, September 1971.
6. Gaffey, T. M., et al, "Analysis and Model Tests of the Proprotor Dynamics of a Tilt-Proprotor VTOL Aircraft," presented at the Air Force V/STOL Technology and Planning Conference, September 1969.
7. Ribner, H. S., "Propellers in Yaw," NACA Report 820, 1944.
8. Bird, B. J. and Blankenship, B. L., "Program AGAJ68, Rotorcraft Flight Simulation," BHC Report 599-068-904, September 1959.
9. Grande, D. L., "Some Effects of Random Turbulence on Weapon-System Performance," Aerospace Engineering 21, 35-43, 1962.
10. Press, H. and Meadows, M. T., "A Reevaluation of Gust-Load Statistics for Applications in Spectral Calculations," NACA TN3540, 1955.
11. Bird, B. J., et al, "A Stability and Control Prediction Method for Helicopters and Stoppable Rotor Aircraft," AFFDL-TR-69-123, Volumes I through IV, February 1970.
12. Holbrook, J. W., "A Low-Speed Wind-Tunnel Test of the 0.20-Scale Bell Helicopter Model 300," LTV Report LSWT 311, January 20, 1970.
13. Vaughn, J. B., "A Low-Speed Wind-Tunnel Force Test of the 0.20-Scale Bell Helicopter Model 300," LTV Report LSWT 333, May 15, 1970.

IX. REFERENCES - Continued

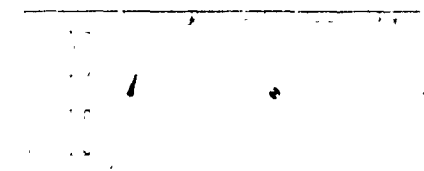
14. Vaughn, J. B., "A Low-Speed Wind-Tunnel Test of the Aeroelastic 0.20-Scale Bell Helicopter Model 300," LTV Report LSWT 361, April 14, 1971.
15. Holbrook, J. W., "A Low-Speed Wind-Tunnel Force Test of the 0.20-Scale Bell Helicopter Model 300," LTV Report LSWT 366, May 11, 1971.
16. Hammond, G., "NASA-Langley Research Center Transonic Dynamics Tunnel Test of an Aeroelastic Bell Helicopter Model 300," to be published.
17. Cox, C. R., "Rotor Noise Measurements in Wind Tunnels," Proceedings Third CAL/AVLABS Symposium, Buffalo, New York, Aerodynamics of Rotary Wing and V/STOL Aircraft, Volume 1, June 1969.
18. Cox, C. R., "Full-Scale Helicopter Rotor Noise Measurements in Ames 40- by 80-Foot Wind Tunnel," Bell Helicopter Company Report 576-099-052, July 1967.
19. Lowson, M. V. and Ollerhead, J. B., "Studies of Helicopter Rotor Noise," Wyle Laboratories, Inc., U. S. Army Aviation Materiel Laboratories, Technical Report 68-60, May 1968.
20. Schlegel, R. G., King, R. J., and Mull, R. H., "Helicopter Rotor Noise Generation and Propagation," Sikorsky Aircraft, U. S. Army Aviation Materiel Laboratories, Technical Report 66-4, October 1966.
21. Lowson, M. V., "Thoughts on Broadband Noise Radiation by a Helicopter," Wyle Laboratories, Inc., Report WR 68-20, December 1968.
22. Hartman, J. R. and Soderman, P. T., "Determination of the Acoustical Properties of the NASA-Ames 40- by 80-Foot Wind Tunnel," Working Paper No. 237, Ames Research Center, Moffett Field, California, August 1967.
23. Guest, S. H. and Adams, B. B., "Methods of Determining the Excess Attenuation for Ground-to-Ground Noise Propagation," National Aeronautics and Space Administration Report SP-189, October 1968.



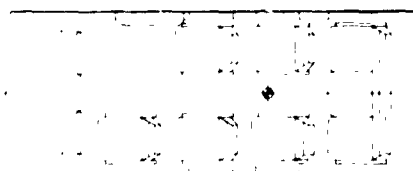
LITTER LOADING



RESCUE HOIST



FOLD-DOWN SEAT
HIGH DENSITY SEATING
W/ REAR

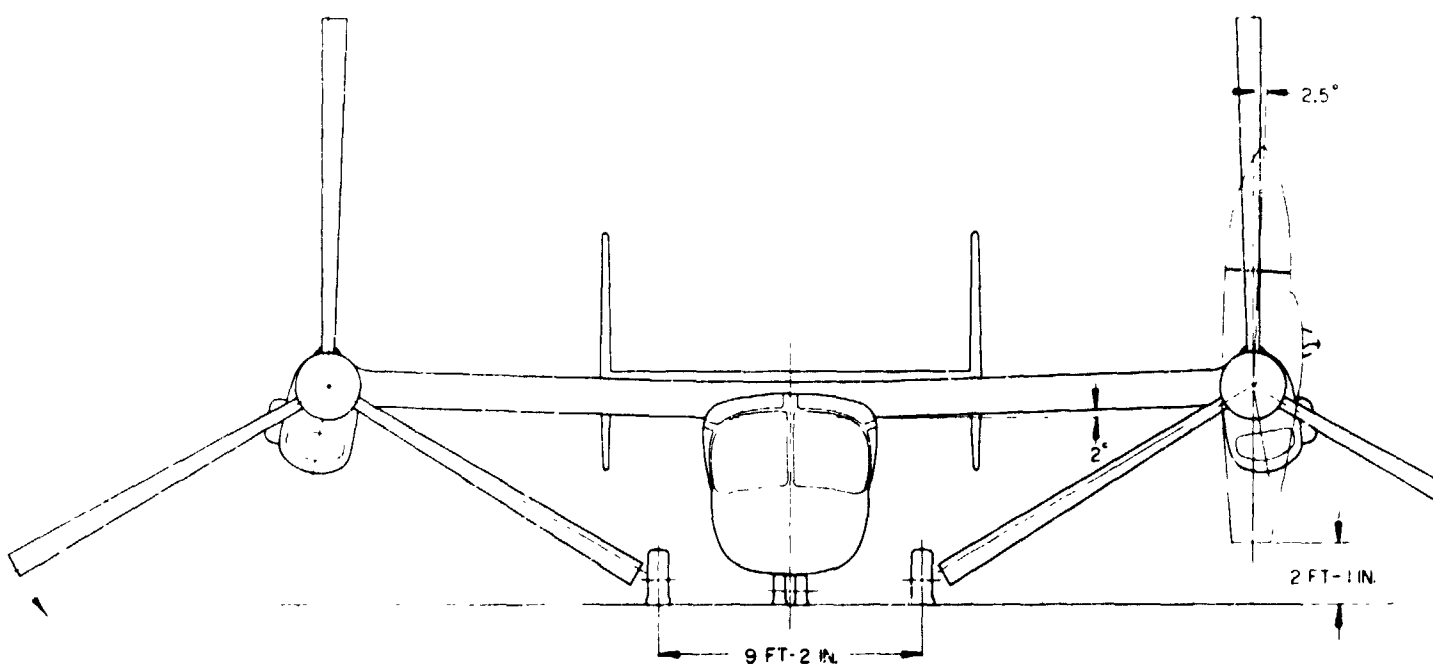


10-PLACE SEATING



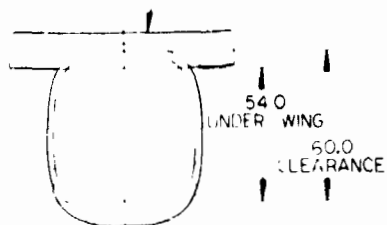
INSTRUMENT

POTENTIAL INTERNAL ARRANGEMENTS

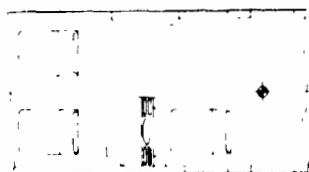


FOLDOUT FRAME 1

WING



60.0



INSTRUMENT CONSOLE

PROPELLOR POSITIONED TO SHOW FLAPPING CLEARANCE

35 FT-4 IN

32 FT-2 IN.

12° FLAPPING

1.5°

22 FT-5 IN

12 FT-1 IN.

15 FT-8 IN.

7 FT-5 IN.

2 FT-0 IN.

17 FT-10 IN.

1 FT-0 IN.

41 FT-0 IN.

42 FT-1 IN.

GROUND LINE

16.5°

FOLDOUT FRAME

2

REVISED BY
A 12/7/77

CHARACTERISTICS

WEIGHTS

NORMAL GROSS	12,400	LB
LANDING GROSS	9,500	LB
STOL GROSS	15,000	LB

POWER PLANT

MANUFACTURER & MODEL	PRATT & WHITNEY	PT6C-40 (VX)	
MAX CONT POWER	(2x990)	1,990	SHP
30 MINUTE POWER	(2x1150)	2,300	SHP
POWER LOADING (30 MIN)	(NORMAL GROSS WEIGHT)	5.4	LB/HP

PROPELLOR

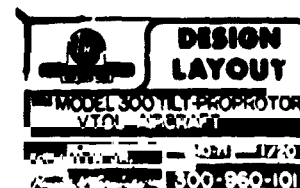
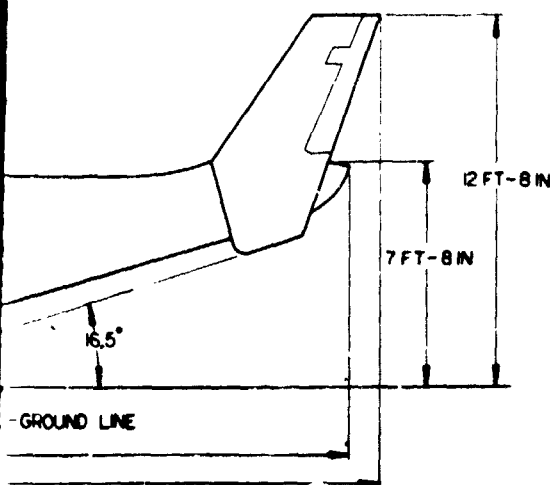
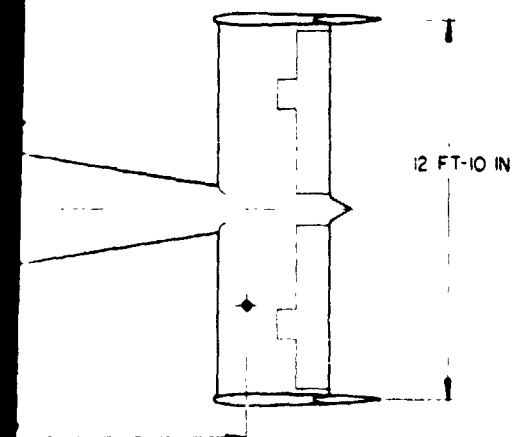
DIAMETER	25	FT
DISC AREA / ROTOR	491	SQ FT
DISC LOADING	12.6	LB / SQ FT
BLADE AIRFOIL	(NORMAL GROSS WEIGHT)	
	NACA 64-935	$\alpha = 0.3$
	NACA 64-208	$\alpha = 0.3$
BLADE CHORD	14	IN
SOLIDITY	.089	
BLADE TWIST-EFFECTIVE	45	DEGREES
TIP SPEED	740	FT / SEC
	600	FT / SEC
	HELIicopter MODE	
	AIRPLANE MODE	

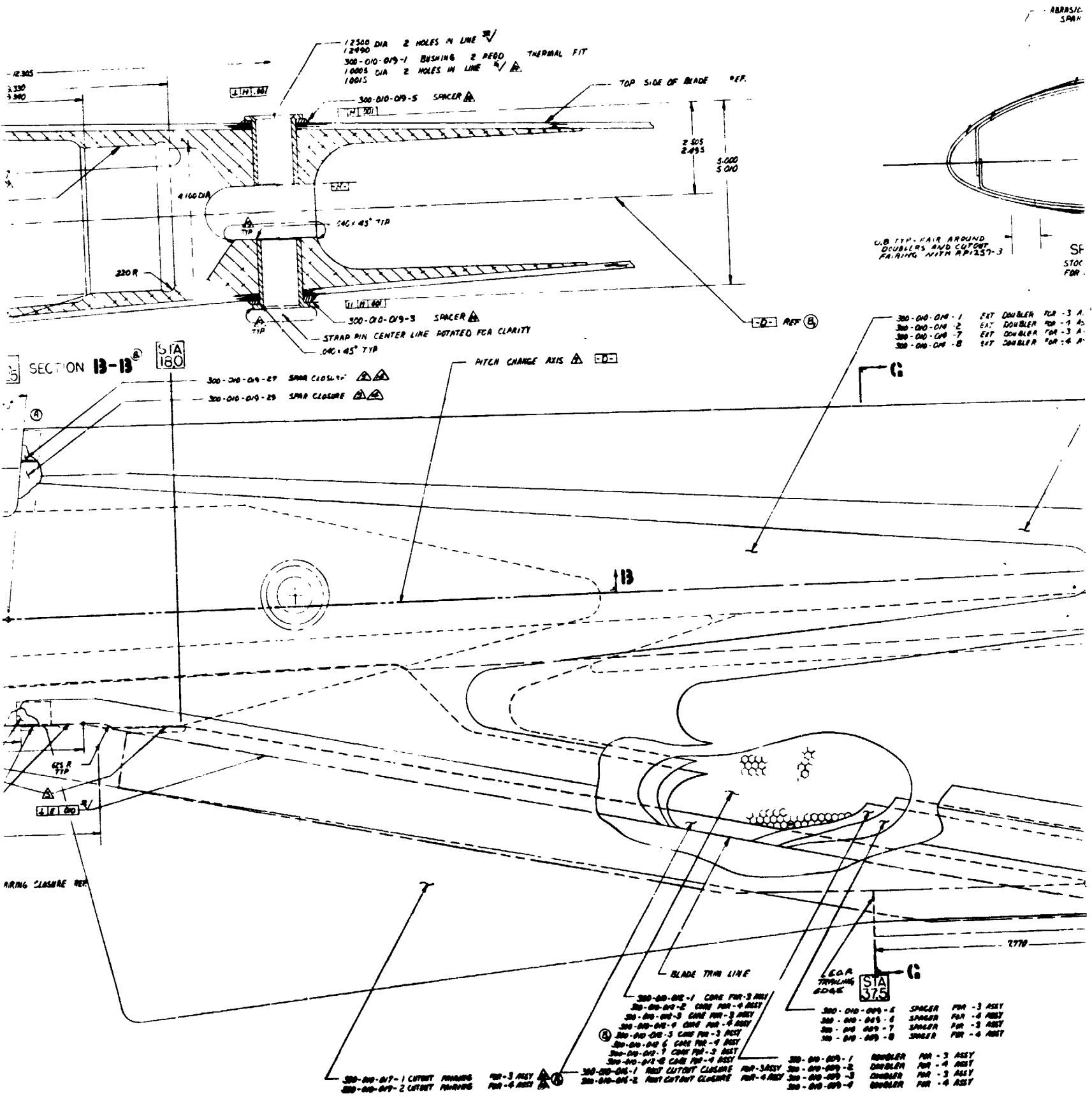
WING

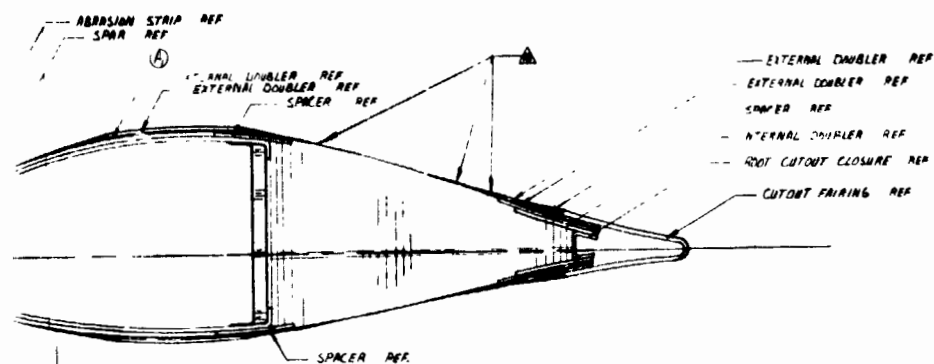
SPAN	34.6	FT
AREA	181	SQ FT
WING LOADING	68.5	LB / SQ FT
ASPECT RATIO	6.6	
AIRFOIL	NACA 64A223	MODIFIED
FLAP AREA / SIDE	5.5	SQ FT
FLAPERON AREA / SIDE	10.1	SQ FT
	TIP & ROOT	
	AFT OF HINGE	
	AFT OF HINGE	

EMPENNAGE

HORIZONTAL TAIL	AREA	50.25	SQ FT
	ASPECT RATIO	3.28	
ELEVATOR AREA TOTAL	AFT OF HINGE	13.0	SQ FT
VERTICAL TAIL	AREA TOTAL	50.5	SQ FT
	ASPECT RATIO	2.4	
RUDDER AREA TOTAL	AFT OF HINGE	7.5	SQ FT





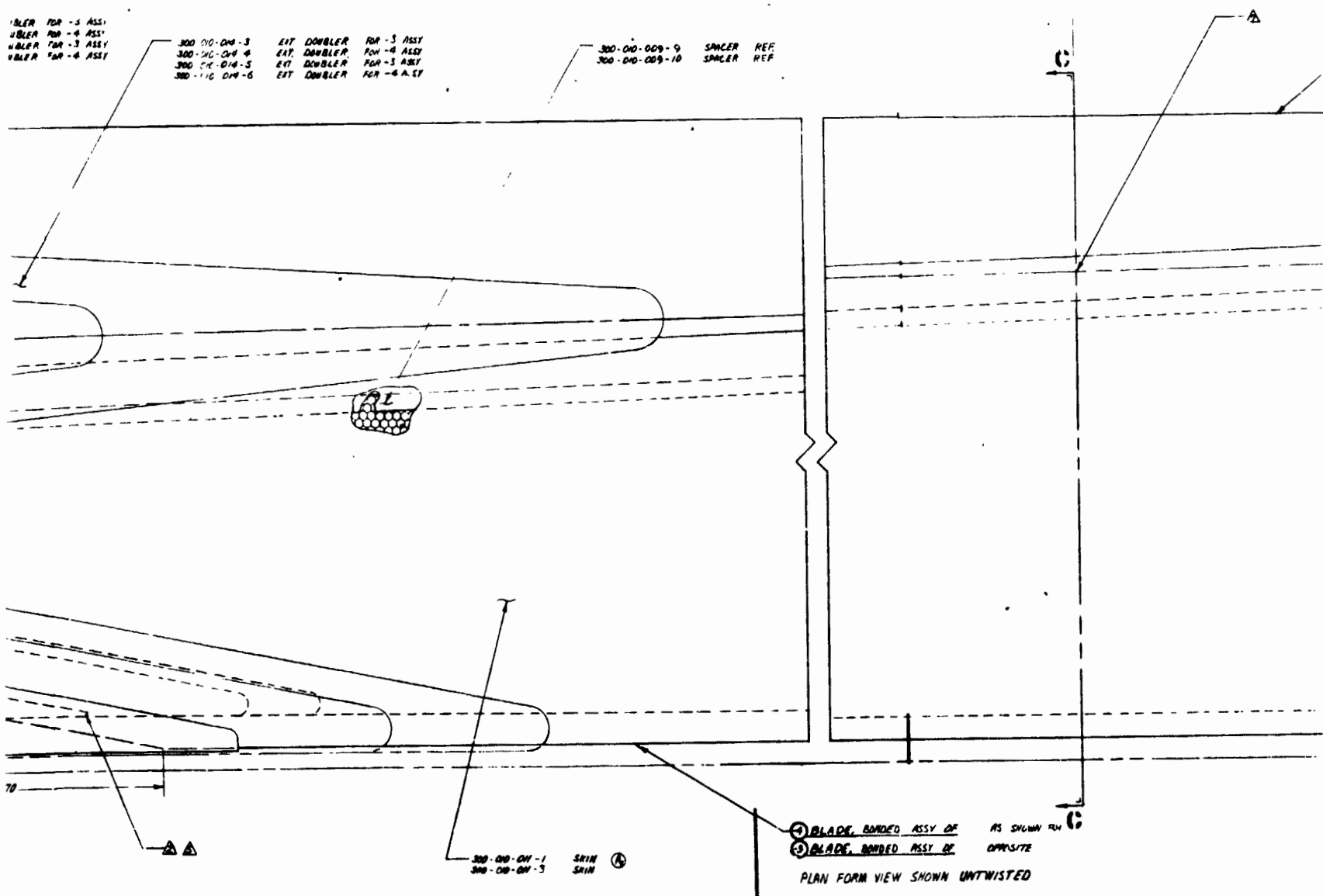


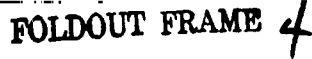
STA
112.5

DOUBLER FOR -3 ASSY
DOUBLER FOR -4 ASSY
DOUBLER FOR -3 ASSY
DOUBLER FOR -4 ASSY

300-010-014-3 EXT DOUBLER FOR -3 ASSY
300-010-014-4 EXT DOUBLER FOR -4 ASSY
300-010-014-5 EXT DOUBLER FOR -3 ASSY
300-010-014-6 EXT DOUBLER FOR -4 ASSY

300-010-009-9 SPACER REF
300-010-009-10 SPACER REF



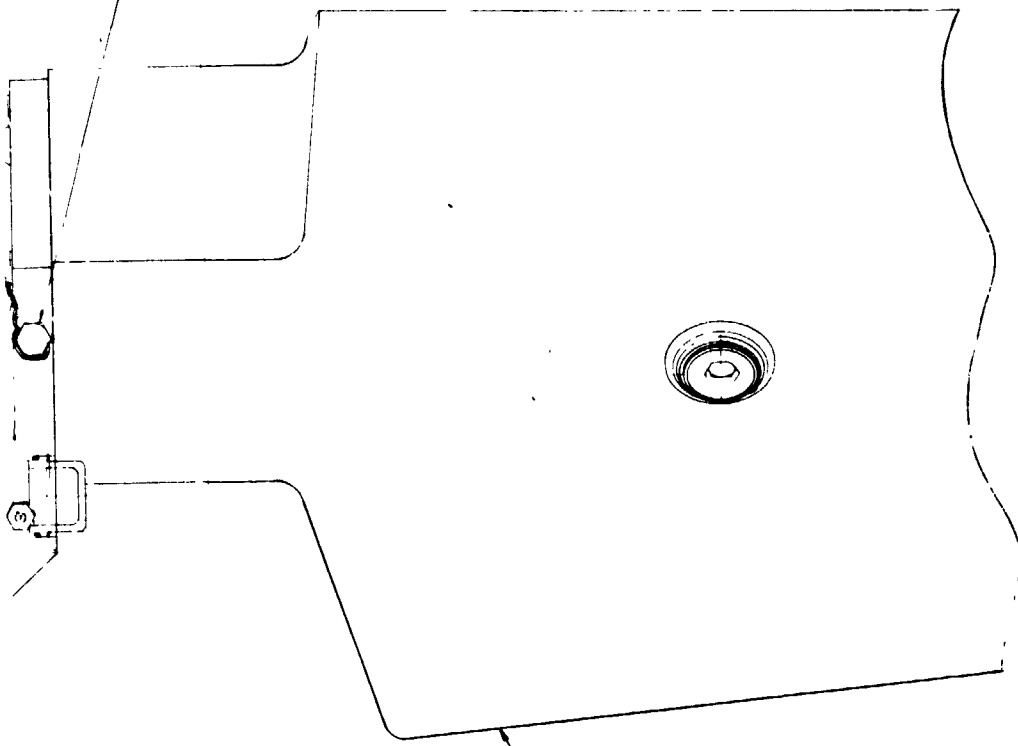
[illegible][illegible][illegible]

FOLDOUT FRAME, DO NOT TAP A ME.

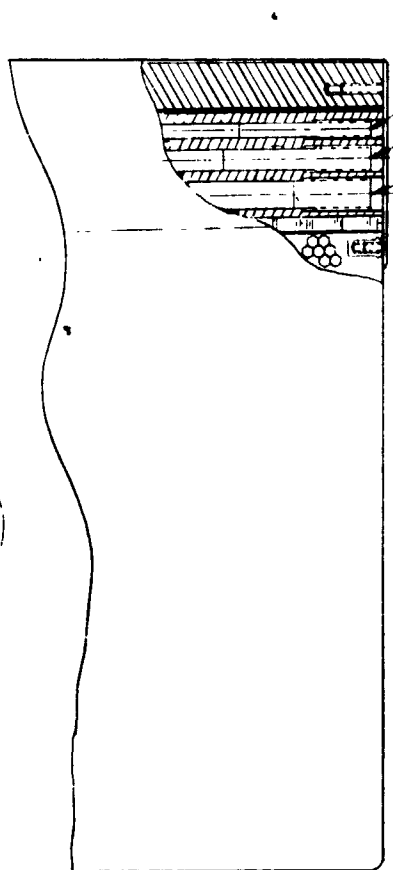


4 REQ'D
 R. 4 REQ'D UNDER NUT
 4 REQ'D UNDER NUT
 1/2" IN-LB
 CUTTER, 4 REQ'D

MS 20995-52 LOCK WIRE
 3 PLACES REMOVE CUTTER
 PIN IF PRESENT



300-010-001-1 BLADE ASSY, LH, 3 REQ'D (OPPOSITE)
 300-010-001-2 BLADE ASSY, RH, 3 REQ'D (SHOWN)



300-010-019-7 B.
 300-010-019-9 B.
 300-010-019-11 B.
 300-010-019-13 B.
 300-010-019-15 B.
 300-010-019-17 B.

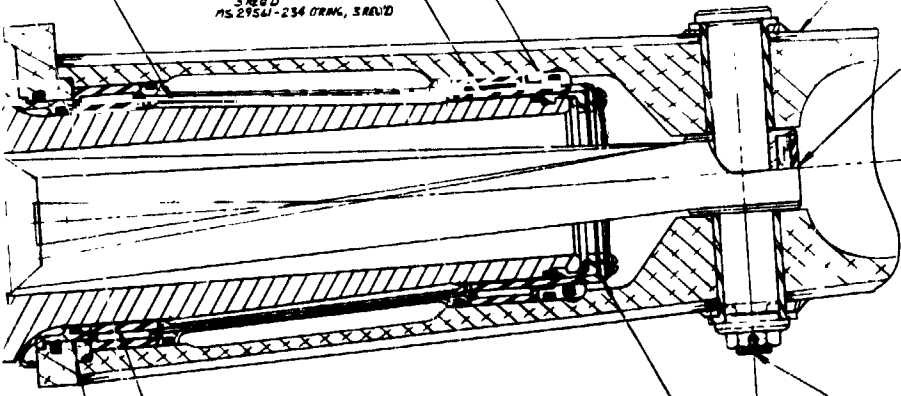
105-1 SEAL ASSY

300-010-107-1 CLAMP SET, 3 REQ'D

300-010-107-1 SPACER, INNER, 3 REQ'D
 300-010-104-1 RACE, BEARING, 3 REQ'D
 MS 29541-234 ORAC, 3 REQ'D

BLADE ROTATED FOR CLARITY

300-010-10 STRAP ASSY
 3 REQ'D



IR-602065 90-1 INNER RACE, 3 REQ'D
 REF 2M-010-251 BEARING INNER RACE

300-010-107-5 RING, 3 REQ'D
 MS 29541-240 O RING, 3 REQ'D

300-010-104-1 BOLT, 3 REQ'D
 300-010-104-5 NUT, 3 REQ'D
 TORQUE TO 88-120 IN LB
 MS 24465-578 PIN CUTTER, INSTALL
 PER OPS PW-6043, 3 PLACE

(SHOWN)
 105-1 SEAL ASSY
 105-1 SEAL ASSY
 105-1 SEAL ASSY

REV	DATE	BY	300-010-100
-----	------	----	-------------

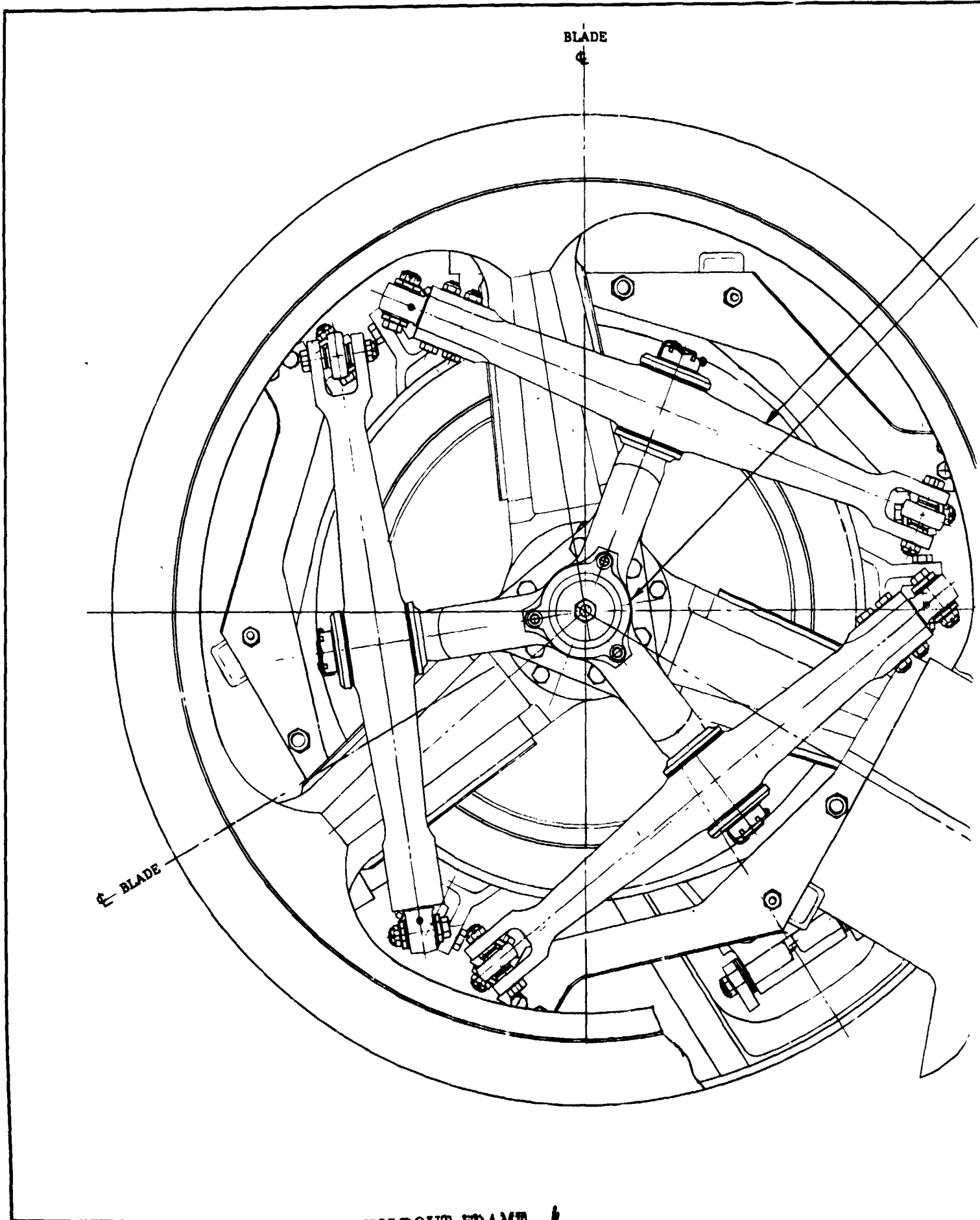
3	3	1R 142015-90-1	INNER RACE	A
AR	AR	1R 134	ADHESIVE	
4	4	BRO	PRO SEAL	
		LCN/2 BRO	NUT	PURCHASE BRO 1 SPS PARTS
4	4	MS 2445-308	PIN CUTTER	
AR	AR	MS 20175-25	LOCK WIRE	
1	1	MS 20002-2	WASHER	
3	3	MS 1250-200	O RING	
3	3	MS 21821-254	O RING	
3	3	MS 2445-372	PIN CUTTER	
6	6	MS 17825-4	NUT	
4	4	MS 20032-8	WASHER	
4	4	AMS 1308-36	BOLT	
1	1	AN 750-1	NAME PLATE	
12	12	AN 90-916L	WASHER	
18	18	AN 140-1016L	WASHER	
18	18	AN 308-10-8	SCREW	
6	6	AN 174-21	BOLT	
1	1	300-00-208-1	UNIVERSAL JOINT ASSY	
1	1	101-1	BRACKET AN	
1	1	101-2	BRACKET AN	
1	1	101-3	SAUM	
1	1	101-4	RETAINER	
1	1	101-5	CLAMP SET	
1	1	101-6	RING	
1	1	101-7	SPACER	
1	1	101-8	NUT	
1	1	101-9	JOINT ASSY	
1	1	101-10	SEAL ASSY	
1	1	101-11	RACE BEARING	

1 FILL SPINDLE BINS & TRUNKMAN BAGS CANTIES WITH SAME POW-30
MIL-1 2004 BIL BY WORKING ALL ARE OUT 45 BIL
IS ADDED FALL UNTIL RESERVOIRS ARE 1/2 FULL.
THIS PART IS LOWER RACE OF 204-000-251-1 BEARING
BAND WITH EPON 934 PER FM 40335
2 LOCKWIRE 1 CRITTER PER PER BPS FM 40443
3 TORQUE PER BPS FM 40408 EXCEPT AS SHOWN
4 FOR HUB ASSY NO. 8 HUB SERIAL NO.
MARK PER BPS FM 4050.

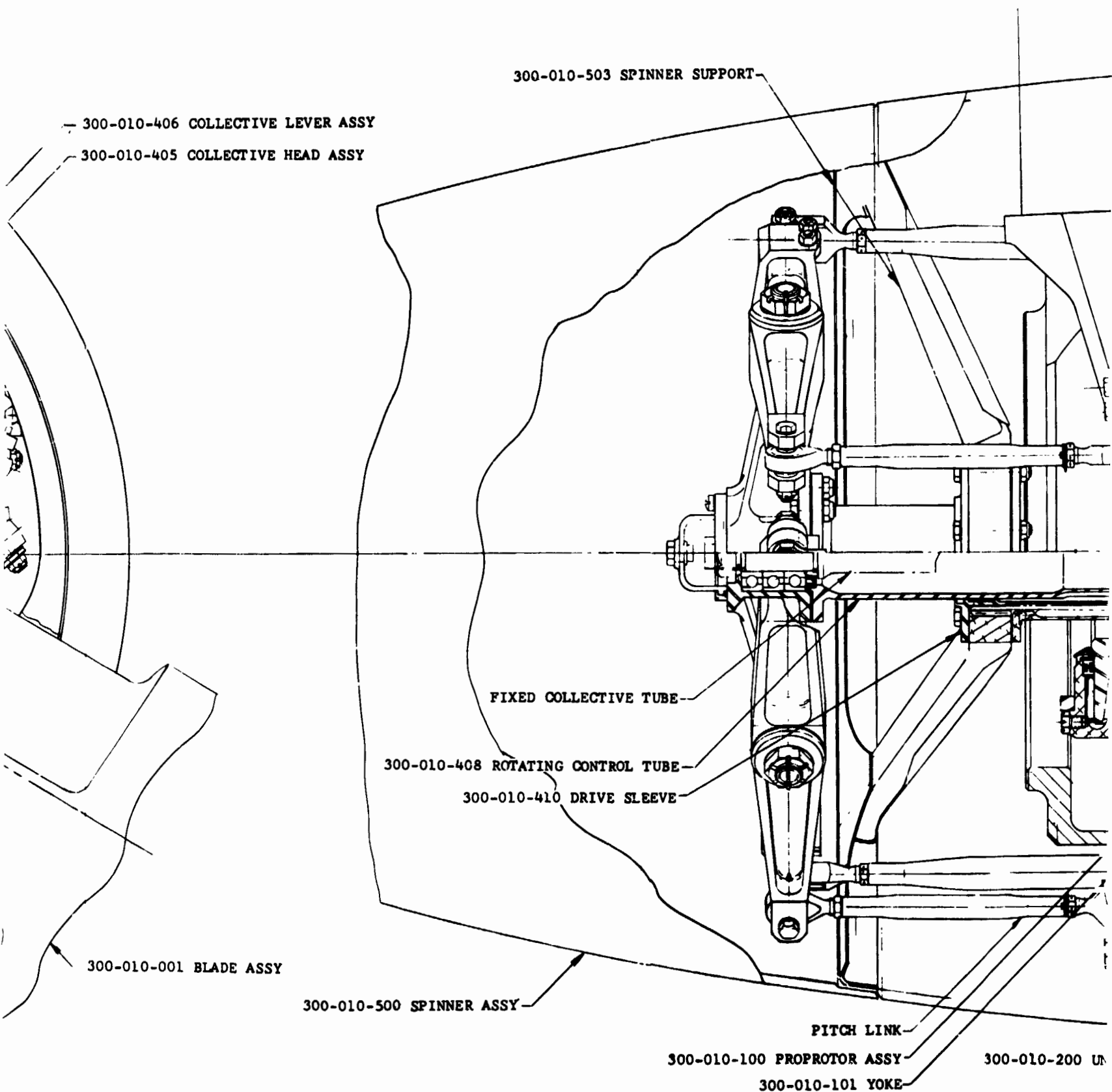
[illegible]

10

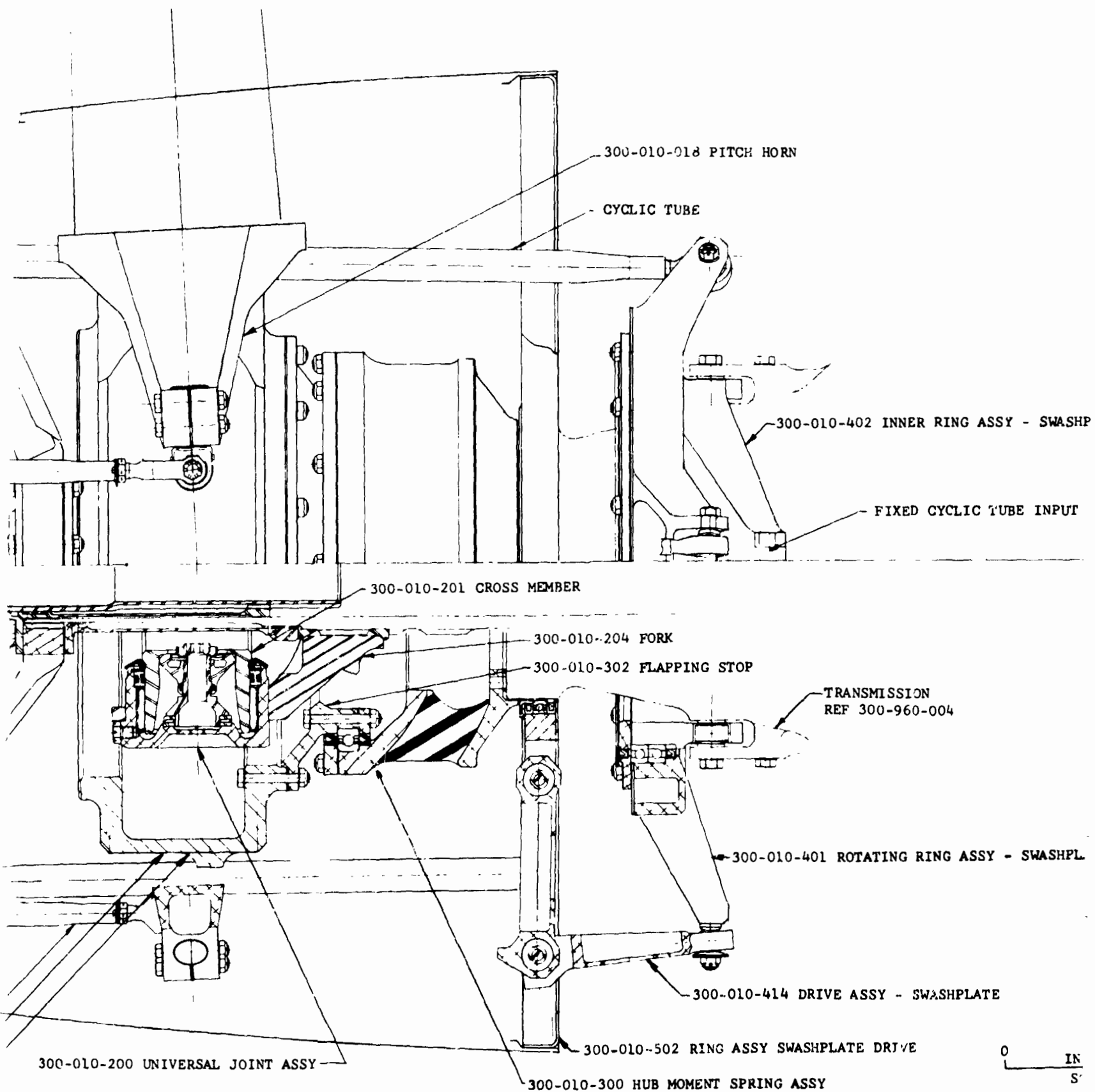
FOLDOUT FRAME 3



FOLDOUT FRAME

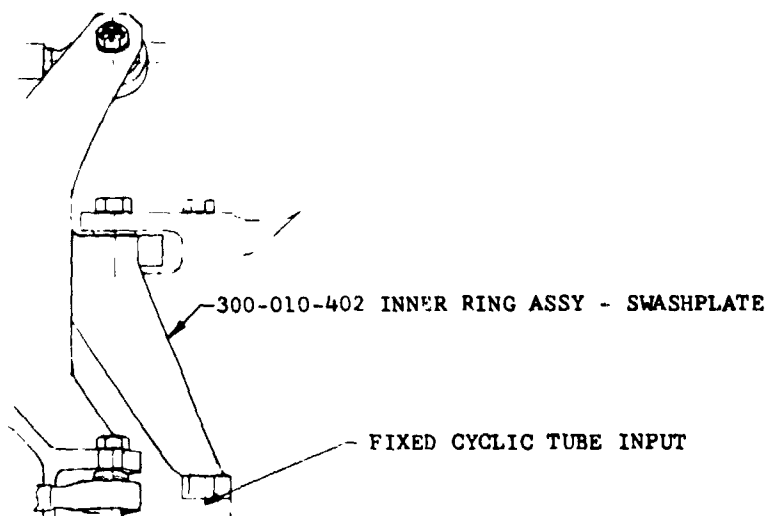


FOLDOUT FRAME 2

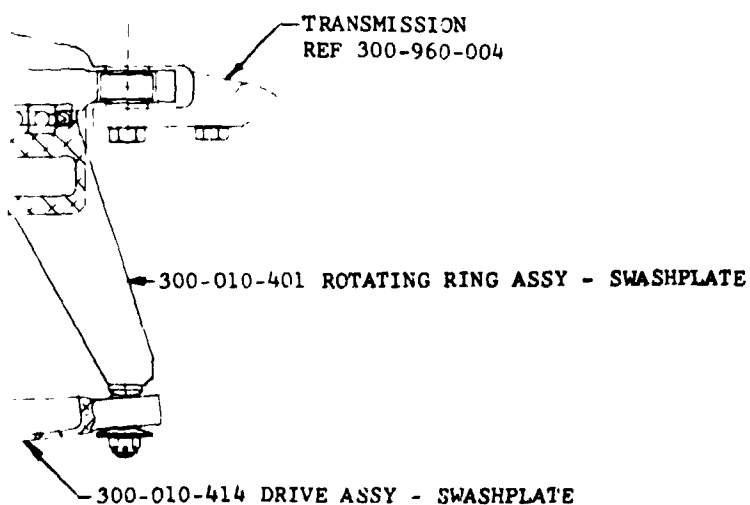


10-018 PITCH HORN

C TUBE



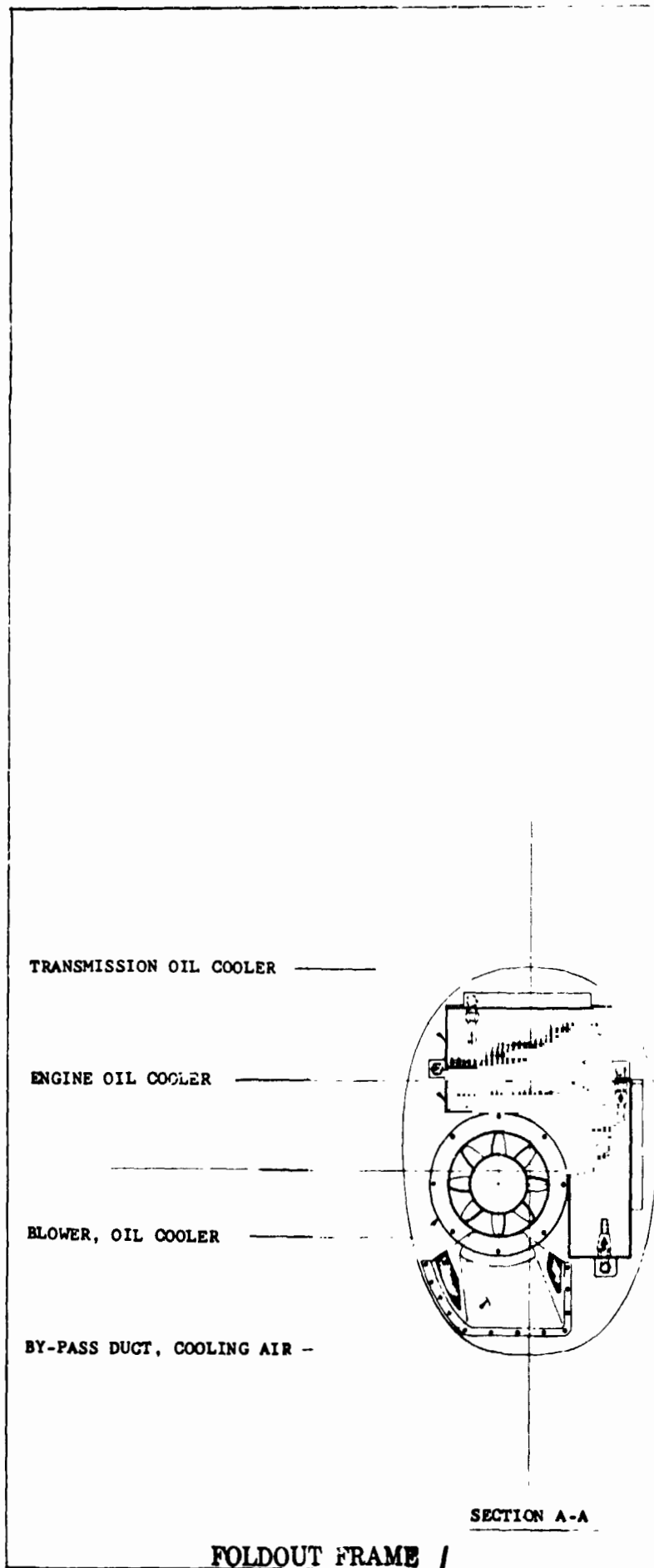
FORK
FLAPPING STOP



10-502 RING ASSY SWASHPLATE DRIVE
HUB MOMENT SPRING ASSY

0 INCHES 5
SCALE

		DESIGN LAYOUT	
PROPRATOR AND CONTROLS			
COVINGTON		8-69	
<i>Carte</i>		300-960-002	



SPINDLE
 COLLECTIVE CONTROL
 CYCLIC CONTROL 300-960-005 FIXED CONTROLS -
 FIXED CONTROL MOUNT

FIREWALL SHUT-OFF VALVE, FUEL
 BLOWER DRIVE SHAFT
 BLOWER, OIL COOLER BY-PASS
 STARTER-GENERATOR

EJECTOR, INDUCTION BY-PASS

PLENUM, INDUCTION BY-PASS
 FIRE EXTINGUISHER
 FUEL PRESSURE TRANSMITTER
 FUEL FILTER, ENGINE
 OIL FILTER, ENGINE

GAS PRODUCER CONTROL
 ENGINE AIR INLET SCREEN
 FIRE EXTINGUISHER
 FIREWALL SHUT-OFF VALVE, FUEL
 CLOSE-OUT BAFFLE, FIREWALL

BAFFLE, OIL COOLER
 PRESSURE TRANSMITTER, FUEL
 GAS PRODUCER CONTROL
 TRANSMISSION OIL COOLER
 BLOWER, OIL COOLER
 EJECTOR, INDUCTION BY-PASS

PLENUM SEAL

STARTER GENERATOR

ENGINE OIL COOLER

COWL SUPPORT

BLOWER DRIVESHAFT

FIRE DETECTOR
 FILTER, ENGINE FUEL
 FILTER, ENGINE OIL
 INDUCTION BAFFLE
 SCREEN, INDUCTION ANTI-ICE

WINGS - WING

300-960-007 WING
AIR-INLET - HOT SEC
CONVERSION ACTUATOR

FAIRING

TRANSMISSION OIL M
HYDRAULIC RESERVOIR

FUSE STA
300.00

TRANSMISSION OIL FILTER
CYCLIC CONTROL
FIREWALL
COLLECTIVE CONTROL

HYDRAULIC & FUEL EXTENDABLE TUBES
300-960-004 MAIN TRANSMISSION
COWL CONVERSION DOOR
HYDRAULIC SWIVELS

FIREWALL

CYLINDER, COLLECTIVE
CYLINDER, CYCLIC CO
ENGINE EXHAUST STA
TURNING VANE, EXHA
BAFFLE, EJECTOR SE
EJECTOR, EXHAUST
CONVERSION DOWN-ST
HYDRAULIC PUMP
INLET, COMPARTMENT

ACTUATOR FAIRING
CONVERSION ACTUAT
POWER TURBINE GOV
SPEED SELECT ACTU
DROOP COMPENSATO
TORQUEMETER & POW

ENGINE AIR INLET

FIREWALL

FIRE DETECTOR
PT6C-40 ENGINE
FIREWALL

VIEW LOOKING INB'D - R.H. NACELLE

FOLDOUT FRAME 2

SECTION
OR

MANIFOLD
AIR & FILTER

TRACE AT WING STA. 193.00

IVE CONTROL
CONTROL

ACK
AUST
EPARATOR

STOP

NT COOLING

300-910-001 BLADE ASSY

300-960-002 PROPRTOR AND CONTROLS

SPINNER

W.L. 100.00

UP

OUTB'D

WING STA
193.00

10°

HYDRAULIC PUMP
HYDRAULIC RESERVOIR & FILTER

ROTATING CONTROLS

ACTUATOR FAIRING CONVERSION

TRANSMISSION OIL PUMP & FILTER

FIREWALL, INB'D CONVERSION

CYLINDER, CYCLIC CONTROL
CYLINDER, COLLECTIVE CONTROL

SPEED SELECT ACTUATOR

POWER TURBINE GOVERNOR


300-960-004 MAIN TRANSMISSION

TORQUEMETER & POWER TURBINE SENSOR

TRANSMISSION OIL SCAVENGE LINE

FIREWALL, UPPER

0 10
INCHES
SCALE

		DESIGN LAYOUT	
INBOARD PROFILE - NACELLE			
BUSBEE	8/69		
300-960-003			

TRANS LUB PUMP
1 PRESSURE ELEMENT
FOR 15 GPM AND
3 SCAVENGE ELEMENTS
FOR 32 GPM TOTAL.
MIL-L-7808 OR
MIL-L-23699 LUB
3 GAL LUB SUMP

43T
(REF)

LUB PUMP DRIVE
GEAR - 45T

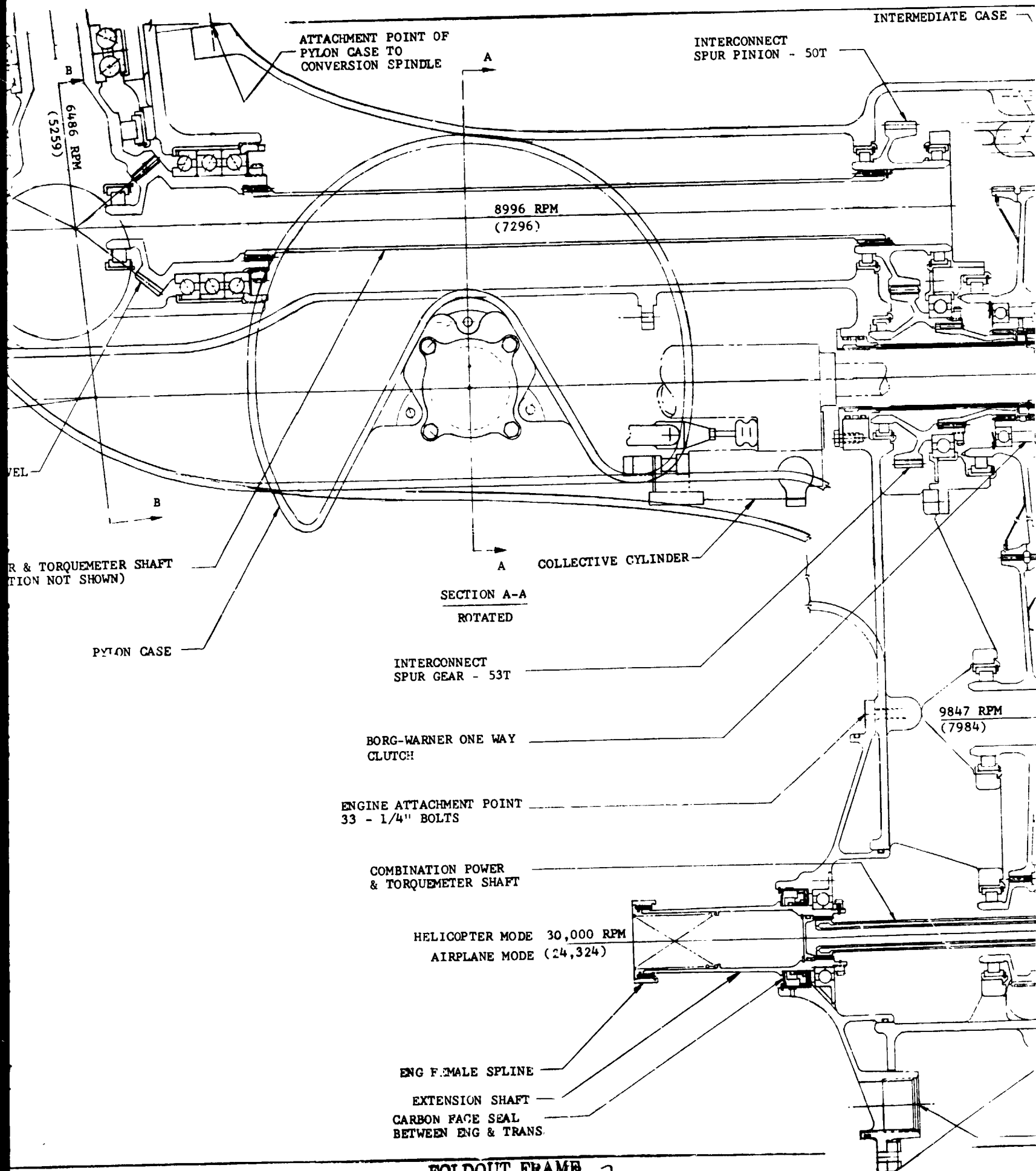
SPIRAL BEVEL
43T

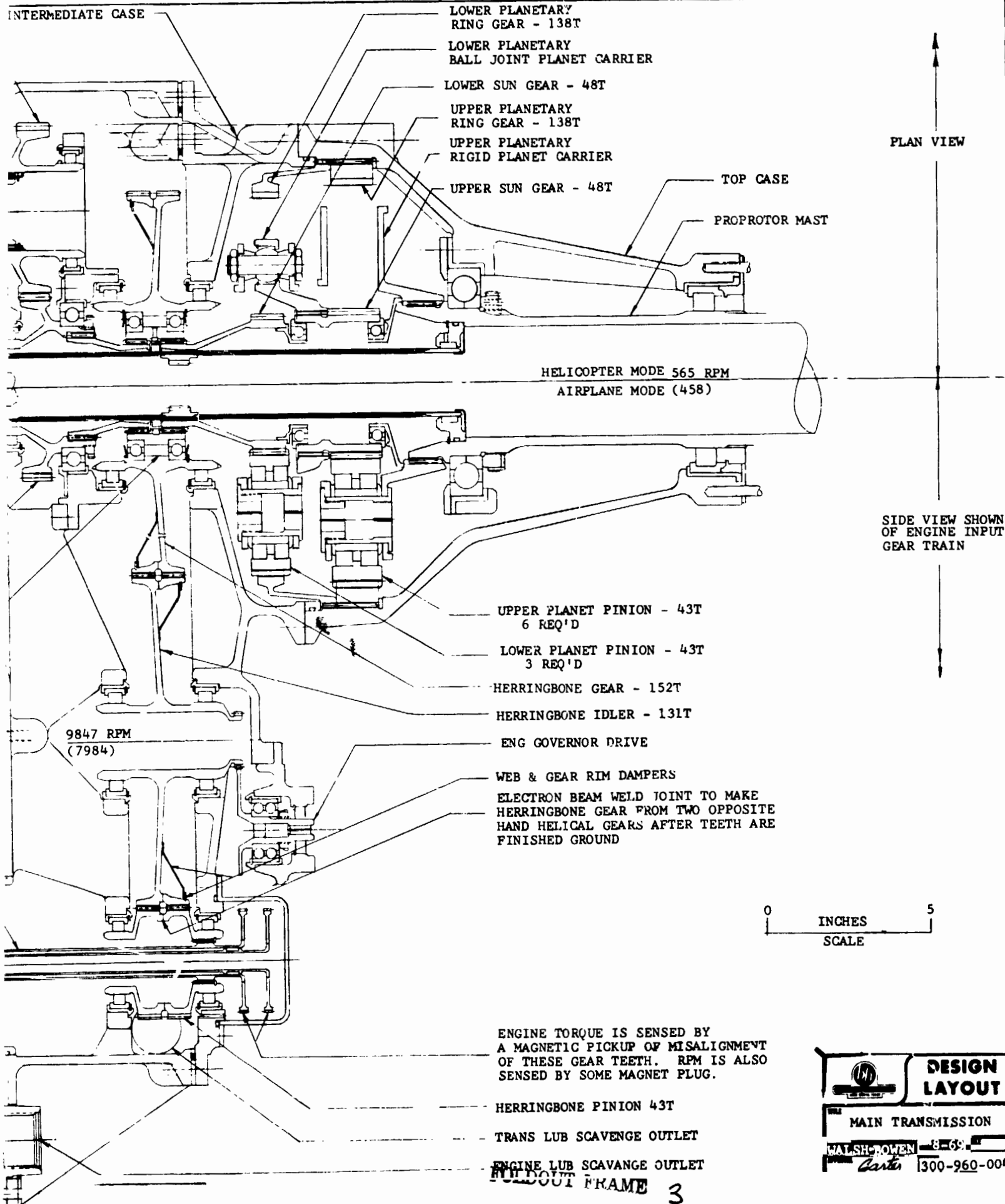
SPIRAL BEVEL
31T

SECTION B-B

COMBINATION POWER & TORQUEM
(TORQUEMETER PORTION NOT SH

6486 RPM
(5259)





CONTROL PHASING ACTUATOR
(REF 300-960-007)

FLAP DRIVE ACTUATOR

DRIVESHAFT

AILERON

COLLECTIVE CONTROL TO LEFT ROTOR ---

AILERON CONTROL TO LEFT ROTOR ---

CYCLIC CONTROL TO LEFT ROTOR ---

DIFFERENTIAL COLLECTIVE PHASING LEVERS ---

COLLECTIVE RANGE-SHIFT CRANK ---

COLLECTIVE CONTROL FROM PILOT ---

DIRECTIONAL CONTROL FROM PILOT ---

CONTROL TO RUDDER (REF 300-960-006) ---

DIFFERENTIAL

DIFFERENTIAL

FORE AND AFT CONTROL FROM PILOT ---

LATERAL CONTROL FROM PILOT ---

CONTROL TO ELEVATOR (REF 300-960-008) ---

CENTERLINE AIRCRAFT

FOLDOUT FRAME /

COLLE

- DRIVESHAFT INTERCONNECT GEARBOX (REF)

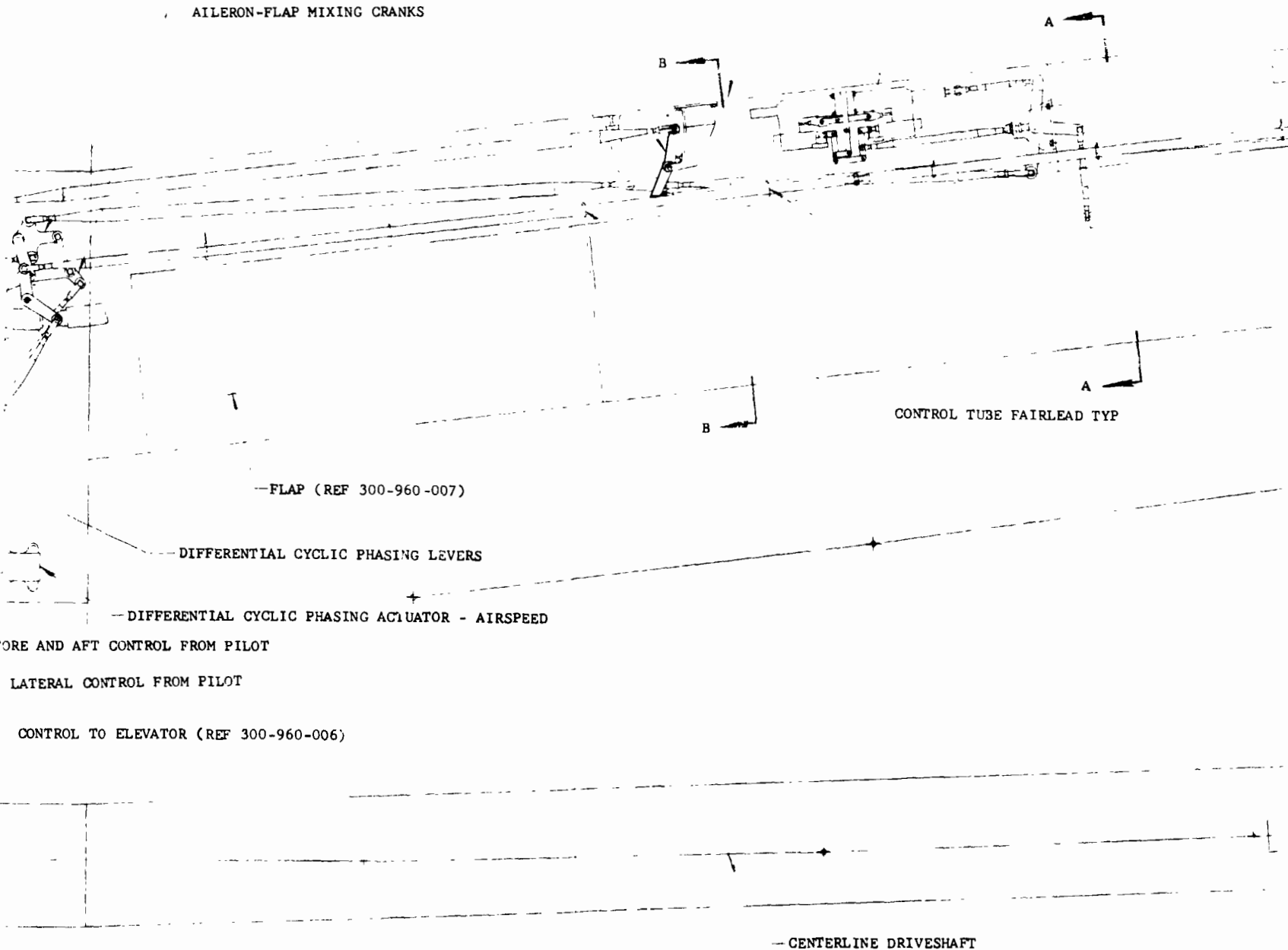
- AFT SPAR

TRANSMISSION (REF 3

COLLECTIVE WING DEFLECTION
ISOLATION BELLCRANK

- AILERON SERVO ACTUATOR

AILERON-FLAP MIXING CRANKS



-FLAP (REF 300-960-007)

-DIFFERENTIAL CYCLIC PHASING LEVERS

-DIFFERENTIAL CYCLIC PHASING ACTUATOR - AIRSPEED

CONTROL TUBE FAIRLEAD TYP

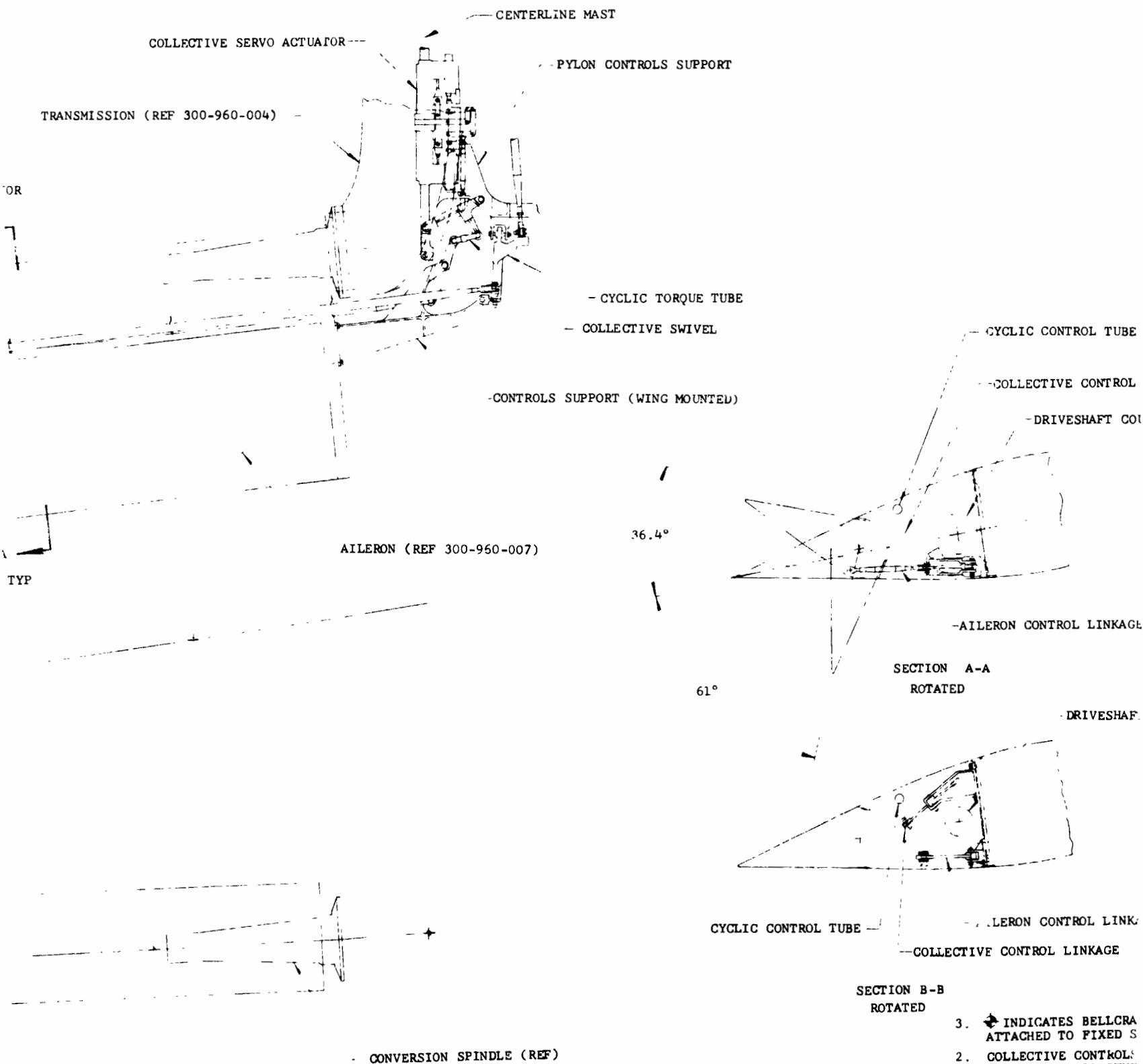
- CENTERLINE DRIVESHAFT

FORE AND AFT CONTROL FROM PILOT

LATERAL CONTROL FROM PILOT

CONTROL TO ELEVATOR (REF 300-960-006)

NE AIRCRAFT



3. * INDICATES BELL CRA ATTACHED TO FIXED S
 2. COLLECTIVE CONTROL POSITION - ALL OTHER NEUTRAL POSITION
 1. ALL CONTROLS SHOWN
- NOTES

A REVISED FLAPERON [2-72] ANGLES

- CYCLIC CONTROL TUBE

- COLLECTIVE CONTROL TUBE

- DRIVESHAFT COUPLING (REF)

-AILERON CONTROL LINKAGE

SECTION A-A
ROTATED

DRIVESHAFT (REF)

0 10
INCHES
SCALE

A

CONTROL TUBE --

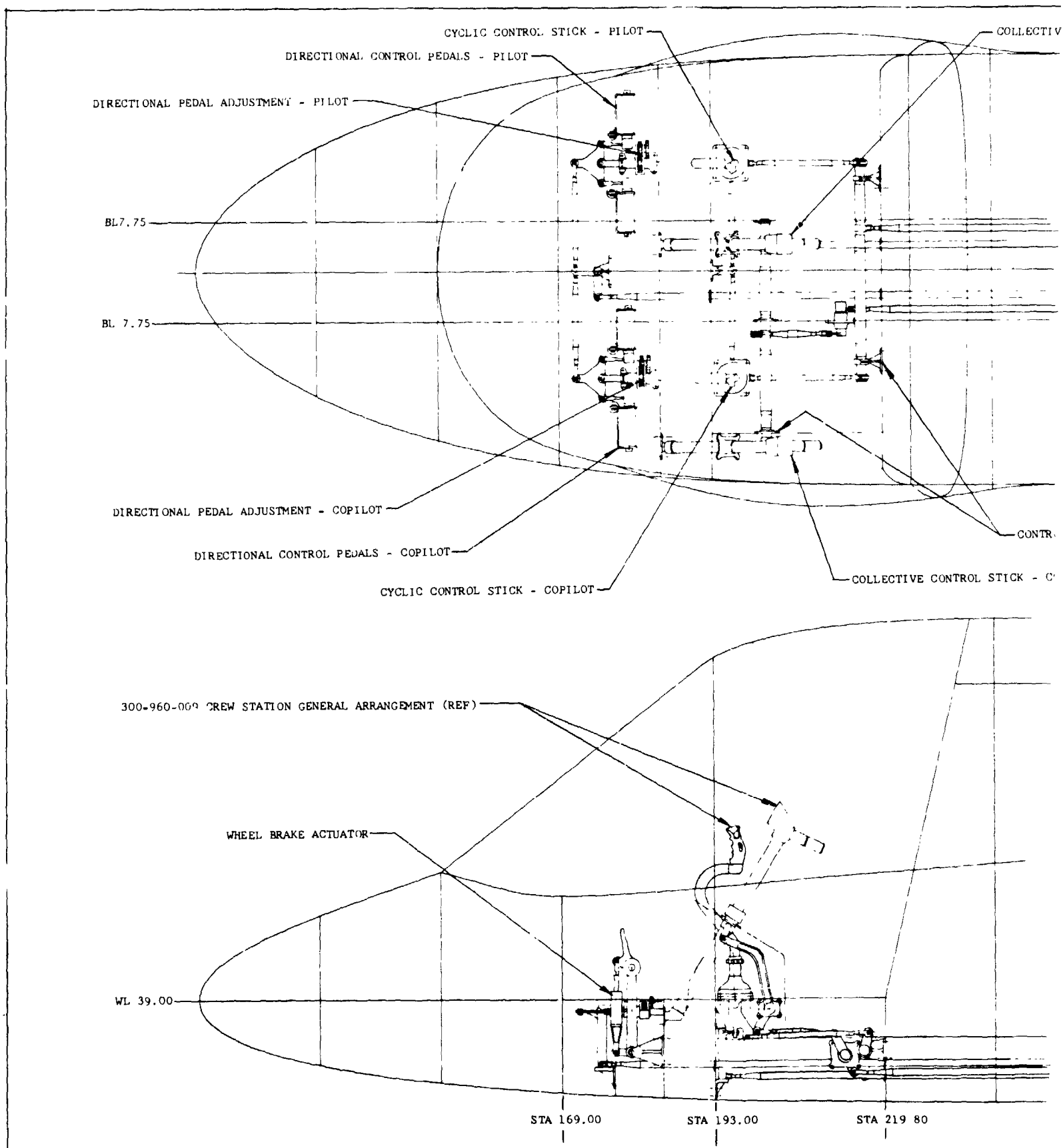
--AILERON CONTROL LINKAGE

COLLECTIVE CONTROL LINKAGE

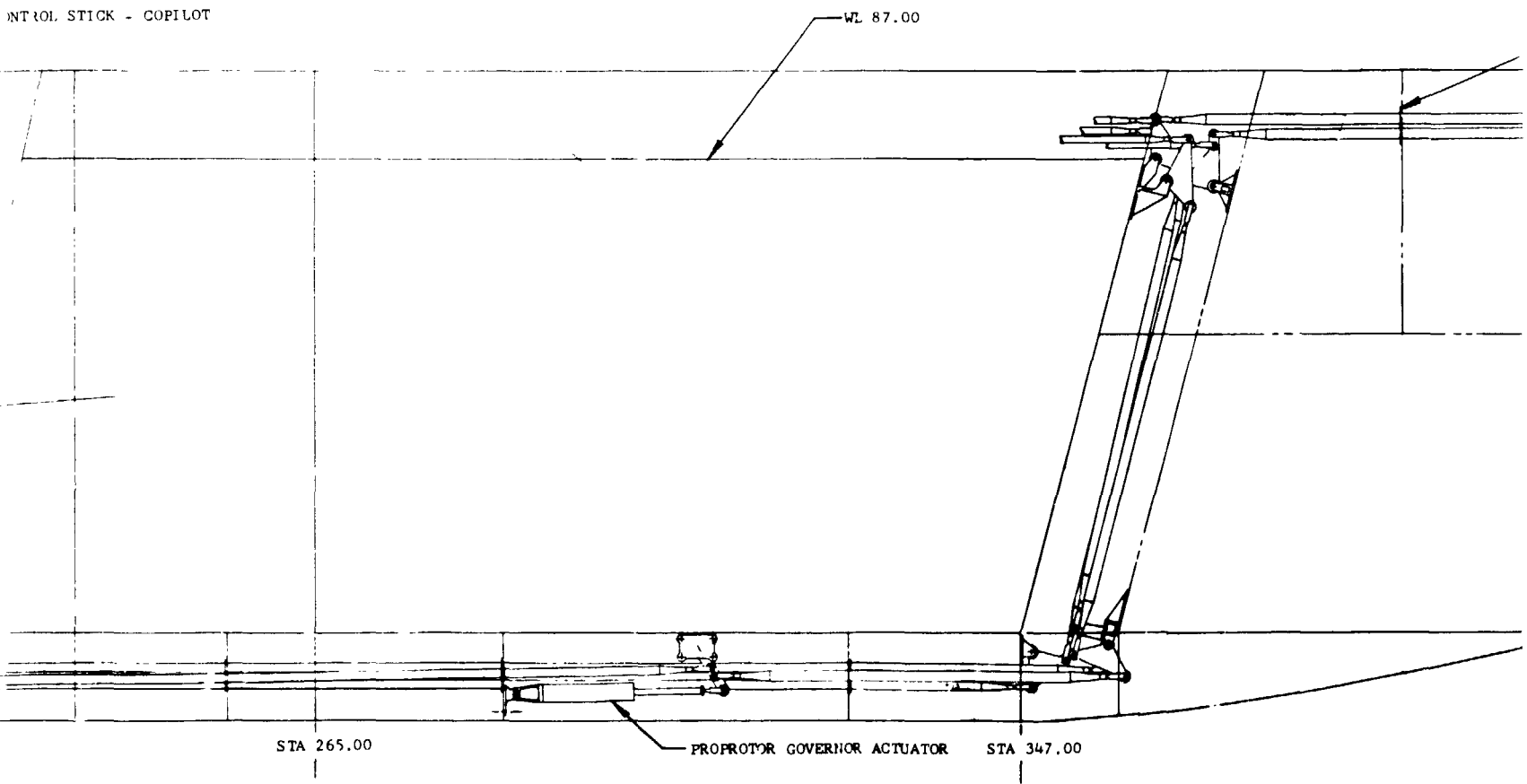
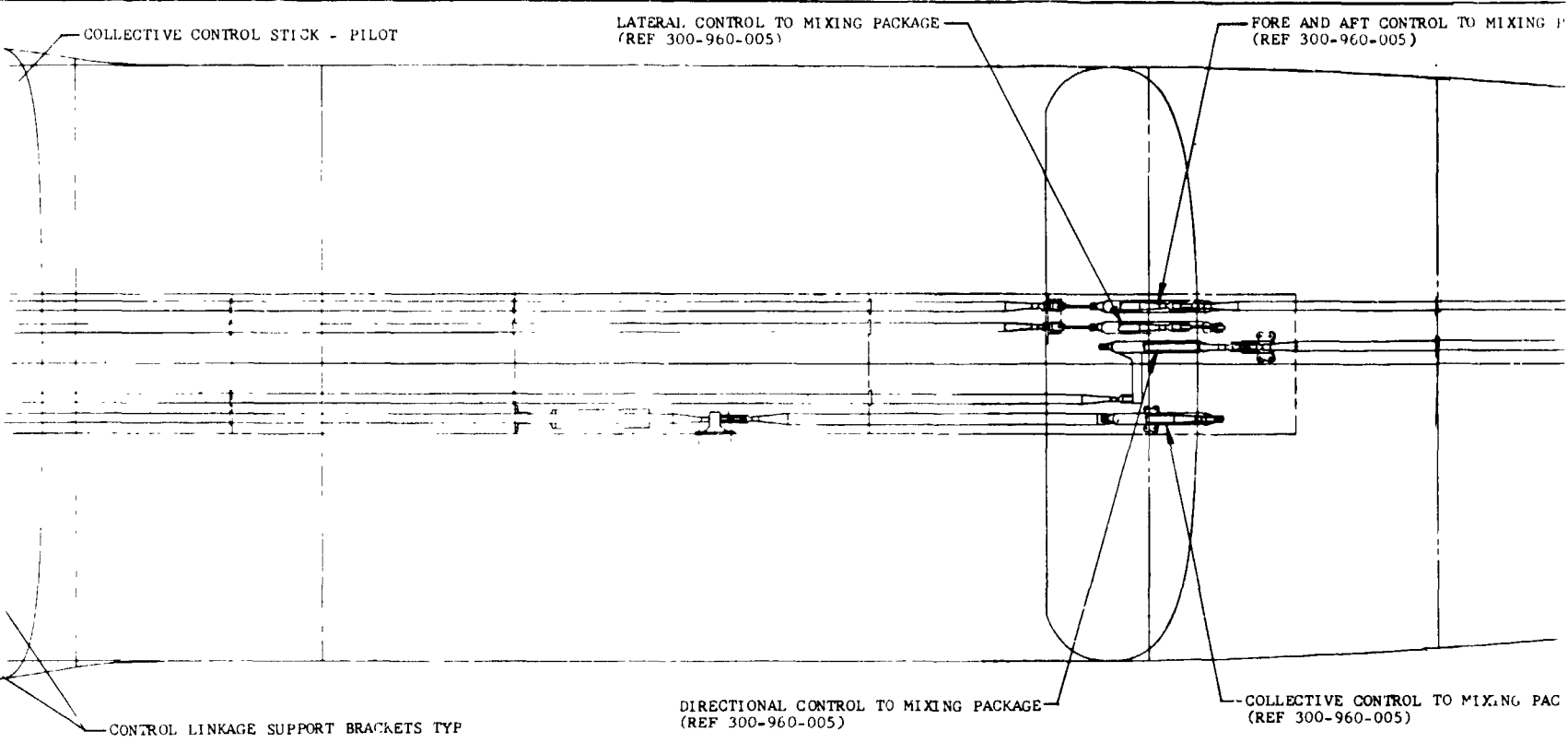
SECTION B-B
ROTATED

3. * INDICATES BELLCRANK PIVOT POINTS ATTACHED TO FIXED STRUCTURE
 2. COLLECTIVE CONTROLS SHOWN IN MAX PITCH POSITION - ALL OTHER CONTROLS SHOWN IN NEUTRAL POSITION
 1. ALL CONTROLS SHOWN IN AIRPLANE MODE
- NOTES

 DESIGN LAYOUT	
FIXED CONTROLS - WING	
ESSARY	8-69
Int.	300-960-005



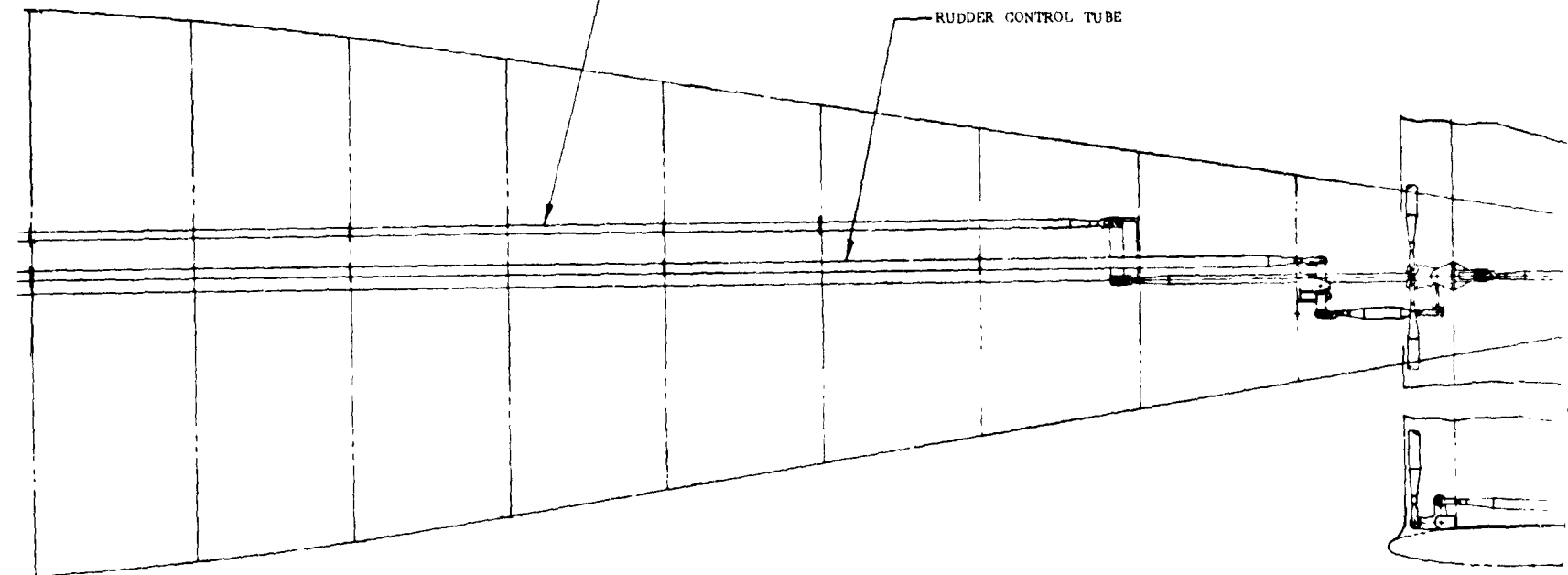
FOLDOUT FRAME /



WL TO MIXING PACKAGE

ELEVATOR CONTROL TUBE

RUDDER CONTROL TUBE



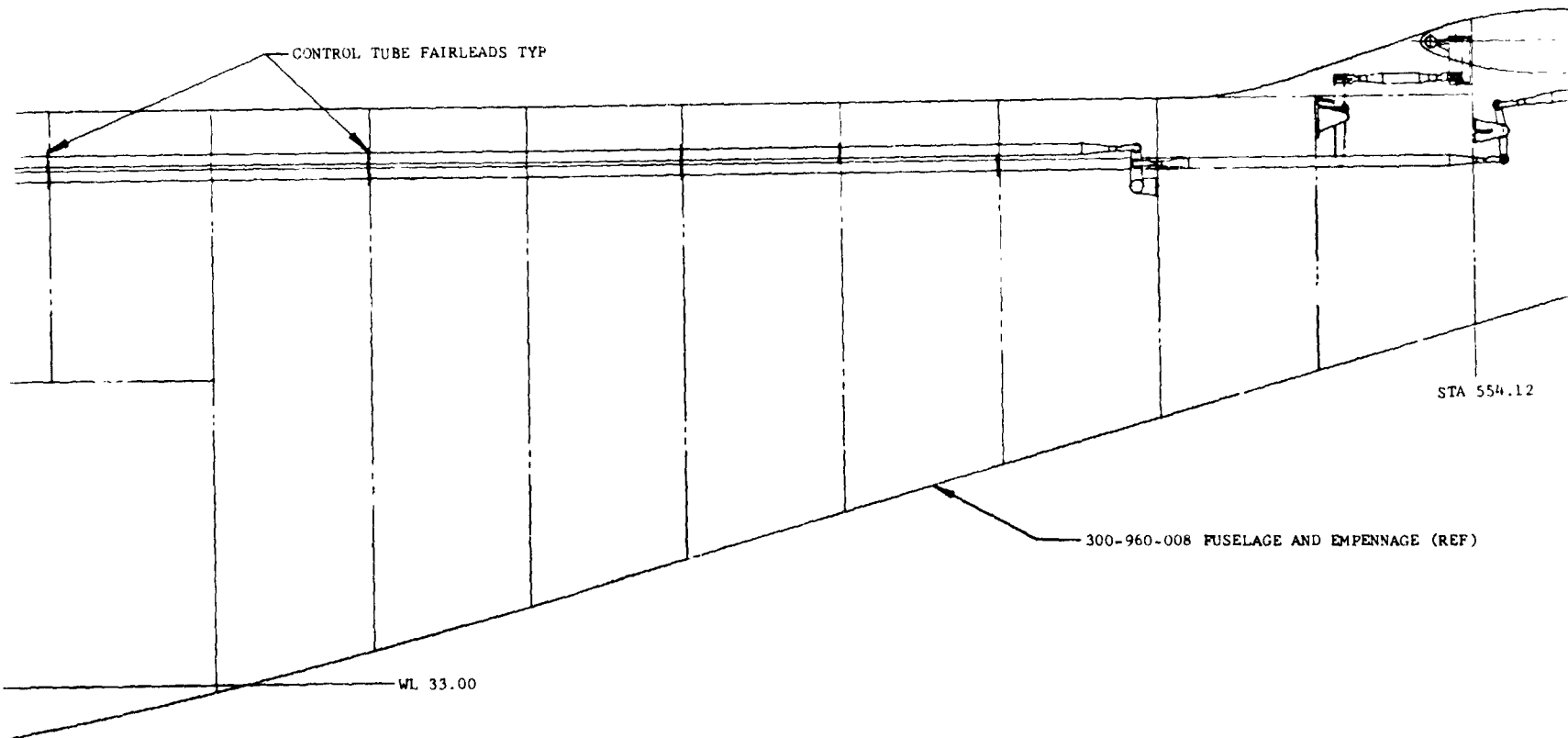
L TO MIXING PACKAGE

CONTROL TUBE FAIRLEADS TYP

STA 554.12

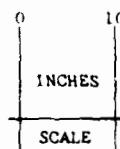
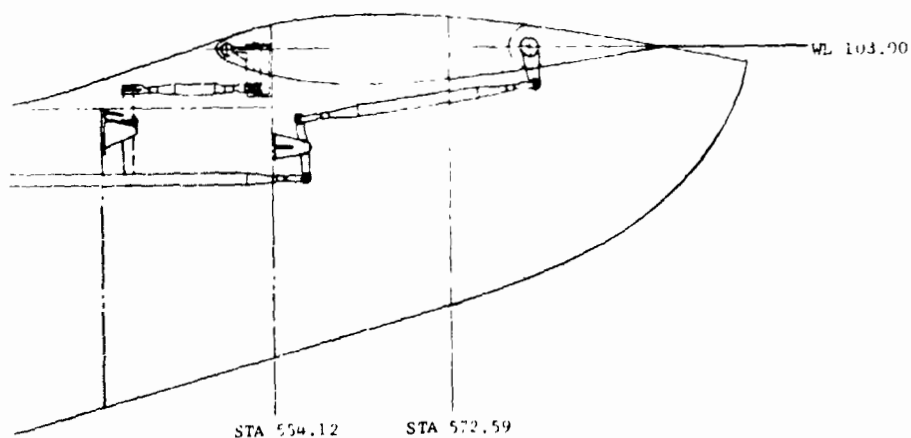
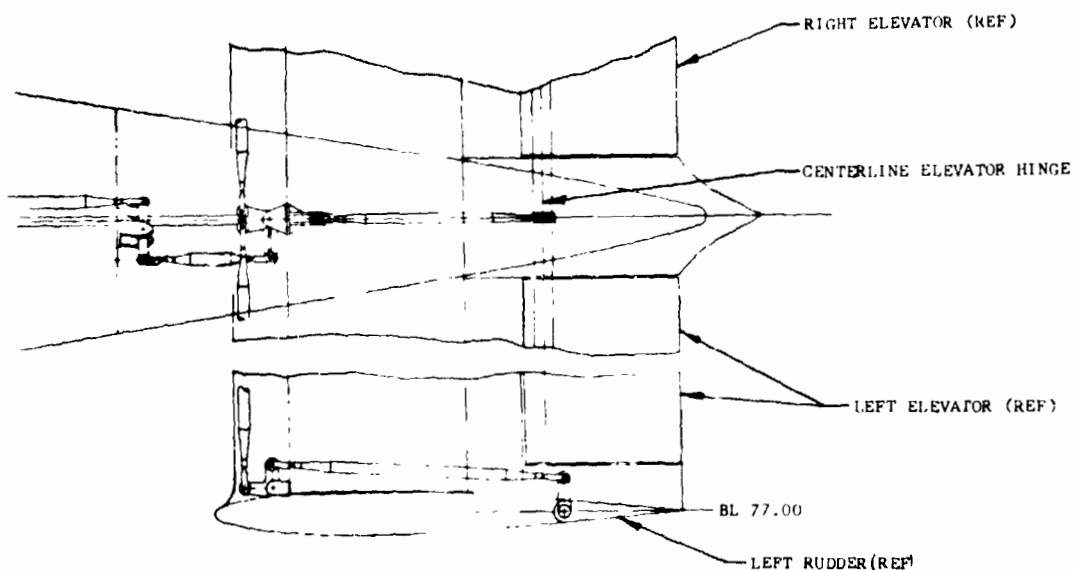
300-960-008 FUSELAGE AND EMPENNAGE (REF)

WL 33.00



FOLDOUT FRAME 3

REV	DATE	BY	CHKD	APP'D
1	2-72	22		
2	2-72	22		
3	2-72	22		
4	2-72	22		
5	2-72	22		
6	2-72	22		
7	2-72	22		
8	2-72	22		
9	2-72	22		
10	2-72	22		



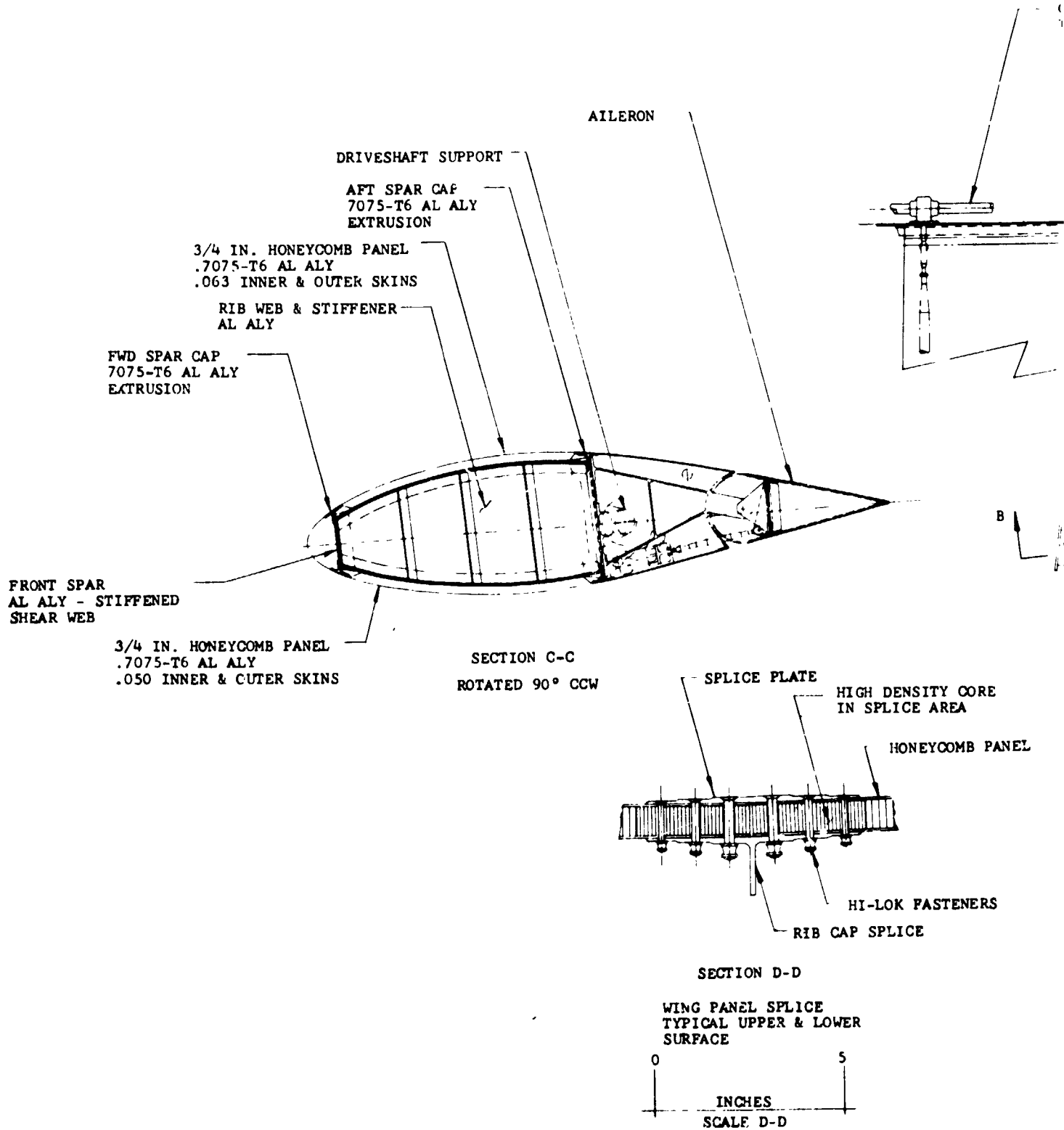
FUSELAGE AND EMPENNAGE (REF)

2. COLLECTIVE CONTROLS SHOWN IN MAX PITCH POSITION - ALL OTHER CONTROLS SHOWN IN NEUTRAL POSITION
1. ALL CONTROLS SHOWN IN AIRPLANE MODE

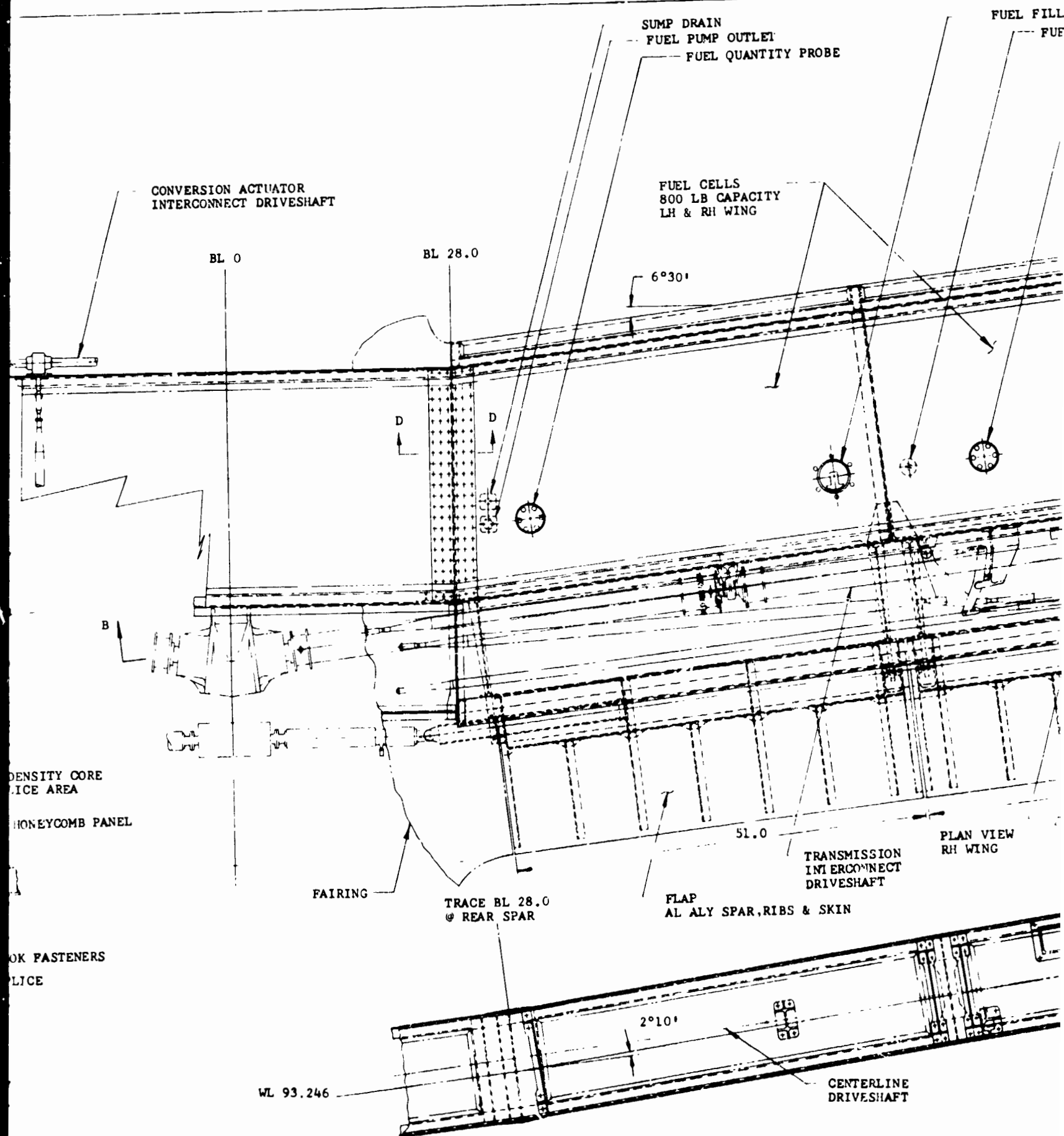
NOTES

DESIGN LAYOUT	
FIXED CONTROLS FUSELAGE	
ESSARY	8-69
300-960-006	

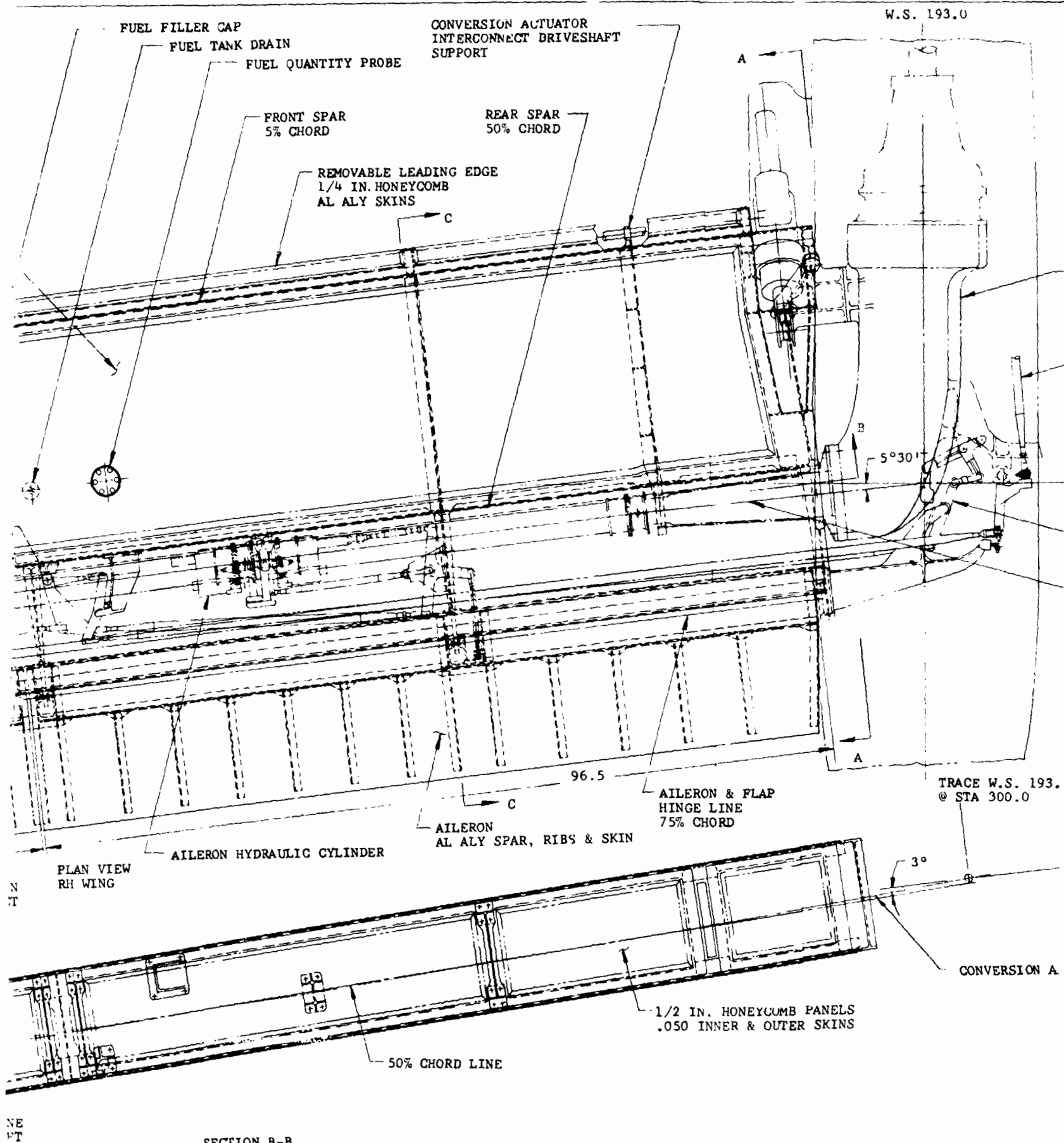
FOLDOUT FRAME 4



FOLDOUT FRAME



FOLDOUT FRAME 2



W.S. 193.0

PYLON DOWN STOP
BRACKET

MAIN TRANSMISSION
REF 300-960-004

CYCLIC CONTROL
REF 300-960-005

STA 300.0

COLLECTIVE CONTROL
REF 300-960-005

CONVERSION AXIS

CONVERSION ACTUATOR

7075-T6 AL ALY MACHINED

SECTION A-A

TRACE W.S. 193.0
@ STA 300.0

WL 100.0

CONVERSION AXIS

0 10
INCHES
SCALE

	DESIGN LAYOUT
	WING ASSEMBLY
	G. SMITH 8-69
	<i>Butler</i> 300-960-007

FOLDOUT FRAME +

BL 7.75

WINDSHIELD STRETCHED ACRYLIC

CAST ACRYLIC

STRETCHED ACRYLIC

WL 87.0

WL 39.0

STA 112.0

STA 131.0

STA 148.0

STA 169.0

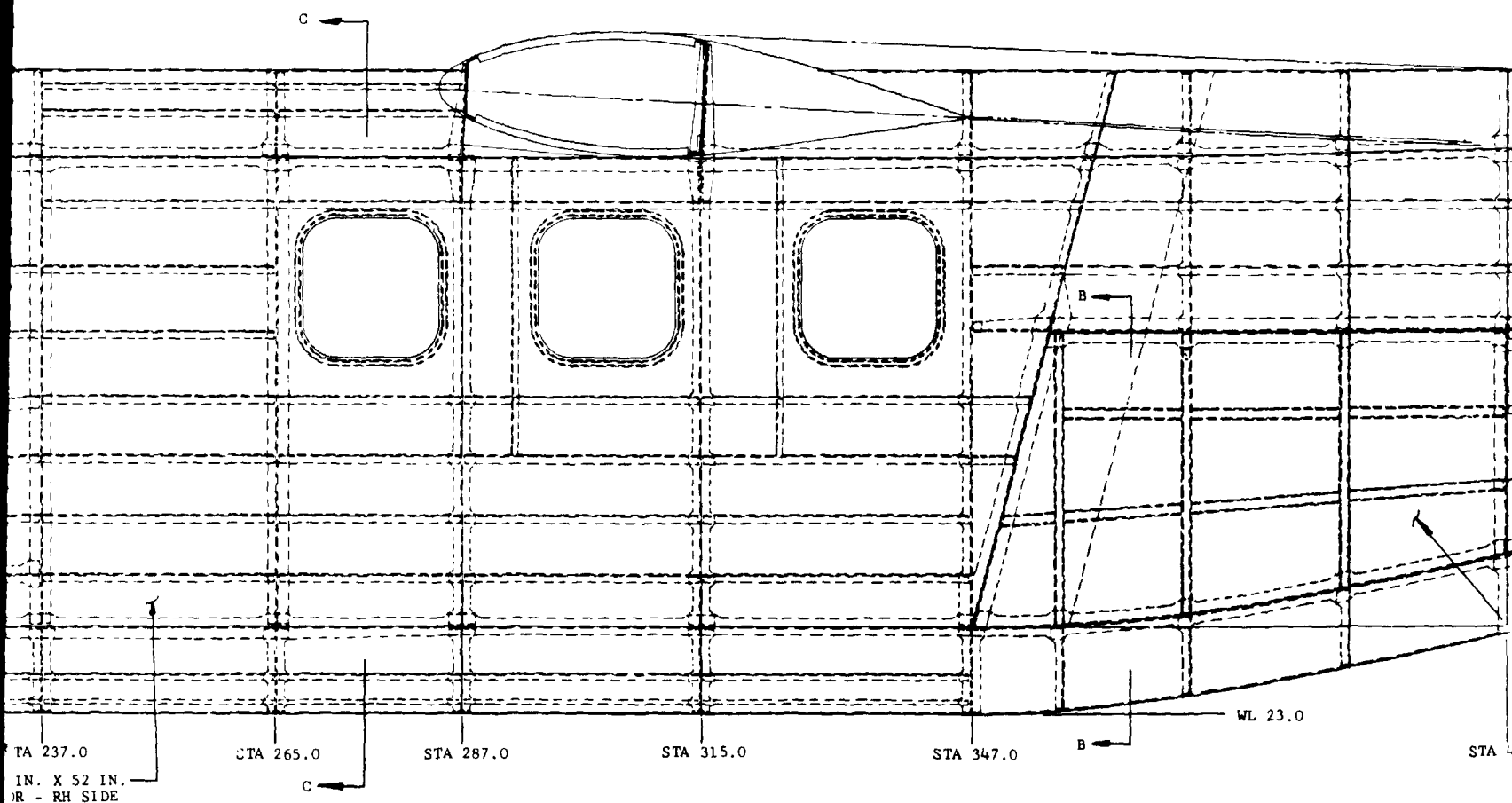
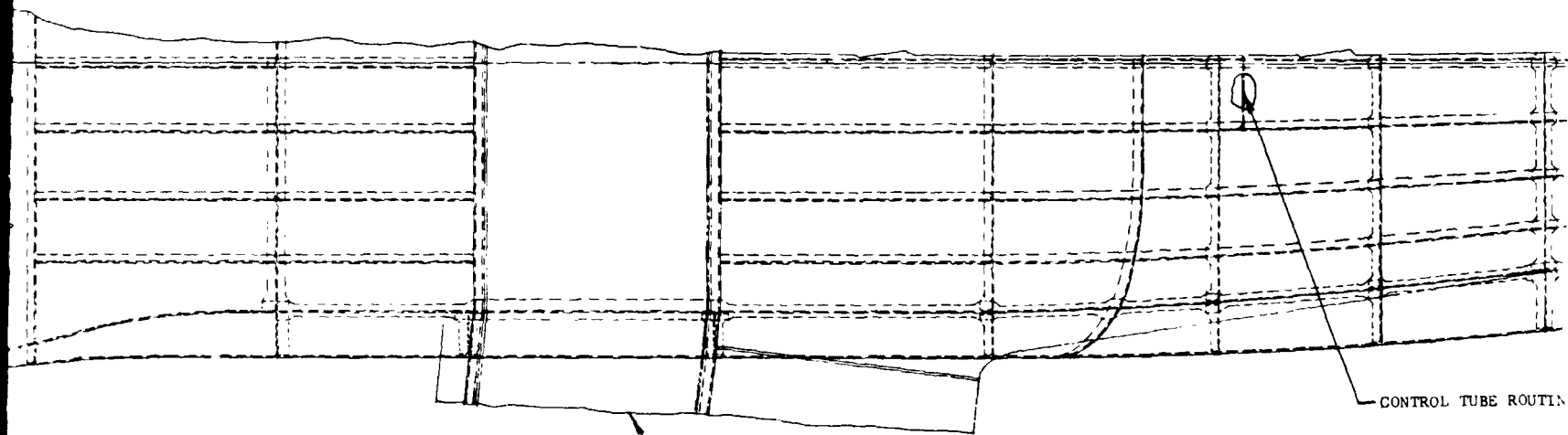
STA 193.0

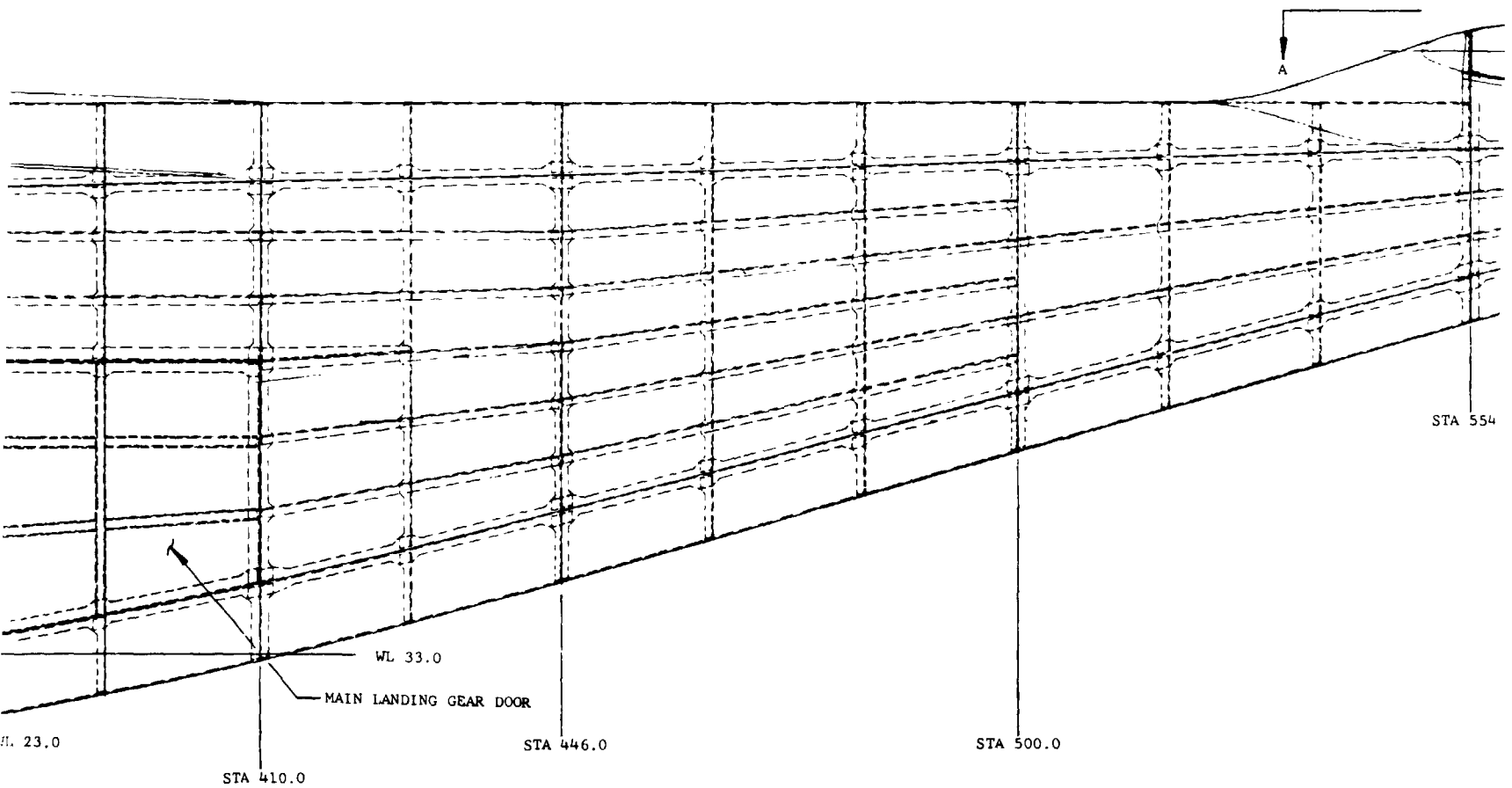
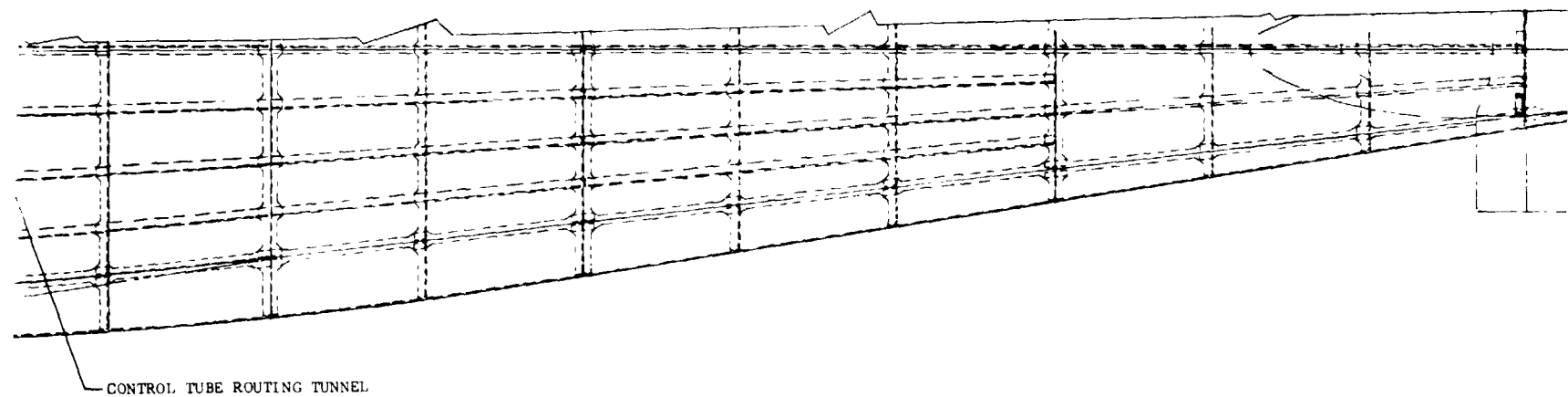
STA 219.8

STA 237.0

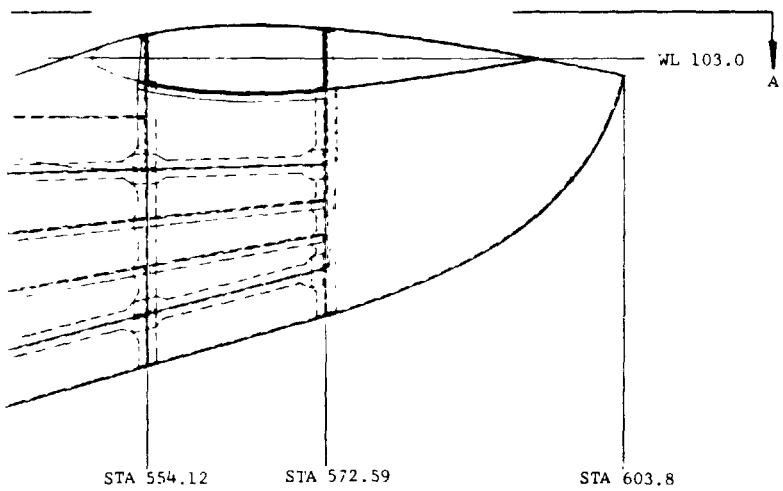
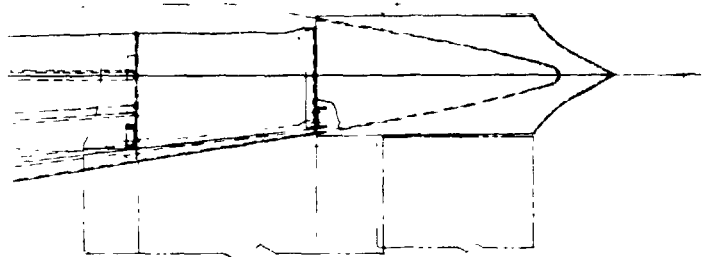
28 IN. X 52 IN.
DOOR - RH SIDE

FOLDOUT FRAME /



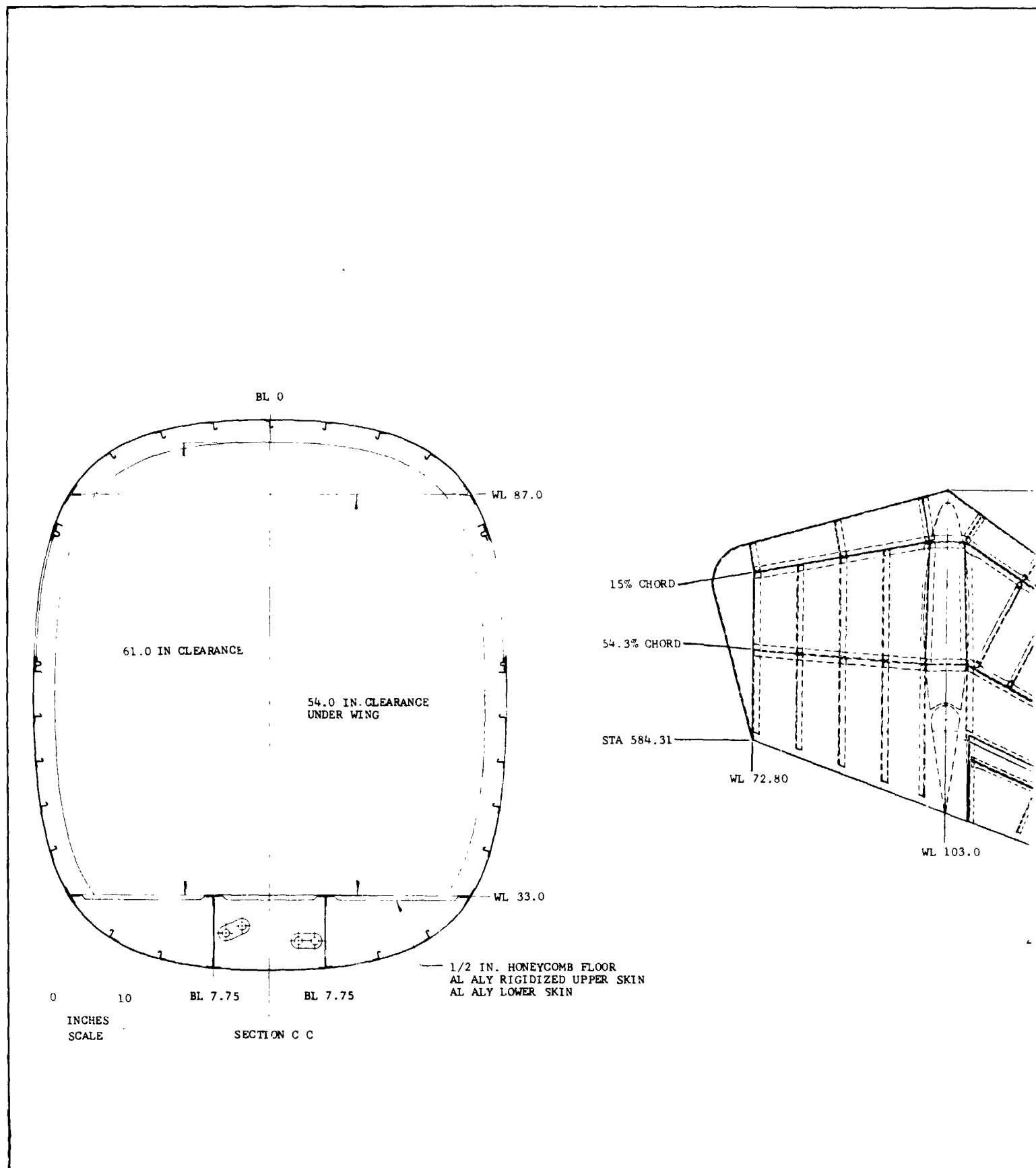


SYMBOL	DESCRIPTION	DATE
A	ADDED TAIL CONFIG.	2-72

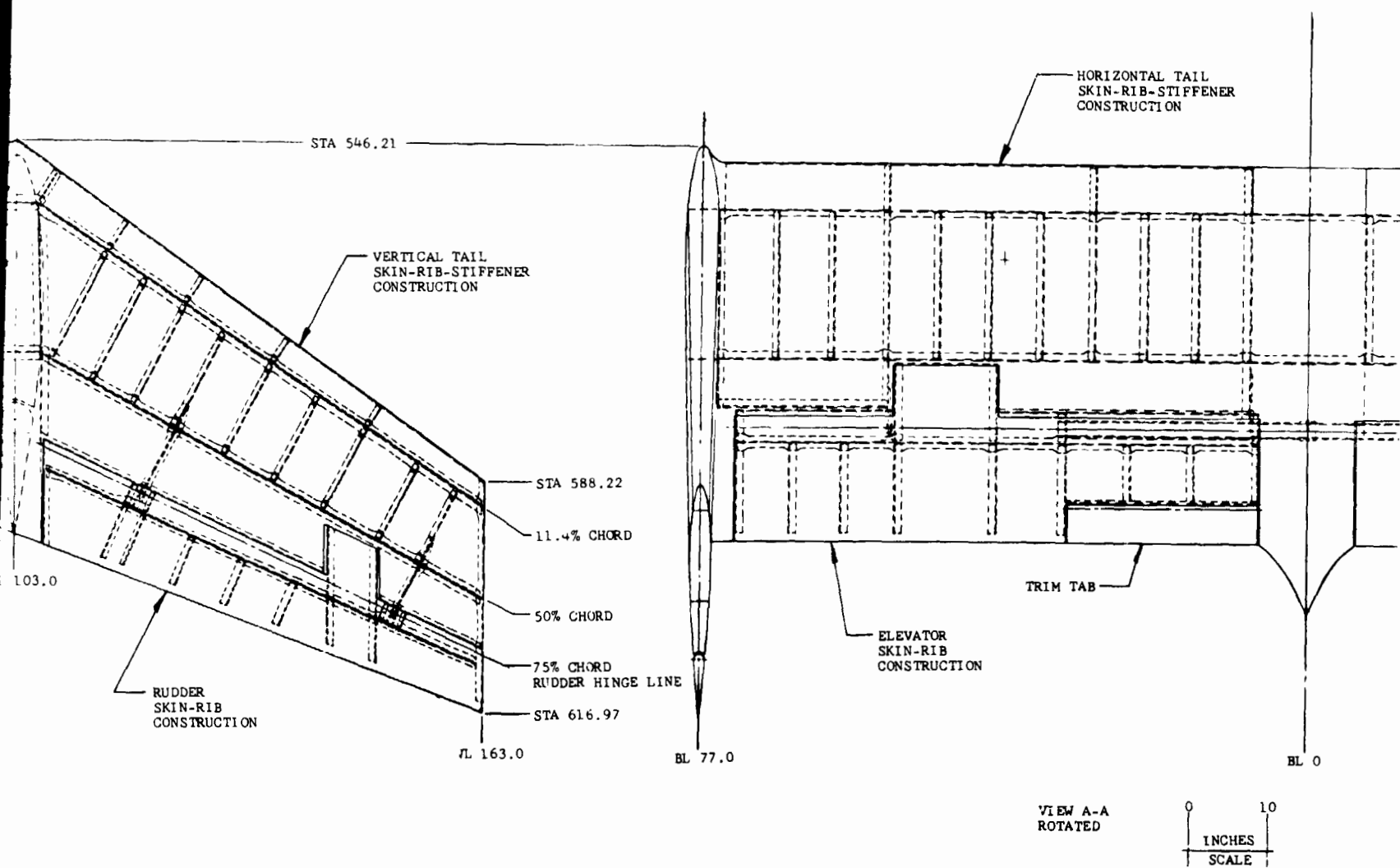


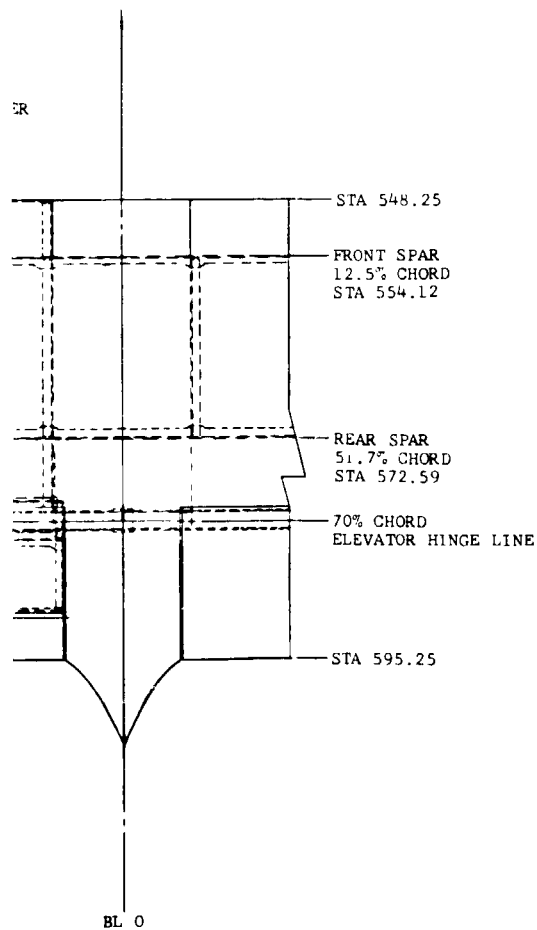
0 10
INCHES
SCALE

DESIGN LAYOUT	
FUSELAGE AND EMPENNAGE	
G. SMITH	2-72 SHT 1
<i>Butler</i>	300-960-008

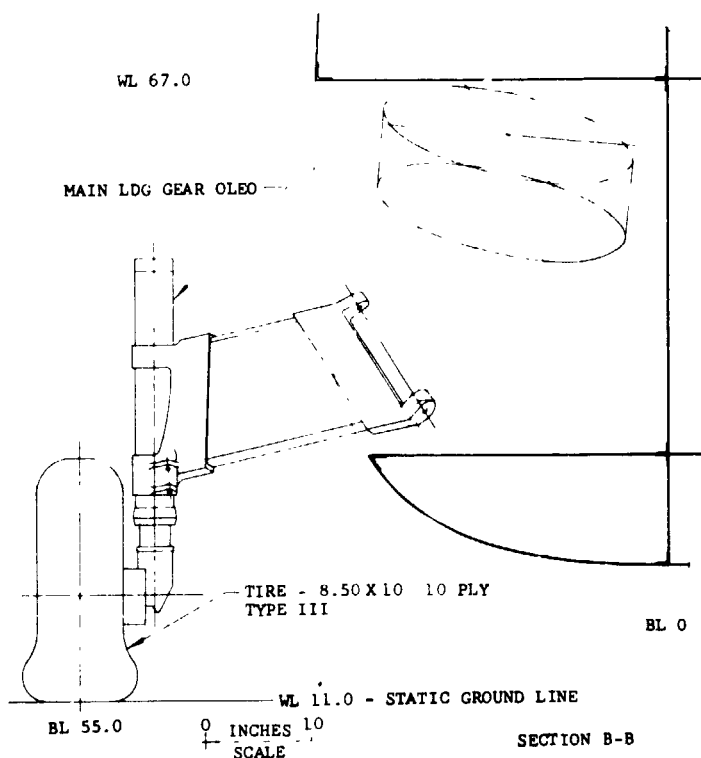
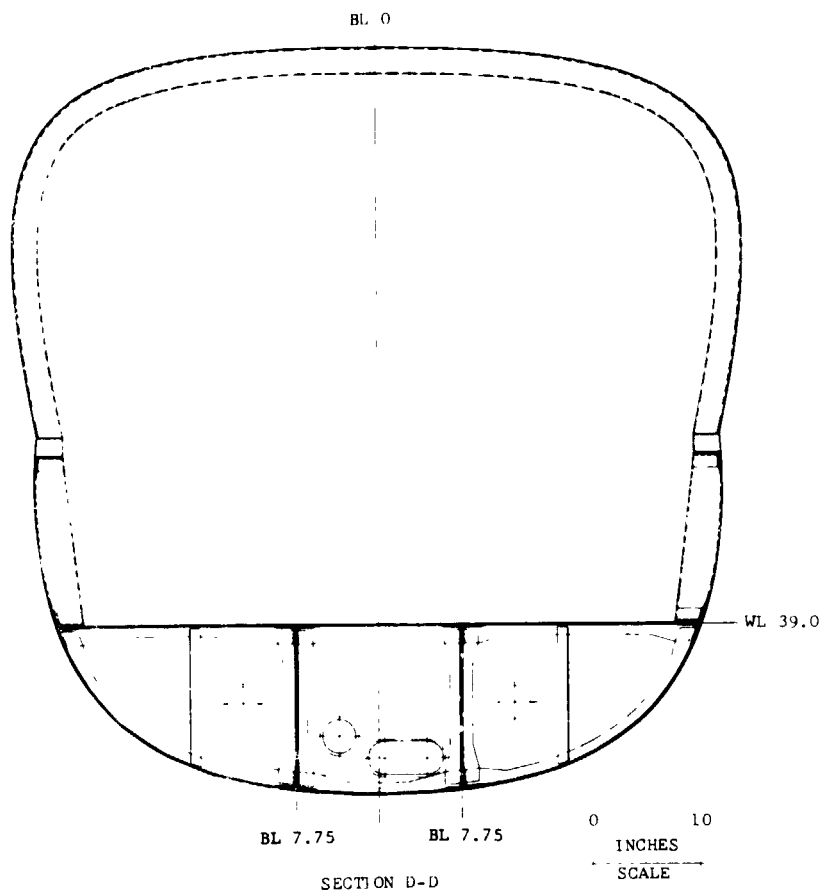


FOLDOUT FRAME /

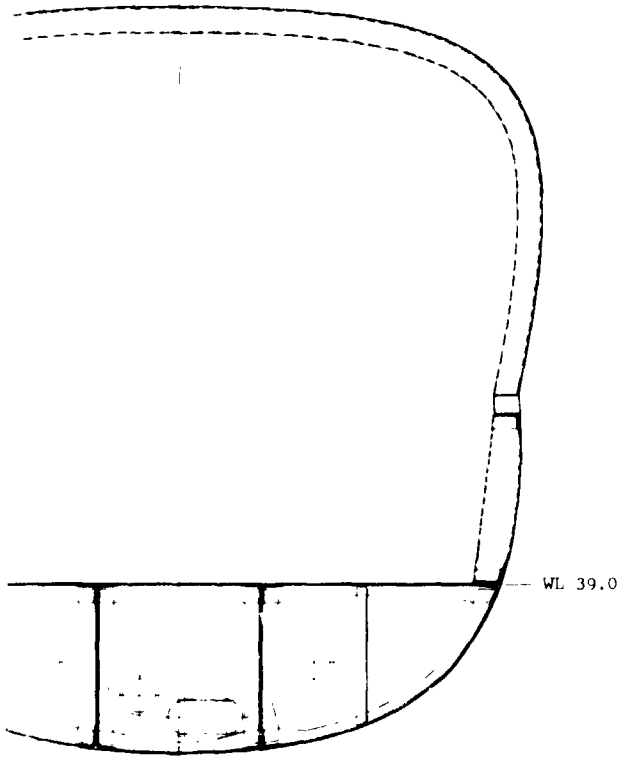




10
INCHES
SCALE



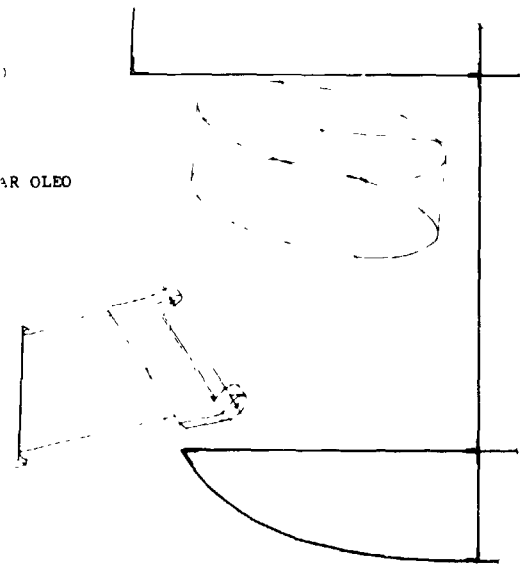
BL 0



BL 7.75 BL 7.75 0 10 INCHES SCALE

SECTION D-D

AR OLEO




- TIRE - 8.50 X 10 10 PLY TYPE III

BL 0

WL 11.0 - STATIC GROUND LINE 0 INCHES 10 SCALE

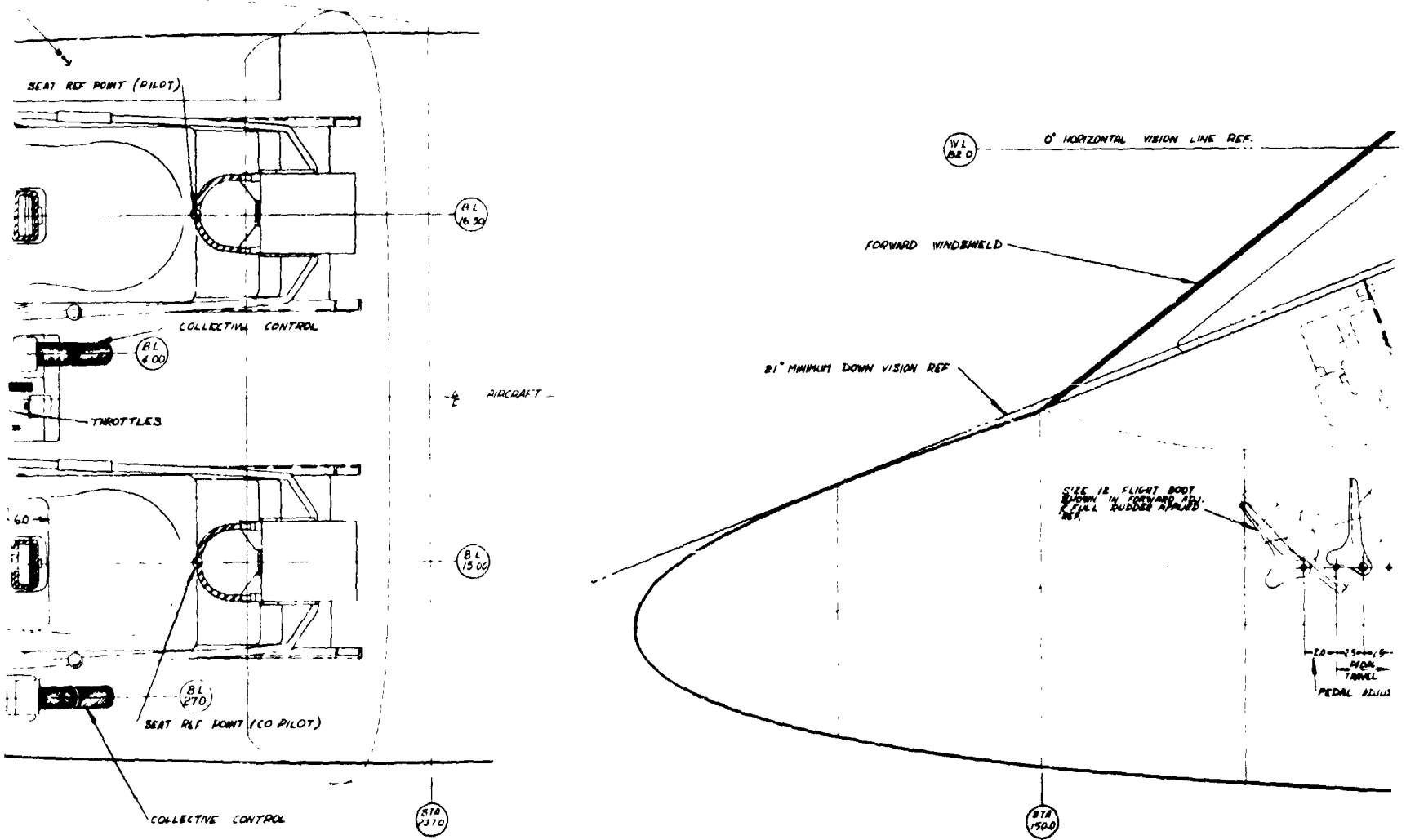
SECTION B-B

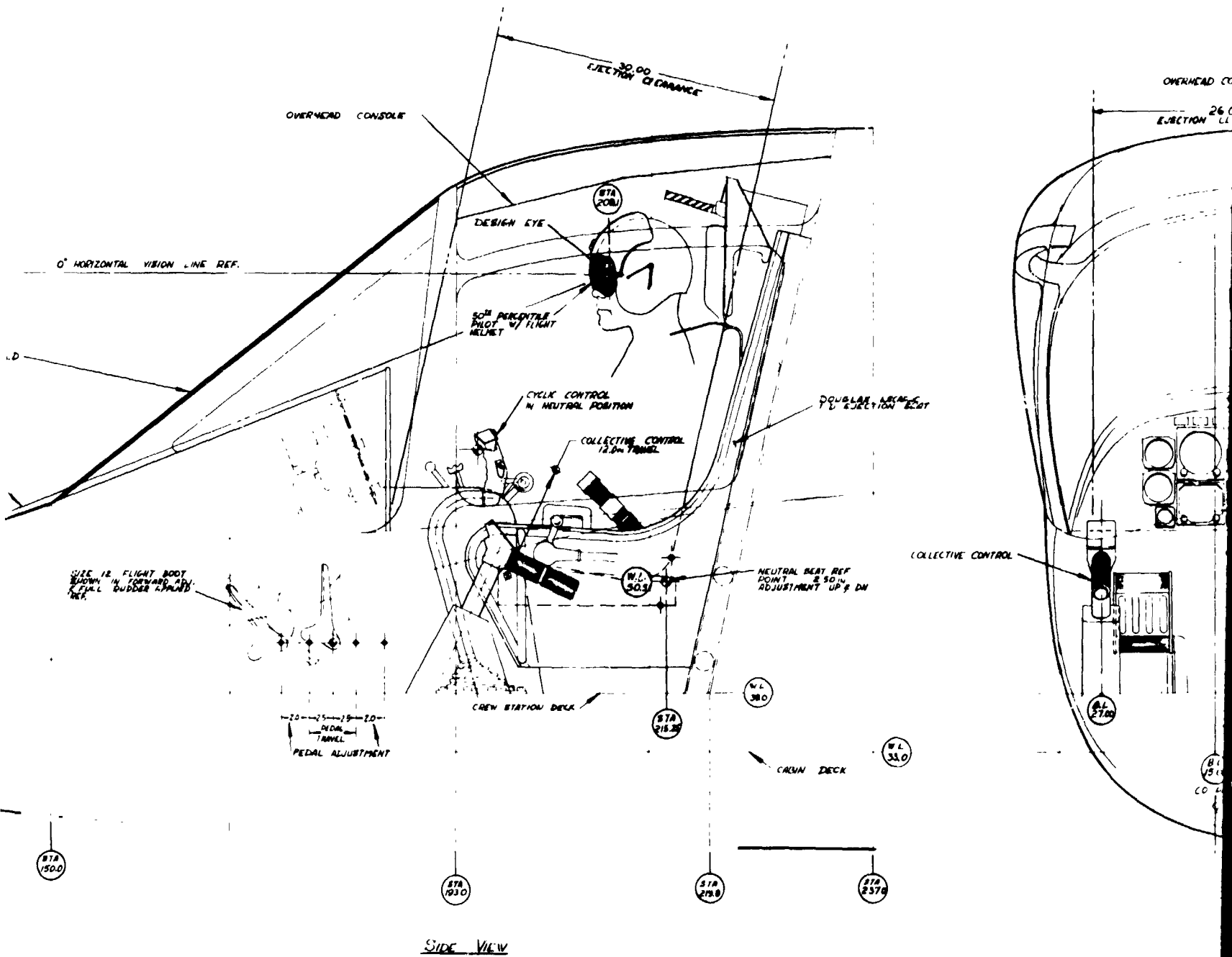
		DESIGN LAYOUT	
FUSELAGE AND EMPENNAGE			
G. SMITH		2-72/SHT 2	
<i>Smith</i>		300-960-008	

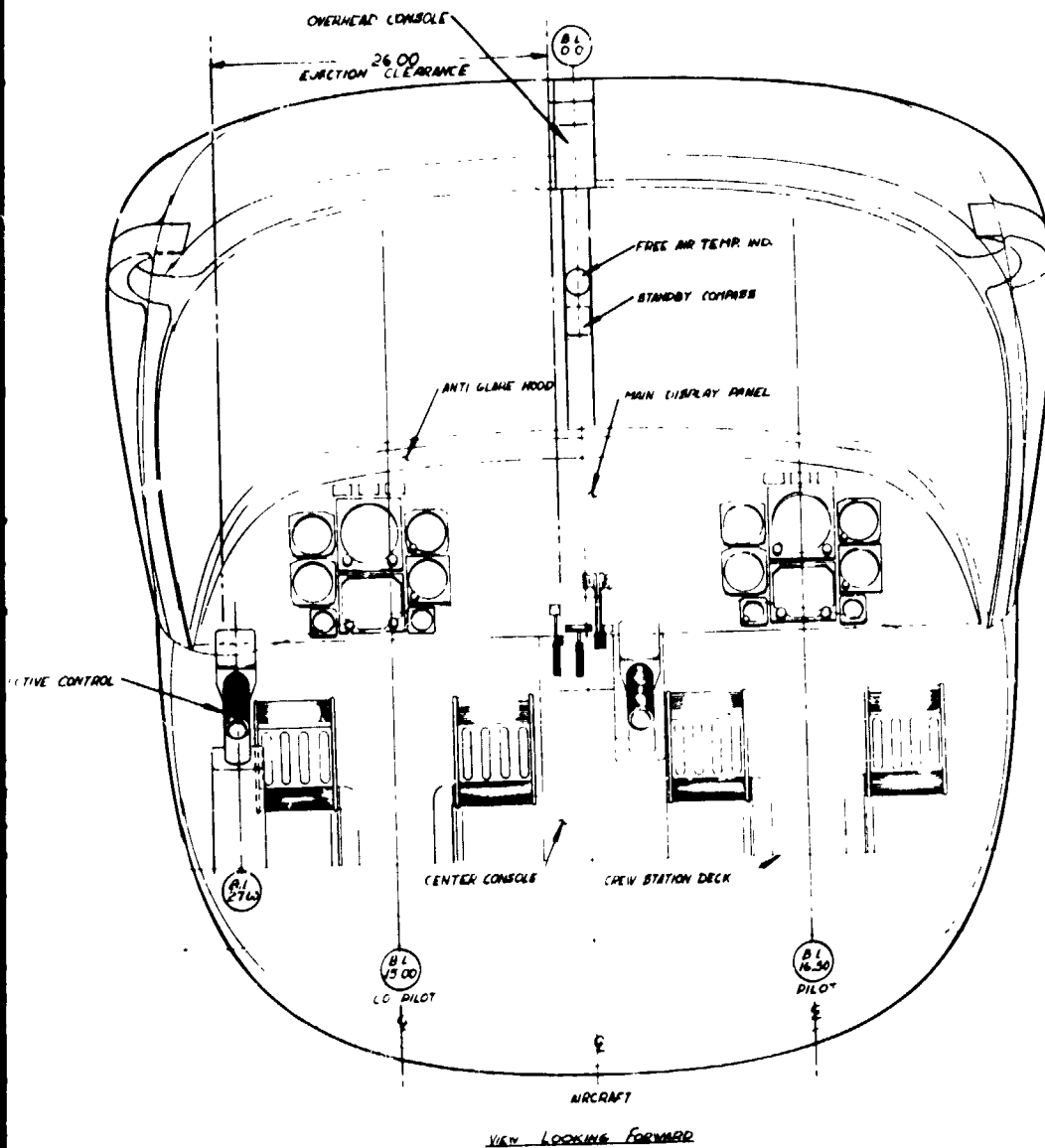
A

FOLDOUT FRAME 4


OVERHEAD CC







INCHES
SCALE 10

 DESIGN LAYOUT	
MODEL 300 CREW STATION GENERAL ARRANGEMENT	
Designer: H. WHITE Date: 12-5-55	Part: 1/2 Drawing No: 300-960-009

FOLDOUT FRAME 4